UNIVERSITY OF STIRLING

DEPARTMENT OF CHEMISTRY

Multiple Phase Equilibria in Polar Polymer Solutions
Containing Poly(acrylic acid)

by

Brian Trevor Swinyard

Submitted for the degree of
Doctor of Philosophy

April 1985

ABSTRACT

The cloud-point curves for solutions of poly(acrylic acid) in 1,4-dioxane, 1,4-dioxane/water mixtures, tetrahydrofuran and tetrahydrofuran/water mixtures as a function of molecular weight and solvent composition were determined. These systems are unusual in that they exhibit three phase separation boundaries on raising the temperature from room temperature to 500K designated as pseudo-LCST (p-LCST), UCST and LCST behaviour respectively in order of increasing temperature. Systems consisting of poly(acrylic acid) together with small chain poly(ethylene glycol)s and poly(propylene glycol)s in 1,4-dioxane were also studied and, in general, they exhibited simple LCST behaviour.

Critical points for the pseudo-LCST phase separation boundary were determined for the higher molecular weight poly(acrylic acid)s in 1,4-dioxane, using the phase volume ratio method. The variation of the intrinsic viscosity of solutions below the pseudo-LCST was measured as a function of temperature increasing towards the phase separation boundary.

The structure and possible complex formation in the system at temperatures below the pseudo-LCST were determined using laser raman spectroscopy. Preferential solvation studies, using light scattering techniques, were also made on the mixed solvent system 1,4-dioxane/water, from which data were obtained which could be compared with those derived from solution viscosity. The variation of the enthalpic interaction parameter, χ_h, was determined from heat of dilution data derived from microcalorimetry experiments.

The cloud-point curves for the poly(acrylic acid) in 1,4-dioxane system were compared to poly(N-isopropylacrylamide) in water, which exhibited simple LCST behaviour and aqueous solutions of poly(vinyl alcohol) which formed a closed-loop of immiscibility.

ACKNOWLEDGEMENTS

C O N T E N T S

Contents (contd.)

Contents (contd.)

Contents (contd.)

CHAPTER ONE

INTRODUCTION

1.1 INTRODUCTION

When homogeneous binary mixtures of two liquids are examined as a function of temperature the appearance of a phase separation boundary will depend on the type of system under study. Liquid pairs may exist as one phase homogeneous solutions at high temperatures and exhibit a phase separation boundary on cooling resulting in a two phase system. This type of phase separation behaviour, as illustrated in Fig 1.1a, is referred to as Upper Critical Solution behaviour and the maximum temperature at which immiscibility is encountered is often referred to as the upper critical solution temperature, UCST. This type of behaviour can be seen in the system of water and isobutanol.[1] Alternatively, on heating a homogeneous solution phase separation may also occur, as shown in Fig 1.1b. This type of phase separation behaviour is referred to as Lower Critical Solution behaviour and the minimum temperature below which the solution is homogeneous and above which phase separation occurs is called the lower critical solution temperature, LCST. This type of behaviour is seen in mixtures of water and triethylamine.[1] The somewhat perverse names lower and upper critical solution behaviour are a result of observations on small molecule mixtures where a closed-loop of immiscibility, completely surrounded by a miscibility region, Fig 1.1d, has been reported, typified by solutions of water and nicotine.[2]

Analogous situations can be encountered in polymer solutions although the corresponding phase equilibria are more complex because of the size difference between the polymer and the solvent and the differing intermolecular forces involved. When a polymer is mixed with a liquid there are basically two stages in the dissolution process. Initially the solvent molecules diffuse into the polymer producing a swollen gel and the process may stop at this stage if the polymer-polymer
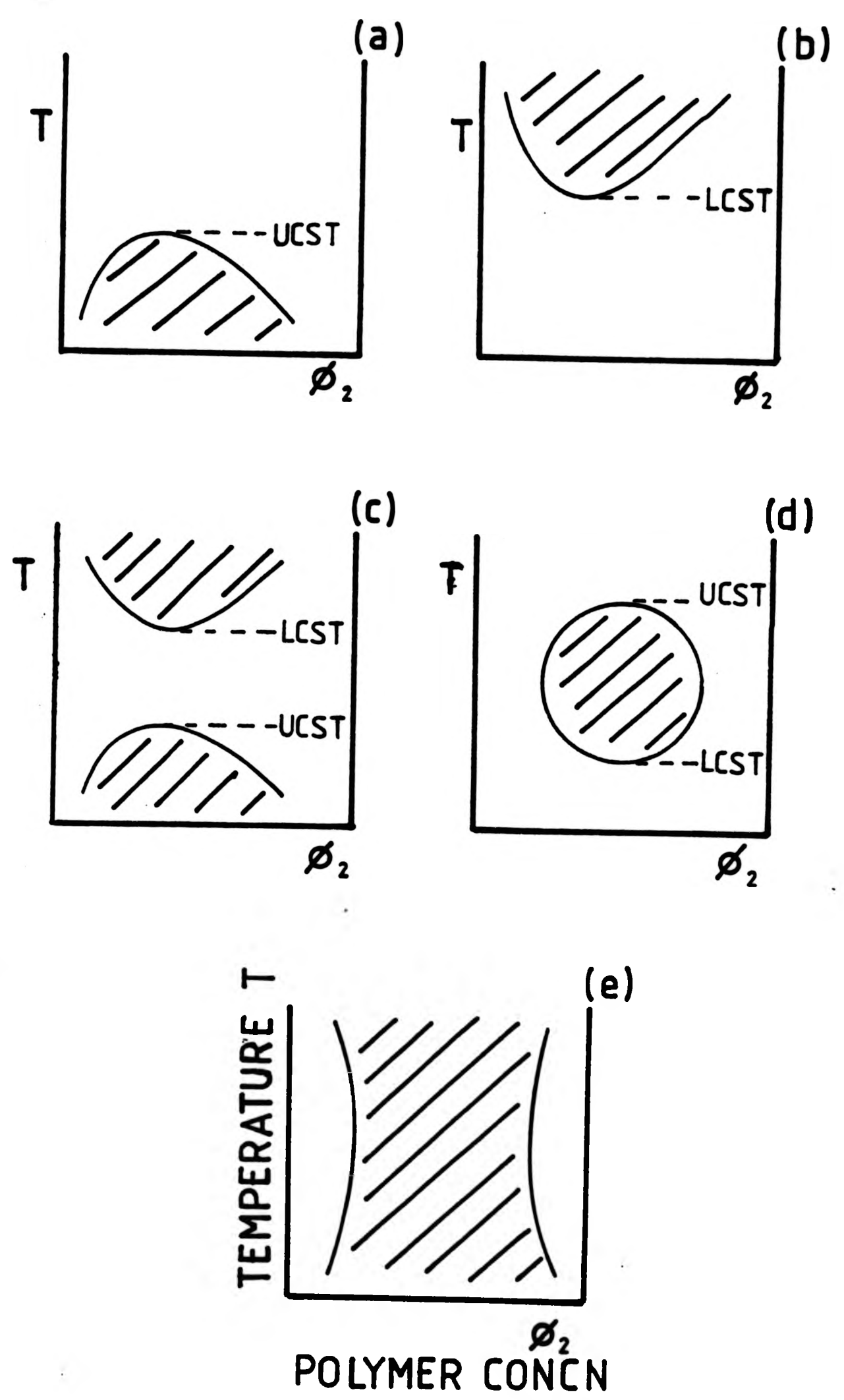
FIG 1.1 : Examples of types of phase equilibria occurring in polymer solutions.

intermolecular forces are high because of crosslinking, crystallinity or strong hydrogen bond interactions, for example. The second stage, the actual 'solution' process, takes place if these forces can be overcome.

UCST behaviour, as shown by diisobutyl ketone solutions of polyisobutylene,[3] was the most commonly observed phenomenon in polymer solution studies until Rowlinson[4] reported that LCST behaviour could be seen in aqueous polyethylene oxide solutions. It was later demonstrated that non-polar polymer/solvent systems underwent phase separation at elevated temperatures, Fig 1.1c, for example cellulose acetate in acetone,[5] and it was shown that this was a general phenomenon for such systems. In general, in polar polymer solutions, LCST behaviour is shown with only a few systems which also exhibit UCST behaviour at higher temperatures[4] (closed-loop type behaviour).

In certain cases, if a poor quality solvent is chosen, the UCST and LCST can be made to approach each other until they coalesce to form an 'hourglass' type diagram, Fig 1.1e, showing limited miscibility across the complete temperature and composition ranges, as seen with poly(ethylene glycol) in tert-butylacetate.[6]

When a binary solution separates into two phases, since these phases must be in equilibrium with each other, the chemical potentials of the components, 1 and 2, in each phase must be equal (generally the polymer is denoted by component 2).

$$\mu_1' = \mu_1'' \qquad\qquad 1.1$$

$$\mu_2' = \mu_2'' \qquad\qquad 1.2$$

(single primes denote the dilute phase and double primes the concentrated

phase). This can only be fulfilled if two points on the curve of the
free energy of mixing, ΔG_m, as a function of composition of one of the
components have a common tangent. As shown in Fig 1.2a there is only
one common tangent to a curve with two minima, A and B. Hence, the
point of contact of this tangent with the curve denotes ϕ_2' and ϕ_2'',
the volume fraction of polymer, for the two phases, at a temperature,
T. The locus of these points as a function of temperature defines the
binodal for the system on a plot of temperature of phase separation
against polymer composition, as shown in Fig 1.2b. These points, ϕ_2'
and ϕ_2'', can be joined by a tie line. At compositions $\phi_2' < \phi_2''$ and
$\phi_2' > \phi_2''$ one phase exists at temperature T.

There are also two points of inflection, C and D, on the curve in
Fig 1.2a. In the region AD and CB the system remains stable with
respect to a phase that differs by a small amount, in composition, from
that at C and D. The system is not stable, however, to the phases with
composition ϕ_2' and ϕ_2''. The locus of these inflection points as a
function of temperature define a spinodal, the limit of metastability, in
Fig 1.2b. Between C and D the system is unstable and separates into two
phases with composition ϕ_2' and ϕ_2'' at either end of the tie line.

A critical point, E, for the system can be defined where the binodal
and spinodal curves touch although not necessarily the maximum of the
curve in Fig 1.2b (or minimum if LCST behaviour is being considered).

1.2 UCST BEHAVIOUR

An expression for ΔG_m can be derived from the lattice theory of
polymer solutions of Flory[7] and Huggins.[8] The theory is based on
the number of different arrangements of n_1 moles of monomer and n_2
moles of x-mer (polymer with x chain 'segments') on a quasi-chemical
lattice assuming no preferential interactions between like and unlike
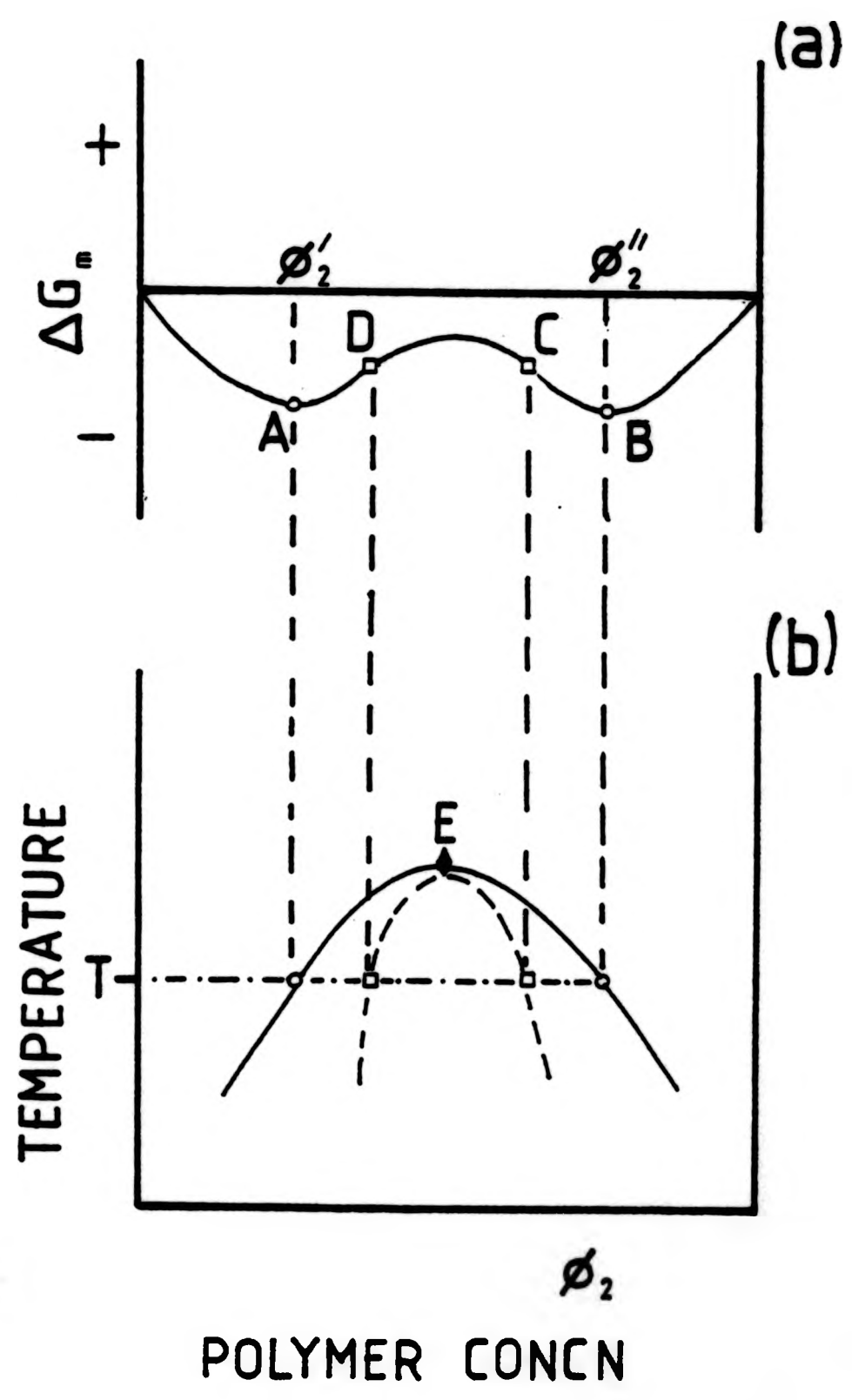
FIG 1.2 : Binodal and spinodal curves defined by the locus of
temperature on the phase diagram and on the corresponding
free energy diagram.

species which would affect the probability of finding a certain molecule or segment of a molecule, in a specific lattice site.   The 'combinatorial' entropy of mixing, ΔS_m,[7] can then be expressed as

$$\Delta Sm = -R[\phi_1 \ln \phi_1 + (\phi_2/x) \ln \phi_2] \qquad\qquad 1.3$$

in which no lattice dependant terms appear.[9-11]

The heat of mixing, ΔH_m, can be given by a Van Laar type expression[12,13] in terms of an energy interaction parameter, X, which is defined by

$$kT\chi = z\Delta w_{12}x_1 \qquad\qquad 1.4$$

where z is the number of nearest neighbours of a polymer segment or a solvent molecule which has x_1 segments instead of one[7] and Δw_{12} is an interchange energy for a pair of contacts as given by

$$\Delta w_{12} = w_{12} - 1/2 (w_{11} + w_{12}) \qquad\qquad 1.5$$

Thus ΔH_m is given by

$$\Delta H_m = RT\chi\phi_1\phi_2 \qquad\qquad 1.6$$

By combining equations 1.3 and 1.6

$$\Delta G_m = RT[\phi_1 \ln \phi_1 + (\phi_2/x) \ln \phi_2 + X\phi_1\phi_2] \qquad\qquad 1.7$$

When differentiated with respect to component 1, the change in chemical

potential, of the solvent, on mixing is obtained.

$$\Delta\mu_1 = RT[\ln(1-\emptyset_2) + (1 - 1/x)\emptyset_2 + \chi\emptyset_2^2] \qquad 1.8$$

Since the corresponding equation for $\Delta\mu_2$ is derived from the same energy expression, $\Delta\mu_1$ can be considered alone.

In a particular polymer-solvent system, where there is total miscibility, $\Delta\mu_1$ decreases monotonically with $\emptyset_2$ but as the solvent becomes poorer eventually a minimum and a maximum will appear, as illustrated in Fig 1.3.[7] When these first occur

$$\left(\frac{\partial\Delta\mu_1}{\partial\emptyset_2}\right)_{T,P} = 0 \qquad 1.9$$

$$\left(\frac{\partial^2\Delta\mu_1}{\partial\emptyset_2^2}\right)_{T,P} = 0 \qquad 1.10$$

By differentiation of equation 1.8 and elimination of χ the critical parameters are

$$\emptyset_{2c} = 1/(1 + x^{\frac{1}{2}}) \qquad 1.11$$

and

$$\chi_c = \frac{(1 + x^{\frac{1}{2}})^2}{2x} \approx \frac{1}{2} + \frac{1}{x^{\frac{1}{2}}} \qquad 1.12$$
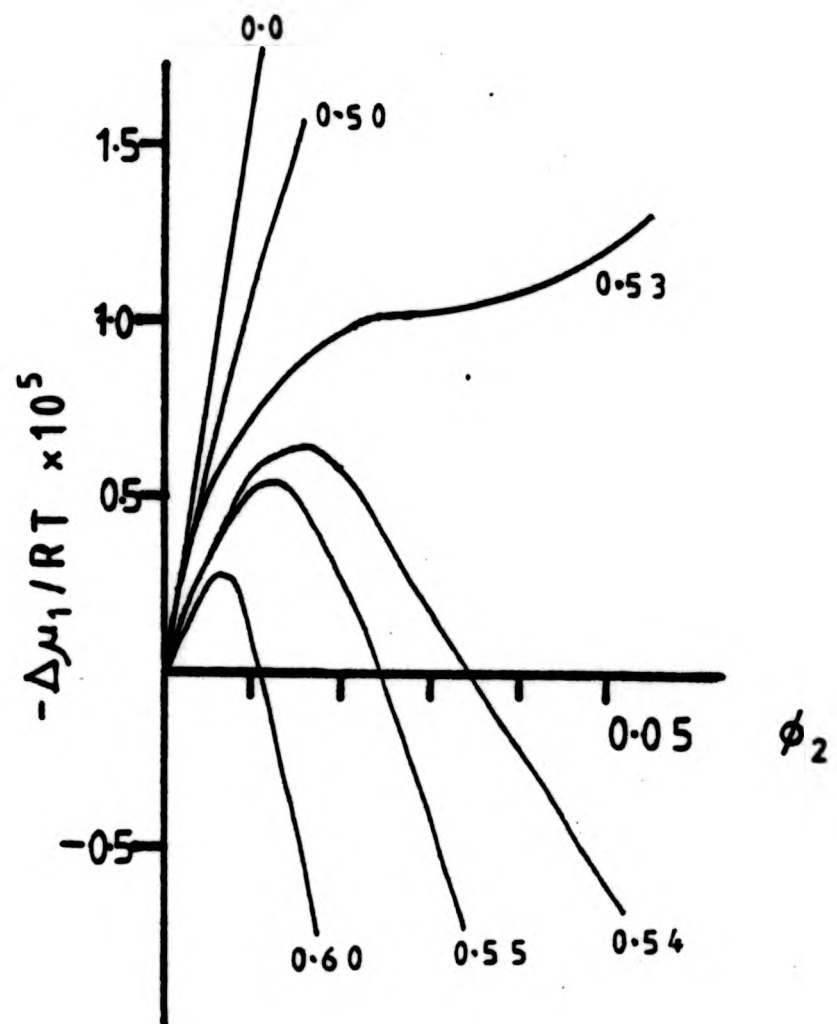
FIG 1.3 : The chemical potential of the solvent in a binary solution
containing a polymer of low concentration (ϕ_2) calculated
for x=1000. (χ values as indicated).

hence χ_c is a small increment larger than 0.5 but approaches it at infinite molecular weight and T_c occurs at lower ϕ_2 for higher molecular weights.

When the Lattice theory is applied to dilute solutions the effect of a non-uniform distribution of polymer concentration throughout the solution has to be taken into account by describing the system in terms of a classical virial expansion of the chemical potential, $\Delta\mu_1$, as a function of ϕ_2.[7,14] Neglecting cubic terms and higher[7]

$$\Delta\mu_1 = -RT(1/2 - \chi)\phi_2^2 \tag{1.13}$$

General enthalpic, κ, and entropic, ψ, parameters derived from the appropriate partial molar quantities

$$\Delta\bar{H}_1 = RT\kappa\,\phi_2^2 \tag{1.14}$$

$$\Delta\bar{S}_1 = R\psi\phi_2^2 \tag{1.15}$$

can be related to χ by

$$\psi - \kappa = 1/2 - \chi \tag{1.16}$$

Using these expressions the variation of T_c with molecular weight, M, can be expressed as

$$\frac{1}{T_c} = \frac{1}{\Theta}(1 - b/M^{\frac{1}{2}}) \tag{1.17}$$

where

$$b = \left(\frac{V_1}{\bar{u}_2}\right)^{\frac{1}{2}} \Big/ \psi \qquad\qquad 1.18$$

and θ is defined by

$$\frac{\theta}{T} = \frac{\kappa}{\psi} \qquad\qquad 1.19$$

(V_1 is the molar volume of the solvent and $\bar{u}_2$ is the partial specific volume of the polymer). This shows that T_c increases in value with increasing molecular weight. From equation 1.17 the parameter θ can be defined as the critical miscibility temperature at infinite molecular weight for a particular polymer-solvent system.

The lattice treatment as applied to dilute solutions can be regarded as a special case of the more general distribution function methods which are termed 'two parameter theories'.[15]

Fig 1.3 shows the variation in χ as a UCST phase separation boundary is approached. As the temperature decreases towards the UCST boundary χ increases through χ_c. When $\chi \geq \chi_c$ there are two values of $\emptyset_2$ with the same $\Delta\mu_1$ and phase separation has occurred.

Using general thermodynamic relationships ΔH_m and ΔS_m can be rearranged to take into account the nearest neighbour interaction contribution from the entropy of mixing of the system.

$$\Delta H_m = -RT^2\left(\frac{\partial \chi}{\partial T}\right)\emptyset_1\emptyset_2 \qquad\qquad 1.20$$

$$\Delta S_m = -R\{\emptyset_1\ln\emptyset_1 + (\emptyset_2/x)\ln\emptyset_2 + \left[\frac{\partial(\chi T)}{\partial T}\right]\emptyset_1\emptyset_2\} \qquad\qquad 1.21$$

χ must now be considered as a parameter with both enthalpic, χ_h, and entropic, χ_s, contributions

$$\chi = \chi_h + \chi_s \qquad 1.22$$

and the variation with temperature can be written in the general form

$$\chi = a + b/T \qquad 1.23$$

where a and b can roughly be identified with the entropic and enthalpic contributions to χ respectively.[16,17] When the system is strongly concentration dependent, χ can be expanded in a power series, when $\emptyset_2$ is small, for both enthalpic and entropic terms[18,19] and χ_i terms are treated as empirical parameters.

$$\chi = \chi_o + \chi_1 \emptyset_2 + \chi_2 \emptyset_2^2 + \cdots \qquad 1.24$$

The entropy term χ_s can also be expanded to include terms which allow for the imperfect randomness in the solution.[20] In polar systems χ could be regarded as a parameter which includes both non-polar and polar contributions.[21]

$$\chi = \chi_{non-polar} + \chi_{polar} = \chi_{np} + \chi_p \qquad 1.25$$

1.3 LCST BEHAVIOUR

The analysis using the Flory-Huggins theory can describe UCST behaviour but as the temperature increases the solvent quality is predicted to increase without limit, hence LCST behaviour cannot be

described. A theory of corresponding states[22,23] or an equation of state theory[24] can be used to describe both UCST and LCST behaviour. Initially, corresponding states theory used a combination of a quasi-crystalline lattice and a flexible cell model but later used an average potential solution theory, independent of lattice, using a smoothed potential cell model to introduce the number of degrees of freedom of a molecule into the partition function for the system.[25] Equation of state theory has a Van der Waals form of the intersegmental energy.[24] Both theories take into account the change of volume on mixing by introducing a 'free-volume' term into various energy expressions. This results in an expression for the heat of mixing, in corresponding state theory,[22,26] of

$$\frac{\Delta H_m}{(x_1 N_1 + x_2 N_2)\phi_1\phi_2/N} = A - B\left(\frac{T}{x_1}\right)^2 \qquad 1.26$$

where $N = N_1 + N_2$ the number of molecules in the solution of components with x_1 and x_2 chain 'segments' with $x_2 \gg x_1 > 1$

$$A = z\Delta w_{12} N_A \qquad 1.27$$

$$B = \frac{10.5k^2}{z\epsilon^*} N_A \qquad 1.28$$

Δw_{12} is the interchange energy defined in terms of the minimum potential well between interacting segments, $-\epsilon^*$,

$$\Delta w_{12} = -\epsilon_{12}^* + 1/2(\epsilon_{11}^* + \epsilon_{22}^*) \qquad 1.29$$

and assuming that $\epsilon_{11}^* = \epsilon_{22}^* = \epsilon^*$.

The entropy of mixing can also be divided up into a Flory-Huggins combinatorial term and a non-combinatorial term which takes into account the change in volume on mixing.[22,26]

$$\frac{T\Delta S_{non-comb}}{(x_1 N_1 + x_2 N_2)\phi_1\phi_2/N} = -2B\left(\frac{T}{x_1}\right)^2 \qquad 1.30$$

The χ parameter, now arises not only from ΔH_m but also from $T\Delta S_{non-comb}$ ($\Delta H_m' = \Delta H_m - T\Delta S_{non-comb}$) hence for $x_2 = \infty$ and $x_1 > 1$

$$\frac{\Delta H_m'}{(x_1 N_1 + x_2 N_2)/N} = A + B\left(\frac{T}{x_1}\right)^2 = RT\chi\phi_1\phi_2 \qquad 1.31$$

which by analogy gives

$$R\chi = \frac{A}{(T/x_1)} + B\left(\frac{T}{x_1}\right) \qquad 1.32$$

This predicts that χ has a minimum in both x_1 and T therefore both UCST and LCST behaviour can be described, as shown in Fig 1.4. Above and below a temperature, T_o, the solvent quality gets poorer

$$T_o^2 = (A/B)x_1^2 \qquad 1.33$$

assuming $\chi_c = 0.5$, from equation 1.32.

$$\frac{T_c}{x_1} = \frac{R/2 \pm [(R/2)^2 - 4AB]^{\frac{1}{2}}}{2B} \qquad 1.34$$

If $4AB < (R/2)^2$ two real roots can be found corresponding to the UCST and LCST boundaries, as in curve (a) in Fig 1.4. If $4AB > (R/2)^2$ then
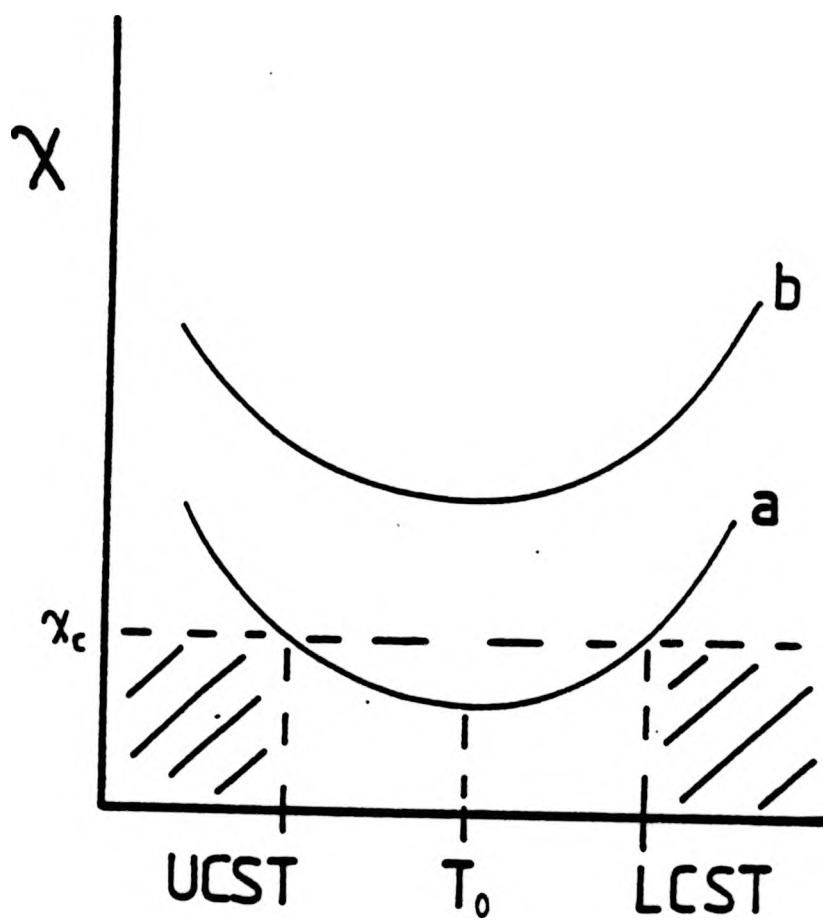
FIG 1.4 : Variation of the interaction parameter χ showing two regions
of immiscibility and two critical solution temperatures
(curve a). Curve b shows the case of a polymer never
miscible in all proportions with the solvent.

there are no real roots and the polymer is immiscible in the solvent, ie χ is never less than 0.5, as in curve (b) in Fig 1.4. Polar polymer solutions exhibit LCST but no UCST behaviour has as yet been detected, at low temperatures. A single LCST boundary can be predicted if A=0. The roots of the equation are then R/2B and zero. From the definitions of A and B, in equations 1.27 and 1.28, it can be seen that as the molecular weight increases (x_2 increases) A increases and B decreases in value. This indicates from equation 1.33, that T_o increases in temperature and from equation 1.32 that the curve of χ against T flattens out (ie the quadratic term gets smaller). Applying this to Fig 1.4, it can be seen that as the molecular weight of the polymer increases the curve goes from (a) to (b). The value of T_c at the UCST boundary, therefore, increases whereas at the LCST boundary, T_c decreases with increasing molecular weight. This is a similar situation to the 'lattice theory for ϕ_{2c} as a function of molecular weight. For both UCST and LCST behaviour ϕ_{2c} decreases as the molecular weight increases.

If the combinatorial and free volume terms, incorporated in the χ parameter, are plotted separately as a function of temperature, as seen in Fig 1.5, the increasing importance of the free volume term can be seen at higher temperatures.[27,28]

Essentially, the equation of state theory gives the same results as the corresponding states theory[23] although an exchange interaction parameter, X_{12}, with units of energy/volume which is analogous to Δw_{12}, is used instead of χ. They can be related to each other[29] although the resultant definition of χ differs from that of lattice theory in two respects. Segment fractions are used instead of volume fractions and the 'hard core' volume ratio replaces the ratio of molar volumes. The parameter X_{12} is independent of temperature and
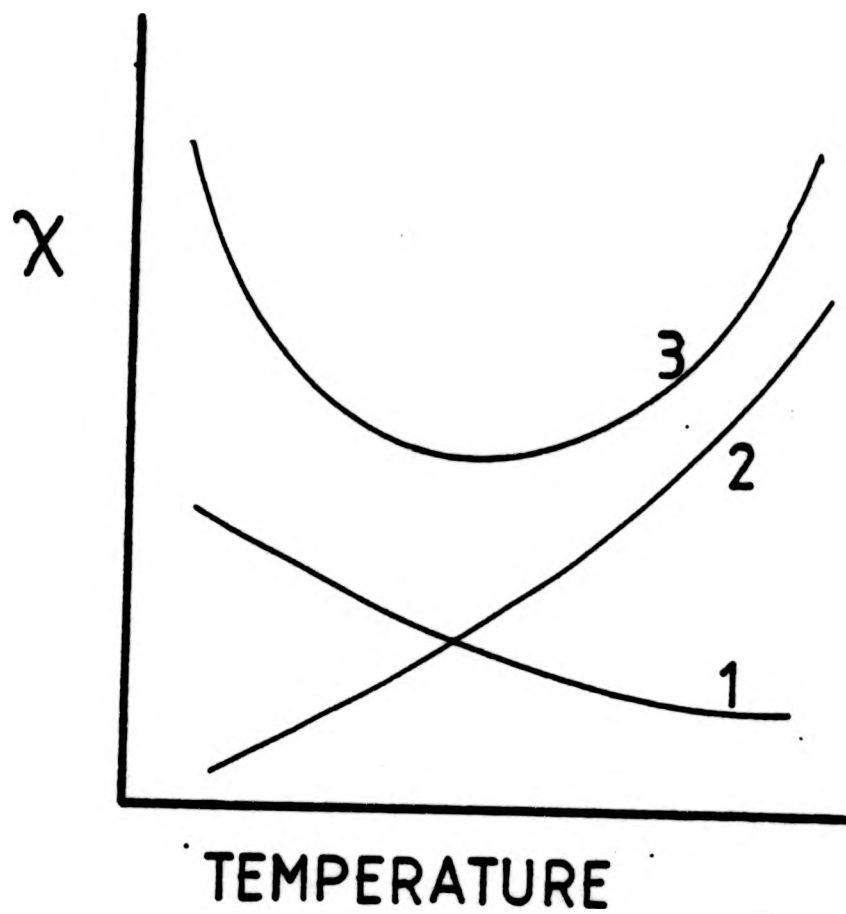
FIG.1.5 : Temperature dependence of the interaction parameter χ.
Curve 3 total , curve 2 contribution due to free volume
dissimilarity between polymer and solvent, curve 1 contribution
due to contact energy dissimilarity between polymer and
solvent.

composition being only a function of the polymer-solvent pair.[24]   If X_{12} is treated as an 'energy density' and not a 'free energy density' another parameter, Q_{12}, is introduced as an entropy interaction parameter[30] which can improve agreement between theory and experiment but should be regarded as an empirical parameter.[24]

No model yet results in a satisfactory expression for the energy functions which apply over the entire range of concentration, although a treatment involving a semi-empirical, poisson weighted linear combination of terms has been proposed.[31]

A model analogous to the scaling law theory of ferromagnetism has been applied to polymer solutions[32] although conclusions in connection with the molecular weight dependence of cloud-point curves[33] have since been refuted.[34]

The above theories can be applied to multicomponents systems. Quasi-binary systems are treated by taking into account the appropriate molecular weight distribution of the polymer.[35,36]   Ternary systems (polymer 1-polymer 2-solvent and polymer-solvent 1-solvent 2) can be treated by regarding X parameters as 'pair interaction parameters', X_{ij}.

A number of theories have been applied to polymer blends and mixtures.[37-44]   Although the complexities of the behaviour of these systems cannot be totally accounted for,[45] it is clear that LCST behaviour, which again cannot be explained by lattice theory,[38,39] is caused primarily not by free volume, but by interaction effects.   This is similar to the situation in polar polymer solutions which only exhibit LCST behaviour.[28]

This study investigates solutions of poly(acrylic acid) in 1,4-dioxane, and related systems, which exhibit three phase separation boundaries after the manner illustrated in Fig 1.6.   On heating a
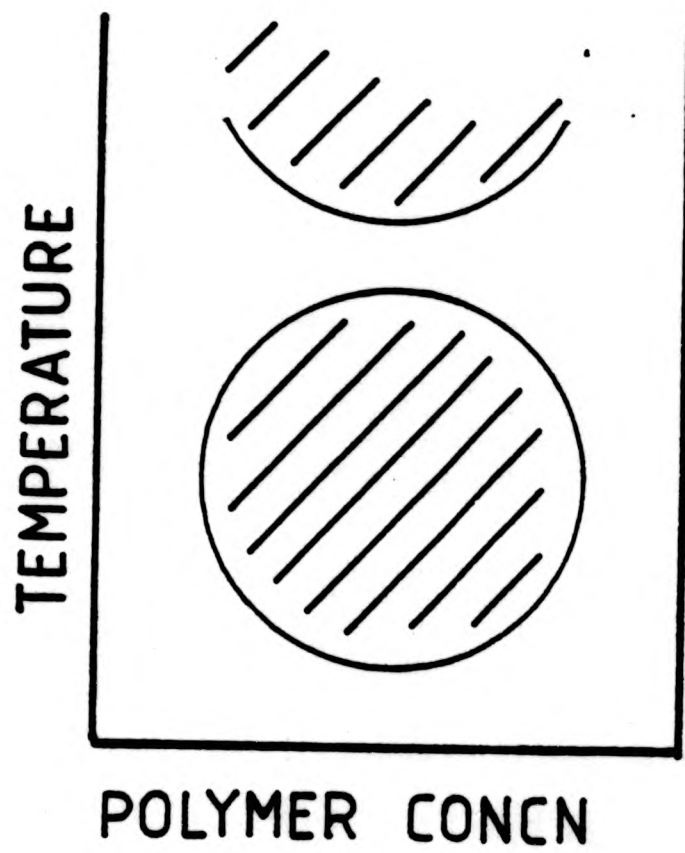
FIG 1.6 : Multipule phase equilibria in a polymer solution showing
a closed-loop type region of immiscibility with another
region of immiscibility at higher temperatures.

homogeneous solution from room temperature the system passes through an LCST boundary into a two phase region. The system then passes through a UCST boundary, at higher temperatures, and once more becomes a one phase system. As the temperature is increased further another LCST boundary is encountered. At this stage the low temperature LCST boundary will be designated as a psuedo-lower critical solution boundary, p-LCST, to distinguish it from the higher temperature LCST boundary, LCST.

1.4 PHASE SEPARATION BEHAVIOUR OF POLY(ACRYLIC ACID)

Lower critical solution behaviour has been reported for the system of poly(acrylic acid) in 1,4-dioxane[45-48] with the θ-temperature determined as 303K.[45,46] This behaviour has been utilised in the fractionation of poly(acrylic acid) using dioxane/water mixtures[49] where the molecular weights of the fractions were found to decrease with increasing precipitation temperature with both dioxane and dioxane/2% water mixtures. It has also been shown that, for a polyacid of molecular weight $5x10^5$ g/mol, the temperature of phase separation increases by 50K upon the addition of 4% water to dioxane[47] using 0.1% polymer solutions.

Similar behaviour has been found in dioxane solutions when small amounts of methanol were added[50] and also under certain conditions in ethanol/water mixtures which has also been used for fractionation.[51]

For the sodium salt of poly(acrylic acid) studies have been carried out either to determine the effect of salt concentration on phase separation at a single temperature, or the phase separation behaviour at one or two salt concentrations or degrees of neutralisation.[46,52] These measurements have been made not only for sodium polyacrylate-sodium chloride but also for unionised poly(acrylic acid)-sodium chloride

systems both of which exhibit the more normal upper critical solution behaviour.   If sodium chloride is replaced by sodium iodide in the sodium polyacrylate system, a more complicated three boundary system has been observed.[53]

In the sodium polyacrylate system, for a fixed sodium chloride concentration the phase separation temperature increases with molecular weight.   Alternatively, for the unionised polyacid, the phase separation temperature, for a polymer concentration <1% has been found to increase by as much as 100K (270-370K) for a sodium chloride concentration range of 0.4-3M.   The polyacid samples had molecular weights of between 10^4-10^6 g/mol with the higher molecular weights giving the greater temperature increase.[54]   Results from the various studies are in good agreement.

Although the phase separation temperatures are proportional to $M^{-\frac{1}{2}}$, the critical points do not coincide with the maximum in the cloud-point curves.   The salt system acts as a simple ternary system and not a quasi-binary one.   The difference in behaviour at different degrees of neutralisation may be due to there being two forms of the polymer, an acid form and a salt form.[54]   It is also possible that intermediate behaviour is due to the formation of incompletely dissociated salts unless the ionised groups are well-separated along the polymer chain and the ions are electrostatically held within the coiled parts of the chains.[55,56]

When hydrochloric acid (0.2M) is used in aqueous systems[57] similar trends, as before, are observed, with the phase separation temperature increasing with salt concentration for the addition of both sodium and lithium chlorides.[57]   Similar trends have also been observed for bivalent chloride salts (eg $MgCl_2$, $CaCl_2$, $BaCl_2$) in both water and

hydrochloric acid (0.01M)[8] as well as aqueous copper sulphate.[46]

Both lower or upper critical solution behaviour have also been observed for the aqueous polyacid system with a variety of 'cationic drugs'[53] (ie hydrochlorides of organic bases).

Aqueous solutions with a second polymer have been studied, notably with poly(ethylene glycol) (see chapter 10).   Systems with polyvinylpyrrolidone[59] and polyacrylamides,[60] have been studied and in both cases lower critical solution behaviour was observed.   The system with aqueous gelatin has been reported[61] and exhibits two regions of immiscibility whilst aqueous solutions with dextran produces a miscible system if the pH is less than 6.[62]

REFERENCES

1. G M Barrow, 'Physical Chemistry' 4th ed, McGraw-Hill, New York, (1979).

2. R T Fowler, J.Soc.Chem.Ind.,Lond. **69**, 565, (1950).

3. A R Schultz, P J Flory, J.Am.Chem.Soc. **74**, 4760, (1952).

4. G N Malcolm, J S Rowlinson, Trans.Faraday Soc. **53**, 921, (1957).

5. H Suzuki, K Kamide, M Saito, Eur.Polym.J. **18**, 123, (1982).

6. S Saeki, N Kuwahara, M Nakata, M Kaneko, Polymer **17**, 685, (1976).

7. P J Flory, 'Principles of Polymer Chemistry', Cornell Univ. Press, Ithaca, New York, (1953).

8. M L Huggins, 'Physical Chemistry of High Polymers', Wiley, New York,, (1958).

9. J H Hildebrand, J.Chem.Phys. **15**, 225, (1947).

10. H C Longuet-Higgins, Disc Faraday Soc. **15**, 73, (1953).

11. M L Huggins, J.Am.Chem.Soc. **52**, 248, (1949).

12. E A Guggenheim, Proc.Roy.Soc. **A183**, 203, (1944).

13. W J C Orr, Trans. Faraday Soc. **40**, 320, (1944).

14. P J Flory, J.Chem.Phys. **12**, 453, (1945).

15. W H Stockmayer, Makromol.Chem. **35**, 54, (1960).

16. M L Huggins, J.Am.Chem.Soc. **86**, 3535, (1964).

17. P J Flory, J.Am.Chem.Soc. **87**, 1833, (1965).

18. H Tompa, 'Polymer Solutions', Butterworth Scientific Publ London, (1956).

19. T A Orofino, P J Flory, J.Chem.Phys. **26**, 1067, (1957).

20. M L Huggins, J.Phys.Chem. **75**, 1255, (1971).

21. H Yamakawa, S A Rice, R Corneliussen, L Kotin, J.Chem.Phys. **38**, 1759, (1963).

22. I Prigogine (with A Bellemans, V Mathot), 'Molecular Theory of Solutions', North Holland Pub. Co., Amsterdam, (1957).

23. D D Patterson, Rubber Chem.Technol. $\underline{40}$, 1, (1967).

24. P J Flory, Disc Faraday Soc. $\underline{49}$, 7, (1970).

25. A Bellemans, C Naar-Colin, J.Polym.Sci. $\underline{15}$, 121, (1955).

26. G Delmas, D D Patterson, Official Digest (Federation Soc. Paint Technol.) $\underline{34}$, 677, (1962).

27. D D Patterson, Macromolecules $\underline{2}$, 672, (1969).

28. D Patterson, A Robard, Macromolecules $\underline{11}$, 690, (1978).

29. R A Orwoll, Rubber Chem.Technol. $\underline{50}$, 451, (1977).

30. B E Eichinger, P J Flory, Trans. Faraday Soc. $\underline{64}$, 2035, (1968).

31. R Koningsveld, W H Stockmayer, J W Kennedy, L A Kleintjens, Macromolecules $\underline{7}$, 73, (1974).

32. D S McKenzie, Phys. Reports $\underline{27}$, 35, (1976).

33. J F Cotton, M Nierlich, F Bove, M Daovo, B Farnoux, G Jannink, R Duplessix, C Picot, J.Chem.Phys. $\underline{65}$, 1101, (1976).

34. G Aharoni, Macromolecules $\underline{10}$, 1408, (1977).

35. R L Scott, J.Chem.Phys. $\underline{13}$, 178, (1945).

36. W H Stockmayer, J.Chem.Phys. $\underline{17}$, 588, (1949).

37. R L Scott, J.Chem.Phys. $\underline{17}$, 279, (1949).

38. H Tompa, Trans. Faraday Soc. $\underline{45}$, 1142, (1949).

39. I C Sanchez in 'Polymer Blends' Vol. 1, Ed D R Paul, S Newman, Academic Press, New York, (1978).

40. I C Sanchez, R H Lacombe, J.Phys.Chem. $\underline{80}$, 2352, (1976).

41. R H Lacombe, I C Sanchez, J.Phys.Chem. $\underline{80}$, 2568, (1976).

42. R Simha, T Somcynsky, Macromolecules $\underline{2}$, 342, (1969).

43. T Somcynsky, R Simha, J.Appl.Phys. $\underline{42}$, 4545, (1971).

44. S Krause in 'Polymer Blends' Vol 1, Ed D R Paul, S Newman, Academic Press, New York, (1978).

45. P J Flory, W R Krigbaum, W B Schultz, J.Chem.Phys. $\underline{21}$, 164, (1963).

46. P J Flory, J E Osterheld, J.Phys.Chem. _58_, 683, (1954).

47. M L Miller, K O'Donnell, J Skogman, J.Colloid.Sci. _17_, 649, (1962).

48. C Cuniberti, V Bianchi, Polymer _15_, 346, (1974).

49. J Lleras, F Abouande, S Combet, C R Acad.Sci.Ser C. _278_, 689, (1974).

50. N A Kuznetsov, Z A Roganova, A L Smolyanskii, Vysokomol.Soedin.Ser C _20_, 791, (1978).

51. J Eliassaf, J.Appl.Polym.Sci. _7_, 59-510, (1963).

52. A Ikegami, N Imai, J.Polym.Sci. _56_, 133, (1962).

53. I Kagawa, R M Fuoss, J.Polym.Sci. _18_, 535, (1955).

54. R Buscall, T Corner, Eur.Polym.J. _18_, 967, (1982).

55. J Bourdais, J.Chim.Phys. _56_, 194, (1959).

56. F T Wall, W B Hill, J.Am.Chem.Soc. _82_, 6599, (1969).

57. J Eliassaf, A Silberberg, J.Polym.Sci. _41_, 33, (1959).

58. N Tanaka, G Hirata, I Utsumi, Chem.Pharm.Bull (Tokyo) _14_, 414, (1966).

59. J Néel, B Sebille, C R Acad.Sci. _250_, 1052, (1960).

60. O V Klenina, E G Fain, Vysokomol.Soedin.Ser A _23_, 1298, (1981).

61. G N Kormanovskaya, V M Zhartovskii, M A Al'Tshuler, V F Abrosenkova, L M Novichkova, V S Zhurina, I Ya Shelomkova, I N Vlodavets, Kolloid Zh _38_, 365, (1976).

62. R J Hefford, Polymer _25_, 979, (1984).

CHAPTER TWO

EXPERIMENTAL TECHNIQUES

2.1 DETERMINATION OF PHASE SEPARATION TEMPERATURES

Although in this study phase separation temperatures were determined
visually, a variety of other techniques have been used including
turbidimetry,[1] viscosity,[2] differential scanning calorimetry
(dsc),[3] nmr[4] and pulse induced critical scattering (PICS).[5]

The polymer solutions were prepared, in situ, in glass tubes of 3mm
internal diameter, at various polymer concentrations $(g/100cm^3)$, based
on $0.3\ cm^3$ solvent.   The polymer was introduced into the tubes in the
form of thin film strips that had been cast from an appropriate
solvent.   The tubes were then flame sealed under vacuum and after total
dissolution of the polymer the phase separation temperatures of the
solutions were determined.

A water bath was used for temperatures up to 353K and a silicone oil
bath for higher temperatures up to approximately 500K, the tubes being
heated at variable rates (0.5-2 K/min).

In all phase separation diagrams LCST phase separation boundaries
are shown by open circles (o), and UCST phase separation boundaries are
indicated by closed circles, (●).   The two phase regions are denoted by
the shaded regions.

2.2 PHASE VOLUME RATIO METHOD

A 'phase volume ratio' method[6,7] was used to determine the
critical polymer concentration, c_c, on the pseudo-LCST phase separation
boundary, which is the lower of the two LCSTs observed, for poly(acrylic
acid)s PAA50, PAA90, PAA150 and PAA300 in dioxane.   Several series of
tubes, prepared as for the phase separation studies, were immersed in a
thermostatted water bath ($\pm$0.02K) at several temperatures, T/K, above
that of the appropriate phase separation temperature, T_p/K.   After

allowing the two phases to separate completely (1-2 hrs) the relative heights of the dilute, 1_d, to the concentrated, 1_c, phases were measured (the cross-sectional areas of the tubes were assumed to be constant) and the value $r = 1_d/1_c$ was plotted against the temperature difference $T-T_p$. At the critical concentration, when $T-T_p=0$, $r=1$. For concentrations above and below the critical concentration, the value of r tends to infinity and zero respectively, as $T-T_p$ tends to zero.

2.3.1 MICROCALORIMETRY

The microcalorimeter used was an LKB 10700-2 Batch Calorimeter System based on a design by Wadsö.[8] In this heat conduction (heat leakage) type microcalorimeter, the integral heat change, Q, is measured indirectly from a change in temperature, ΔT (measured as a voltage difference between thermopiles), during heat exchange with a heat sink. This process can be described by

$$Q = E\Delta T \qquad\qquad 2.1$$

$$\text{or} \quad Q = \varepsilon\int\emptyset dt \qquad\qquad 2.2$$

$$\text{or} \quad Q = \varepsilon A \qquad\qquad 2.3$$

where E and ε are calibration constants. Q is measured as the area under the curve of the variation of some measured quantity, $\emptyset$, with time, t (in area A). ε is calculated by determining the area under the curve when a known amount of electrical heat (I^2Rt heat) is supplied to the system.

The apparatus, shown in Fig 2.1, consisted of an aluminium calorimeter unit (A) placed horizontally in an air thermostatt unit (E) equipped with a motor to rotate the calorimeter unit about its long
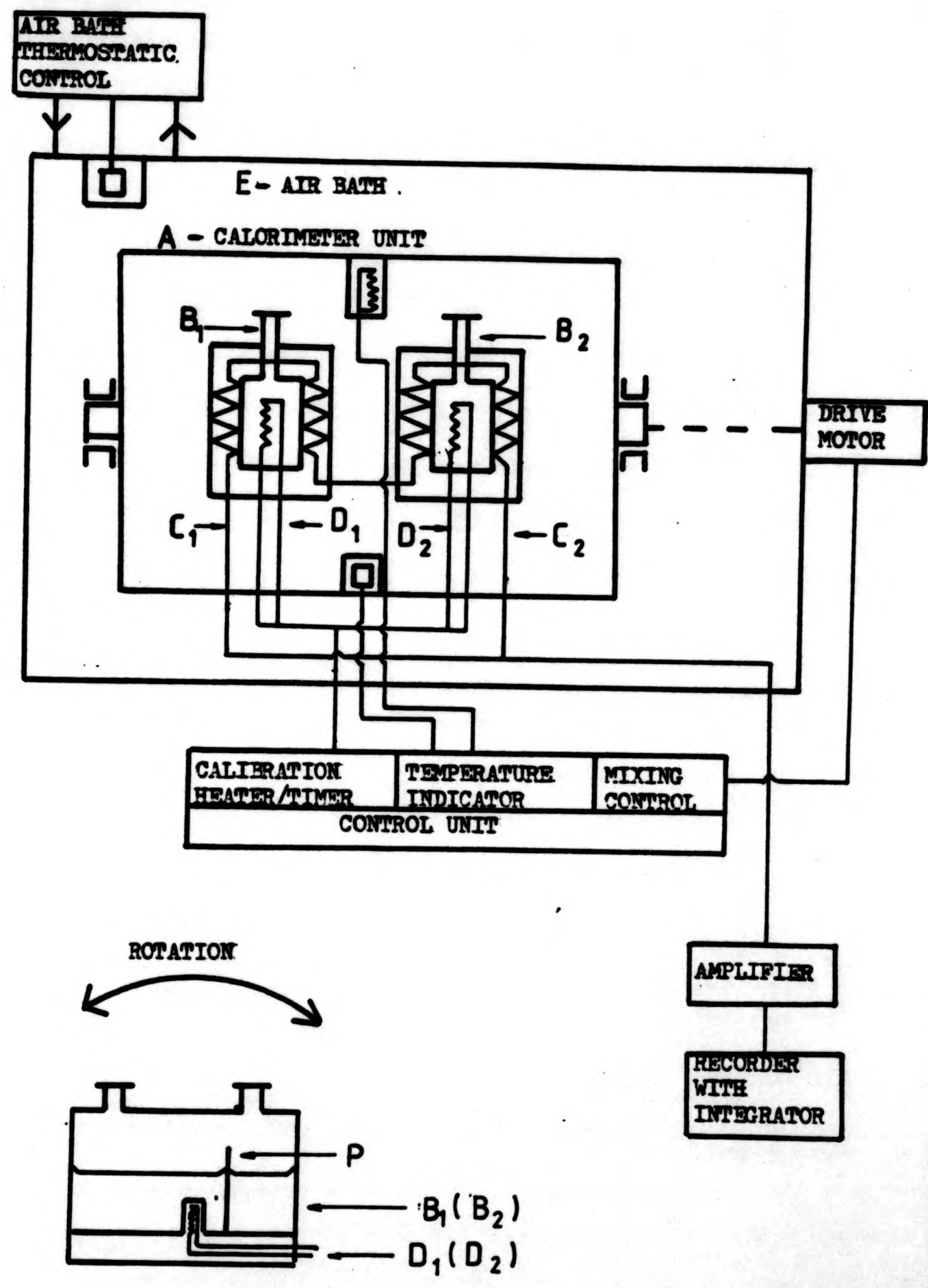
FIG.2.1 : Schematic diagram of microcalorimeter.

horizontal axis during mixing (the mixing time was 50s for 2.5 rotations). The pair of reaction cells (B_1, B_2) within the calorimeter unit were made of 18-carat gold, each cell being divided into two interconnected compartments of differing sizes (2 cm^3 and 4 cm^3) by a partition wall (P). One cell was used as the reaction cell whilst the other was used as a reference cell; thus for heats of dilution measurements, the reference cell was used with solvent in both compartments; the reaction cell had solution in one compartment, and the same, diluting, solvent in the other, in the same relative quantities.

The heat due to the mixing of the different liquids or solutions was detected by the temperature difference between a pair of thermopiles (C_1, C_2) (one in each cell). This difference, registered as a voltage difference, was amplified (Keithley Instruments model 150B) before being recorded as the deflection on a 100mV range recorder equipped with a ball and disc type integrator (Philips PM8000). The area under the curve was determined by counting deflections of the integrator pen.*

The environmental temperature was controlled by an external water heater unit, kept at approximately 10K below the operating temperature. A separate control unit was used to regulate the calibration heaters (D_1, D_2) and timer. An example of the analytical method is given in Fig. 2.2 for the heat of dilution of sample PAA50 in a dioxane/water mixture containing 5.06(wt/vol)% water, at 312K. In this case, the areas give the amount of heat in an exothermic sense.

---

* In most cases here, the area was measured using a precision planimeter.

The area under the curve, A_T, Fig. 2.2a, swept out during the experiment was measured by planimeter as 0.171 units. After each experiment, when a horizontal base line is obtained, the mixing process is repeated again to determine the effect due to the mechanical rotation of the calorimeter unit, A_F, Fig. 2.2a. If during the experiment the mixing process was repeated n times then the area due to the reaction, A_R, is given by

$$A_R = A_T - nA_F$$

In the example $A_R = -0.171 - 2(0) = -0.171$.

The calibration constant ϵ can be determined by measuring the area, A_c, when a known amount of electrical heat, $Q = I^2Rt$, is introduced into the system, from

$$\epsilon = Q/A_c$$

In this case, $I = 16mA$, $t = 2s$ and $R = 50.055\Omega$ which gives $Q = -0.026J$. A_c was measured as -0.230 units, Fig. 2.2b, hence $\epsilon = -0.026/0.230 = 0.113$.

The heat of dilution, ΔH_d, is then given by
$$\Delta H_d = (0.113)(-0.171)$$
$$= -1.93 \times 10^{-2}J$$

2.3.2   CALCULATION OF HEAT OF DILUTION

The heat of dilution, ΔH_d, is related to the final volume fraction, ϕ_2, of solute in a solution, when Δn moles of solvent are
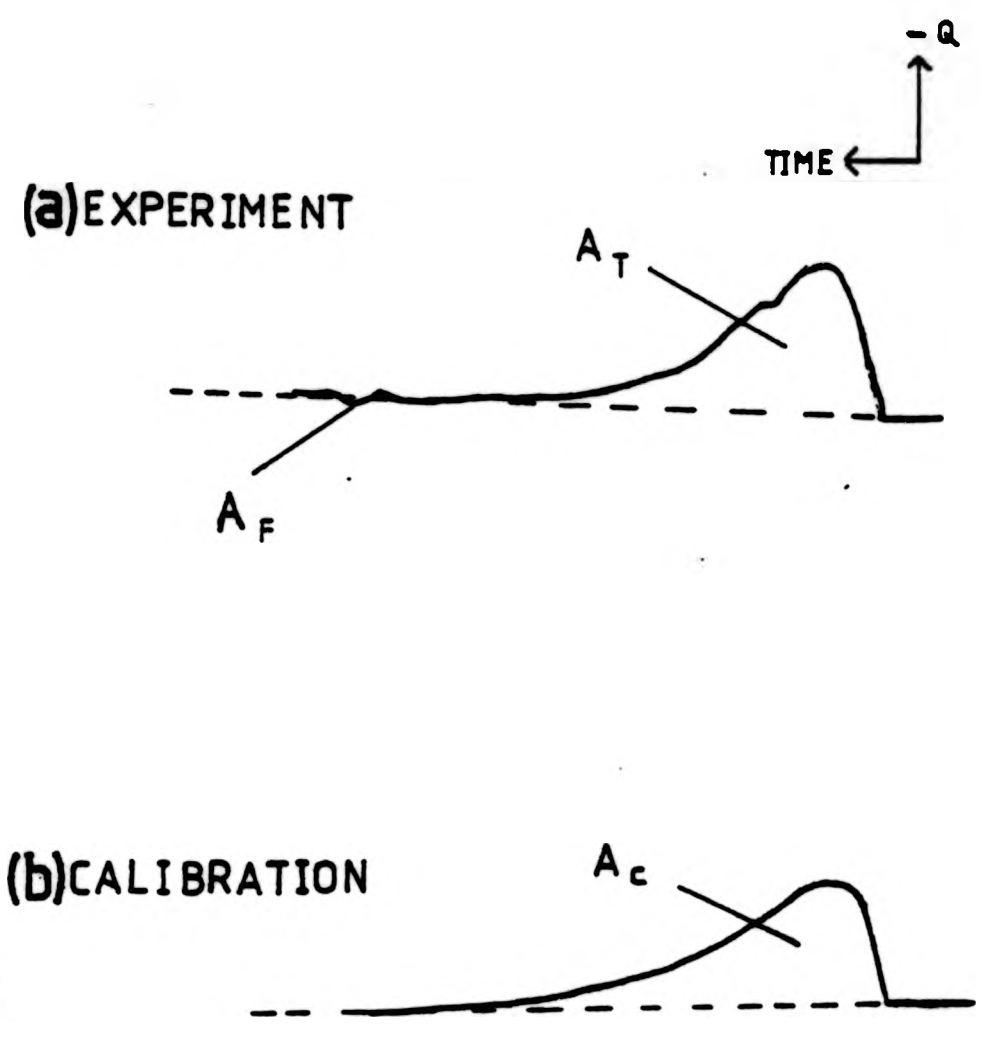
FIG 2.2 : Microcalorimeter example.

(a) ΔH_d for PAA50 in dioxane/5·06(wt/vol)%water at 312 K,

(b) calibration – 16mA for 2s (R=50·055Ω) at 312 K.

added to a solution of initial solute volume fraction, $\emptyset_1$, at a temperature, T/K, by[9]

$$\Delta H_d = RT \, X_h \emptyset_1, \emptyset_2 \, \Delta n \qquad\qquad 2.4$$

where R is the gas constant, and

$$X_h = X_1 + X_2 \emptyset + X_3 \emptyset^2 + \ldots \qquad\qquad 2.5$$

which, alternatively, by neglecting third and higher powers, can be expressed as

$$X_h = X_1 + X_2 (\emptyset_1 + \emptyset_2)/2 \qquad\qquad 2.6$$

The concentration independent parameter, X_1, is equivalent to the κ parameter in dilute theory.[9]

2.3.3 CALCULATION OF HEAT OF MIXING

The heat of mixing, ΔH_m, of two liquids can be directly measured, in terms of the total number of moles of substance, as a function of the mole fraction of one of the components. The total number of moles of liquid is kept constant for each determination.

2.4 SOLUTION VISCOSITY

The measurements of solution viscosity were carried out, using an Ubbelohde viscometer and were timed with a stopwatch measuring to $\pm 0.25s$. The viscometer was immersed in a thermostatically controlled water bath ($\pm 0.02K$). Solutions with concentration of about $1g/100cm^3$

were used initially. Dilution of this solution (5 cm^3) was with successive additions of 2 cm^3, 2 cm^3, 3 cm^3 and 4 cm^3 of solvent. The flowtime for the solvents were greater than 100s and no kinetic energy correction was used. The flowtimes were found by repeated determination until consistent times were recorded. All the solutions, and solvent, were filtered through No 2 glass sinters before use.

The values of intrinsic viscosity, $[\eta]$, were determined from plots of specific viscosity/concentration, η_{sp}/c, against concentration, c (g/100 cm^3), where $[\eta]$ can be defined by

$$\eta_{sp}/c = [\eta] + k'[\eta]^2 c \qquad\qquad 2.7$$

and

$$\eta_{sp} = (t-t_o)/t_o \qquad\qquad 2.8$$

t_o is the flowtime of the pure solvent and t is the flowtime of a solution of concentration c. An alternative analysis to determine $[\eta]$ is through equation 2.9.

$$(\log \eta_r)/c = [\eta] + k''[\eta]^2 c \qquad\qquad 2.9$$

where

$$\eta_r = t/t_o \qquad\qquad 2.10$$

Here, the constant k" is different to k' in equation 2.7. A typical

analysis is shown in Fig. 2.3 for poly(acrylic acid), PAA50, in dioxane at 298, 303, 308 and 313K. [η] is given by the intercept on the η_{sp}/c axis.

Several relationships between [η] of a linear polymer and its molecular weight, M, have been proposed.[10] The most widely used is the Mark-Houwink relationship[11,12]

$$[\eta] = KM^a \qquad\qquad 2.11$$

The Stockmayer-Fixman relationship[13], can also be used to give a measure of the short and long range interactions in the system as given by the values of K_θ and K' respectively in equation 2.12.

$$[\eta]/M^{\frac{1}{2}} = K_\theta + K'M^{\frac{1}{2}} \qquad\qquad 2.12$$

where originally

$$K' = 0.51\,\Phi\,B \qquad\qquad 2.13$$

Φ is a constant and B is related to the χ parameter for the solution through[14] $B = \bar{u}^2(1-2\chi)/V_1N_A$. This equation can be modified to take into account the coil expansion factor, α_η[14]

$$[\eta]/M^{\frac{1}{2}} = K_\theta + 0.346\,\Phi BM^{\frac{1}{2}} \text{ for } 0<\alpha_\eta^3<1.6 \qquad\qquad 2.14$$

or

$$[\eta]/M^{\frac{1}{2}} = 1.05K_\theta + 0.287\,\Phi BM^{\frac{1}{2}} \text{ for } 0<\alpha_\eta^3<2.5 \qquad\qquad 2.15$$

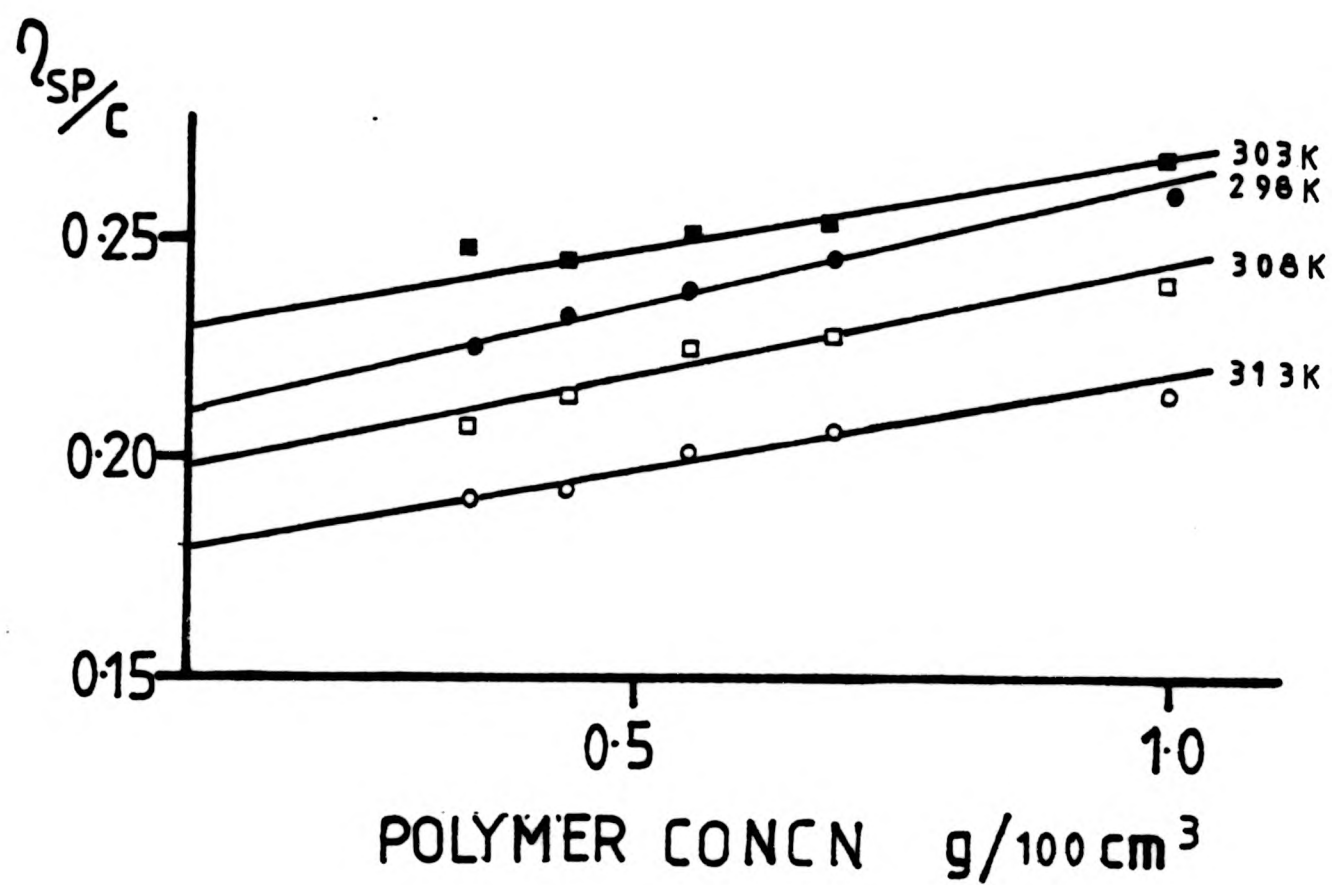FIG 2.3 : Solution viscosity example.

PAA50 in dioxane as a function of temperature.

(298 K(●), 303 K(■), 308 K(□), 313 K(o)).

2.5 MEMBRANE OSMOMETRY

A membrane osmometer can be used to determine the number average molecular weight, $\bar{M}_n$, by measuring the difference in equilibrium osmotic pressure between a pure solvent and a solution of a non-volatile solute in the same solvent when they are separated by a semipermeable membrane. This pressure difference is due to the flow of solvent across the membrane caused by a difference in chemical potential between the pure solvent in the solvent and in the solution.

A Knauer single unit instrument was used, in conjunction with a Knauer electronic temperature measuring instrument which measures the output from an in-built stainless steel pressure measuring system. Regenerated membranes (Sartorius) were used, which had been previously conditioned to the appropriate solvent, to divide the thermostatically controlled measuring cell into two chambers. The equipment is shown schematically in Fig. 2.4. The sample solutions, which ranged between 0.5-10 g/dm^3 in polymer concentration, were introduced into the upper chamber. A series of four or five solutions of different concentration was used. The pressure change was recorded as the deflection of a meter needle which had been calibrated to give a full scale deflection equivalent to the difference in pressure exerted by a column of solvent when it is moved through a vertical height of 10cm. After measurement, the cell is washed out with solvent and the meter needle was re-zeroed. This process does not affect the calibration but it is useful to check it periodically.

The relationship between the osmotic pressure, π, of a solution can be related to the concentration of solute, c g/dm^3, at a temperature T/K, by a virial equation of the form
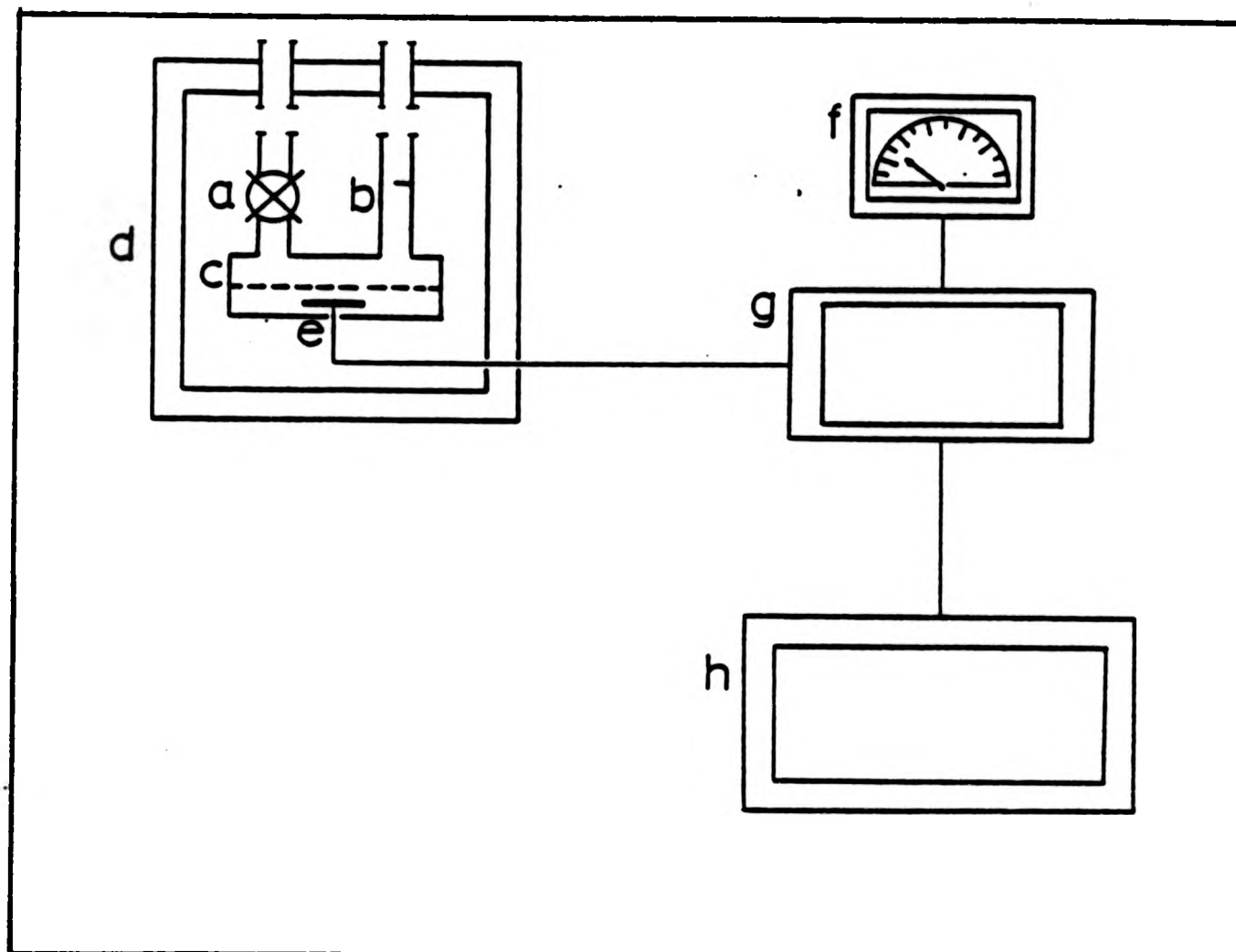
FIG 2.4 : Schematic diagram of membrane osmometer.

    (a) outlet valve

    (b) inlet valve

    (c) membrane

    (d) thermostatted chamber

    (e) pressure detecting membrane

    (f) osmotic pressure dial

    (g) Wheatstone bridge circuit

    (h) chart recorder

$$\pi/RTc = A_1 + A_2c + A_3c^2 + \ldots\ldots \qquad 2.16$$

or

$$\pi/RTc = 1/\bar{M}_n \ (1 + \Gamma_2c + \Gamma_3c^2 + \ldots\ldots \qquad 2.17$$

where $\Gamma_2 = A_2/A_1$ and A_1, Γ_1 are virial coefficients. For dilute solutions, terms in c^2 and higher can be neglected. A plot of π/c for a series of solute concentrations then gives $(\pi/c)_{c=0} = RT/\bar{M}_n$ as the intercept and gives A_2, the osmotic second virial coefficient, from its slope. For large ranges of solute concentration, this may not be linear but can be linearised by plotting $(\pi/c)^{\frac{1}{2}}$ against concentration to determine $(\pi/c)^{\frac{1}{2}}_{c=0}$ and hence $(\pi/c)_{c=0}$.

A sample analysis is given in Fig 2.5 for poly(acrylic acid), PAA300, determined in dioxane at 300K. Both analyses give $\bar{M}_n = 26.2 \times 10^4$ g/mol.

2.6 VAPOUR PRESSURE OSMOMETRY

In a vapour pressure osmometer the depression of the vapour pressure of a solution of a non-volatile solute in a solvent is compared with that of the pure solvent and from that one can measure the number average molecular weight, $\bar{M}_n$. The technique is used to measure $\bar{M}_n$ for a solute which is too low to be measured by membrane osmometry due to permeation of the solute through the membrane. $\bar{M}_n$ values of 50-20000 g/mol are conveniently measured by vapour pressure osmometry.

A Hewlett-Packard 302B instrument was used. It consisted of an insulated, temperature controlled sample chamber, in which two thermistor beads, used as temperature sensing elements, were suspended. They were maintained in equilibrium with a saturated atmosphere of solvent vapour continuously supplied via evaporation from a wick. A series of four or five sample solutions, of different solute concentration, with a maximum
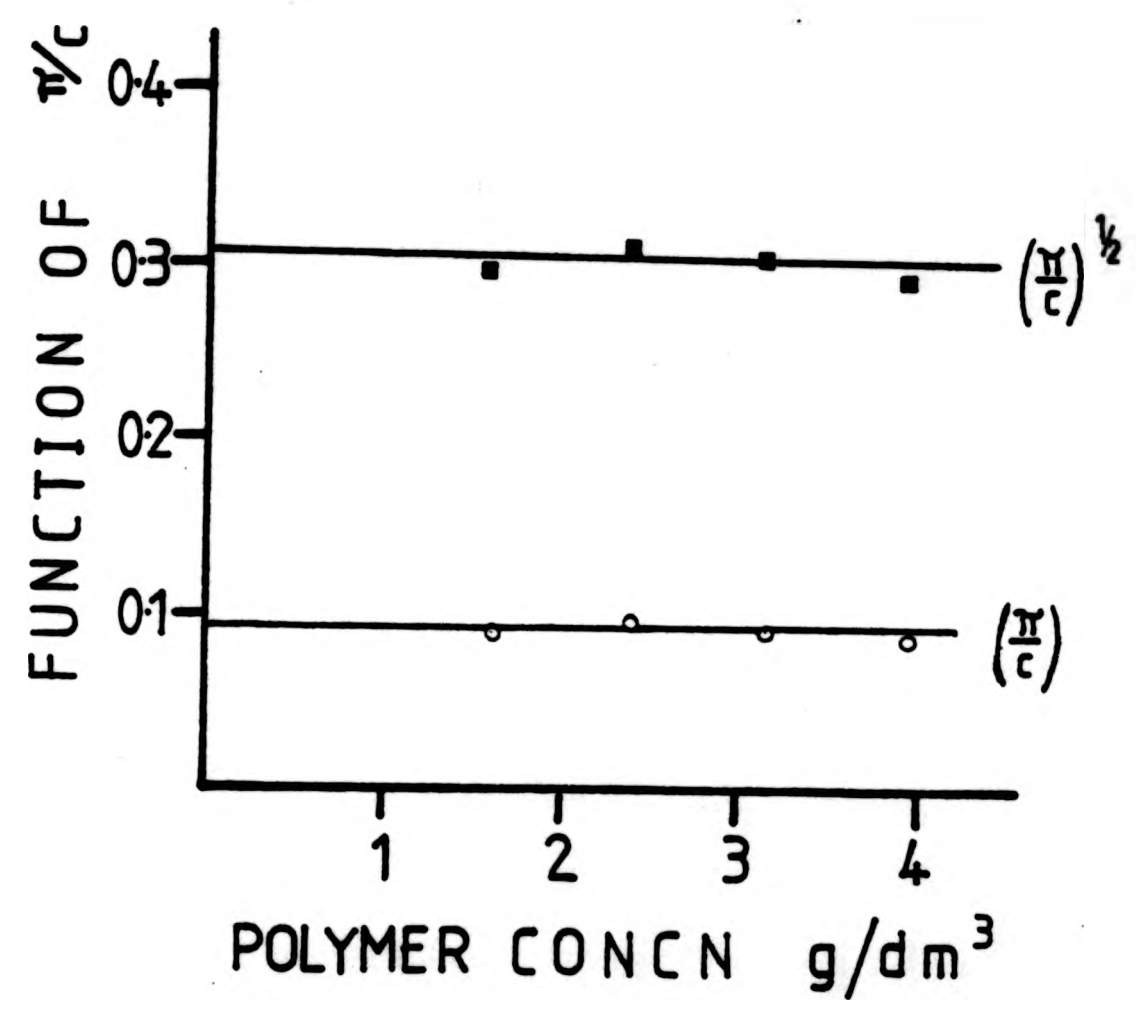
FIG 2.5 : Membrane osmometer example.
PAA300 in dioxane at 300 K

concentration of $30g/dm^3$, and solvent were introduced, as droplets, to the thermistor beads with the aid of a hypodermic syringe. One bead, the reference bead, is coated with solvent during the experiment, the other bead is used for the sample solutions and must be rinsed with solvent between measurements. The temperature difference which is recorded as a voltage difference on a conventional Wheatstone bridge, results from the different rates of evaporation and condensation in the droplets, of the solvent and sample solutions. A diagram of the instrument and the bridge circuit is shown in Fig 2.6.

The variation of the voltage, V (μV), with concentration, $c(g/dm^3)$, can be expressed as a virial equation of the form

$$V/c = (V/c)_{c=o} (1 + \Gamma_2 + \Gamma_3 c^2 + \ldots\ldots) \qquad 2.18$$

where

$$(V/c)_{c=o} = K/\bar{M}_n \qquad 2.19$$

Γ_2 and Γ_3 are virial coefficients and K is a calibration constant which is determined using a standard substance (eg benzil, polystyrene standards) of known molecular weight. The number average molecular weights, $\bar{M}_n$, were determined by both the 'Linear method' (from the slope of a plot of V against c) and the 'Ratio method' (from the intercept of a plot of V/c against c).

An example analysis is shown in Fig 2.7 for the polystyrene standard used to determine the calibration constant, K. The sample used was a Polysciences standard of $\bar{M}_n = 2030$. Both methods described gave
$K = 7.2 \mu V \ dm^3/mol$
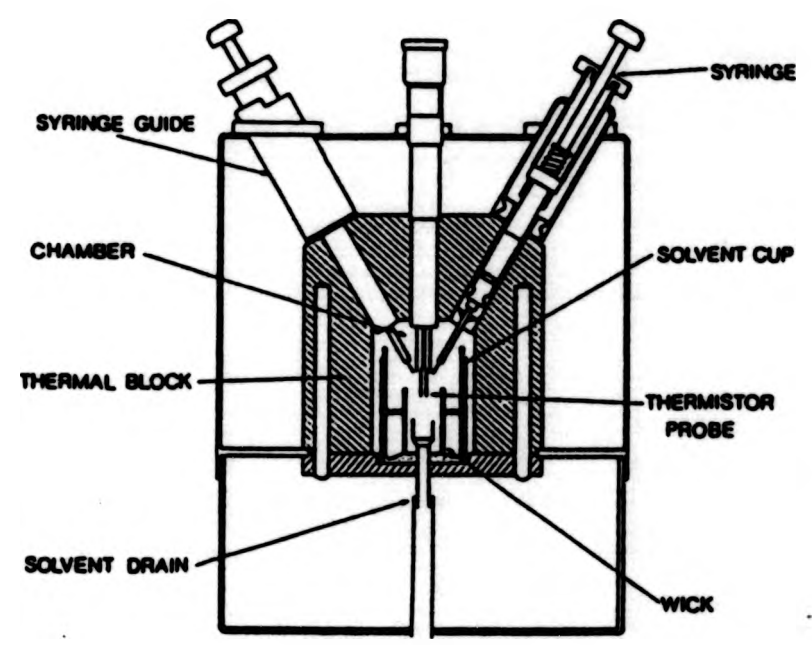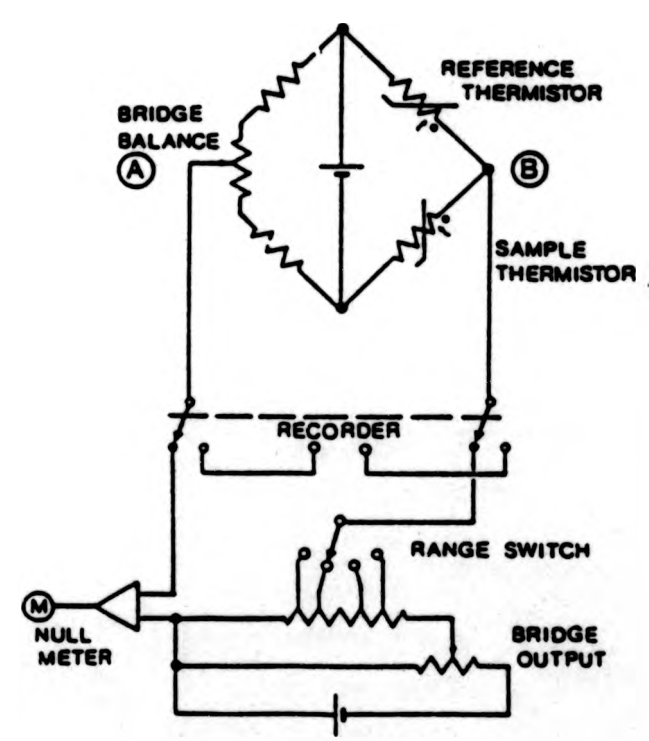
FIG 2.6 : Vapour pressure osmometer.
    (a) Schematic diagram.
    (b) Bridge circuit.
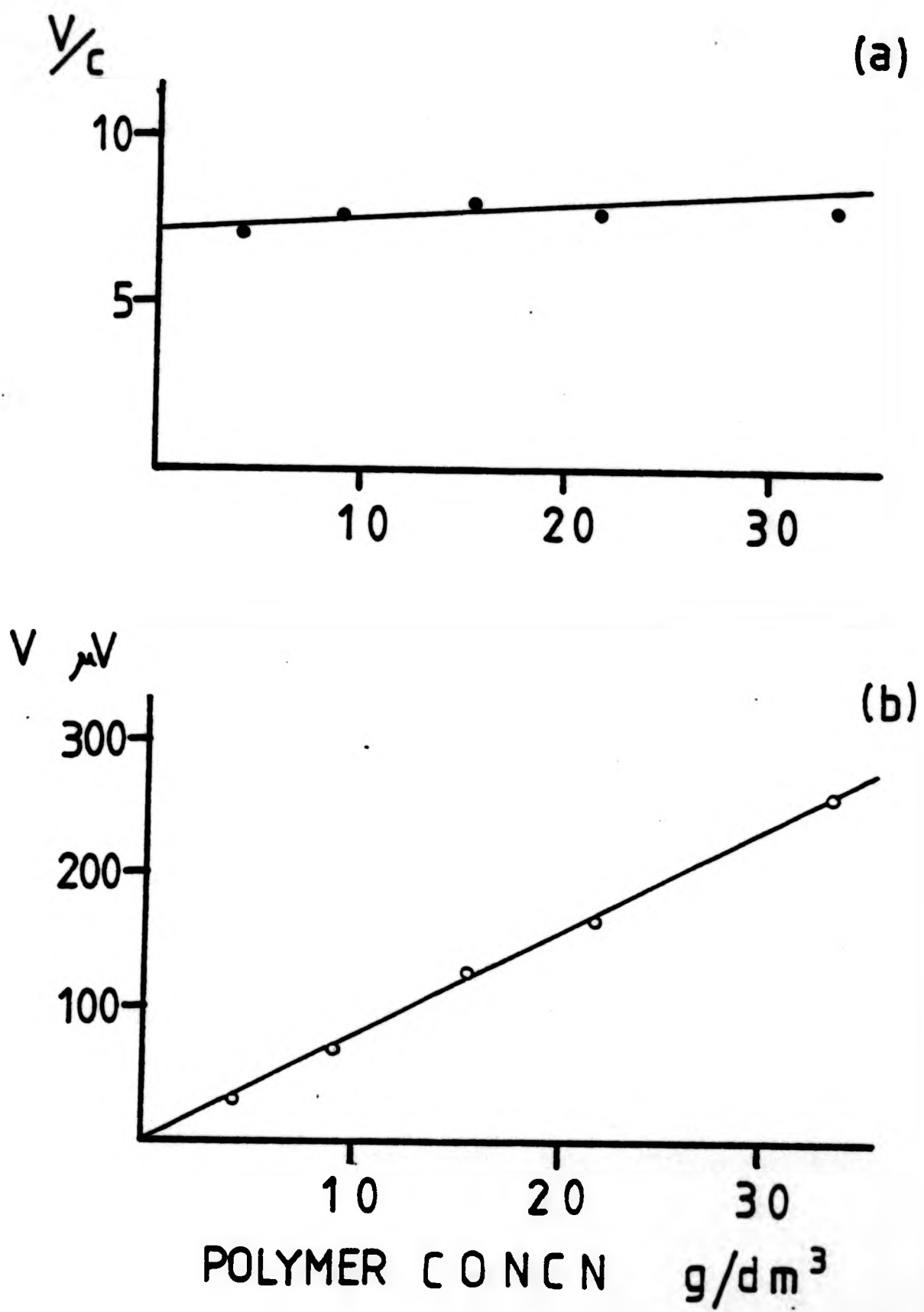
FIG 2.7 : Vapour pressure osmometer example.
polystyrene in dioxane at 328 K.
(a) Ratio method.
(b) linear method.

2.7 LIGHT SCATTERING

The scattering of light by a solution of a small particle (compared to the wavelength of the incident beam, λ_o) can be expressed as

$$\frac{K'c}{R_\theta} = 1/\bar{M}_w + 2A_2c+\ldots \qquad\qquad 2.20$$

where

$$K' = \frac{2\pi^2 \tilde{n}_o^2}{N_o\lambda_o^4}\left(\frac{dn}{dc}\right)^2 (1 + \cos^2\theta) \qquad\qquad 2.21$$

$\tilde{n}_o$ = refractive index of solvent and dn/dc is the refractive index increment of the solution. R_θ is called the Rayleigh ratio and is equal to $(i_\theta r^2/I_o)$ where I_o is the intensity of the incident light, i_θ is the quantity of light scattered per unit volume by one centre at an angle θ to the incident light and r is the distance of the centre from the observer. For small particles, the weight average molecular weight, $\bar{M}_w$, can be calculated from equation 2.20.

For larger particles, where the dimensions are greater than $\lambda/20$, light scattered from different parts of the particle can interfere with each other. This can be taken into account by a particle scattering factor $P(\theta)$ which can be used to modify equation 2.20.

$$\frac{K'c}{R_\theta} = \frac{1}{\bar{M}_w P(\theta)} + 2A_2c+ \ldots \qquad\qquad 2.22$$

Where the molecular weight is expressed as an average because of sample polydispersity. There are two methods used to determine $\bar{M}_w$.

Provided the dissymmetry, z, which is the ratio of the scattered light at two angles symmetrical about 90°, eg i_{45^o}/i_{135^o}, is not too large $\bar{M}_w$ can be calculated from measurement of the scattering

intensity at 90° and two angles symmetrical about 90° eg 45° and 135°.

Alternatively, or when the dissymmetry is large, a double extrapolation method (Zimm Plot) can be used. This method uses the knowledge that the scattering is independent of size at zero angle. Since this is difficult to measure experimentally, a double extrapolation using a modified form of equation 2.22 can be used. Substituting for $P(\theta)$ in equation 2.22

$$\frac{K'c}{R_\theta} = \frac{1}{\overline{M}_w} \left\{ 1 + \left(\frac{16\pi}{3\lambda^2}\right) \sin^2\left(\frac{\theta}{2}\right) <\bar{s}_z^2> \right\} + 2A_2 c \ldots \qquad 2.23$$

where $<\bar{s}_z^2>^{\frac{1}{2}}$ is a shape independent, radius of gyration. Values of $\frac{K'c}{R_\theta}$ at various angles are plotted against $\sin^2\left(\frac{\theta}{2}\right)$ + kc where k is a constant used to make the plot into a reasonable grid pattern.

A Sofica Light Scattering Instrument was used in this study. A schematic diagram is given in Fig 2.8. Light obtained from a water-cooled mercury vapour lamp (1) was passed first through a filter to select the appropriate working wavelength (546nm) and then through a system of polarisers (2). Before entering through the measuring cell, which was immersed in a thermostated vat of Xylene (4), at 298K. The filtered light was collimated (2).

The scattering intensity, I, was detected by a photomultiplier (5), which could be rotated to different angles, to the incident light, for a series of solutions of concentration c, 2c/3, c/2, c/3 ($c = 4 \times 10^{-3}$ g/cm^3), in addition to that of the pure solvent, I_o. All the solutions were filtered through 0.45μm Millipore filters before use. The intensity was measured as the deflection on a galvanometer.

The function $\frac{K'c}{R_\theta}$ was plotted against $\sin^2\left(\frac{\theta}{2}\right)$ +kc. The grid was

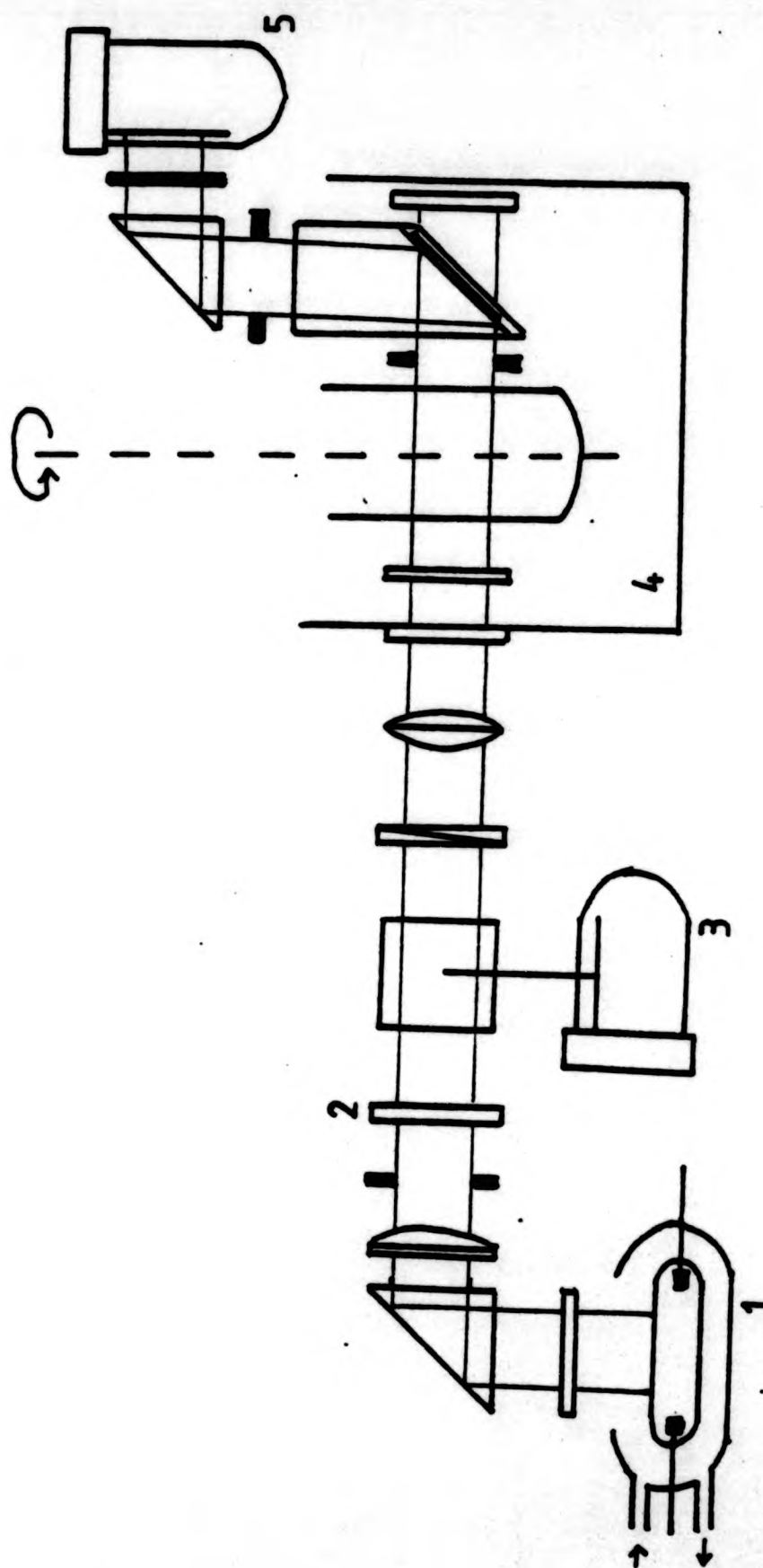FIG 2.8 : Schematic diagram of light scattering instrument.

1   Water cooled mercury vapour lamp.

2   Filter, polariser, variable slit system.

3   Reference photomultiplier.

4   Thermostat vat.

5   Photomultiplier.

extrapolated to both $\theta = 0$ and $C = 0$. These were extrapolated a second time to give $\left(\dfrac{K'c}{R_\theta}\right)_{\substack{c=0 \\ \theta=0}}$, from the reciprocal of which $\bar{M}_w$ can be derived. A_2 was derived from the initial slope of the $\theta = 0$ line and $<\bar{s}_z^2>$ from the initial slope of the $c=0$ line. An example of a Zimm plot is given in Fig 2.9, for sample PAA300 in a mixed solvent of dioxane/water containing 18.67(wt/vol)% water. (The corresponding differential refractometer plot is shown in Fig 2.11b).

2.8 DIFFERENTIAL REFRACTOMETRY

To determine $\bar{M}_w$ by light scattering the refractive index increment (dn/dc) for the system must be measured. This was determined using a Brice-Phoenix differential refractometer which is shown schematically in Fig. 2.10.

It was measured by determining the displacement of monochromatic light when it is passed through a series of solutions of various concentration with respect to that of pure solvent. The displacement, Δd, is related to the refractive index difference, Δn, by

$$\Delta n = k\Delta d \qquad\qquad 2.24$$

where k is a calibration constant determined using standard solutions of known (dn/dc).

After being filtered the light (546nm) was passed through a thermostated rotatable split cell. The light was then focused onto the cross hairs of a travelling microscope equipped with drum and eyepiece scales. The instrument was calibrated using aqueous sodium chloride solutions and (dn/dc) determined as the slope of a plot of Δn against concentration,Δc, $g/100cm^3$. Δd is measured for a series of solutions
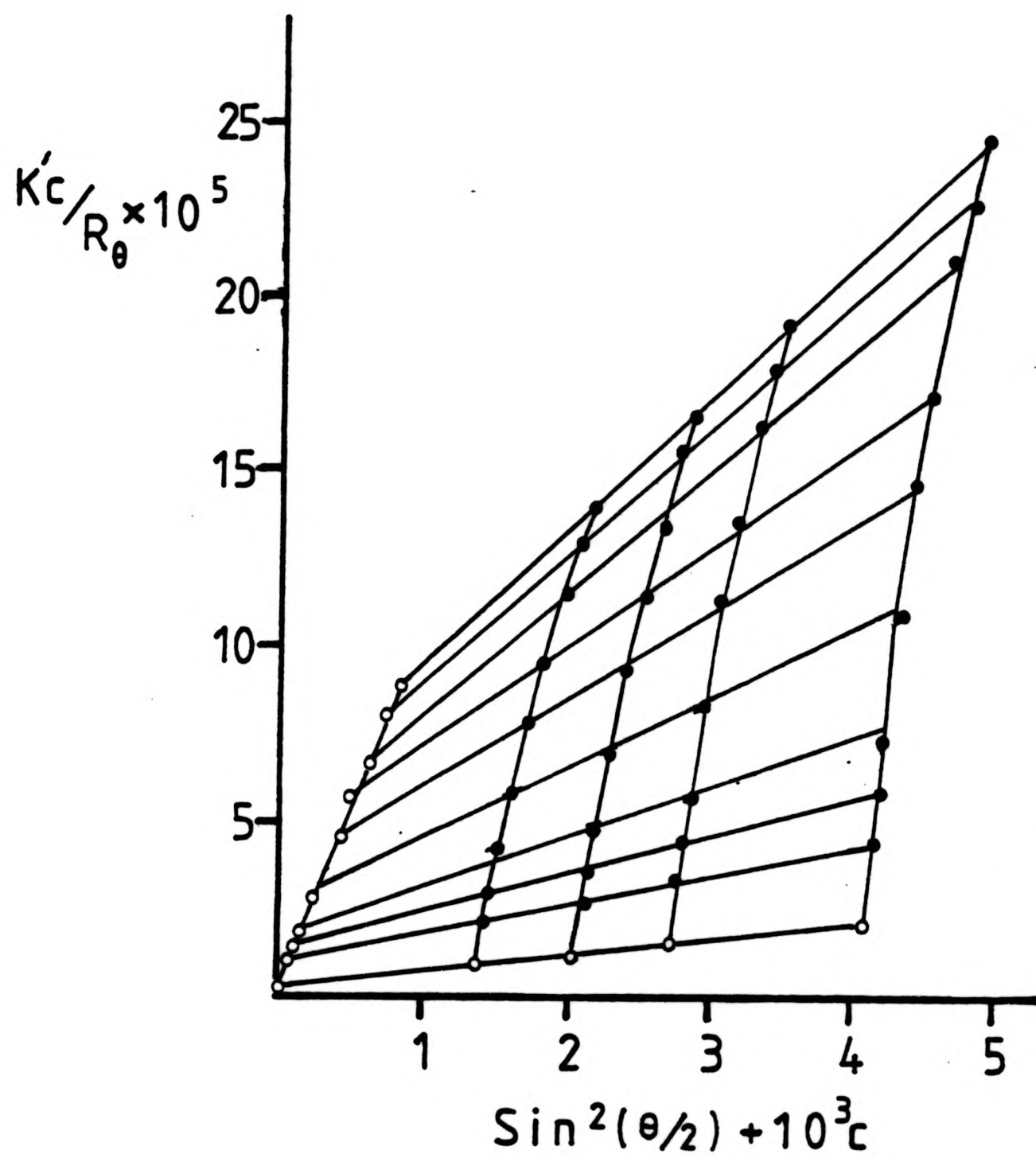
FIG 2.9 : Light scattering example.

PAA300 in dioxane/18·67(wt/vol)% water at 298 K.
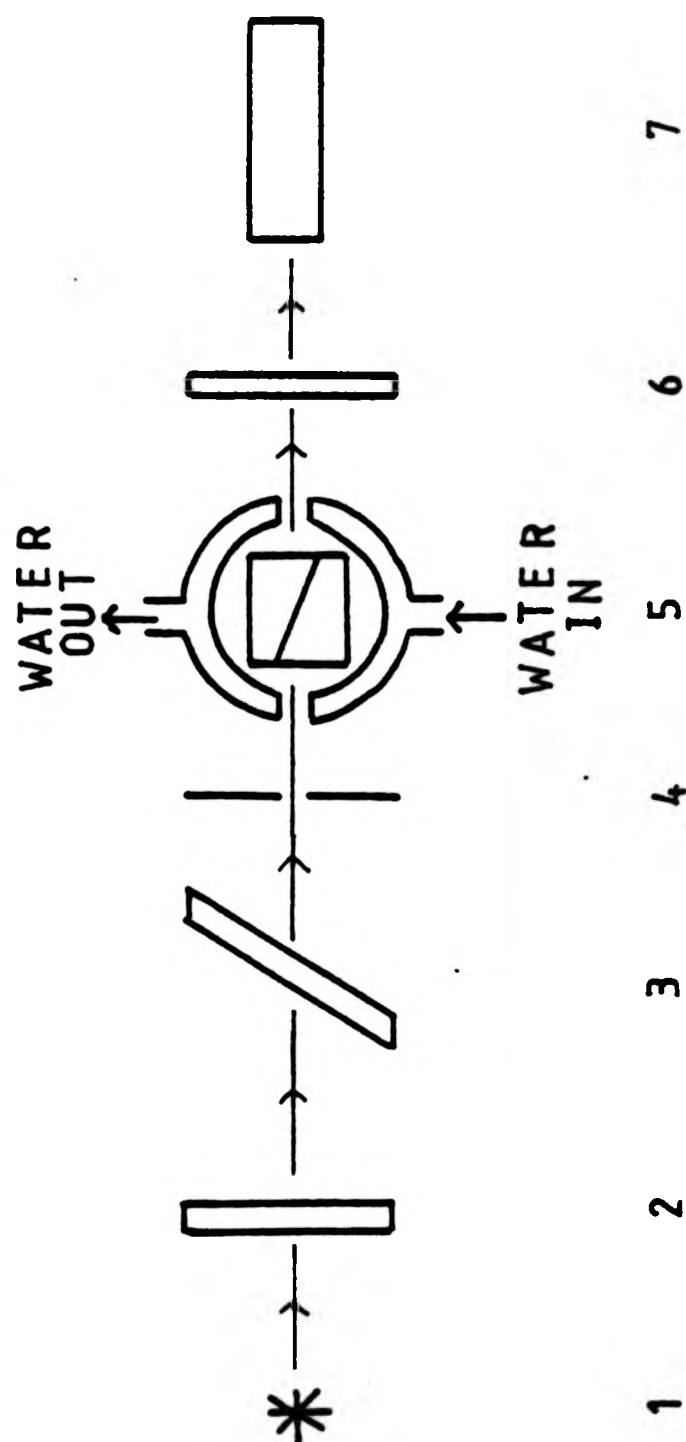
FIG 2.10 : Schematic diagram of differential refractometer.

    1 Light source.

    2 Filter.

    3 Semi-transparent mirror.

    4 Collimating slit.

    5 Cell housing.

    6 Lens.

    7 Travelling microscope.

of aqueous sodium chloride. k is then obtained from the slope of a plot
of Δn against Δd as seen in Fig. 2.11a. The values of Δn for this
system, as a function of concentration, have been determined.[15] In
this case k = 9.71 x 10^{-4}. Fig. 2.11b gives an example of the
determination of dn/dc for sample PAA300 in dioxane containing
18.67(wt/vol)% water by a plot of Δn against concentration, c.

2.9 DIFFERENTIAL SCANNING CALORIMETRY

Differential scanning calorimetry, dsc, is a non-equilibrium
calorimetry technique in which heat flow into or out of a sample and
inert reference is measured. Both sample and reference are maintained
at the same temperature by altering the electric heat currents to the
sample and reference chambers. Heat flow is detected electronically by
measuring the difference in the heating current requirements of sample
and reference. It is displayed as the deflection of a pen on a recorder
as a function of time or temperature.

A Perkin-Elmer DSC-2[16] fitted with a low temperature accessory and
capable of measurement in the temperature range 100-1000K was used.
10-20mg samples were encapsulated in standard aluminium pans. For
measurement at 200K helium was used as the purge gas for the sample and
reference chambers. A Perspex dry box purged with oxygen-free nitrogen
was mounted on the analyser deck to minimise condensation in the vicinity
of the sample and reference holders during sample changeover. A
schematic diagram of the instrument is shown in Fig. 2.12.

The glass transition temperature, T_g, and the melting temperature,
T_m, of samples can be measured. The change in the specific heat,
C_p, of the sample during the transitions is monitored as the
temperature of the sample is continuously changed at some chosen rate.
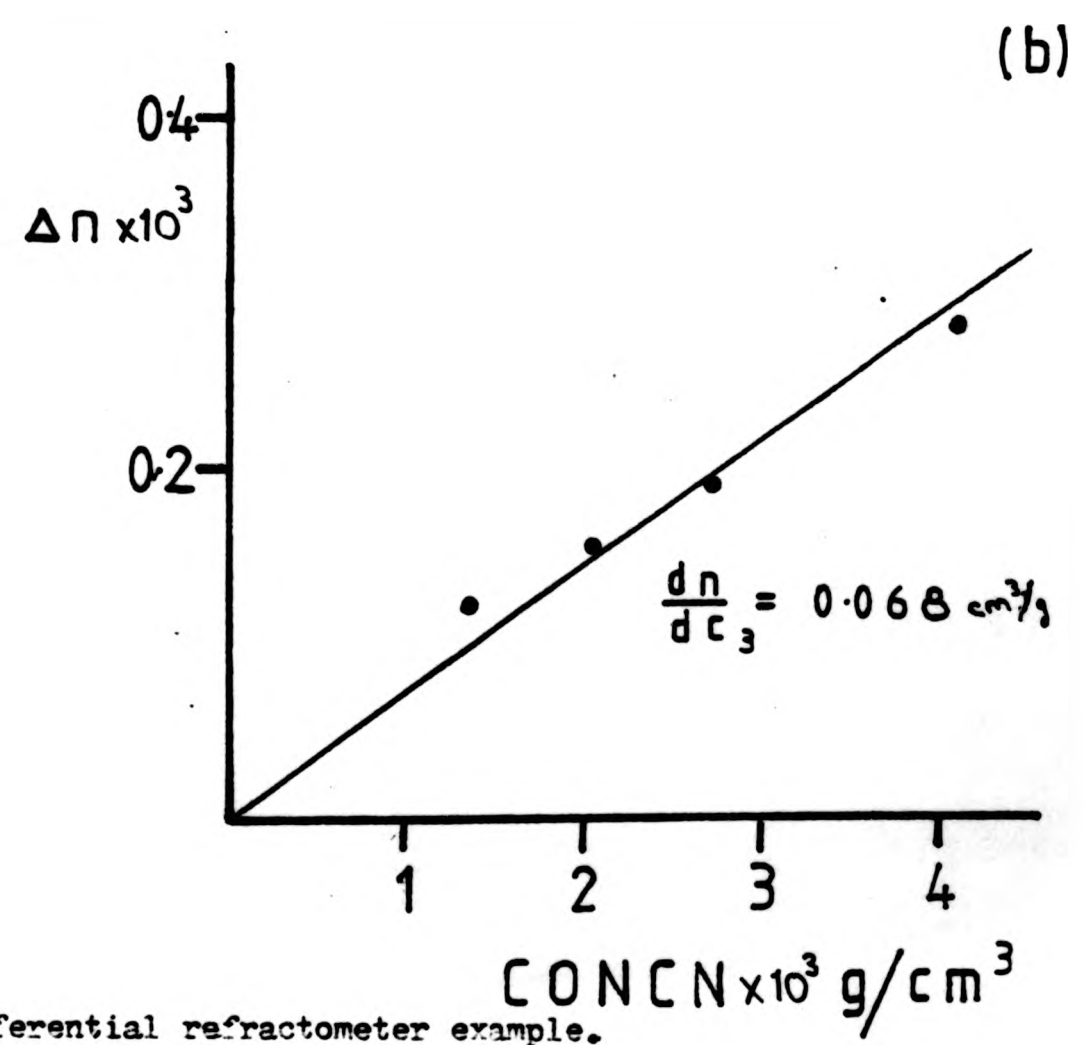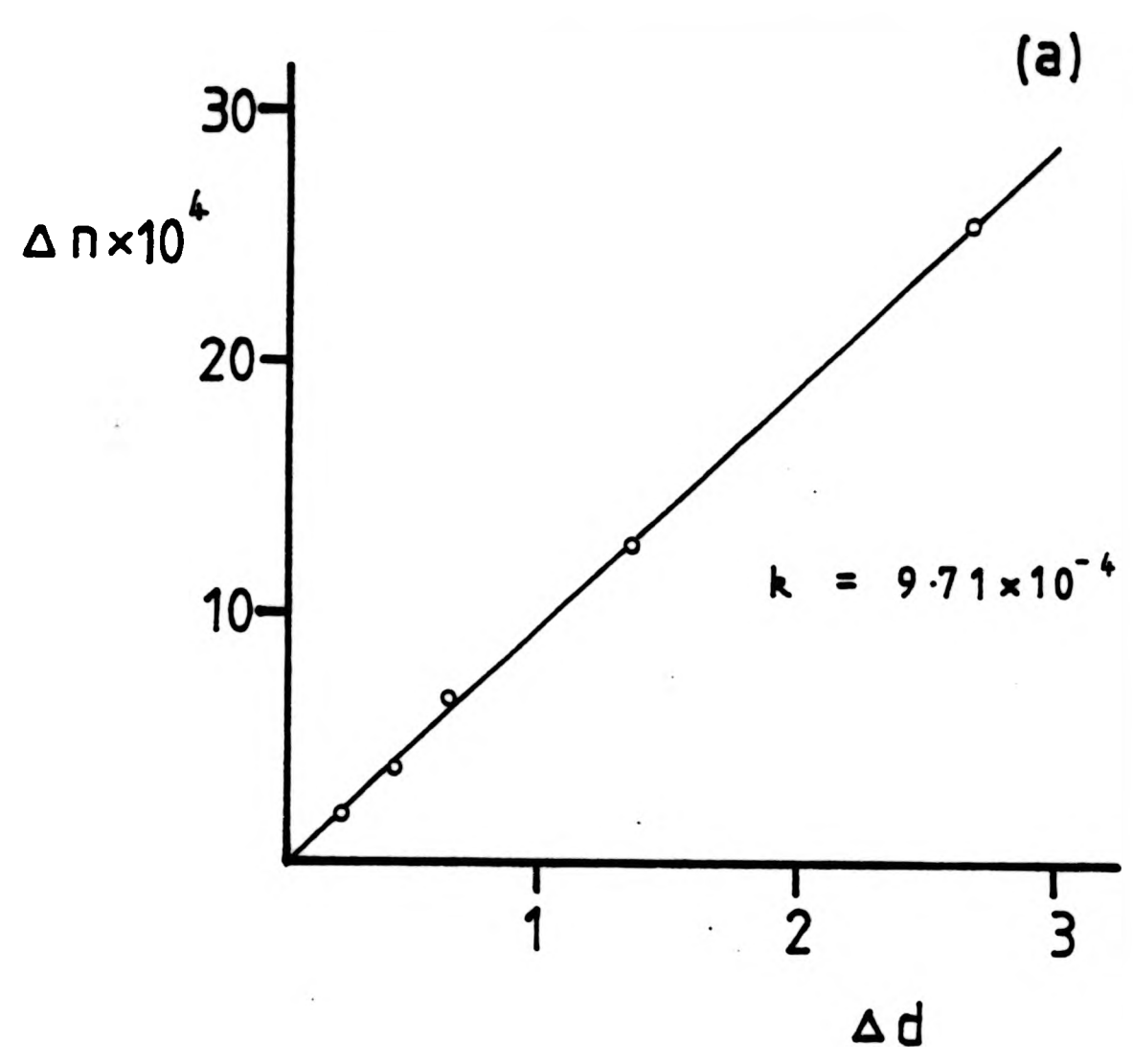
FIG 2.11 : Differential refractometer example.
(a) Calibration aqueous NaCl at 298 K.
(b) PAA300 in dioxane/18·67(wt/vol)% water at 298 K.
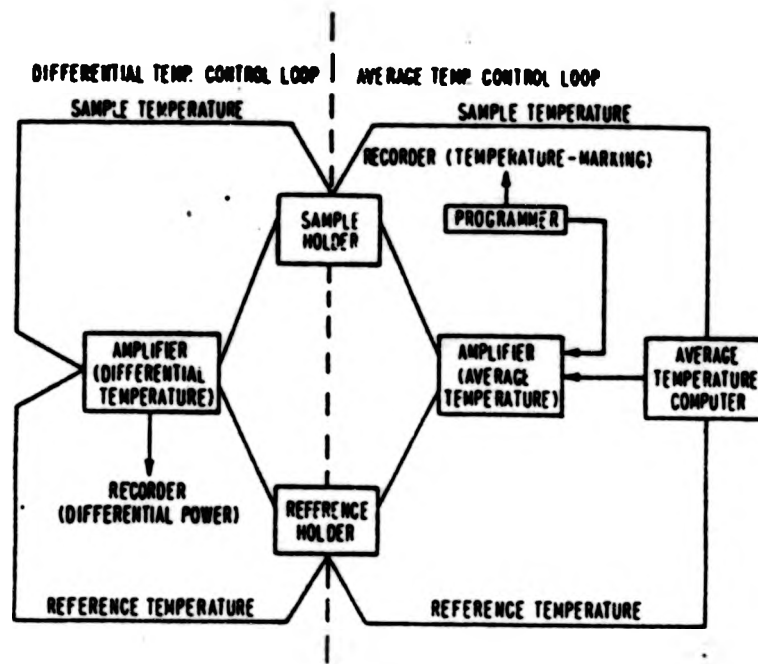
FIG 2.12 : Schematic diagram of differential scanning calorimeter.

The T_g is represented by a sharp change in the value of C_p and hence by a change in the recorder output, Fig. 2.13. The actual temperature of the change is a function of the temperature scan rate. The melting temperature, T_m, is seen as a peak in the recorder output, Fig. 2.14b.

Poly(acrylic acid)/poly(ethylene glycol), PAA5/PEG40, blends were studied in this way. They were scanned at a rate of 20K/min in the temperature range 180–400K. Fig. 2.13 shows an example for a blend with 18.9(wt/vol)% poly(acrylic acid).

2.10 PARTIAL SPECIFIC VOLUME

The partial specific volume, $\bar{u}$, of poly(acrylic acid), PAA150, in dioxane was measured at 298K using a series of 50 cm^3 volumetric flasks which had been calibrated using distilled water. Solutions of polymer concentration 1.2, 1.8 and 3.6 $g/100cm^3$ were made up in these flasks. The partial specific volume was then determined from[17]

$$\bar{u} = \frac{1}{m_2}\left(u - \frac{1}{\rho_1}(m-m_2)\right)$$

2.25

where m is the mass of the solution in the flask with a volume u g/cm^3, which contains a mass m_2 of polymer. ρ_1 is the density of the solvent (dioxane = 1.0336 g/cm^3). $\bar{u}$ for poly(acrylic acid) in dioxane at 298K was measured as 0.780 $\pm$0.001 cm^3/g from the slope of $(u-1/\rho_1 (m-m_2))$ against m_2.

2.11 MISCELLANEOUS TECHNIQUES

2.11.1   Infrared Spectroscopy

Infrared spectra were run on a Perkin-Elmer 577 Grating Infrared Spectrometer. The samples were cast as films on NaCl plates.
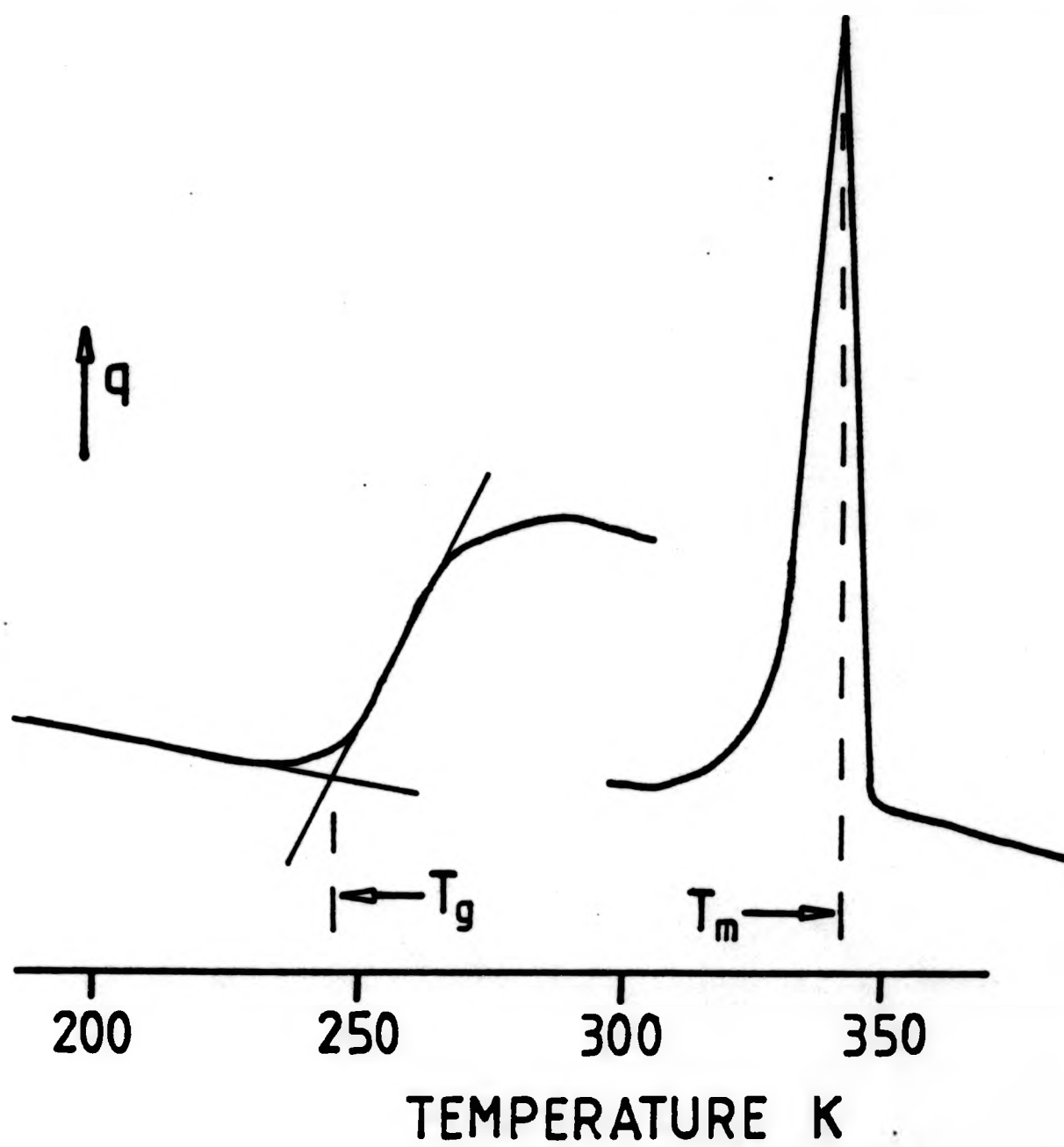
FIG 2.13 : Differential scanning calorimeter example.
PAA5/PEG40(18·90(wt)%) blend.
(q axis not to scale).

2.11.2   Laser Raman Spectroscopy

Laser Raman spectra were run on a Spex Ramalog R5M spectrometer using a coherent CR6 Argon Ion Laser (514.5nm). Samples were used as solutions in thin capillary cells.

2.11.3   Nuclear Magnetic Resonance Spectroscopy

(^{1}H) nmr spectra were run on either a Hitachi Perkin-Elmer R24 (60MHz) or a Perkin-Elmer R32 (90 MHz) spectrometer. Samples were 10-15 (wt/vol)% solutions in $CDCl_3$ with TMS as internal standard.

Acetate contents for the poly(vinyl alcohol) samples were determined on a Bruker WP80 fourier transform nmr spectrometer equipped with an Aspect 2000 minicomputer, in d_6-DMSO with NaTMS as internal reference at 343K over 100-700 transients.

REFERENCES

1. J R Urwin in "Light Scattering from Polymer Solutions", ed M B Huglin, Academic Press, London, (1972).

2. B A Wolf, M C Sezen, Macromolecules **10**, 1010, (1927).

3. E Maderek, B A Wolf, Polym.Bull. **10**, 458, (1983).

4. J-P Cohen-Addad, C Roby, J.Polym.Sci., Polym.Phys.Ed. **19**, 1395, (1981).

5. K W Derham, J Goldsbrough, M Gordon, Pure Appl.Chem. **38**, 97, (1974).

6. R Koningsveld, PhD Thesis, Leiden, (1967).

7. R Koningsveld, A Stavermann, J.Polym.Sci. A2, **6**, 325, (1968).

8. I Wadsö, Acta Chem.Scand. **22**, 927, (1968).

9. G Lewis, A F Johnson, J.Chem.Soc. (A), 1816, (1969).

10. J M G Cowie, Polymer **7**, 487, (1966).

11. H Mark, Der Feste Korper, Leipzig, 103, (1938).

12. R Houwink, J.Prakt,Chem. **155**, 15, (1940).

13. W H Stockmayer, M Fixman, J.Polym.Sci. **C1**, 137, (1963).

14. H Yamakawa, "Modern Theory of Polymer Solutions", Harper and Row, New York, (1971).

15. B P 2000-V Differential Refractometer Operating Manual.

16. Perkin-Elmer DSC-2 Operating Manual.

17. J F Rabek, "Experimental Methods in Polymer Chemistry", Wiley Interscience, New York, (1980).

CHAPTER THREE

POLY(ACRYLIC ACID) SYSTEMS

3.1 POLY(ACRYLIC ACID) SYSTEMS

The phase equilibria of both binary and ternary solutions containing poly(acrylic acid) were studied (ie polymer dissolved in either one or two solvents).

The samples of polymer used were commercially obtained (except PAA17 and PAA20) from Polysciences, as 25 or 50% aqueous solutions and were characterised in 1,4-dioxane* by osmometry.   The lower molecular weights, PAA2, PAA5, PAA17 and PAA20, were characterised using vapour pressure osmometry at 328K, Table 3.1 .   The higher molecular weights were characterised at a number of temperatures between 300 and 310K, by membrane osmometry, Table 3.2 .   PAA17 and PAA20 were supplied by ICI Mond division as aqueous solutions.   PAA20 was Allied Colloids E7 and PAA17 was prepared, by ICI, in an ethanol/water mixture using 4,4'-azobis(4-cyanovaleric acid) as initiator at 353K.   All the polymers were used as dried films cast from aqueous solutions.

The solvents used (dioxane and tetrahydrofuran) were prepared for use by refluxing for 2hr with calcium hydride, followed by distillation.   They were stored over sodium wire or molecular sieves. No difference in behaviour was observed between the two methods of storage over the time between preparation and use.   The water content of the dried dioxane as determined by a Karl-Fischer method, gave consistent results over different batches of dried solvent of less than 0.1% water.

Dioxane/water mixtures were prepared using a known weight of distilled water to a volume of dried dioxane (wt/vol %).   Other 'solvent mixtures' were prepared in a similar manner by addition of a weight of the second component, polyglycol (both liquid and solid), a crown ether

---

*hereafter referred to as dioxane

(12-C-4) or hydrochloric acid (0.01M) to a known volume of dioxane.

The weight average molecular weights of PAA50, PAA150 and PAA300 in dioxane, at 298K, were also determined by light scattering (see Section 5.1).

3.2 CLOUD POINT CURVES - BINARY SOLUTIONS

The phase separation behaviour of poly(acrylic acid) in dioxane for solutions of polymer concentration up to 40 g/100cm^3 are shown in Figs 3.1-3.7. All the molecular weights studied showed three phase boundaries except for PAA2 which exhibited no boundaries and PAA5, Fig 3.1, which exhibited a single high temperature lower critical solution boundary. With increasing temperature these three boundaries are designated as exhibiting pseudo-lower critical solution behaviour, p-LCST, at the lower temperature boundary with upper critical solution behaviour, UCST, at higher temperatures. The highest boundary, in temperature, is considered to show lower critical solution behaviour, LCST. The two designations p-LCST and LCST are used to distinguish between the two lower critical solution boundaries in the system.

Solutions of PAA50 and PAA90 tended to phase separate at similar temperatures, Figs 3.4, 3.5. The two lower temperature boundaries, p-LCST and UCST, occurred at approximately 320 and 420K in both cases with only a relatively small change in temperature with changing polymer concentration. The LCST also showed only a small variation in temperature as a function of polymer concentration but the boundary for PAA90 solutions occurred, generally, at slightly lower temperatures than for PAA50 solutions. (440K for PAA90 solutions and 450K for PAA50 solutions.) A region of complete miscibility over the entire range of polymer concentration studied occurred for both molecular weights.

The p-LCST for PAA150, Fig 3.6, was again at similar temperatures to that for PAA50 and PAA90 solutions but both the higher temperature boundaries were lowered in temperature, to 410K for the UCST and 410K for the LCST. A region of complete miscibility between the UCST and LCST did not occur in this case for the whole polymer concentration range but instead there was an 'extended hourglass' shape. This was also the case for PAA300 solutions in which there was a lowering, in temperature, of all three boundaries, to 300, 380 and 390K for p-LCST, UCST and LCST respectively, Fig 3.7. The closing of the gap between the two upper boundaries occurred at progressively lower polymer concentrations (from 8 $g/100cm^3$ for PAA150 to 5 $g/100cm^3$ for PAA300) as the molecular weight increased.

Solutions of PAA17, Fig 3.2, and PAA20, Fig 3.3, also exhibited 'extended hourglass' shapes but with 'indentations' into the lower temperature two phase region, centred around a polymer concentration of 8.5 $g/100cm^3$. The closure of the miscibility gap occurred at a higher polymer concentration for the higher molecular weight (20 $g/100cm^3$ for PAA20 and 14.5 $g/100cm^3$ for PAA17). The UCST occurred at temperatures similar to PAA50 and PAA90 and the LCST's were observed at lower temperatures than for the higher molecular weights. The p-LCST occurred at 370K for both PAA17 and PAA20.

The solutions of PAA5 showed a single phase separation boundary (LCST) at approximately 430K but with the residue of a more complex system occurring at low polymer concentrations, Fig 3.1.

A phase volume ratio method was used to determine the critical concentration, c_c, and hence the critical temperature, T_c of the p-LCST boundary for PAA50, PAA90, PAA150 and PAA300, Figs 3.8-3.11 . The values obtained are indicated on Figs 3.4-3.7 by the symbol ■ , and are

also in Table 3.3.   The temperature of the various phase boundaries, T_{pm}, occurring at the polymer concentration which gives the minimum in the p-LCST, c_{pm}, are shown in Table 3.4   The values of both T_{pm} and T_c as a function of molecular weight are shown in Fig 3.12, denoted by the symbols o and ■ respectively.   This shows clearly the depression in temperature of the p-LCST and LCST with increasing molecular weight but it also shows that there is a depression in temperature for the UCST boundary.   The transition between a three and a single boundary (LCST) system occurs at a molecular weight ($\bar{M}_n$) of approximately 5×10^3 g/mol.   The single boundary LCST can be seen to be a continuation of the p-LCST and not the higher temperature LCST and so the mechanism of phase separation must be the same as at the p-LCST boundary.

A comparison of the variation of the phase separation boundaries with temperature, expressed as the minimum and critical temperatures, shows similar trends for the p-LCST curves.   The trends for the two higher temperature boundaries are similar but the critical temperature plot indicates that the critical points may not be detectable for these two boundaries above a molecular weight ($\bar{M}_n$) of approximately 17×10^4 g/mol.   The corresponding temperature minimum curves for these two higher temperature boundaries are parallel and therefore may not reflect the formation and disappearance of the 'extended hourglass' as well as the critical temperature curves.   Both measurements give polymer concentrations, c_c and c_{pm}, which decrease with increasing molecular weight as shown in Fig 3.13.

An estimation of the 'theta-temperature' (θ-temperature) for the system can be found by plotting either temperature T_{pm} or T_c, against $\bar{M}_n^{-\frac{1}{2}}$ where the θ-temperature is given by extrapolation to $\bar{M}_n^{-\frac{1}{2}} = 0$.[1]   Since both sets of points are scattered a linear

regression analysis was performed on the combined values. This gave a value of 297K, Fig 3.14. This value is in reasonable agreement with the accepted value of 303K for this system[2] although this was reported for dioxane containing 2-4% water.

Similar behaviour was observed when the cloud point curves were measured for tetrahydrofuran, THF, solutions of poly(acrylic acid). The phase separation boundaries for PAA5, PAA50 and PAA90 solutions were determined and are shown in Fig 3.15 and Fig 3.16. PAA5 solutions exhibited a single phase separation boundary, above 370K, Fig 3.15 , which is lower in temperature than the corresponding dioxane curve, Fig 3.1. Sample PAA50 exhibits, as before, three phase separation boundaries at 290, 405 and 415K for p-LCST, UCST and LCST. Again these occur at lower temperatures than the dioxane system, Fig 3.4, with the gap between the UCST and LCST being much closer and with the gap closing at 9 g/100cm^3. PAA90 solutions were totally insoluble. The general trends, when compared with those of the dioxane system, indicate that THF is a poorer solvent for poly(acrylic acid) then dioxane.

In all cases, although the cloud-point curves were reproducible when determined as the temperature was raised, they were not necessarily reproducible if the precipitation temperatures were determined by progressively lowering the temperature which may indicate a tendency for supercooling to occur. There was also evidence of the formation of a little gelatinous solid in the tubes on cooling from the higher temperatures.

The ir spectra of PAA50 CAST FROM solutions of approximately 3g/100cm^3 polymer IN DIOXANE before and after heating to 367, 435 and 465K, for approximately two hours, gave coincident peaks except for the solution heated to 465K which showed the absence of a peak at 610 cm^{-1}, possibly due to the

disappearance of vinyl end groups on the polymer, Fig 3.17. The
solution heated to 367K, on cooling, was still a homogeneous solution.
Unheated solutions of PAA5, PAA50 and PAA90 gave coincident peaks.

3.3 CLOUD POINT CURVES - AQUEOUS TERNARY SOLUTIONS

In the system PAA50 in dioxane/water mixtures, for polymer
concentrations of up to $20g/100cm^3$, three phase separation boundaries,
analogous to the single solvent system, were observed for mixtures
containing less than 12(wt/vol)% water. At higher water contents, up to
20(wt/vol)%, a single LCST phase separation boundary was observed.
Solutions containing 25, 30, 40 and 100(wt.vol)% water, in the solvent,
showed total solubility within the range of temperatures studied, Fig
3.18-3.23 .

The solutions containing 1.02, 2.52 and 4.99(wt/vol)% water, Fig
3.18-3.20, exhibit LCST and UCST at similar temperatures (using the same
nomenclature as before). The temperatures of these phase separation
boundaries are effectively independent of polymer concentration,
occurring at 450 and 425K respectively. These temperatures are similar
to those for the corresponding single solvent systems, Fig 3.4 . The
region of miscibility between these phase separation boundaries extends
over the entire polymer concentration range studied. The temperature of
the p-LCST boundary increases with increasing water content up to
12.05(wt/vol)% water which is the lowest water content to exhibit single
LCST behaviour, Fig 3.23. As with the UCST and LCST, the p-LCST for all
these water contents are essentially independent of polymer
concentration. For the solutions with 7.49(wt/vol)%, Fig 3.21, and
9.99(wt/vol)% water, Fig 3.22, the region of miscibility, between the
UCST and LCST boundaries, forms an 'extended hourglass'. The closure of

the gap occurs at $7g/100cm^3$ for 7.49(wt/vol)% water and 6 $g/100cm^3$ for 9.99(wt/vol)% water. The temperature at which the UCST occurs was again constant, at 420K, whilst the LCST decreased in temperature and the p-LCST increased, in temperature, in going to higher water contents.

The three solutions containing 12.05, 14.87 and 19.72(wt/vol)% water, Fig 3.23, all showed single LCST behaviour, the temperatures of which were observed to move to higher temperatures as the water content increased.

The movement of the phase separation boundaries, as a function of water content, at a polymer concentration of $2g/100cm^3$ is shown in Fig 3.24, Table 3.5 . This indicates that the UCST is relatively constant in temperature with the LCST decreasing in temperature until they merge at approximately 11(wt/vol)% water content. The temperature of the p-LCST increases with water content and appears to merge with the other two phase separation boundaries at 11-12(wt/vol)% water content. Fig 3.24 also indicates that the single LCST system is a continuation of the p-LCST and would therefore be expected to have a similar mechanism of phase separation.

Similar phase equilibria were obtained when PAA17 was used, instead of PAA50, as can be seen in Fig 3.25-3.27. The UCST was again observed at similar temperatures (420K), for all percentages of water. It also occurred at similar temperatures when PAA50 was used. The p-LCST was found to increase and the LCST to decrease in temperature with increasing water content. The region of miscibility between the UCST and LCST phase boundaries disappeared at a faster rate than that seen in the PAA50 solutions. The single phase separation boundary, here, is formed above 4(wt/vol)% water, Fig 3.27. The temperature of the p-LCST phase boundary, at polymer concentrations greater than $8.5g/100cm^3$, increased

faster than at lower polymer concentrations as the water content increased. For PAA17 in the single solvent, the corresponding cloud-point curve also shows 'indentations' into the lower two phase regions at approximately 8.5g/100cm^3 (see Fig 3.2).

As with the single solvent, a gelatinous solid was observed after heating to higher temperatures, but as before, the phase separation boundaries were reproducible in the heating process although not necessarily in the cooling process. The rate of original dissolution of the polymer was found to increase as the water content was increased.

When water was replaced by 0.01M hydrochloric acid the cloud-point curves for solutions of PAA50 were located at temperatures similar to the aqueous dioxane system indicating that the phase separation behaviour is not necessarily pH dependent, in this case, Fig 3.28 .

As with the single solvent, when water was added to PAA50 in tetrahydrofuran the resulting phase behaviour indicated that this is a poorer solvent than the corresponding system with dioxane, see Fig 3.29. The LCST and UCST phase boundaries occur at lower temperatures than with the single solvent THF, with the gap between them closing at lower polymer concentrations, at 2.5g/100cm^3. The p-LCST occurs at higher temperatures than for the single solvent.

REFERENCES

1.   T G Fox Jr, P J Flory, J.Phys.Colloid.Chem. **53**, 197 (1949).

2.   P J Flory, W R Krigbaum, W B Schultz, J.Chem.Phys. **21**, 164, (1953).
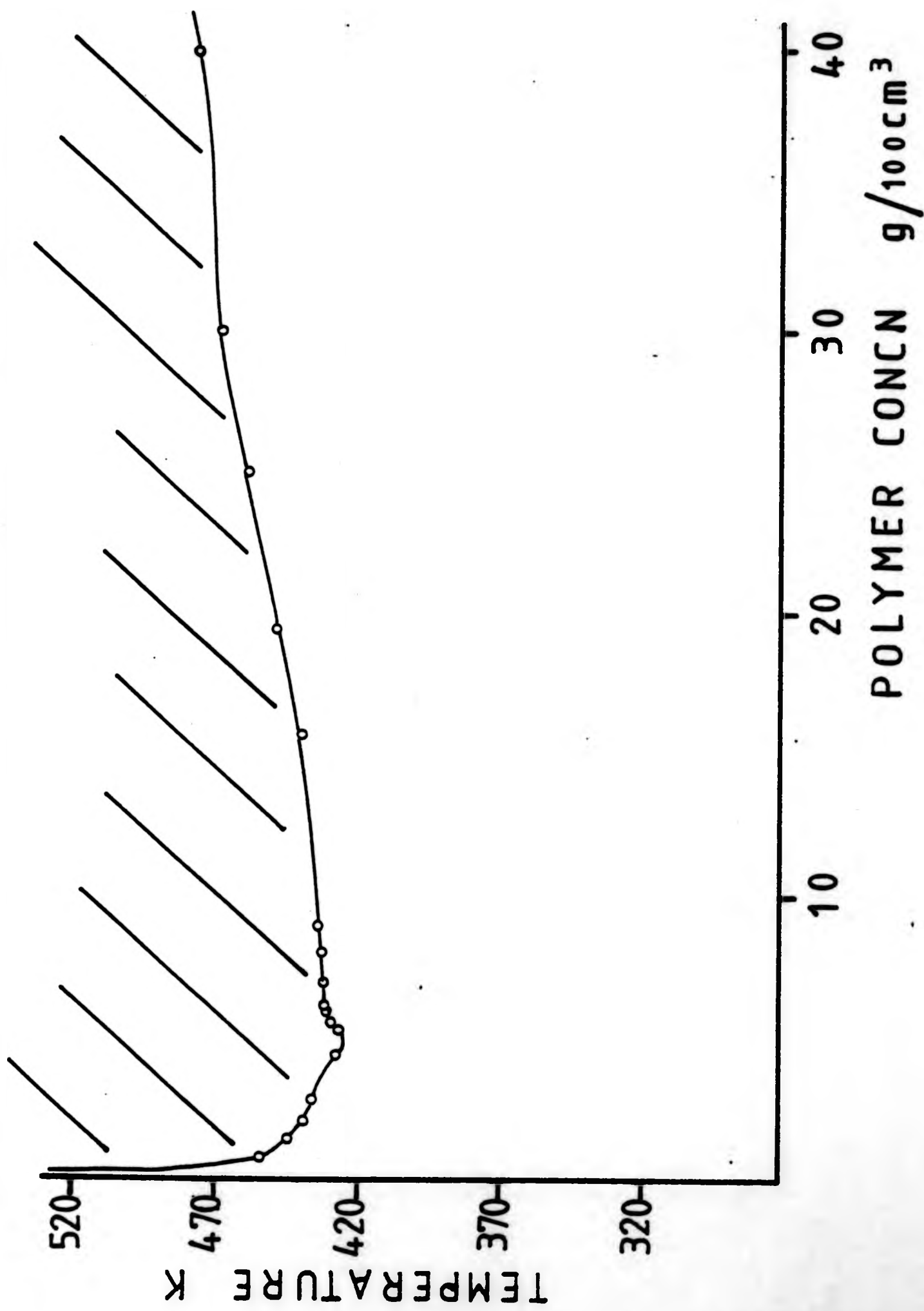
FIG 3.1 : Cloud point curve for poly(acrylic acid) PAA5 in dioxane.
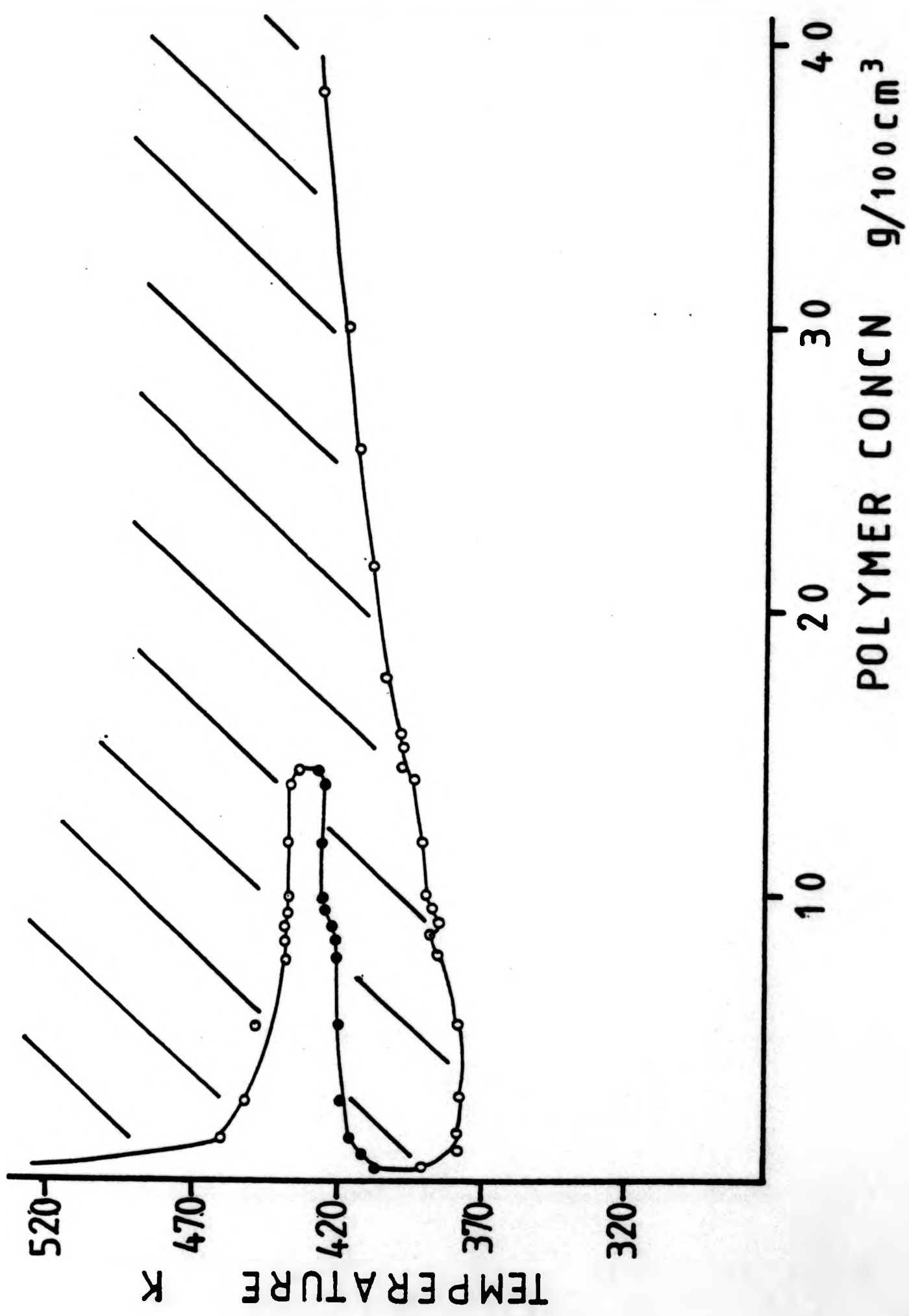
FIG 3.2 : Cloud point curve for poly(acrylic acid) PAA17 in dioxane.
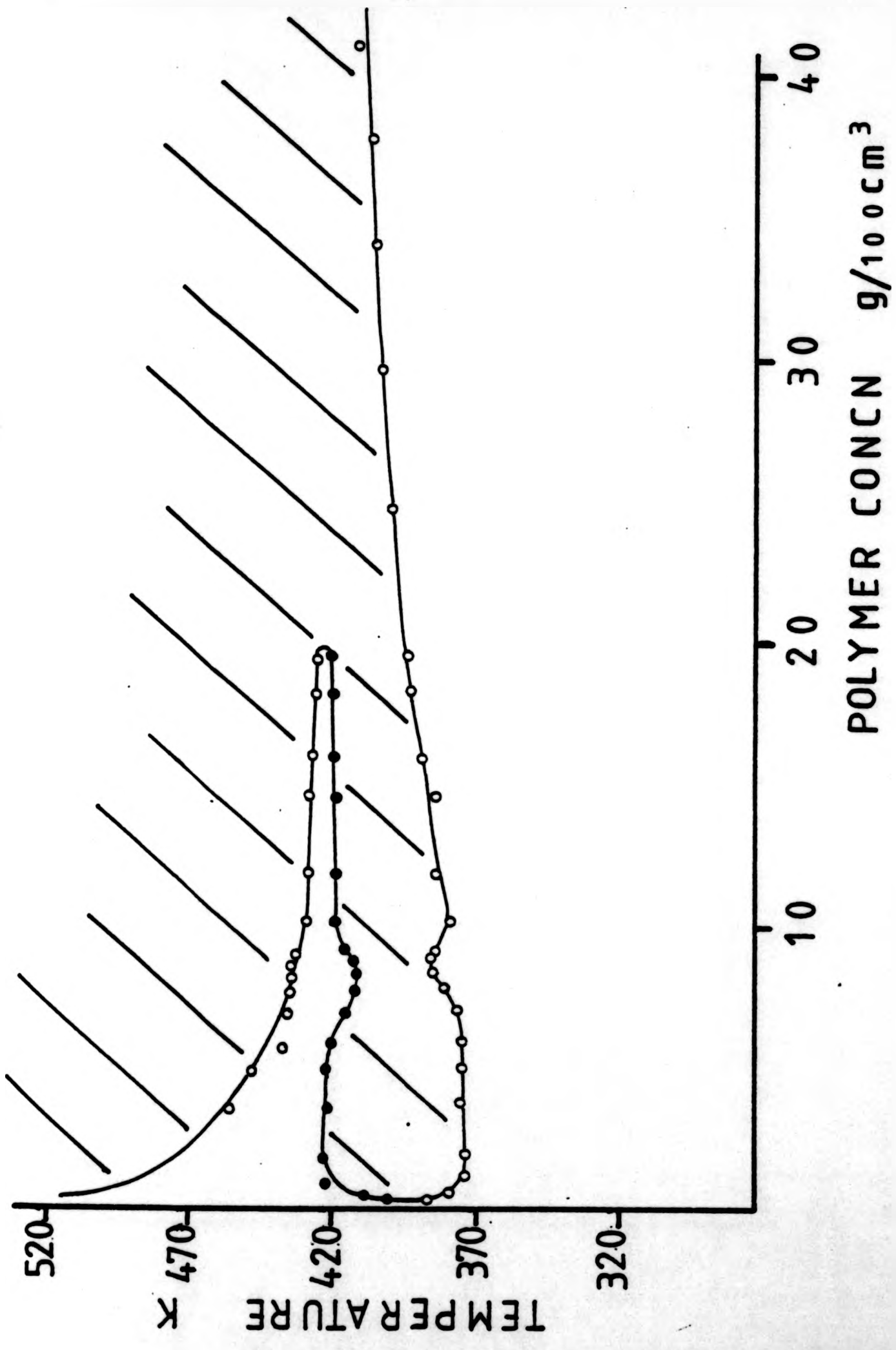
FIG 3.3 : Cloud point curve for poly(acrylic acid) PAA20 in dioxane.

69
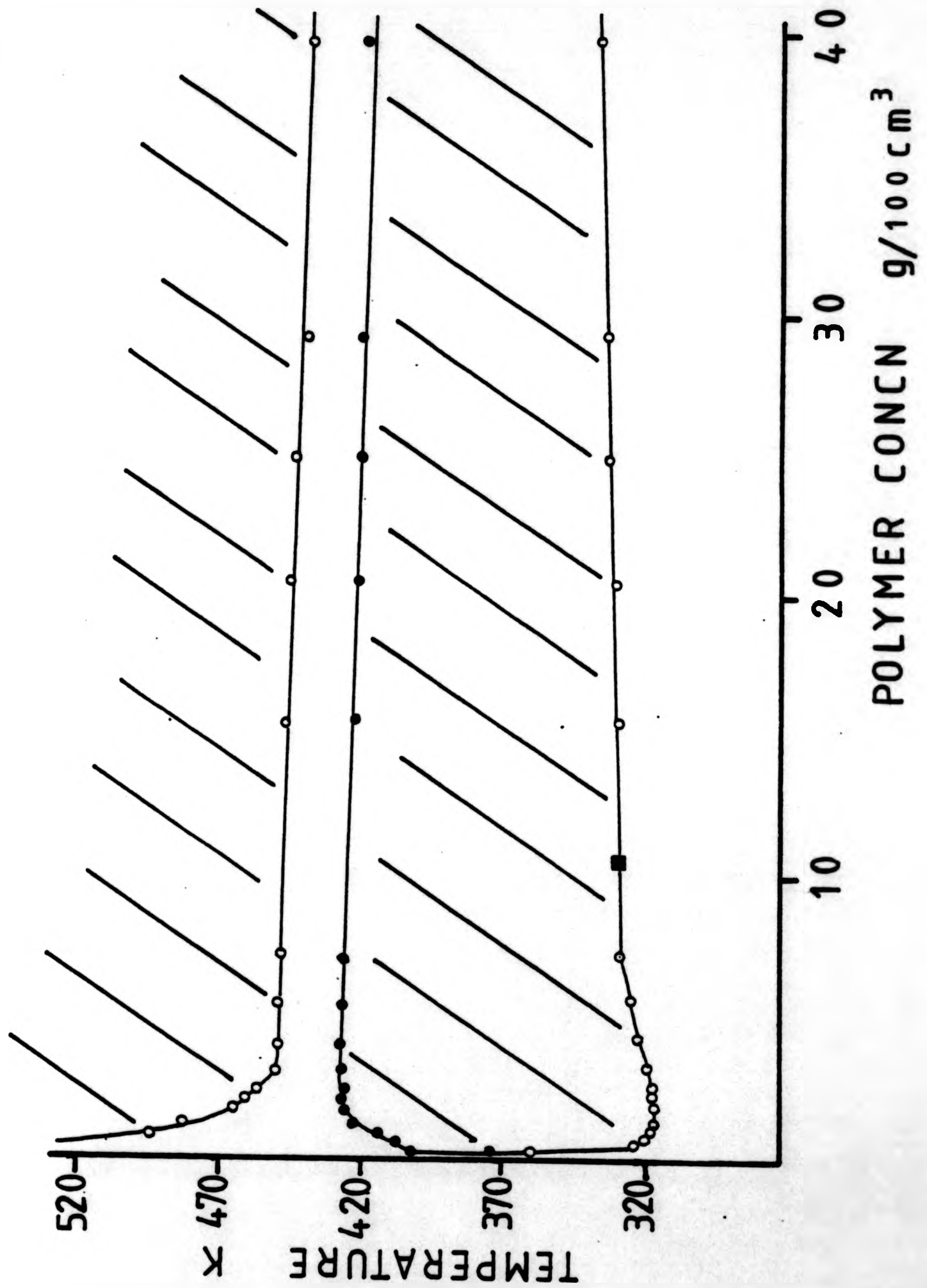
FIG 3.4 : Cloud point curve for poly(acrylic acid) PAA50 in dioxane.
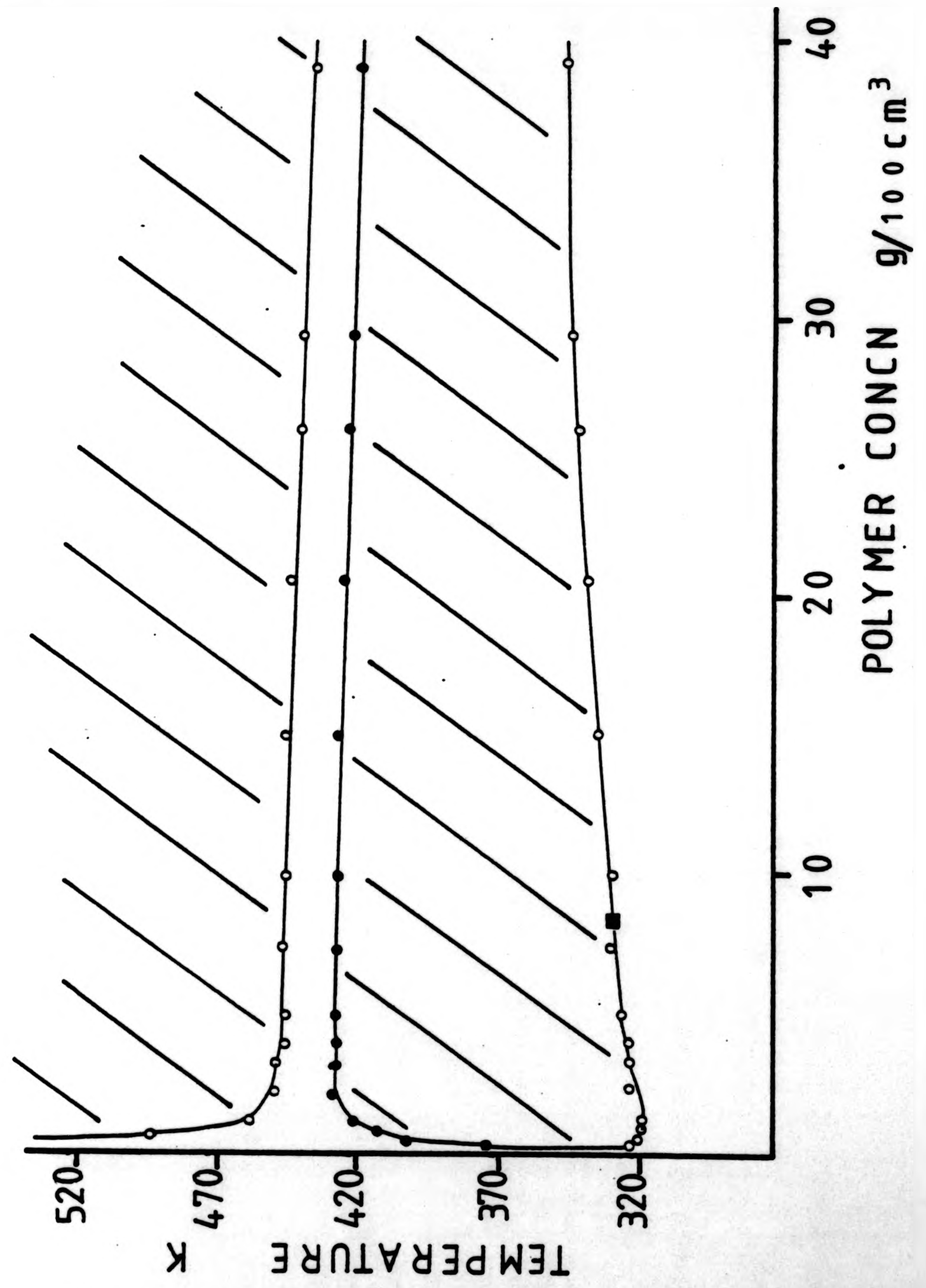
FIG 3.5 : Cloud point curve for poly(acrylic acid) PAA90 in dioxane.
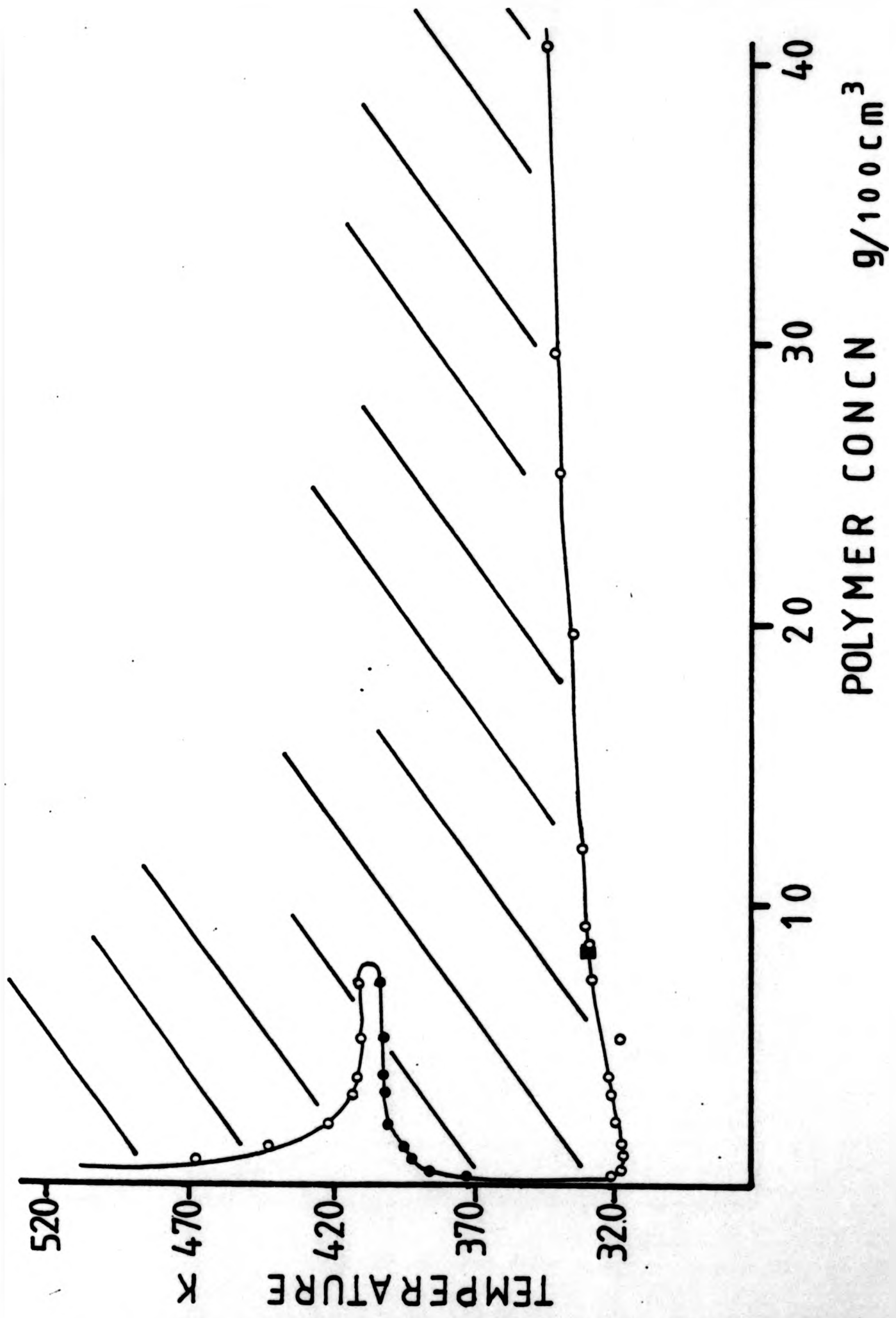
FIG 3.6 : Cloud point curve for poly(acrylic acid) PAA150 in dioxane.
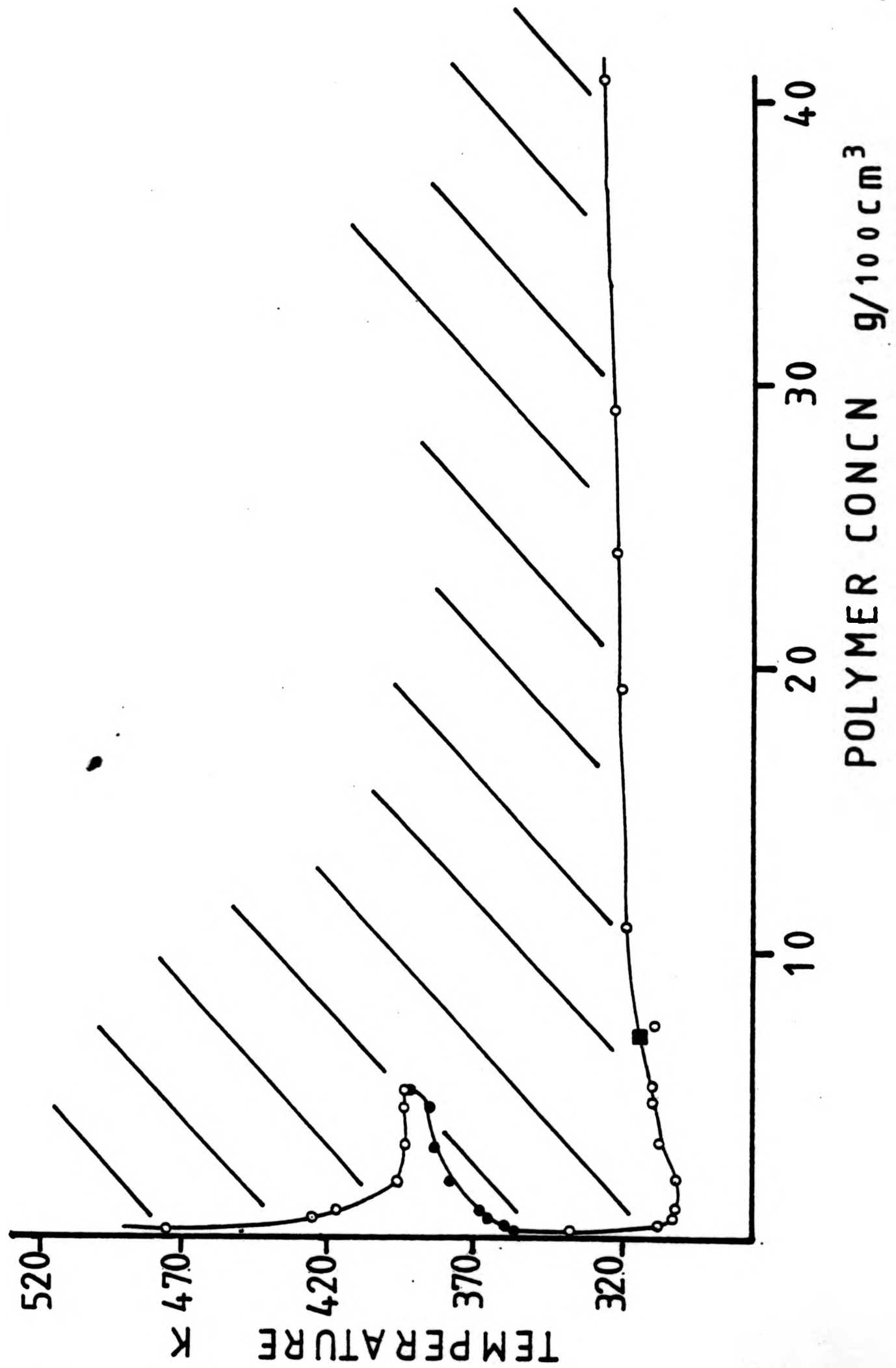
FIG 3.7 : Cloud point curve for poly(acrylic acid) PAA300 in dioxane.
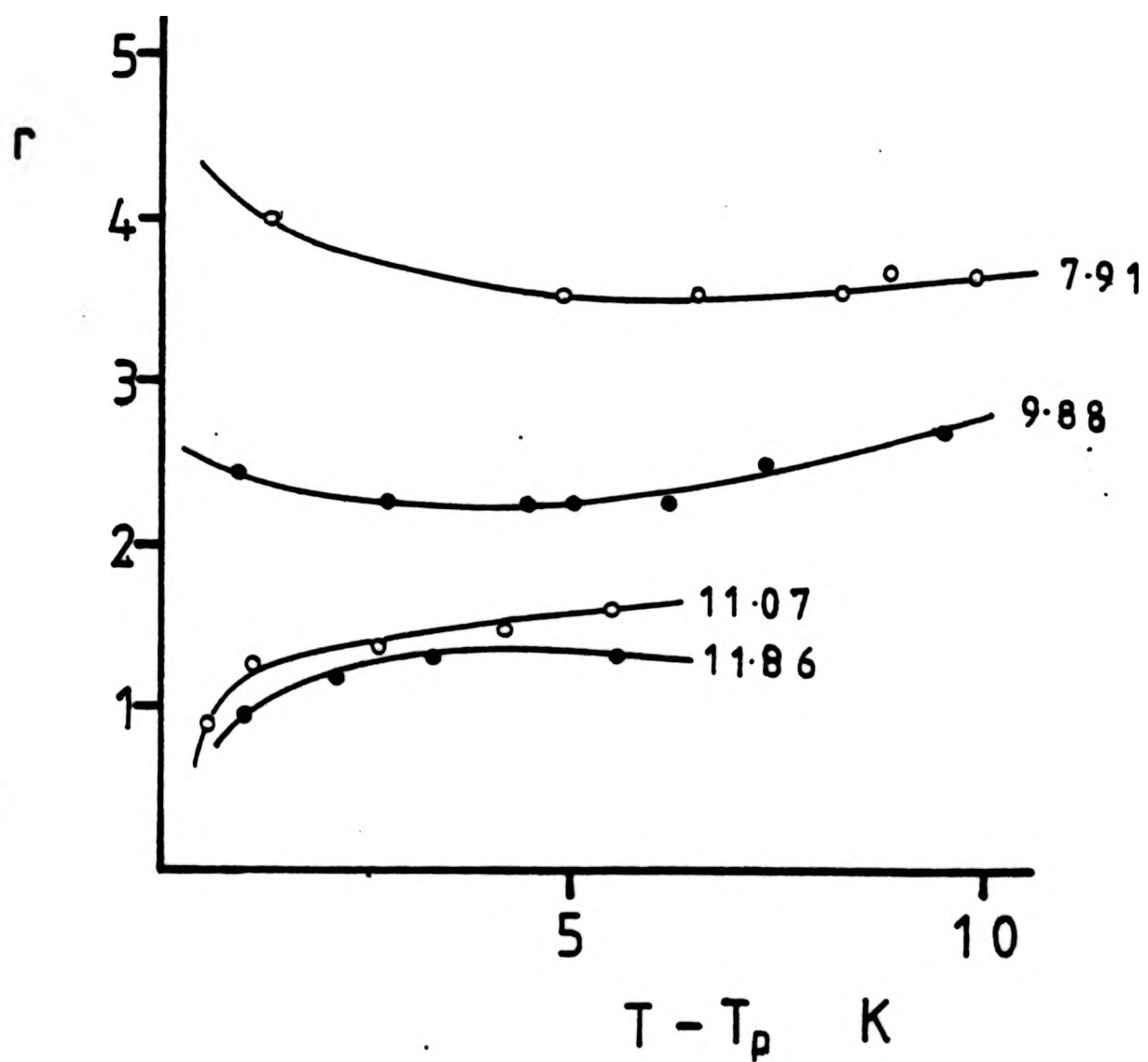
FIG 3.8 : Phase volume ratio, r, against T-T$_p$ for
poly(acrylic acid) PAA50 in dioxane.
(concn as indicated, g/100cm^3).
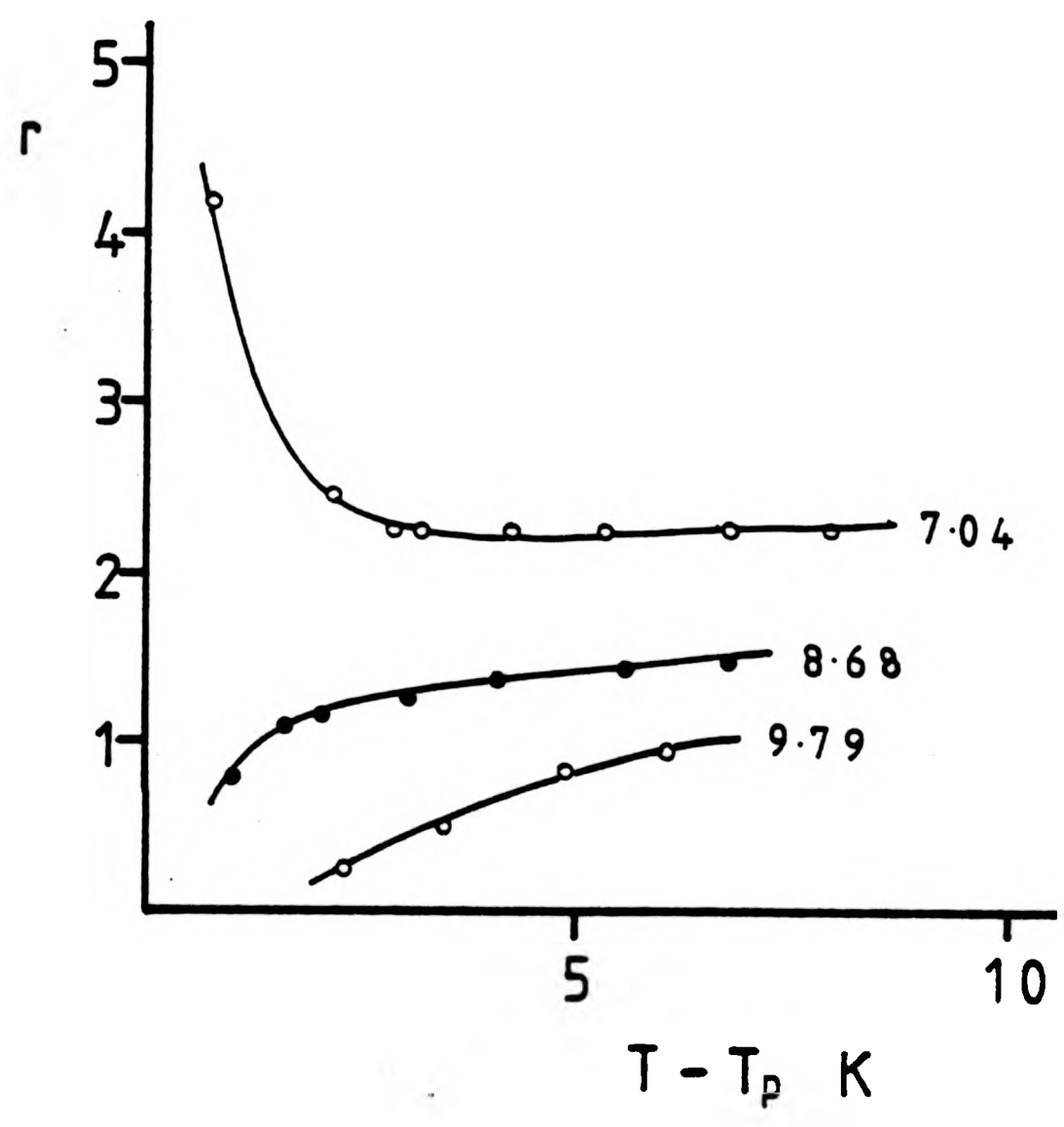
FIG 3.9 : Phase volume ratio, r, against $T-T_p$ for
poly(acrylic acid) PAA90 in dioxane.
(concn as indicated, $g/100cm^3$).
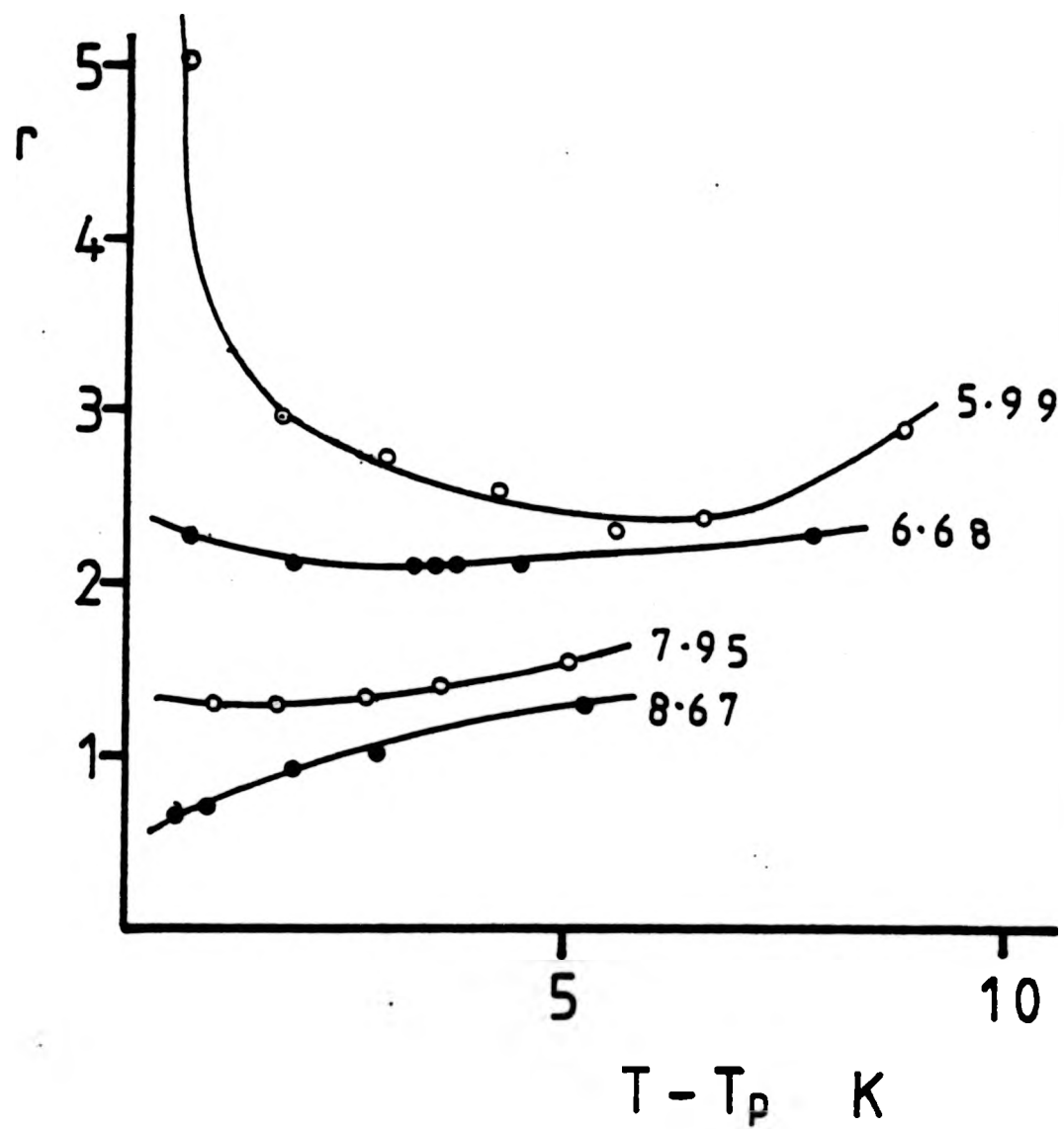
FIG 3.10 : Phase volume ratio, r, against T-T$_p$ for
poly(acrylic acid) PAA150 in dioxane.
(concn as indicated, g/100cm^3).
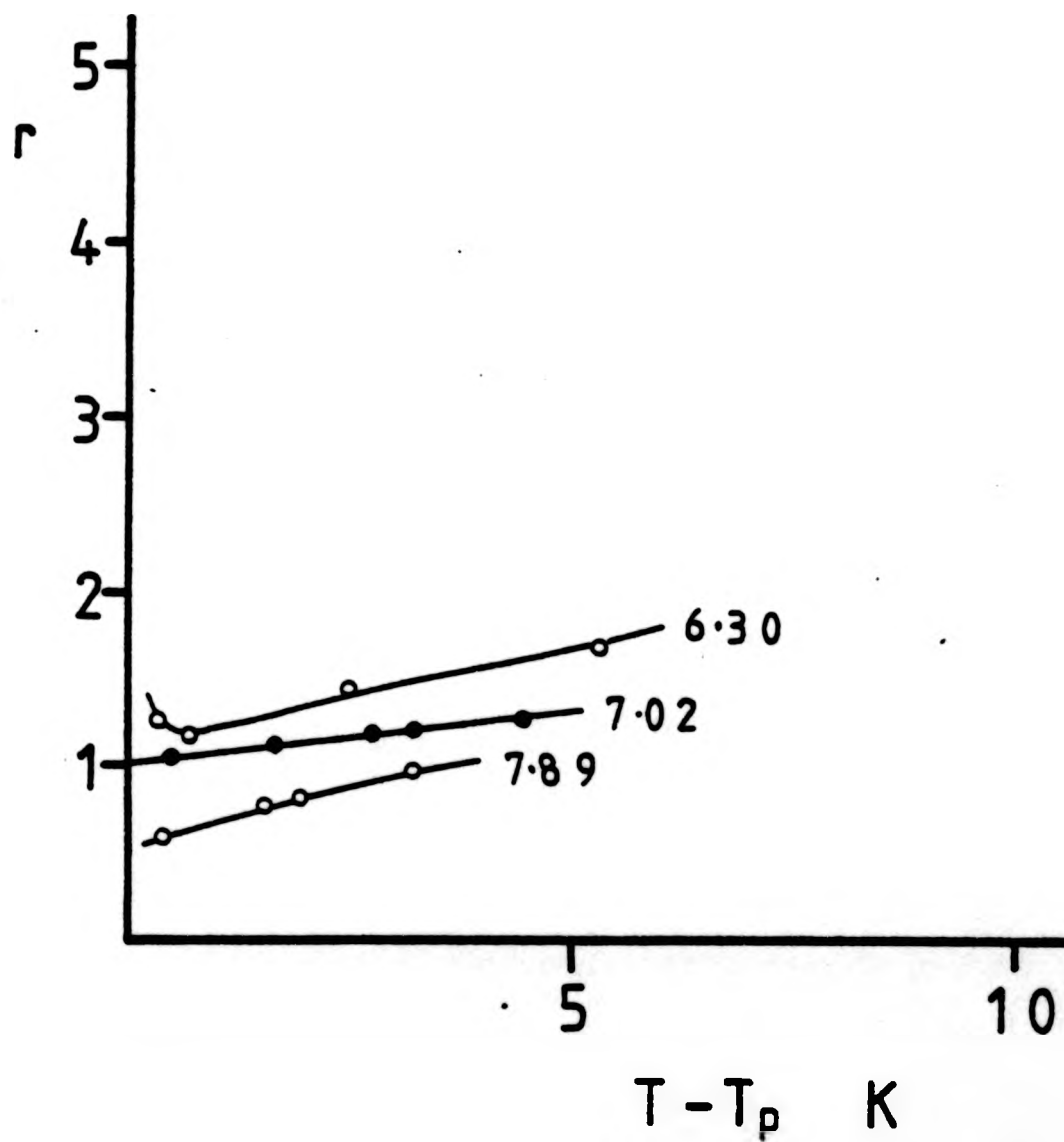
FIG 3.11 : Phase volume ratio, r, against $T-T_p$ for
poly(acrylic acid) PAA300 in dioxane.
(concn as indicated, $g/100cm^3$).
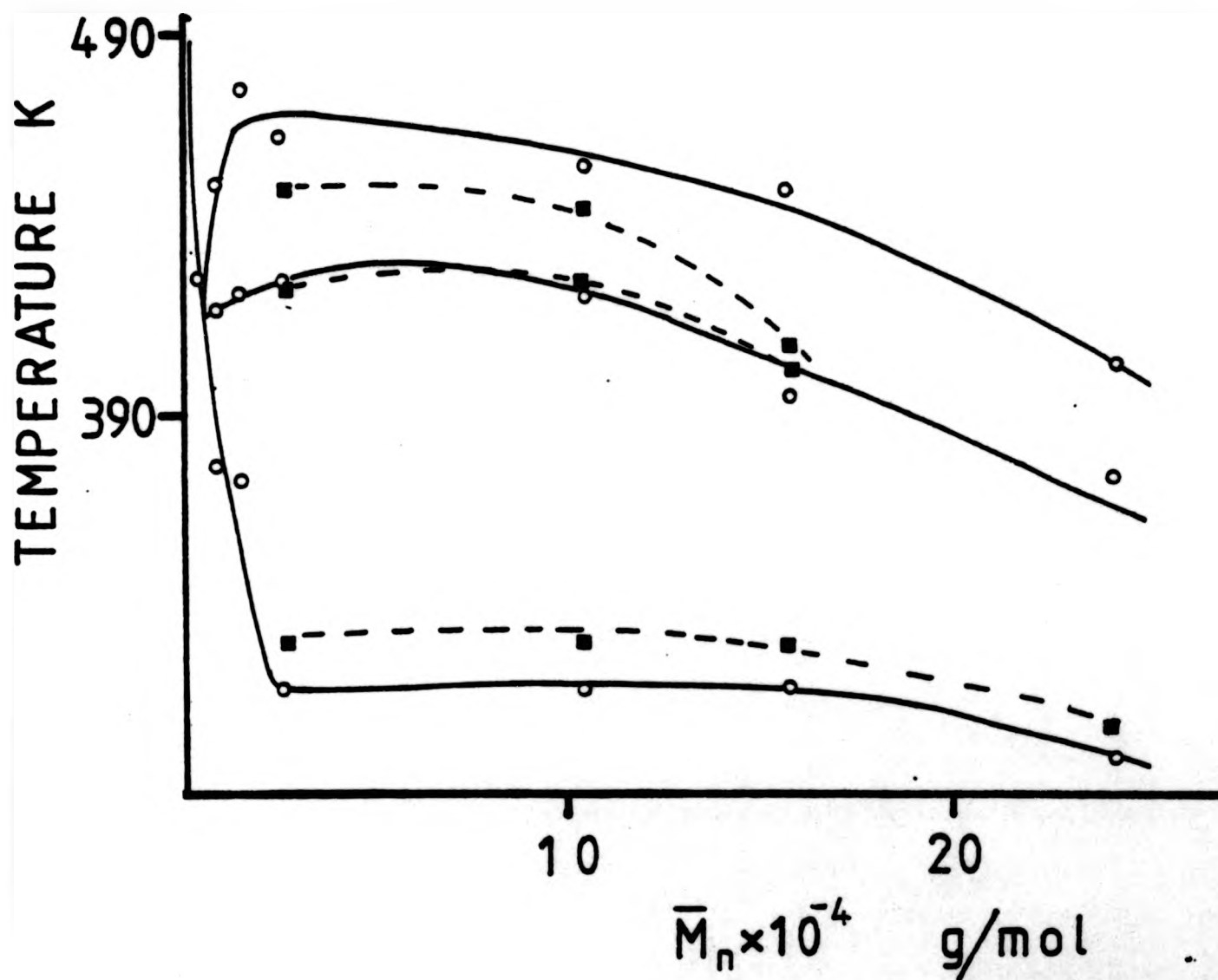
FIG 3.12 : Temperatures of phase separation T_{pm} (o) and T_c (■) of polymer concentrations C_{pm} and C_c as a function of $\bar{M}_n$ for poly(acrylic acid) in dioxane.
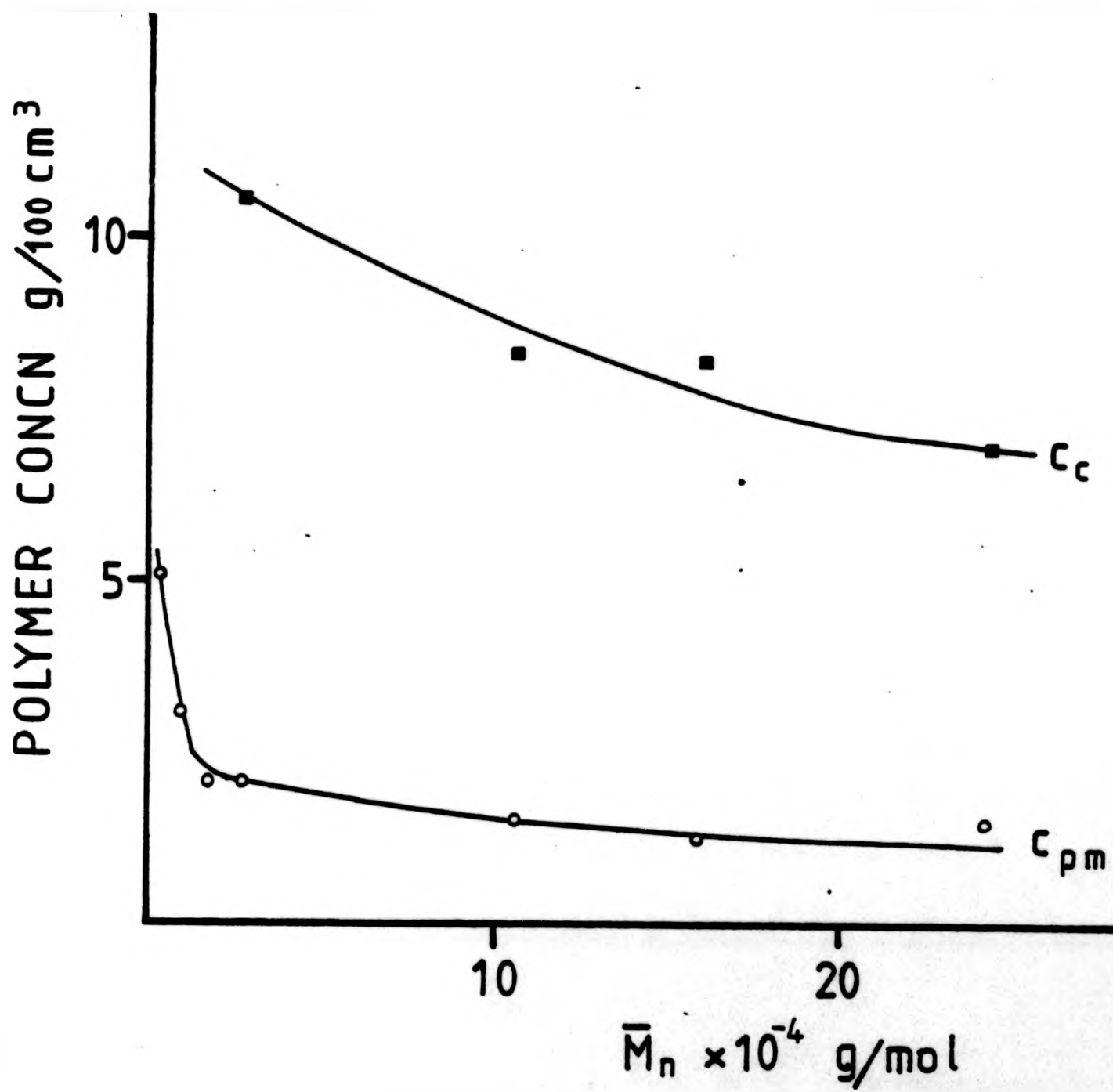
FIG 3.13 : Polymer concentrations C_{pm} (o) and C_c (■) as a function of $\overline{M}_n$ for poly(acrylic acid) in dioxane.
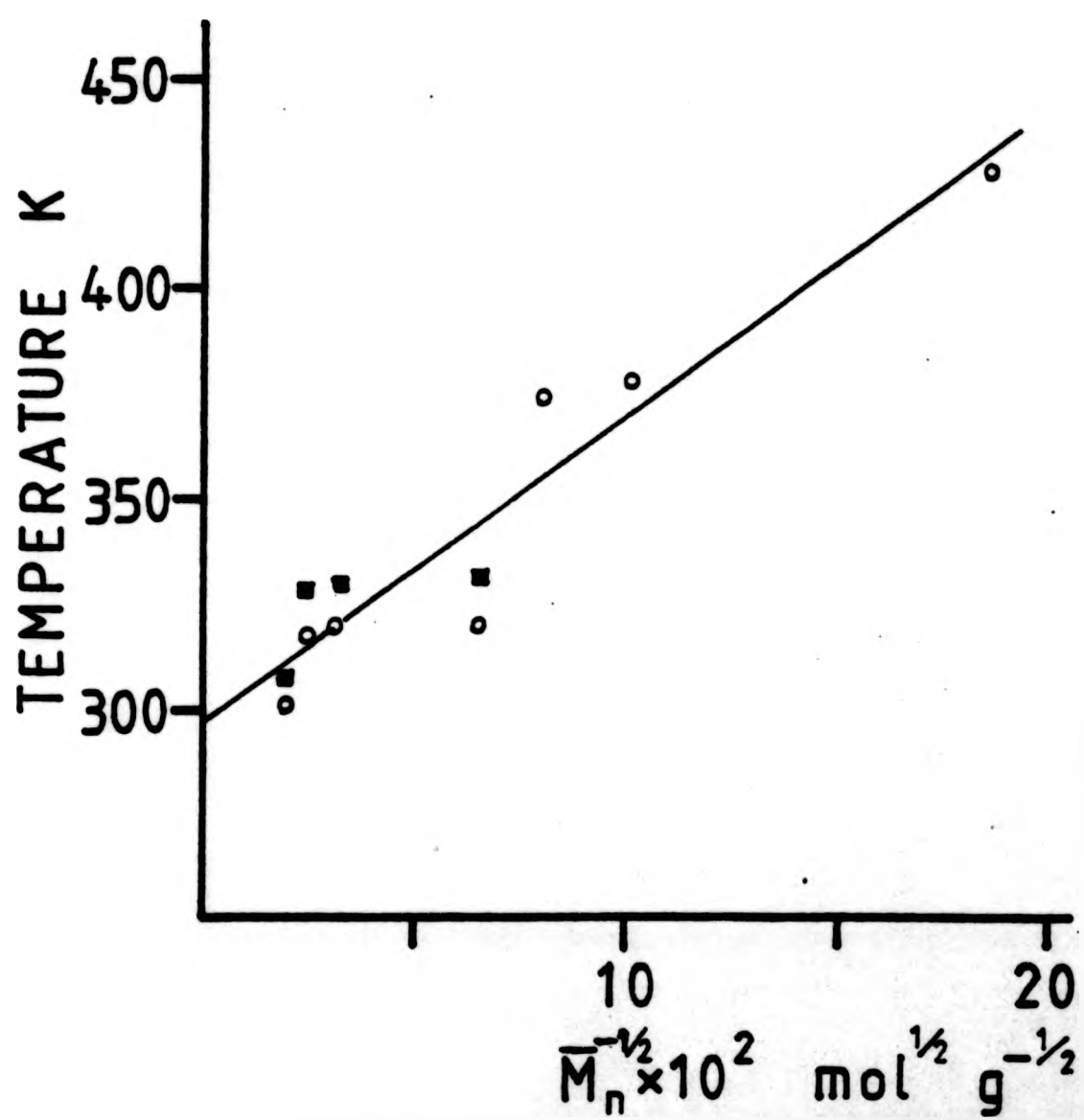
FIG 3.14 : Temperatures of phase separation T_{pm} (o) and T_c (■) as
a function of $\overline{M}_n^{-\frac{1}{2}}$ for poly(acrylic acid) in dioxane.
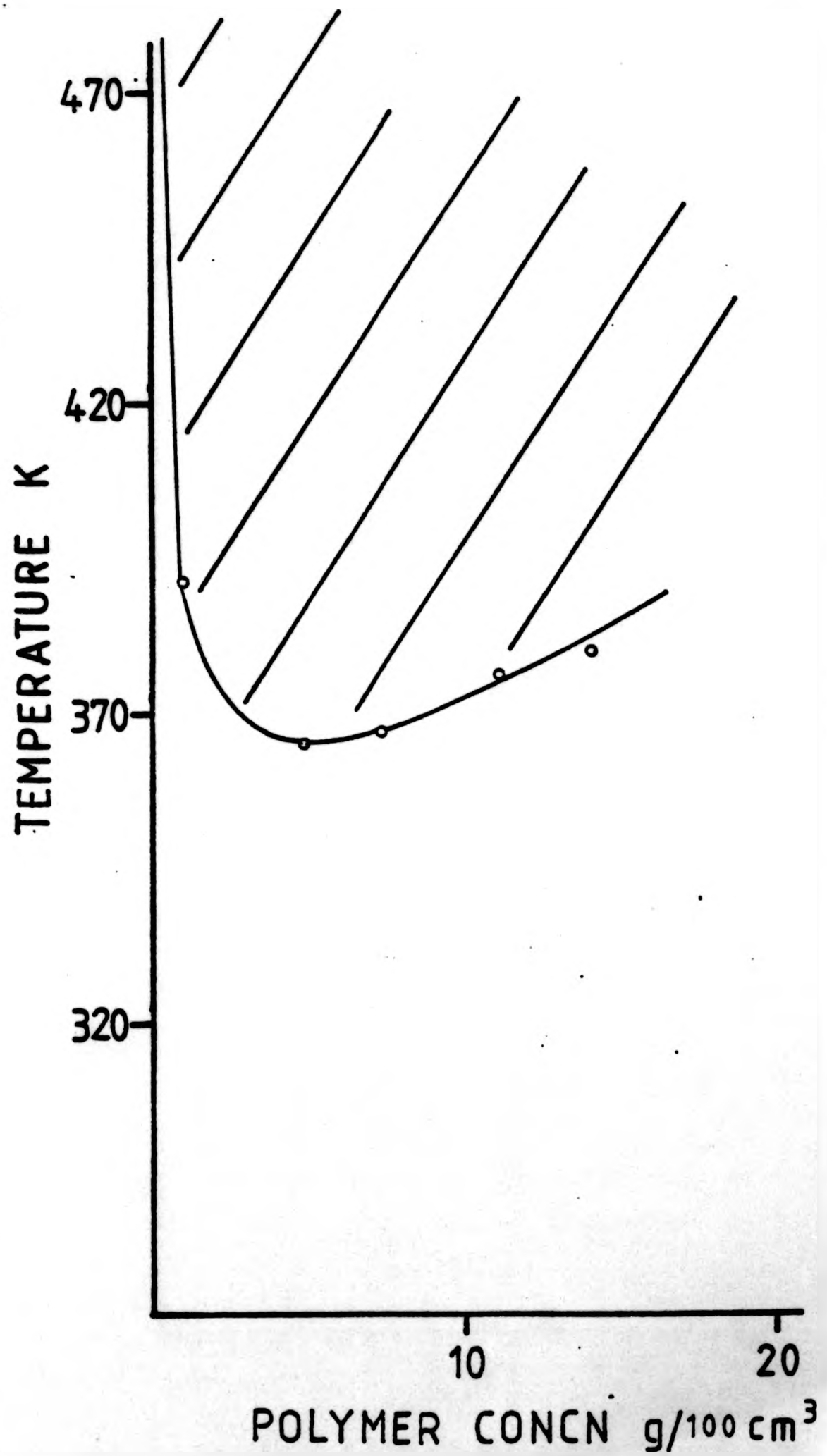
FIG 3.15 : Cloud point curve for poly(acrylic acid) PAA5 in
tetrahydrofuran.
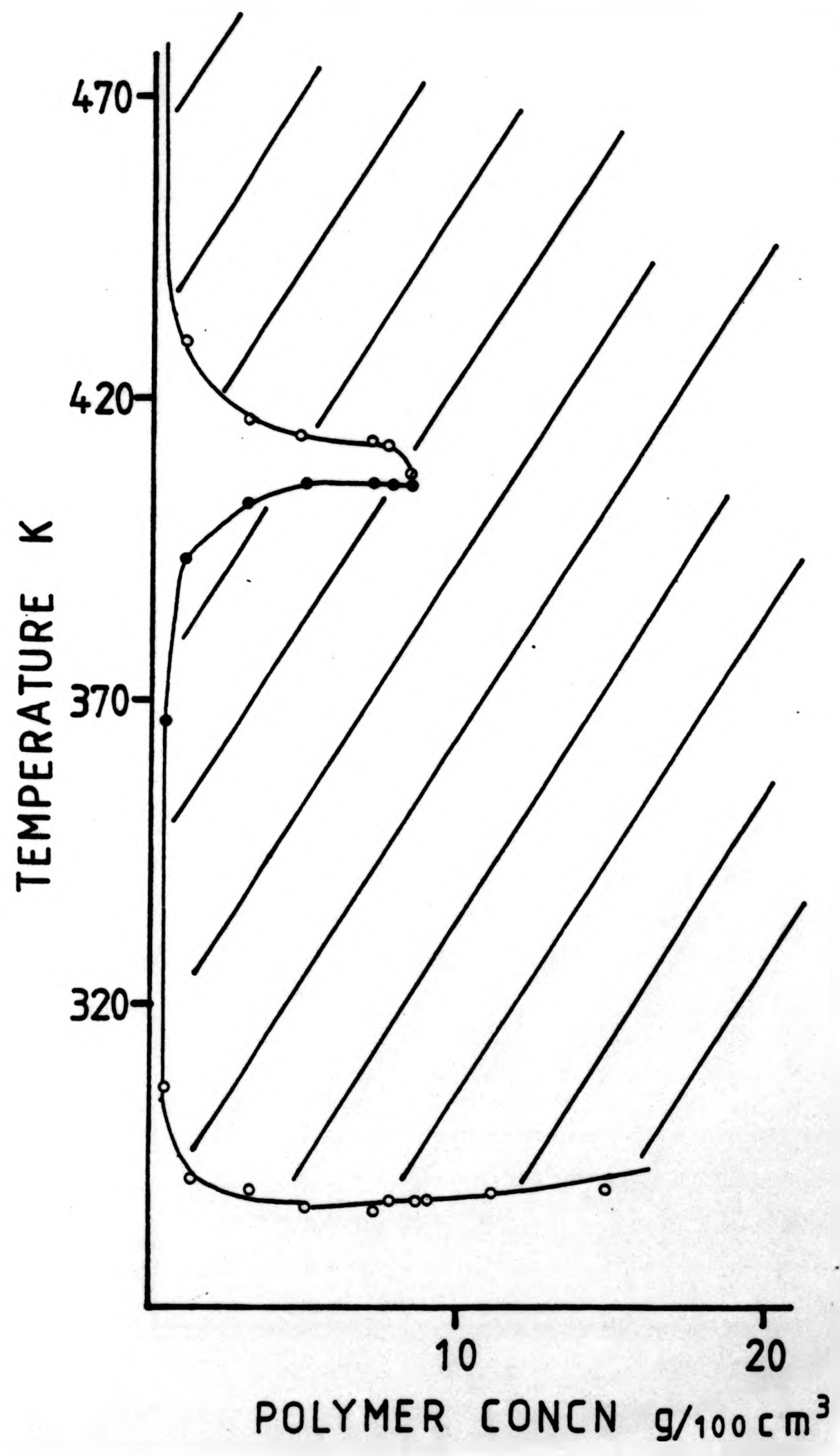
FIG 3.16 : Cloud point curve for poly(acrylic acid) PAA50 in
tetrahydrofuran.
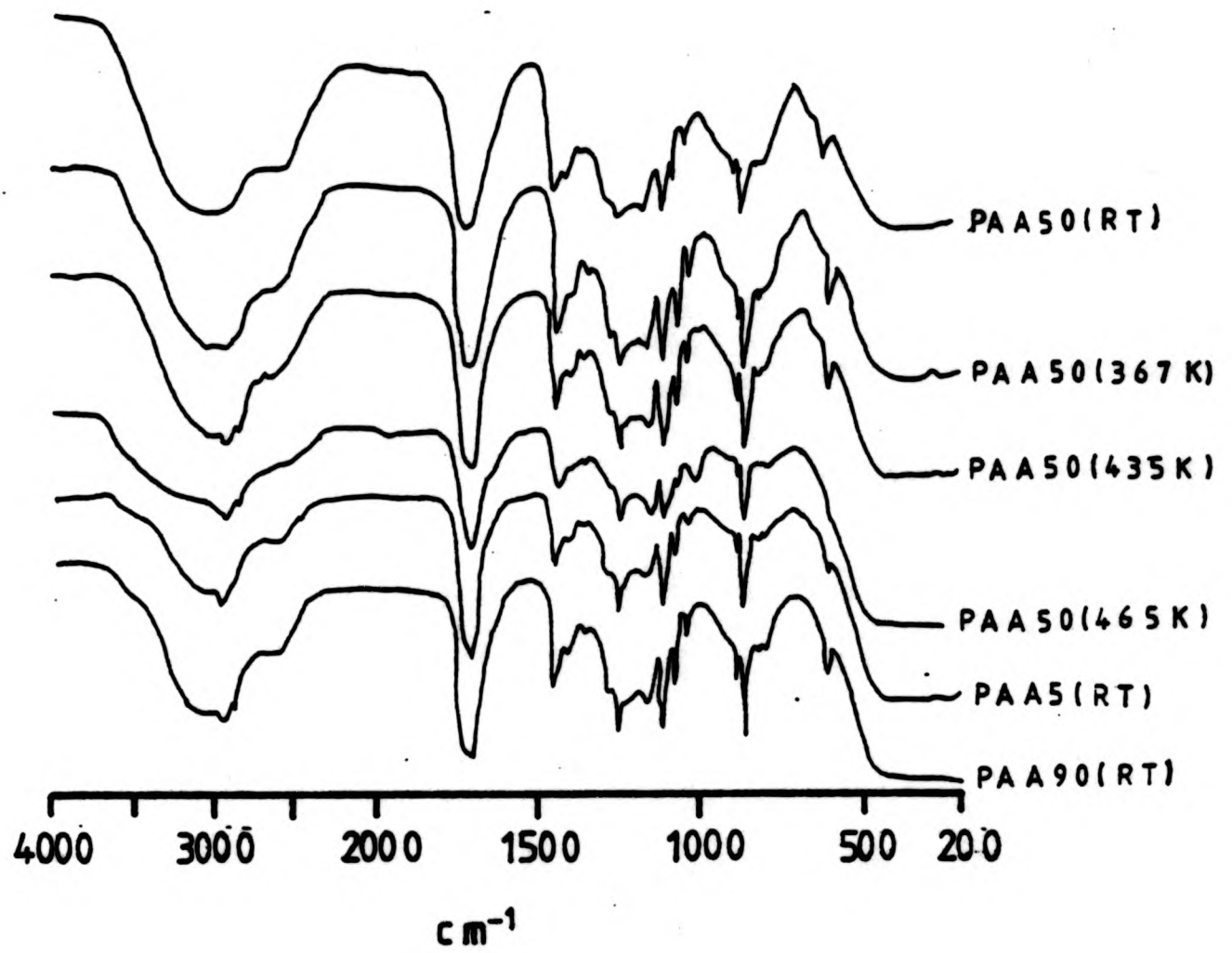
FIG 3.17 : ir spectra for poly(acrylic acid) (as indicated).
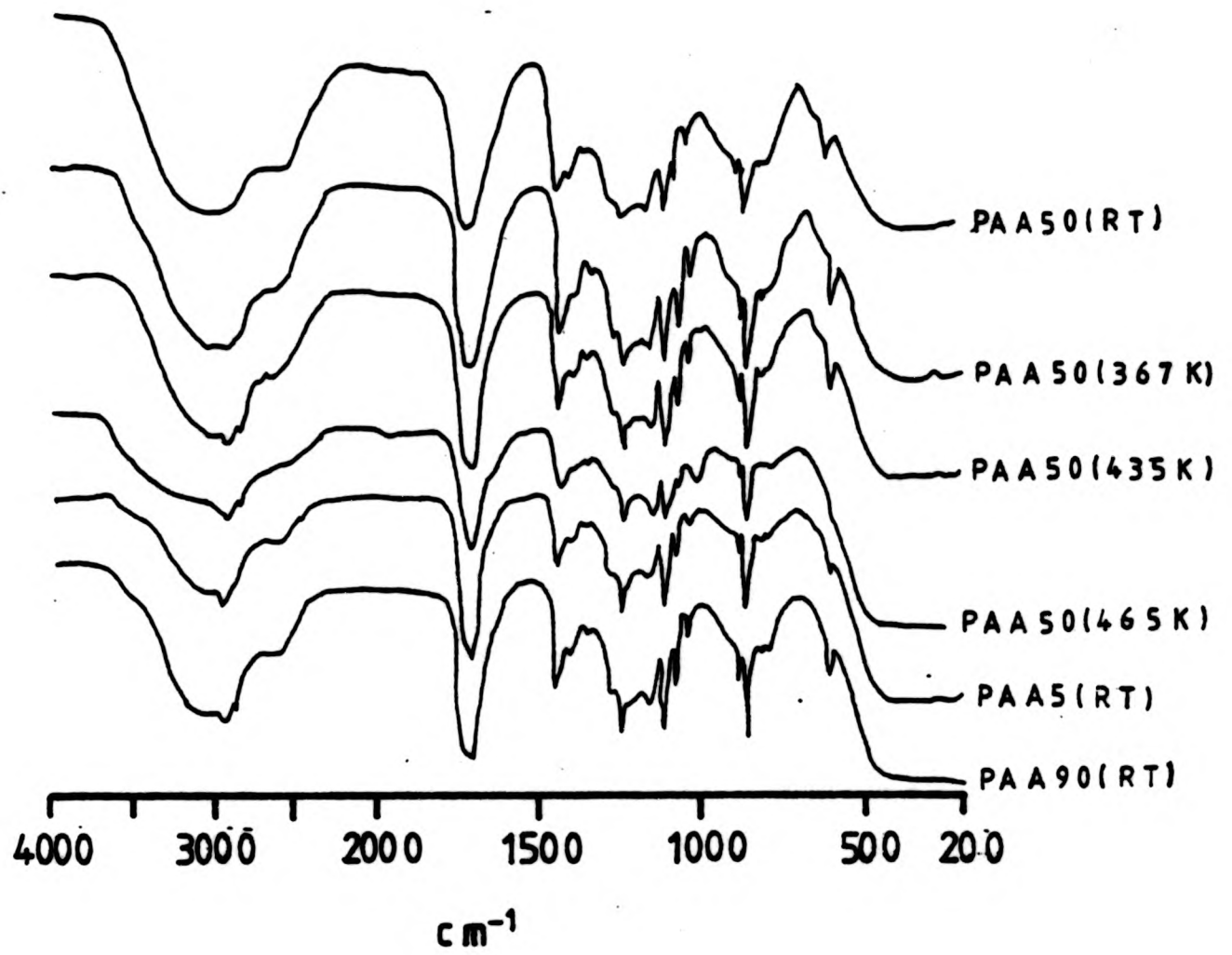
FIG 3.17 : ir spectra for poly(acrylic acid) (as indicated).
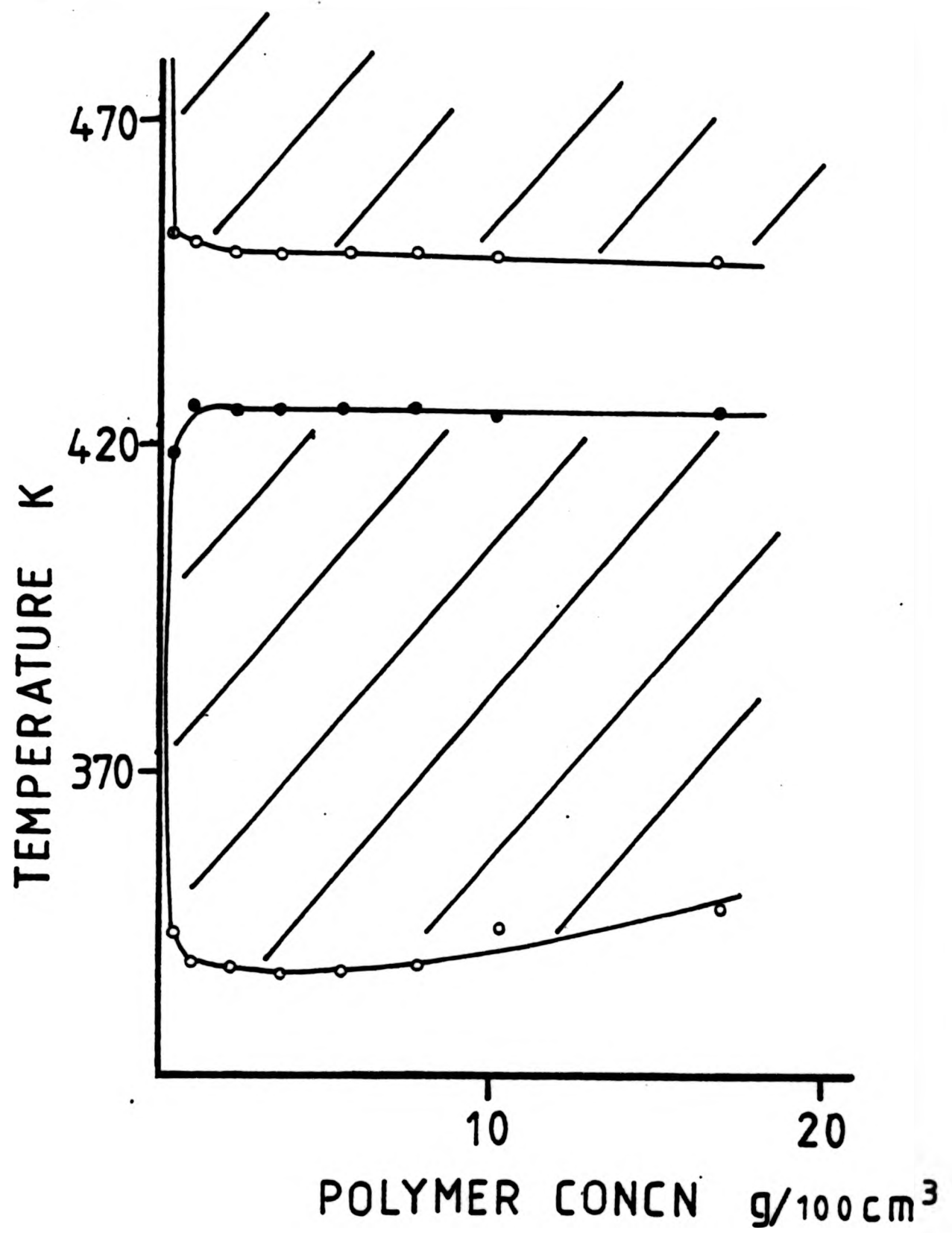
FIG 3.18 : Cloud point curve for poly(acrylic acid) PAA50 in dioxane/1.02(wt/vol)% water.
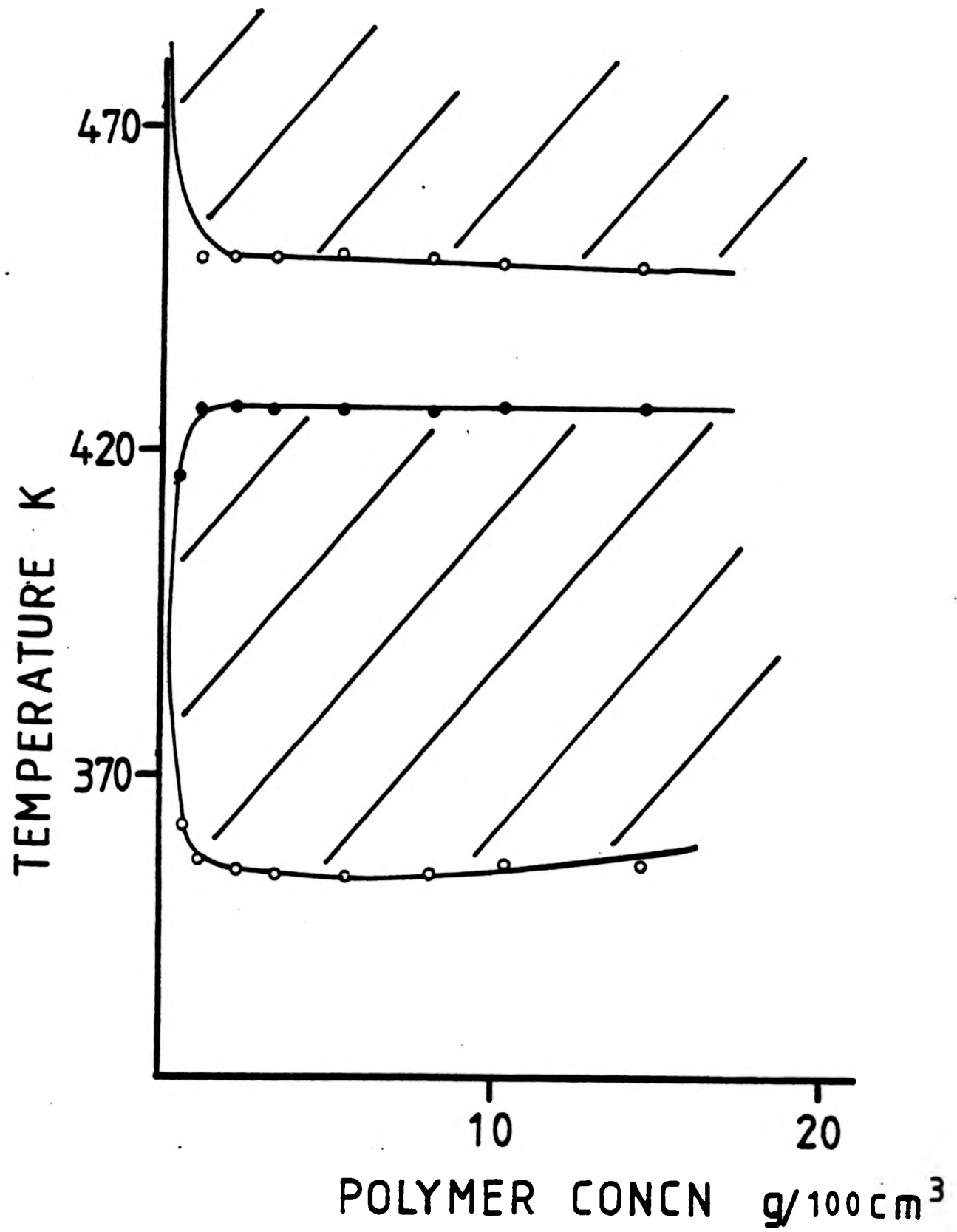
FIG 3.19 : Cloud point curve for poly(acrylic acid) PAA50 in
dioxane/2.52(wt/vol)% water.
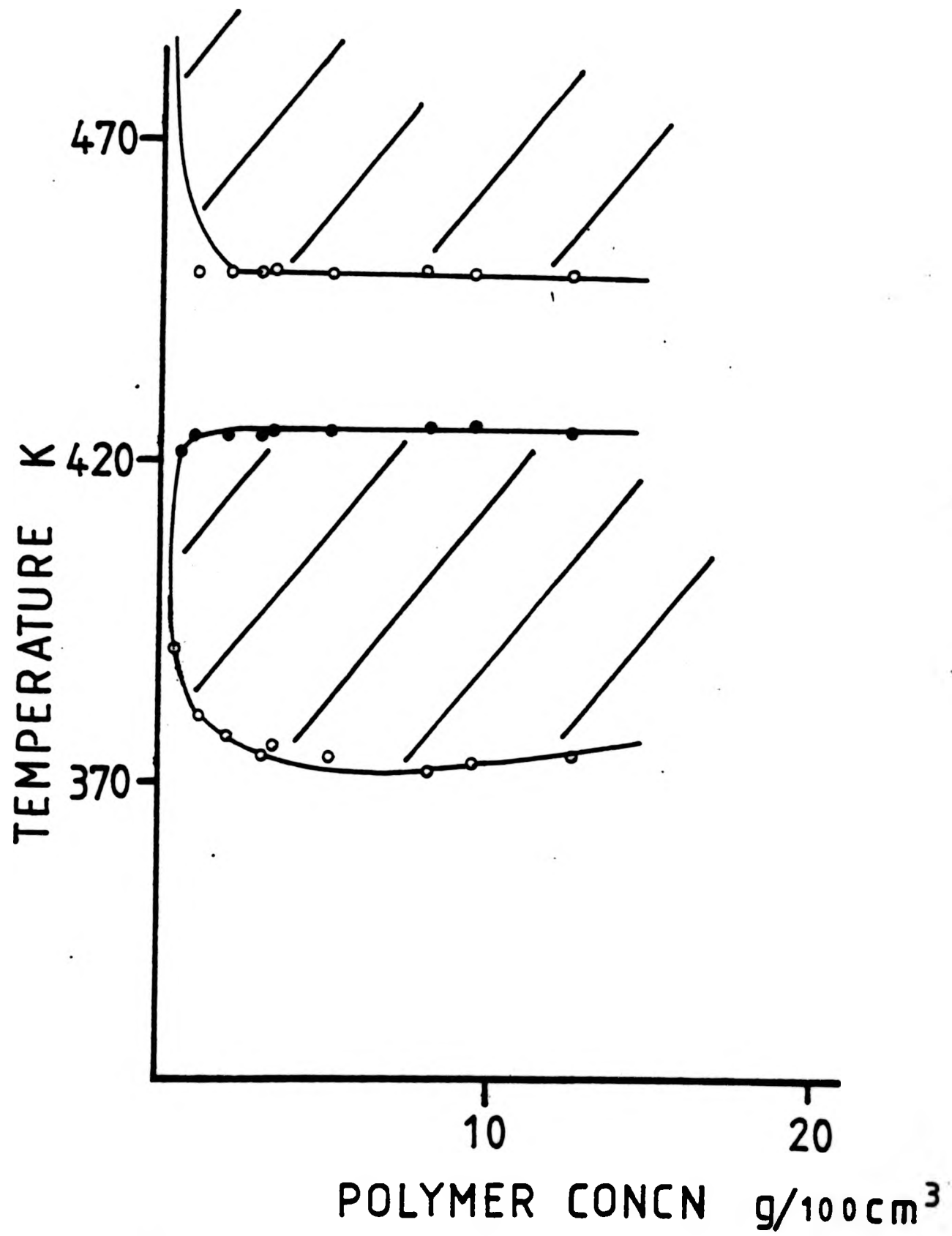
FIG 3.20 : Cloud point curve for poly(acrylic acid) PAA50 in
dioxane/4.99(wt/vol)% water.
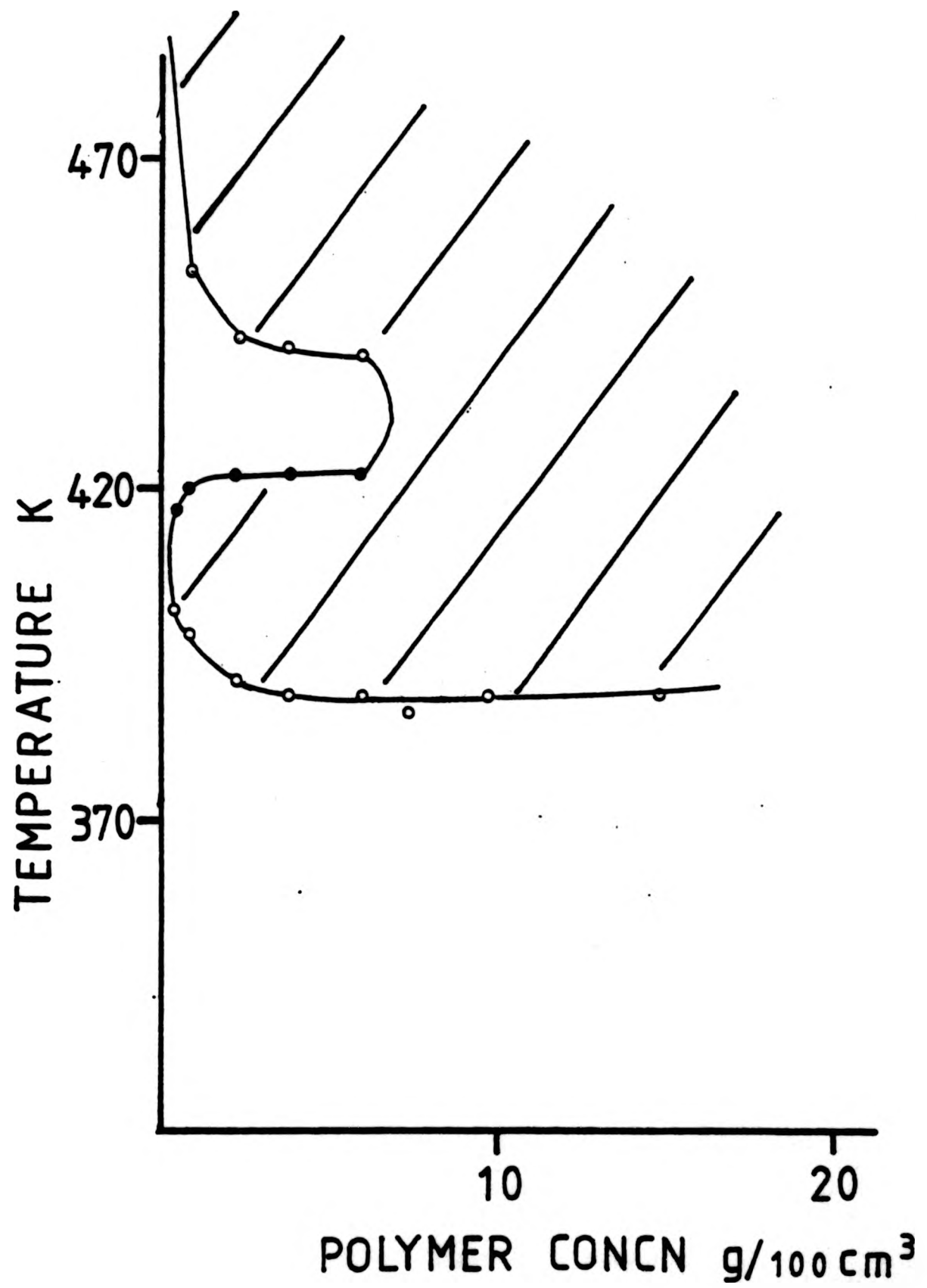
FIG 3.21 : Cloud point curve for poly(acrylic acid) PAA50 in
dioxane/7.49(wt/vol)% water.
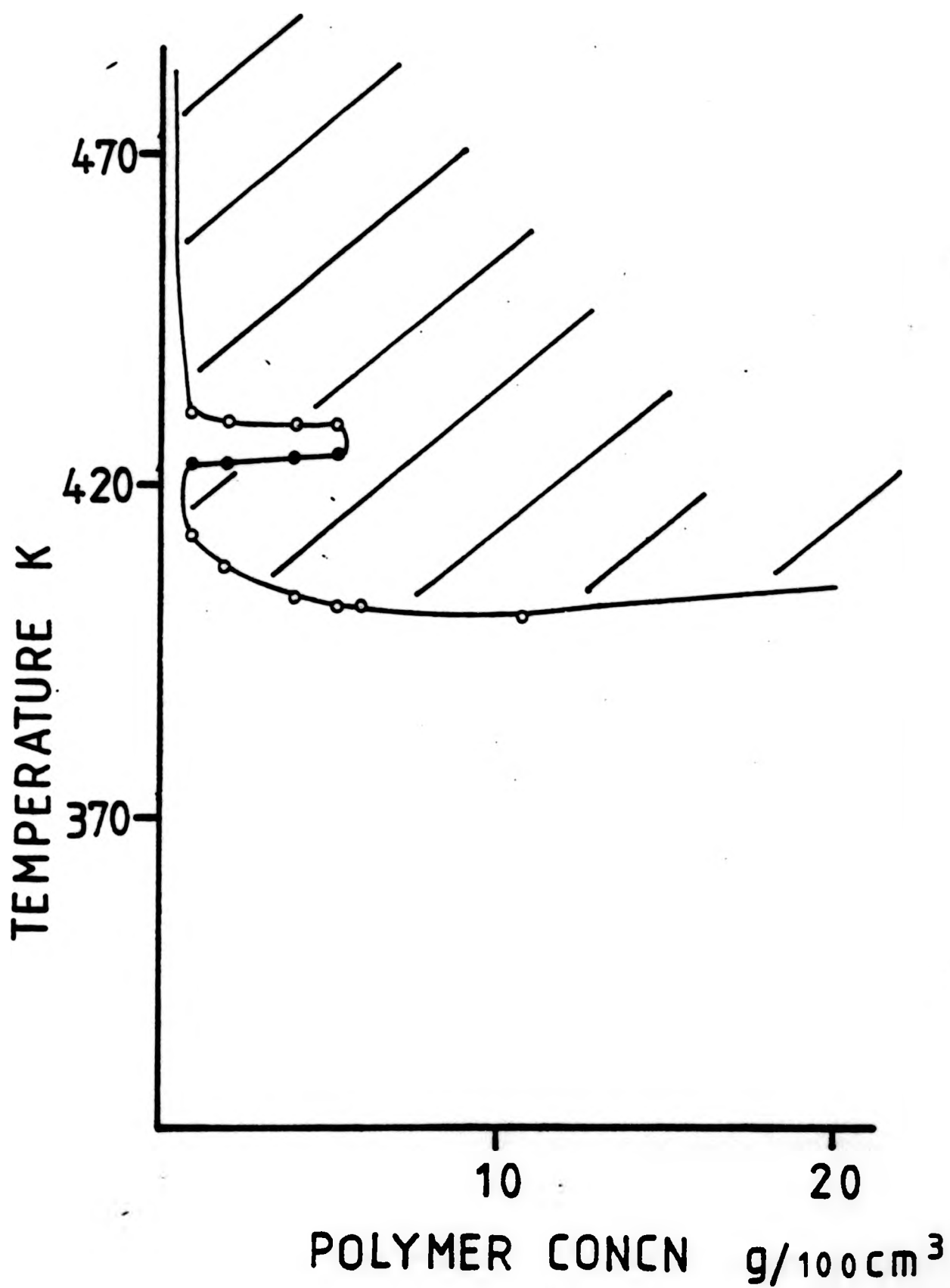
FIG 3.22 : Cloud point curve for poly(acrylic acid) PAA50 in
dioxane/9.99(wt/vol)% water.
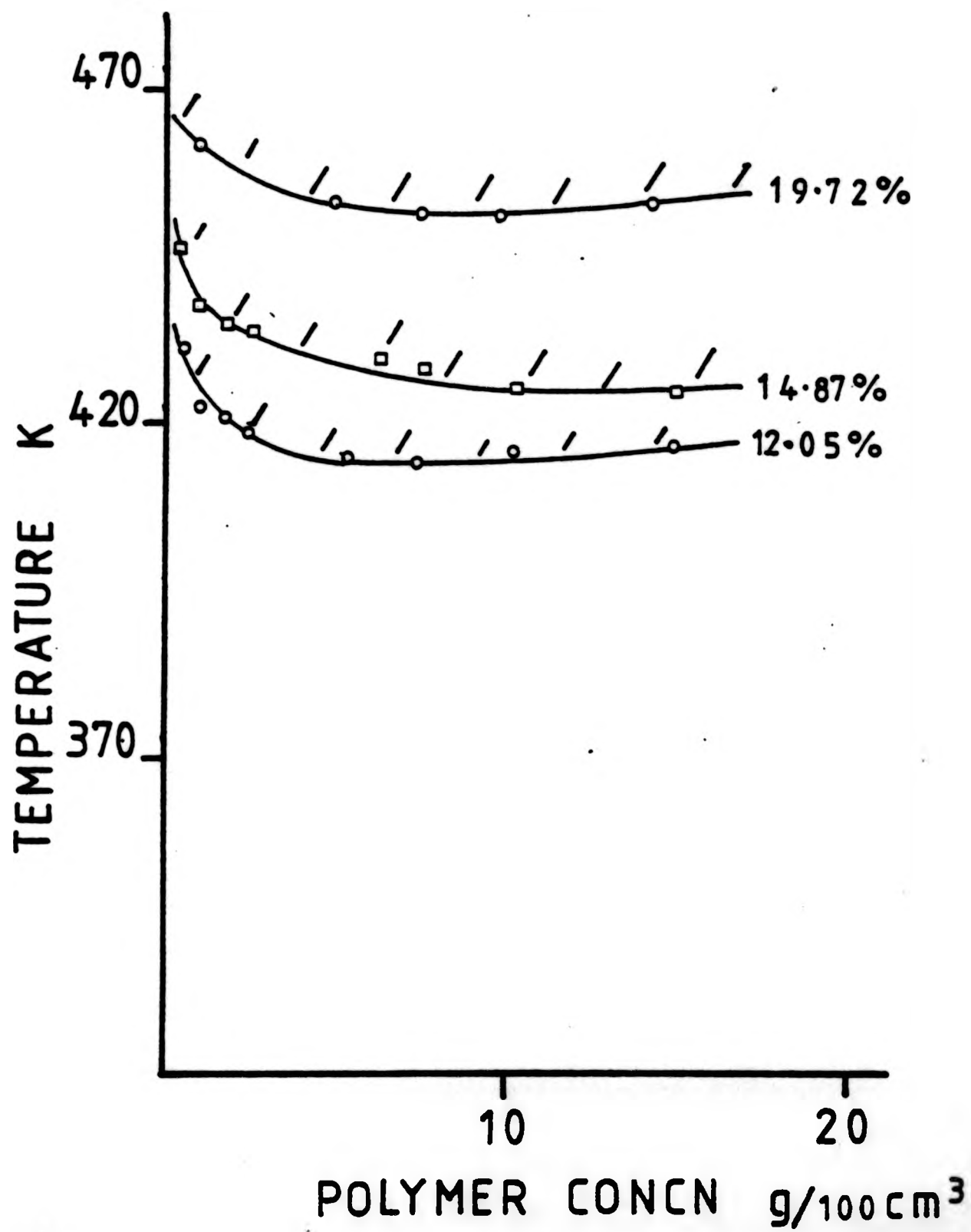
FIG 3.23 : Cloud point curve for poly(acrylic acid) PAA50 in
dioxane/water.
(water content : 12·05(o),14·87(□) and 19·72(wt/vol)%(o)).
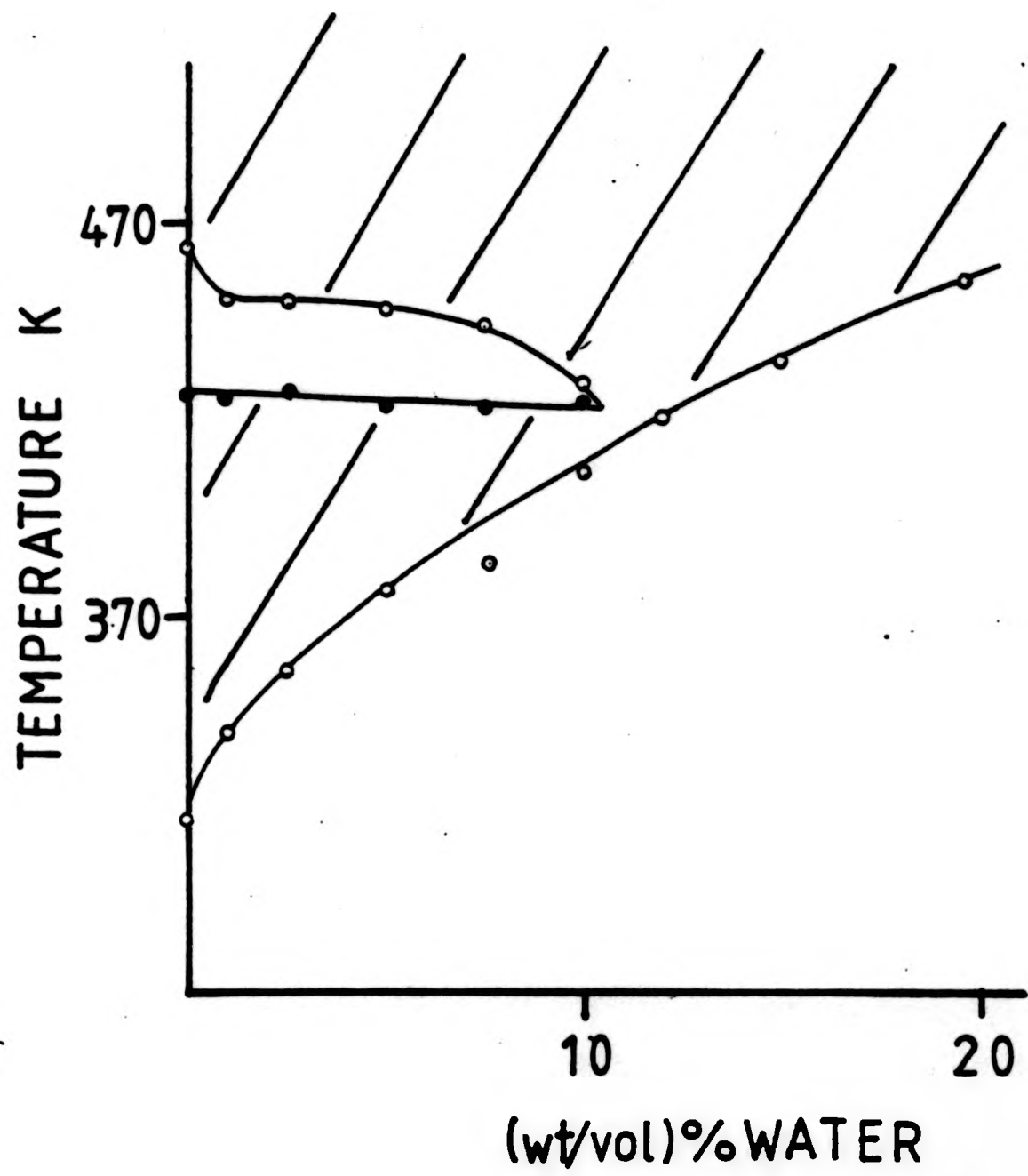
FIG 3.24 : Temperature of phase separation for poly(acrylic acid) PAA50
in dioxane/water mixtures, at $2g/100cm^3$ polymer, as a
function of water content.
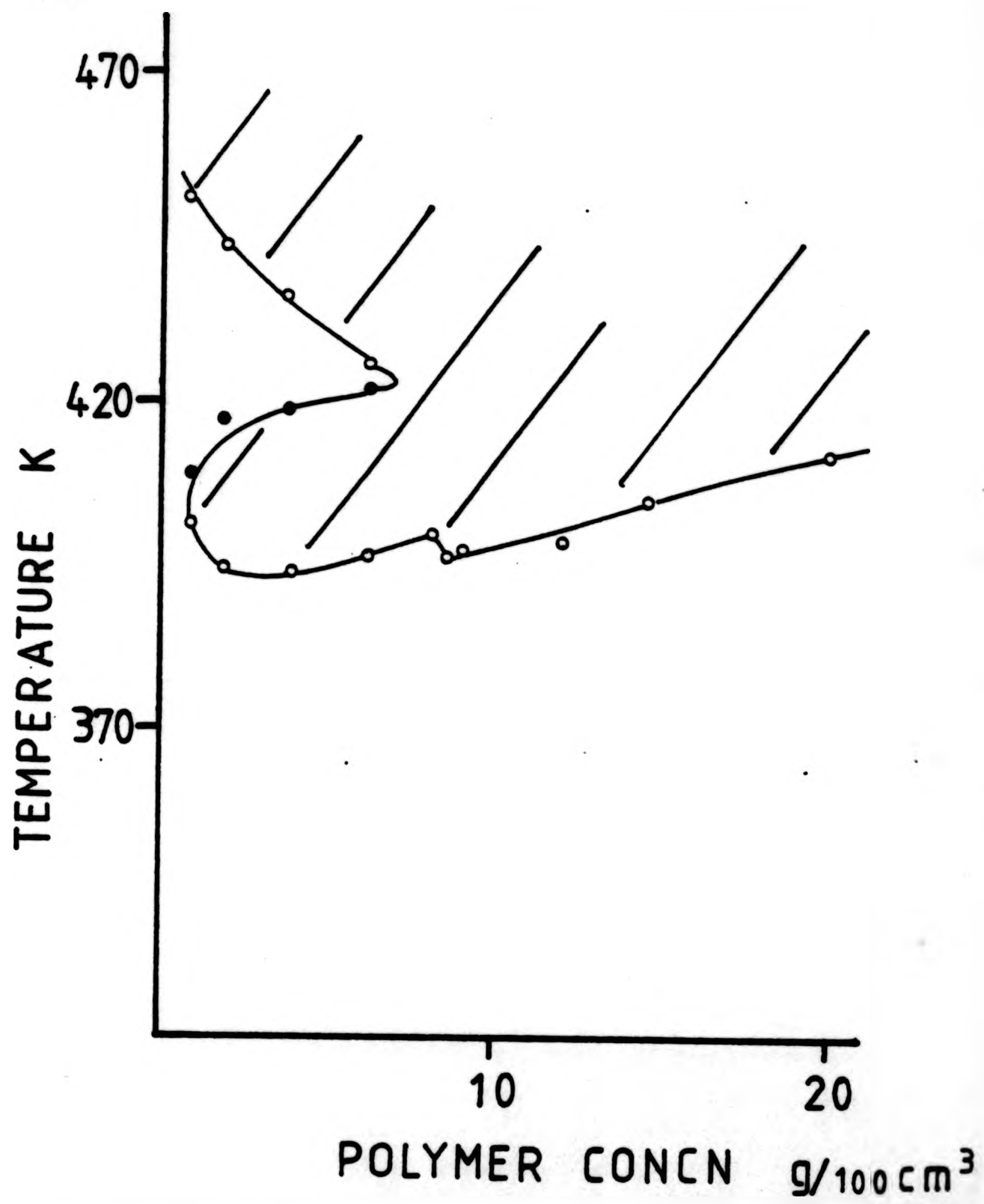
FIG 3.25 : Cloud point curve for poly(acrylic acid) PAA17 in dioxane/1.02(wt/vol)% water.
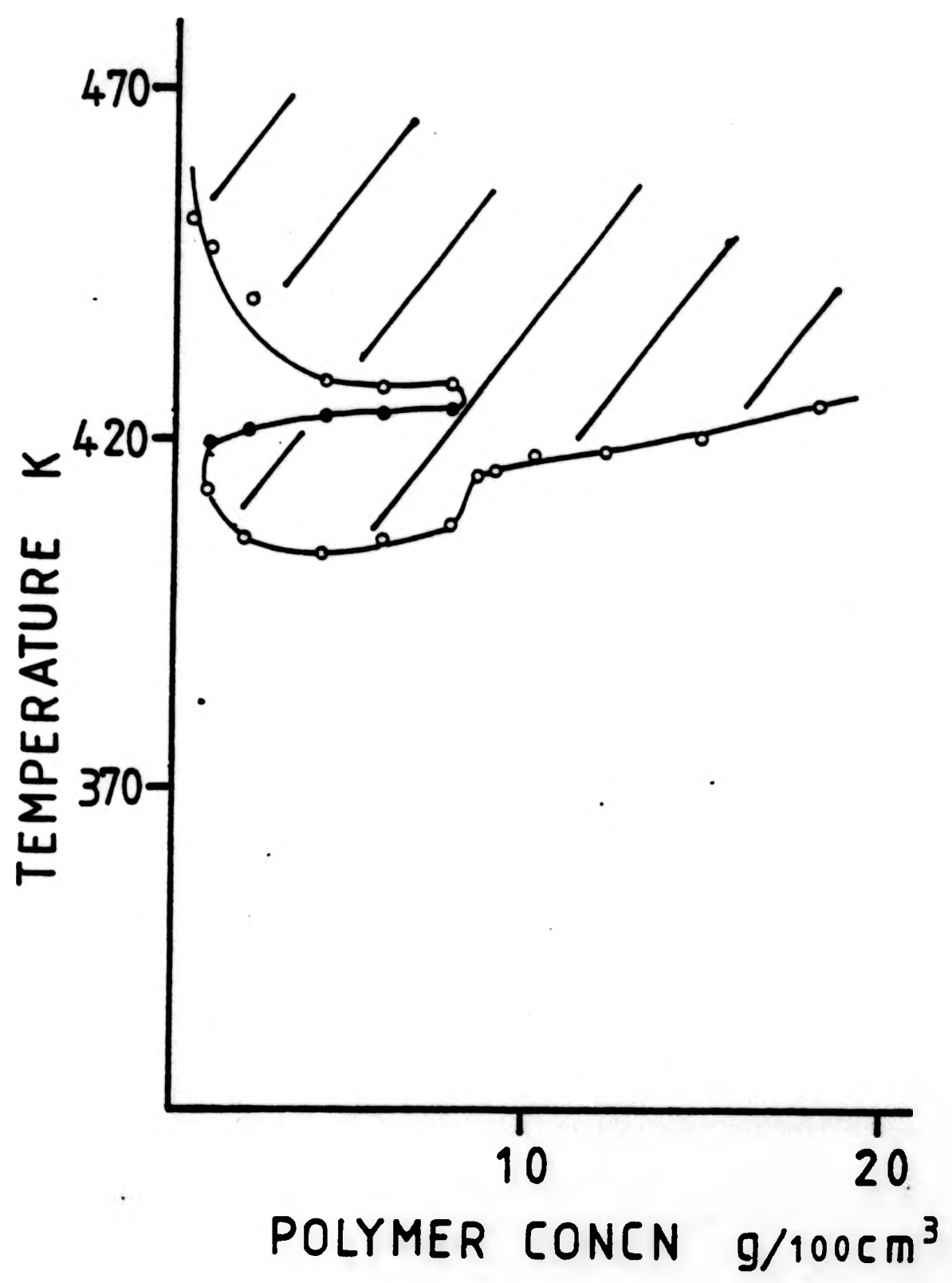
FIG 3.26 : Cloud point curve for poly(acrylic acid) PAA17 in dioxane/2.55(wt/vol)% water.
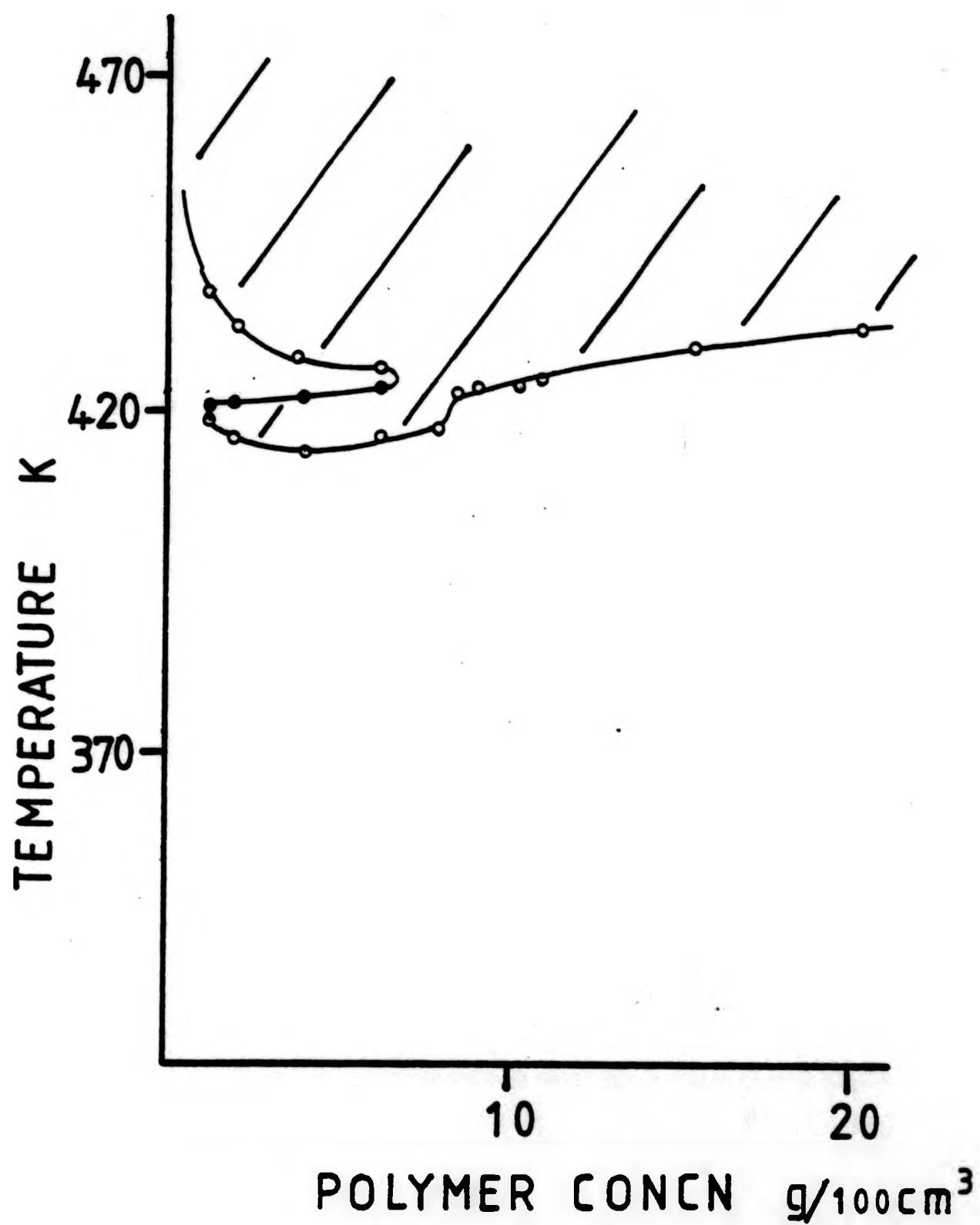
FIG 3.27 : Cloud point curve for poly(acrylic acid) PAA17 in
dioxane/4·01(wt/vol)% water.
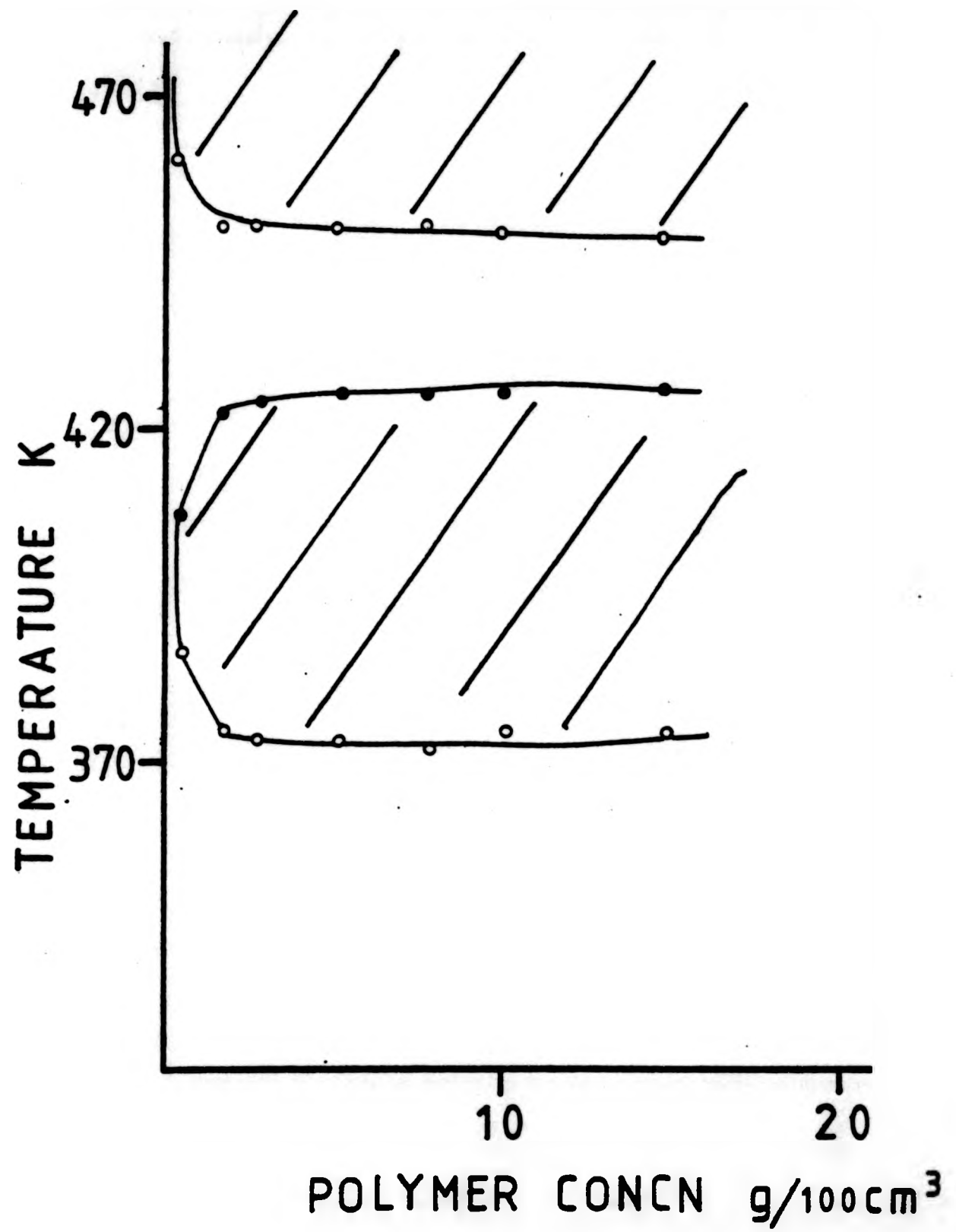
FIG 3.28 : Cloud point curve for poly(acrylic acid) PAA50 in dioxane/5.00(wt/vol)% 0.01M hydrochloric acid.
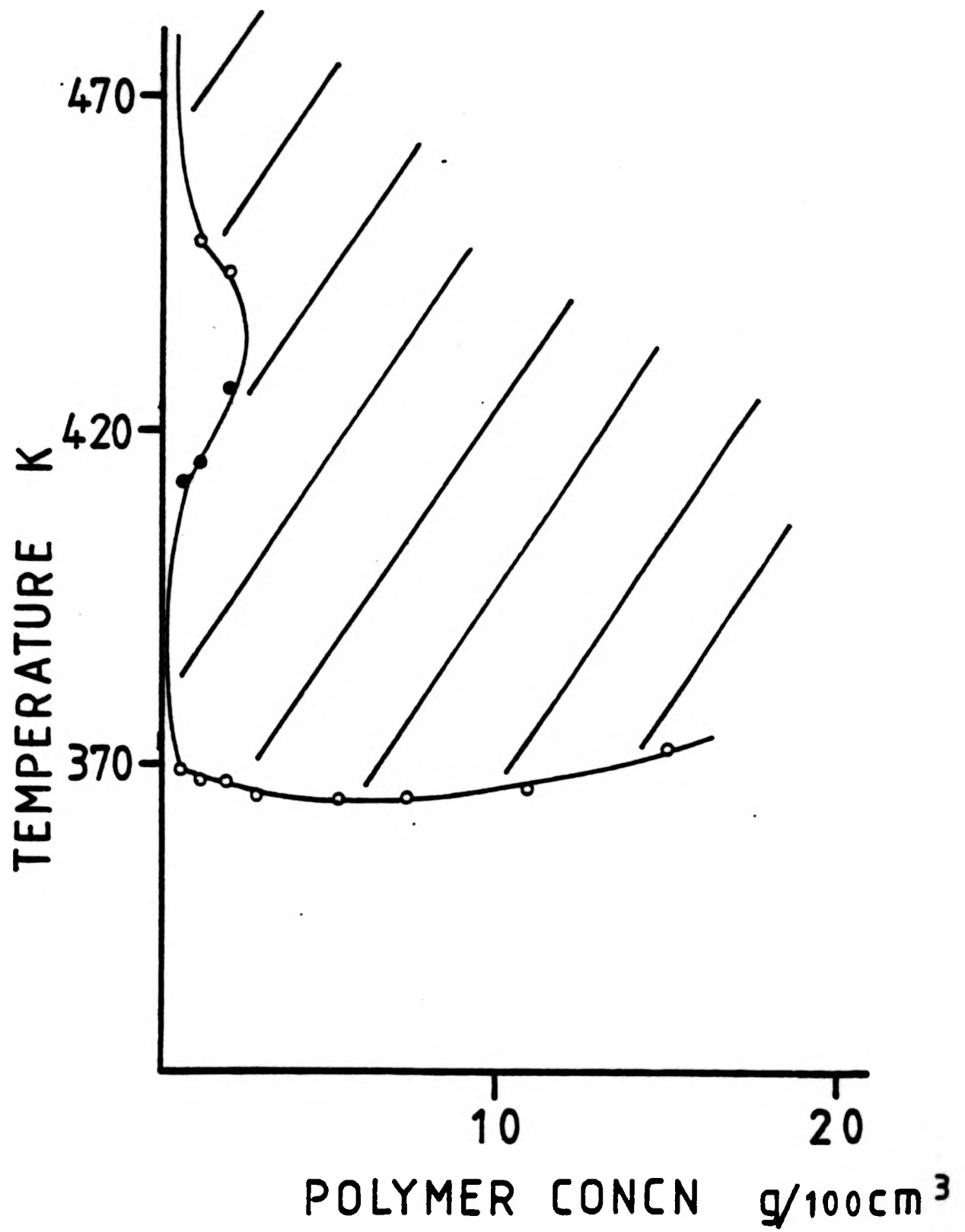
FIG 3.29 : Cloud point curve for poly(acrylic acid) PAA50 in
tetrahydrofuran/2·51(wt/vol)% water.

TABLE 3.1 $\bar{M}_n$ for poly(acrylic acid) determined in dioxane at 328K by vapour pressure osmometry

PAA No	$\bar{M}_n \times 10^{-4}$/ g/mol	
	Nominal	Experimental
PAA2	0.18	0.164 ± 0.02
PAA5	0.50	0.291 ± 0.03
PAA17	1.70	0.970 ± 0.09
PAA20	2.00	1.600 ± 0.14

TABLE 3.2 $\bar{M}_n$ for poly(acrylic acid) determined in dioxane by membrane osmometry

PAA No	Nominal MWx10^{-4}	Temp /K	$\bar{M}_n \times 10^{-4}$/g/mol		$A_2 \times 10^4$/ cm^3 mol/g^2
			Exptl.	Average	
PAA50	5.00	300	2.71		$+0.47 \pm 0.03$
		303	2.57		$+0.26 \pm 0.01$
		306	2.42	2.57 ± 0.15	$+0.31 \pm 0.02$
PAA90	9.00	300	10.40		$+0.19 \pm 0.01$
		303	9.95		$+0.09 \pm 0.006$
		306	11.20	10.50 ± 0.70	$+0.30 \pm 0.02$
PAA150	15.00	300	15.00		$+1.67 \pm 0.19$
		303	14.70		$+0.02 \pm 0.002$
		306	17.60	15.80 ± 1.80	$+0.47 \pm 0.05$
PAA300	30.00	300	26.20		-0.02 ± 0.0004
		303	25.70		-0.05 ± 0.001
		306	26.50		-0.07 ± 0.0014
		308	26.30	26.20 ± 0.52	-0.07 ± 0.0014

TABLE 3.3   Temperature of phase separation., T_c, at critical concentration, c_c.

PAA No	c_c/ g/100 cm^3	T_c, Temp/K		
		p–LCST	UCST	LCST
PAA50	10.51	331	426	448
PAA90	8.28	330	427	445
PAA150	8.23	329	404	409
PAA300	7.02	308	–	–

TABLE 3.4   Temperature of phase separation , T_{pm}, at minimum of p–LCST curve, c_{pm}.

PAA No	c_{pm}/ g/100 cm^3	T_{pm}, Temp/K		
		p–LCST	UCST	LCST
PAA2	–	–	–	–
PAA5	5.0	–	–	427
PAA17	3.0	378	419	442
PAA20	2.0	374	423	(476)
PAA50	2.0	319	426	464
PAA90	1.5	319	423	456
PAA150	1.25	318	395	450
PAA300	1.5	299	373	403

TABLE 3.5   Temperatures of phase separations of $2g/100cm^3$ polymer
solutions as a function of water content.

(wt/vol)% water	Temperature/K		
	p-LCST	UCST	LCST
0.00	318.5	426	464
1.02	339	424	449
2.52	355	426	449
4.99	376	423	448
7.49	383	422	443
9.99	406	423	428
12.05	-	-	420
14.87	-	-	435
19.72	-	-	455
24.81	-	-	-
29.72	-	-	-
39.85	-	-	-
100.00	-	-	-

CHAPTER FOUR

SOLUTION VISCOSITY

4.1 SOLUTION VISCOSITY - BINARY SOLUTION

The intrinsic viscosity, $[\eta]$, was measured for all poly(acrylic acid) samples in dried dioxane at 298, 303, 308 and 313K except for sample PAA300. This sample was measured at 298K only because of its proximity to the phase separation temperature for $1g/100cm^3$ solutions of this sample.

In general, as can be seen in Fig 4.1 and Table 4.1, the higher the molecular weight of the sample the higher the intrinsic viscosity. The two lower molecular weight samples, PAA2 and PAA5, gave good parallel straight lines which decrease in intrinsic viscosity with increasing temperature. All other samples gave curves with a maximum at approximately 305K. Above this temperature all the samples gave decreasing intrinsic viscosity with increasing temperature.

The Mark-Houwink relationships for this system were established at each temperature, Figs 4.2-4.5, and the values obtained are given in Table 4.2. Both the exponent, a, and pre-exponential factor, K, are relatively constant at 0.4 and 3×10^{-3} $100cm^3/g$ respectively. The value of the exponent appears to be low. For a θ-solvent, in which the polymer coil achieves its unperturbed dimensions, the accepted value is 0.5.

A Stockmayer-Fixman analysis was also carried out on this system (see Fig 4.6, Table 4.3) noting that as shown in the example in Fig 4.6 the points are very scattered. From these two relationships a variety of molecular parameters can be derived. These derived parameters and the results obtained using the various modified Stockmayer-Fixman relationships,[1] together with corresponding values obtained for the aqueous ternary system are discussed later.

The parameter K' in the Stockmayer-Fixman relationship, which leads

to a value of the X parameter is of note here because its negative value is highly unusual. This parameter can be associated with 'long-range interactions' whereas K_θ can be associated with 'short-range interactions'. The analysis given here appears to indicate that as the temperature is increased 'long-range interactions' become more favourable whilst the 'short-range interactions' become less important.

A study of the change of intrinsic viscosity, for PAA50 at 298K, with time indicates little change in $[\eta]$ over a period of 36 days, Table 4.4, Fig 4.7 and so no apparent aging effect of any significance is encountered here.

4.2 SOLUTION VISCOSITY - AQUEOUS TERNARY SOLUTIONS

The intrinsic viscosity of PAA5, PAA17, PAA50 and PAA150 at 303K, was determined as a function of water content in the mixed solvent, up to 20(wt/vol)% water. For solutions of PAA50 and PAA150 there is an increasing trend in $[\eta]$ with increasing water content but the trends for PAA5 and PAA17 are less well defined. For PAA5 solutions $[\eta]$ appears to be decreasing whilst for PAA17 solutions it appears to be increasing slowly, Table 4.5, Fig 4.8 .

Mark-Houwink and Stockmayer-Fixman analyses were carried out, as before, and the results are given in Tables 4.6 and 4.7 respectively. The value of K generally decreases but the value of a increases. The resulting curve of the exponent, a, as a function of water content gives turning points at 8% water (maximum) and 10.5% water (minimum) as shown in Fig 4.9. The value of K_θ appears to be relatively constant but, again, for water contents up to approximately 5 (wt/vol)% K' has a negative value. Above this water content the values of K' are positive, Table 4.7.

A study of the variation of [η] for PAA50 as a function of water content, over the full range of solvent compositions, at 298K. This indicates distinct changes in trends at 12 (wt/vol)% (cf Fig 3.24), 25 (wt/vol)% and 49 (wt/vol)% water, Fig 4.10.

The equivalent Mark-Houwink and Stockmayer-Fixman analyses were also carried out on a system using neutralised poly(acrylic acid) in water, ie poly(acrylic acid) in water with the pH adjusted to 6.7 with tetramethylammonium bromide, at 303K. This system resulted in a very low value of the Mark-Houwink exponent (0.21) and a large K (22.9 x 10^{-3} 100cm^3/g). The system also gives a relatively large negative value of K'(-4.03 x 10^{-6} 100cm^3 mol/g^2), (see Tables 4.5, 4.6, 4.7).

4.3 DISCUSSION

If 303K is taken as the θ-temperature for the system of poly(acrylic acid) in dioxane[2,3] then the Mark-Houwink exponent is taken as 0.5. Previous work on this system has been based on this assumption[3] and a study by Welch[4] states that the results obtained are similar to the Newman data but fails to quote values. An analysis of the previously published data[3] using a linear regression analysis yields a relationship

$$[\eta] = 1.26 \times 10^{-3} \ M^{0.47} \qquad\qquad 4.1$$

as opposed to the relationship usually cited[3]

$$[\eta] = 0.85 \times 10^{-3} \ M^{0.5} \qquad\qquad 4.2$$

Weight average molecular weights were used as opposed to the number averages used in this work. However, the assumption of an exponent of

A study of the variation of [η] for PAA50 as a function of water content, over the full range of solvent compositions, at 298K. This indicates distinct changes in trends at 12 (wt/vol)% (cf Fig 3.24), 25 (wt/vol)% and 49 (wt/vol)% water, Fig 4.10.

The equivalent Mark-Houwink and Stockmayer-Fixman analyses were also carried out on a system using neutralised poly(acrylic acid) in water, ie poly(acrylic acid) in water with the pH adjusted to 6.7 with tetramethylammonium bromide, at 303K. This system resulted in a very low value of the Mark-Houwink exponent (0.21) and a large K (22.9 x 10^{-3} 100cm^3/g). The system also gives a relatively large negative value of K'(-4.03 x 10^{-6} 100cm^3 mol/g^2), (see Tables 4.5, 4.6, 4.7).

4.3 DISCUSSION

If 303K is taken as the θ-temperature for the system of poly(acrylic acid) in dioxane[2,3] then the Mark-Houwink exponent is taken as 0.5. Previous work on this system has been based on this assumption[3] and a study by Welch[4] states that the results obtained are similar to the Newman data but fails to quote values. An analysis of the previously published data[3] using a linear regression analysis yields a relationship

$$[η] = 1.26 \times 10^{-3} M^{0.47}$$

4.1

as opposed to the relationship usually cited[3]

$$[η] = 0.85 \times 10^{-3} M^{0.5}$$

4.2

Weight average molecular weights were used as opposed to the number averages used in this work. However, the assumption of an exponent of

0.5 would appear to be reasonable. It is interesting to note that residual impurities, in the polymer, of 2 and 4% water were quoted for the various samples in the Newman paper. From Fig 4.9, an exponent of 0.5 is given when the system has approximately 3% water present, and so the data are not inconsistent when this is considered. The low Mark-Houwink exponents could be due to branching of the chain but in the light of the above this would appear not to be encountered here.

The molecular dimensions of the polymer can be determined through the pre-exponential factor, K, in the Mark-Houwink relationship.[5]

$$[\eta] = \left(\frac{\Phi <r_z^2>^{3/2}}{M^{1+a}} \right) M^a = KM^a \qquad 4.3$$

This relationship assumes that $[\eta] \propto M^{-1}$ and $\Phi = 2.5 \times 10^{21}$ ml, the normally accepted 'best' experimental value, when $[\eta]$ is in $100 cm^3/g$ ($<r_z^2>^{1/2}$ is then given in cm).

The Stockmayer-Fixman relationship can give a measure of the unperturbed dimension of the polymer, $<r_o^2>$, through the parameter K_θ

$$K_\theta = \frac{\Phi}{6^{3/2}} \left[\left(\frac{1 - \cos\theta}{1 + \cos\theta} \right) \frac{\sigma^2 1^2}{M_u} \right]^{3/2} \qquad 4.4$$

where the angle θ is the bond angle between chain atoms, 1 is the bond length and M_u is the molecular weight of the repeat unit. The parameter σ, the steric hindrance parameter can also be given by[6]

$$\sigma = \left(\frac{<r_o^2>}{<r_{0F}^2>} \right)^{1/2} \qquad 4.5$$

$\langle r^2_{OF} \rangle$ is the dimension of the molecule for the case where the steric hindrance is removed but the angular restriction is retained, ie free rotation.

Using the quoted values above in equation 4.4

$$\sigma = 14.0 \, K_\theta^{1/3} \qquad\qquad 4.6$$

In addition the characteristic ratio, C_∞, can be defined by[6]

$$C_\infty = \frac{\langle r_o^2 \rangle}{nl^2} = \left(\frac{1 + \cos\theta}{1 - \cos\theta}\right)\sigma^2 = 2\sigma^2 \qquad\qquad 4.7$$

(n is the number of main chain bonds).

The values for $(\langle r_z^2 \rangle / \bar{M}_n)^{1/2}$, $(\langle r_o^2 \rangle / \bar{M}_n)^{1/2}$, σ and C_∞ for the single solvent system as a function of temperature are given in Table 4.8 and for the mixed solvent system as a function of water content in Table 4.9. A value of 770×10^{-4} nm has been derived previously[8,9] for $(\langle r_z^2 \rangle / \bar{M}_n)^{1/2}$ for the single solvent system at 303K which is in reasonable agreement with the results obtained here.

The Stockmayer-Fixman equation[1]

$$[\eta] = K_\theta + 0.51 \, \Phi B \, M^{1/2} \qquad\qquad 4.8$$

$$K' = 0.51 \, \Phi B \qquad\qquad 4.9$$

can be used in modified forms depending on the value of the radius expansion coefficient, α_η,[1]

$$[\eta]/M^{1/2} = K_\theta + 0.346 \; \Phi \, BM^{1/2} \; \text{for} \, 0 < \alpha_\eta^3 < 1.6 \qquad\qquad 4.10$$

or

$$[\eta]/M^{1/2} = 1.05K_\theta + 0.287 \; \Phi \, BM^{1/2} \; \text{for} \; 0 < \alpha_\eta^3 < 2.5 \qquad\qquad 4.11$$

α_η is given by[1]

$$[\eta] = [\eta]_\theta \alpha_\eta^3 \qquad\qquad 4.12$$

The value of $(<r_o^2>/M)^{1/2}$ derived from these modified equations is little affected. Using equation 4.12 it is changed by 2%. The main effect is on K' and thus on the parameter B. This parameter is related to the parameter χ through equation 4.13[6]

$$B = \bar{u}^2 \, \frac{(1-2\chi)}{V_1 N_A} \qquad\qquad 4.13$$

where V_1 is the molar volume of the solvent and $\bar{u}$ is the specific volume of the polymer in the solvent. It is also related to the excluded-volume parameter[1], z, by

$$z = (3/2\pi)^{3/2} \, (B/A^3) \, M^{1/2} \qquad\qquad 4.14$$

where

$$A^2 = <r_o^2>/M \qquad\qquad 4.15$$

The negative values of K' would indicate that χ is greater than 0.5. These effects are left until the thermodynamic conditions involved at p-LCST phase separation boundaries are considered (section 13.2).

The variation of $(<r_{\bar{z}}^2>/M)^{1/2}$ and $(<r_o^2>/M)^{1/2}$ as a function of temperature for the single solvent system is shown in Fig 4.11 (see also Table 4.8). The curvature in the $(<r_z^2>/M)^{1/2}$ plot reflects that shown by the variation of intrinsic viscosity for the individual molecular weights as can be seen in Fig 4.1. This trend is also seen in the variation in the Mark-Houwink exponent, Table 4.2 . $(<r_o^2>/M)^{1/2}$ gives a linear relationship with temperature in this region so that extrapolation to a temperature where $<r_z^2> = <r_o^2>$, a measure of the θ-temperature, is very difficult.

The Mark-Houwink exponent, as previously noted, is always less than 0.5 in this temperature range indicating that the molecular dimensions of the polymer coil should be smaller than the expected unperturbed value. This would appear to be confirmed by Fig 4.11 which gives a value of $(<r_z^2>/M)^{1/2}$ which is always smaller than the expected unperturbed dimension. The dimension also appears to be getting smaller as the temperature is increased towards a p-LCST phase separation boundary.

The curves for the molecular dimensions in the mixed solvent system are more complicated and are given separately in Fig 4.12 for $(<r_z^2>/M)^{1/2}$ and in Fig 4.13 for $(<r_o^2>/M)^{1/2}$. The Mark-Houwink exponent for the mixed solvent system is 0.5 at approximately 3% water so that at this water content $<r_z^2>$ would be expected to be equal to $<r_o^2>$. Both curves give maxima at this water content. A plot of $(<r_z^2>/M)^{1/2} - (<r_o^2>/M)^{1/2}$ as a function of water content, Fig 4.14, however, gives $<r_z^2> = <r_o^2>$ at approximately 5% water. Both Fig 4.12 and Fig 4.13 give similar trends with an additional maximum at 10.5% water and a minimum at 8% water (cf trends in Fig 4.9). Below 5% water it can be seen from Fig 4.14 that the molecular dimension of the coil is smaller than the

expected unperturbed value whilst above 5% it is larger. These trends would appear, in general, to be similar to those that are indicated by the variation in Mark-Houwink exponent.

An alternative to using number average molecular weights in the equations would be to use weight averages (as used in the previous work[3]). Using $\bar{M}_w$ data determined by light scattering (see chapter 5) for PAA50 and PAA150 at 303K, the values obtained for K, a, K_Θ and K' are 5.22×10^{-3} $^{100cm^3/g}$, 0.34, 1.09×10^{-3} $^{100cm^3mol^{1/2}/g^{3/2}}$ and -0.67×10^{-6} $^{100cm^3mol/g^2}$ respectively. The corresponding values determined from Newman's data, at 303K, are 1.22×10^{-3} $^{100cm^3/g}$, 0.47, 8.84×10^{-4} $^{100cm^3mol^{1/2}/g^{3/2}}$ -6.3×10^{-8} $^{100cm^3mol/g^2}$. Since the data here are only actually derived from two values, a dubious procedure, it is not surprising that the values do not agree. However, Table 4.10 gives the molecular parameters derived from both sets of data which appear to be in reasonable agreement. The similarity in the values of $(\langle r_z^2 \rangle / \bar{M}_w)^{1/2}$ could be another indication that chain branching is not encountered here. The corresponding value purely derived by light scattering data by Newman is $773(\pm 30) \times 10^{-4}$ nm mol$^{1/2}/g^{1/2}$

Corrections can be made to equate the different results (ie from light scattering or viscosity) using a modified Mark-Houwink equation.[3]

$$[\eta] = \left[\left(\frac{\Phi}{q}\right) \frac{\langle r_z^2 \rangle^{3/2}}{\bar{M}_w^{1+a}} \right] \bar{M}_w^{\,a} \qquad 4.16$$

where[3]

$$q = \left(\frac{\bar{M}_w}{\bar{M}_n}\right)^{13/8} \qquad 4.17$$

Since the ratios $(\bar{M}_w/\bar{M}_n)$ for the samples PAA50, PAA150 and PAA300 are 3.49, 1.94 and 2.52, this correction could not be expected to improve the agreement.[3]

Most viscometric studies on this system have been into the effect of adding various salts to aqueous poly(acrylic acid) and the effect of partial neutralisation.[2,8,12,14] It has been generally found that viscosity increases with increasing degrees of neutralisation.[15] The addition of an electrolyte results in no postponment of the molecular expansion (which is not the case with poly(methacrylic acid)[16]) and the concentration and temperature dependence at different degrees of neutralisation (for NaBr additive) resemble those for non-polar polymers in non-polar solvents.[17]

The Mark-Houwink exponent has been found to range from 0.5 - 0.9 as the solution is neutralised[18] from a strongly coiled molecule in 1.2 - 1.5N aqueous hydrochloric acid[19] to a loosely bound one at low degrees of ionisation.[20] The steric hindrance parameter, σ, has been found to range from 2.38 (at 288K)[18] for a fully charged species to 1.85 (at 303K)[7] for the non-ionised acid in dioxane. The values of σ obtained here, for $\bar{M}_n$ based data, appear to be too large if the acid is considered un-ionised although the values based on $\bar{M}_w$ data are more in keeping with the values quoted above.

The viscosity in the water system may be affected by CO_2 uptake from the atmosphere, not only from the distilled water, which in the distilling process looses its 'buffer' effect, but also from the alkylammonium polyacrylate itself.[10] This effect appears to be minimal since the solutions were adjusted in pH immediately before use and there was no sign of a polyelectrolyte effect during the course of

the experiments.   Any 'iceberg' structure formation around the
tetramethylammonium species[11] which would have increased the viscosity
of the system also appears to have been minimal (the tetramethyl salt was
used because of its low hydrophobicity[11]).

REFERENCES

1. H Yamakawa, "Modern Theory of Polymer Solutions", Harper and Row, New York, (1971).

2. P J Flory, W R Krigbaum, W B Schultz, J.Chem.Phys. 21, 164, (1953).

3. S Newman, W R Krigbaum, C Laugier, P J Flory. J.Polym.Sci. 14, 451, (1954).

4. G J Welch, Polymer 16, 68, (1975).

5. P J Flory, "Principles of Polymer Chemistry", Cornell University Press, Ithaca, New York, (1953).

6. H G Elias, "Macromolecules 1", Plenum Press, New York, (1977).

7. 'Polymer Handbook', Ed J Brandrup, E H Immergut, Wiley-Interscience, New York, (1967).

8. P J Flory, J E Osterheld, J.Phys.Chem. 58, 653, (1954).

9. C Cuniberti, U Bianchi, Polymer 15, 346, (1974).

10. P V Wright, Makromol.Chem. 176, 801, (1975).

11. N Ise, K Mita, T Okubo, J.Chem.Soc., Faraday Trans. I 69, 106, (1973).

12. A Silberberg, S Eliassaf, A Katchalsky, J.Polym.Sci. 23, 259, (1957).

13. J Eliassaf, A Silberberg, J.Polym.Sci. 41, 33, (1959).

14. L Bardel, J Bontoux, A Faucon, Trav.Soc.Pharm.Montpellier 22, 238, (1962).

15. G Markers, Angew.Makromol.Chem. 11, 85, (1970).

16. G Barone, V Crescenzi, F Quadrifoglio, Ric.Sci. 35,(11A), 393, (1965).

17. G E Heckler, T E Newlin, D M Stern, R A Stratton, J R Witt, J D Ferry, J.Colloid.Sci. 15, 294, (1960).

18. A Takahashi, M Nagasawa, J.Am.Chem.Soc. 86, 543, (1964).

19. A Dobry, F Boyer-Kawenoki, Macromol.Chem. 6, 157, (1951).

20. J N Davenport, P V Wright, Polymer 21, 227, (1981).
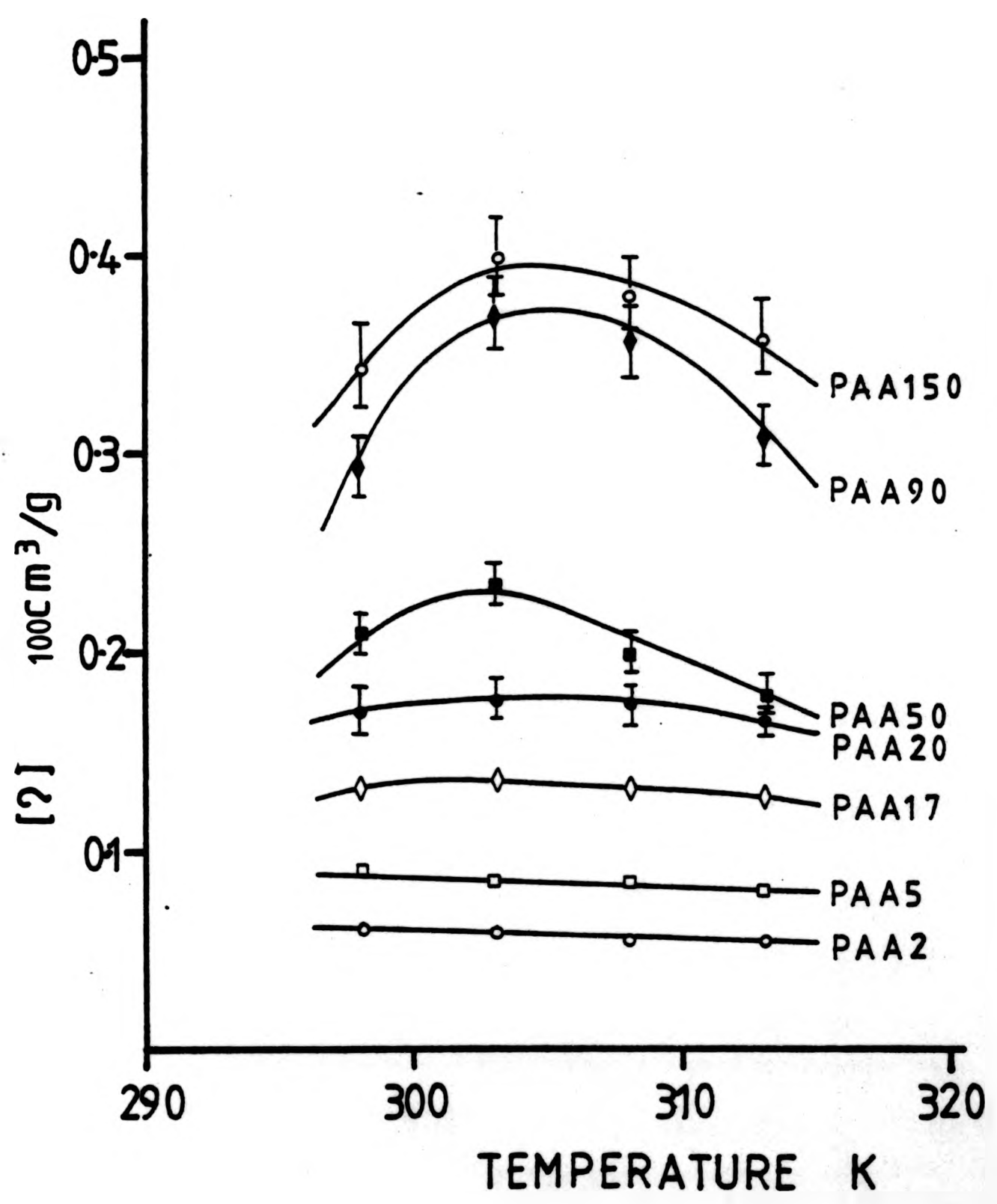
FIG 4.1 : Variation of intrinsic viscosity,[η], with temperature
for poly(acrylic acid) in dioxane.
(samples as indicated).
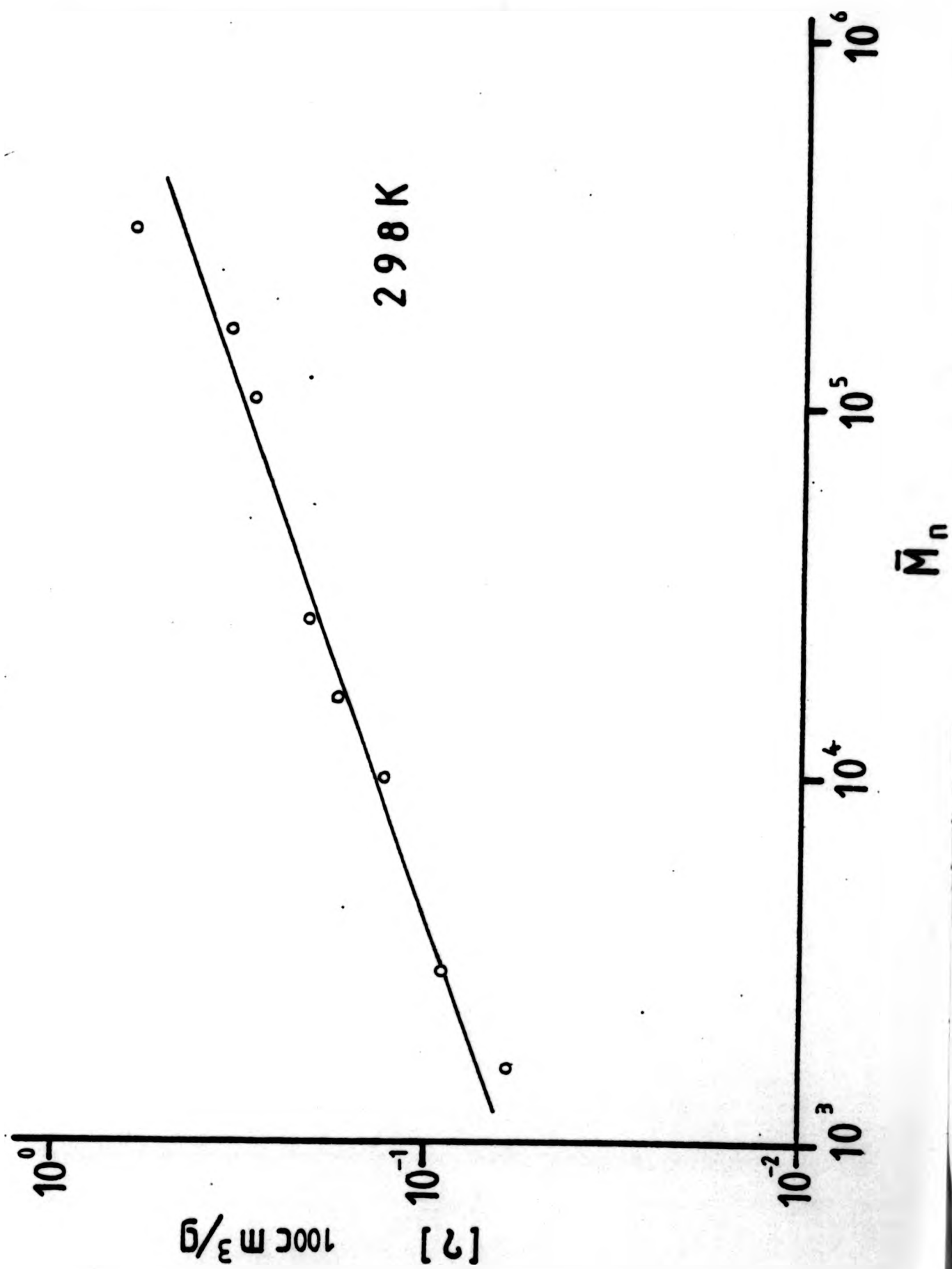
FIG 4.2 : Mark-Houwink analysis for poly(acrylic acid) in
dioxane at 298 K.
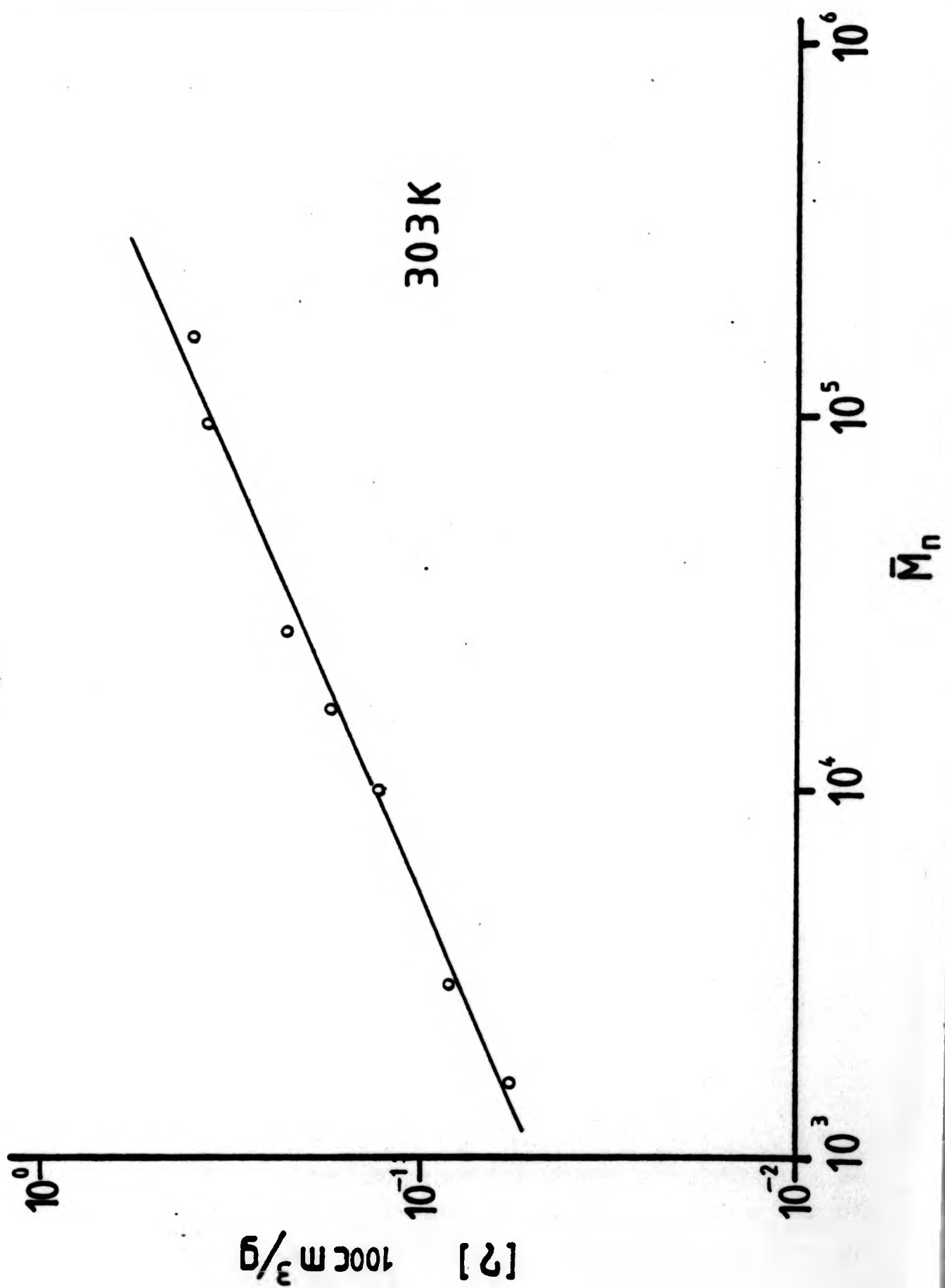
FIG 4.3 : Mark-Houwink analysis for poly(acrylic acid) in dioxane at 303 K.
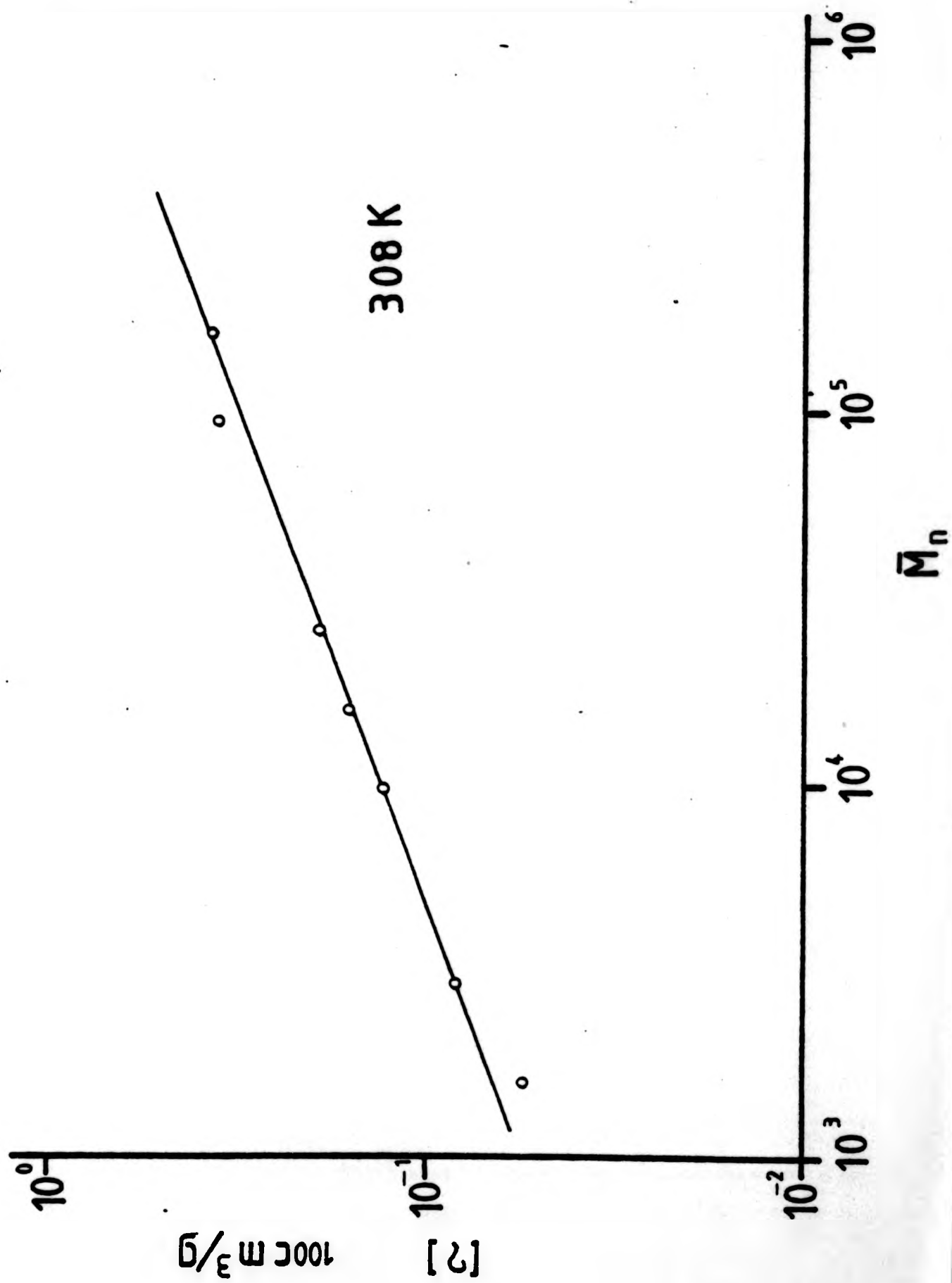
FIG 4.4 : Mark-Houwink analysis for poly(acrylic acid) in dioxane at 308 K.
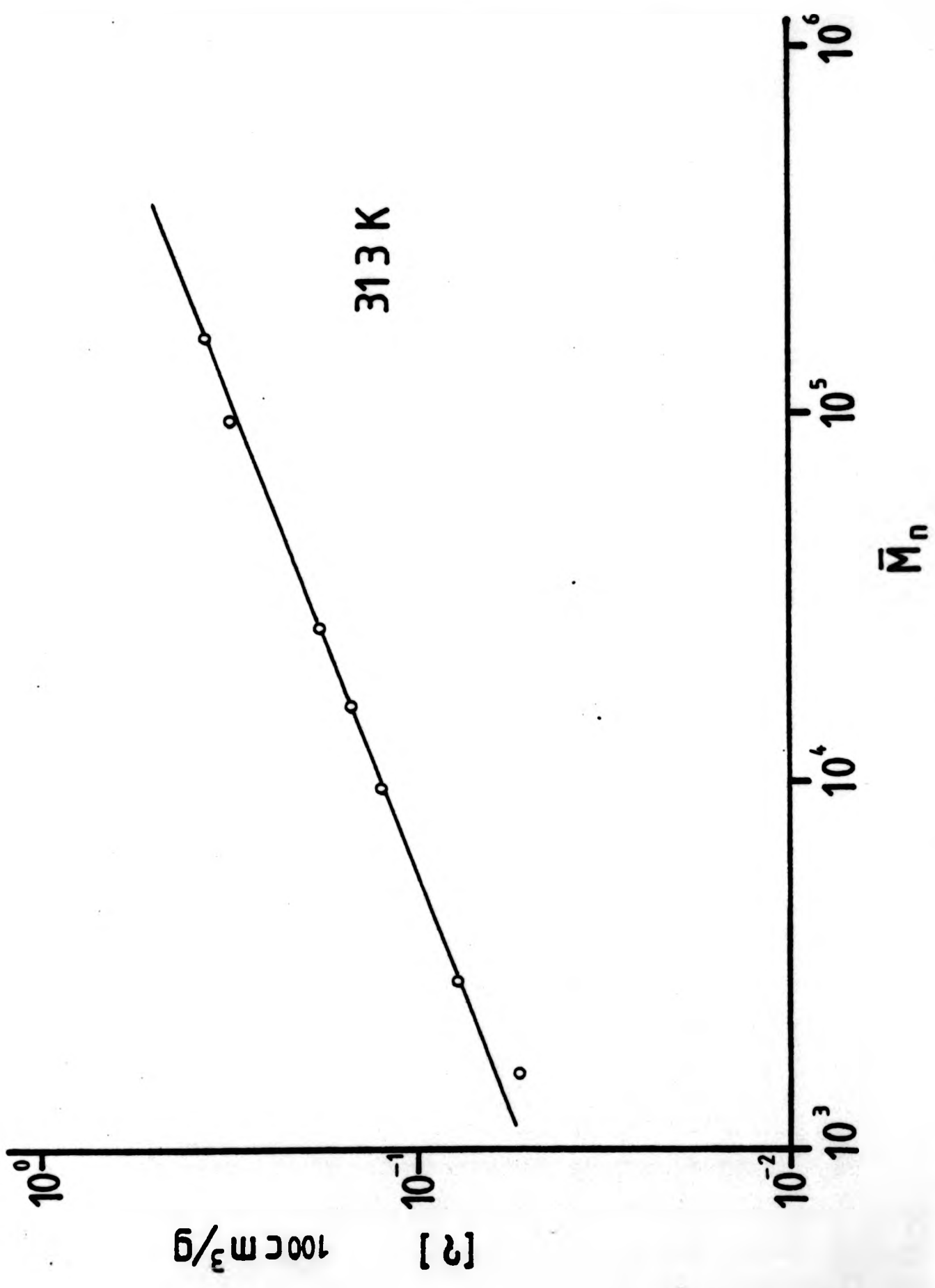
FIG 4.5 : Mark-Houwink analysis for poly(acrylic acid) in dioxane at 313 K.
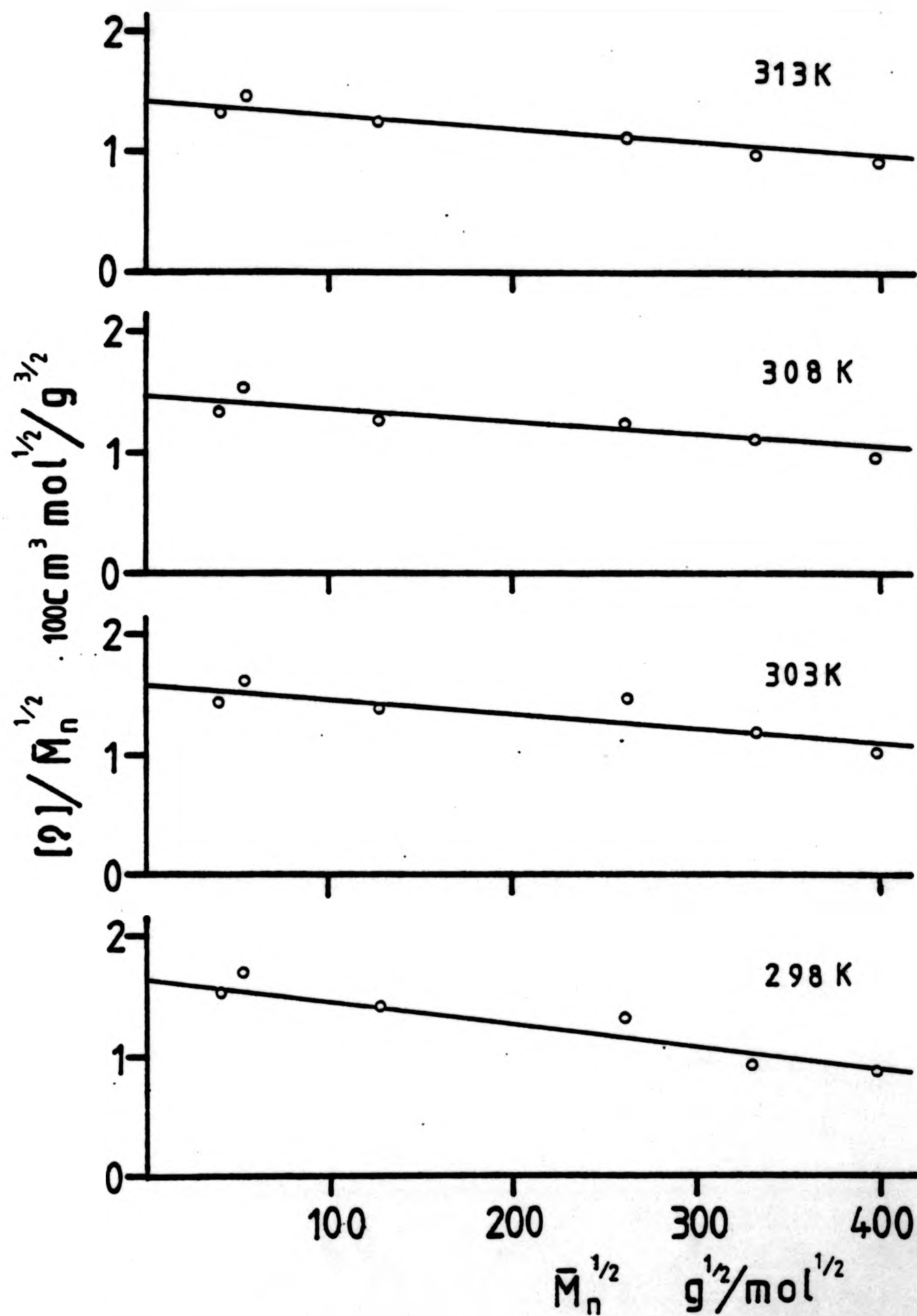
FIG 4.6 : Stockmayer-Fixman analysis for poly(acrylic acid) in dioxane.
(Temperatures as indicated).
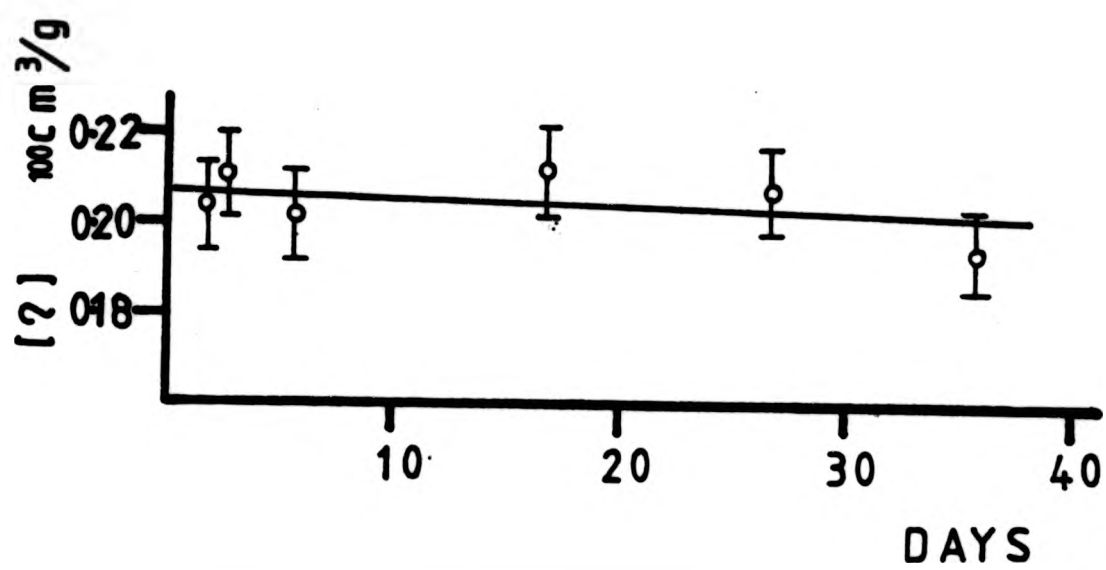
FIG 4.7 : Variation of intrinsic viscosity,[η], with time for
poly(acrylic acid) PAA50 in dioxane at 298 K.
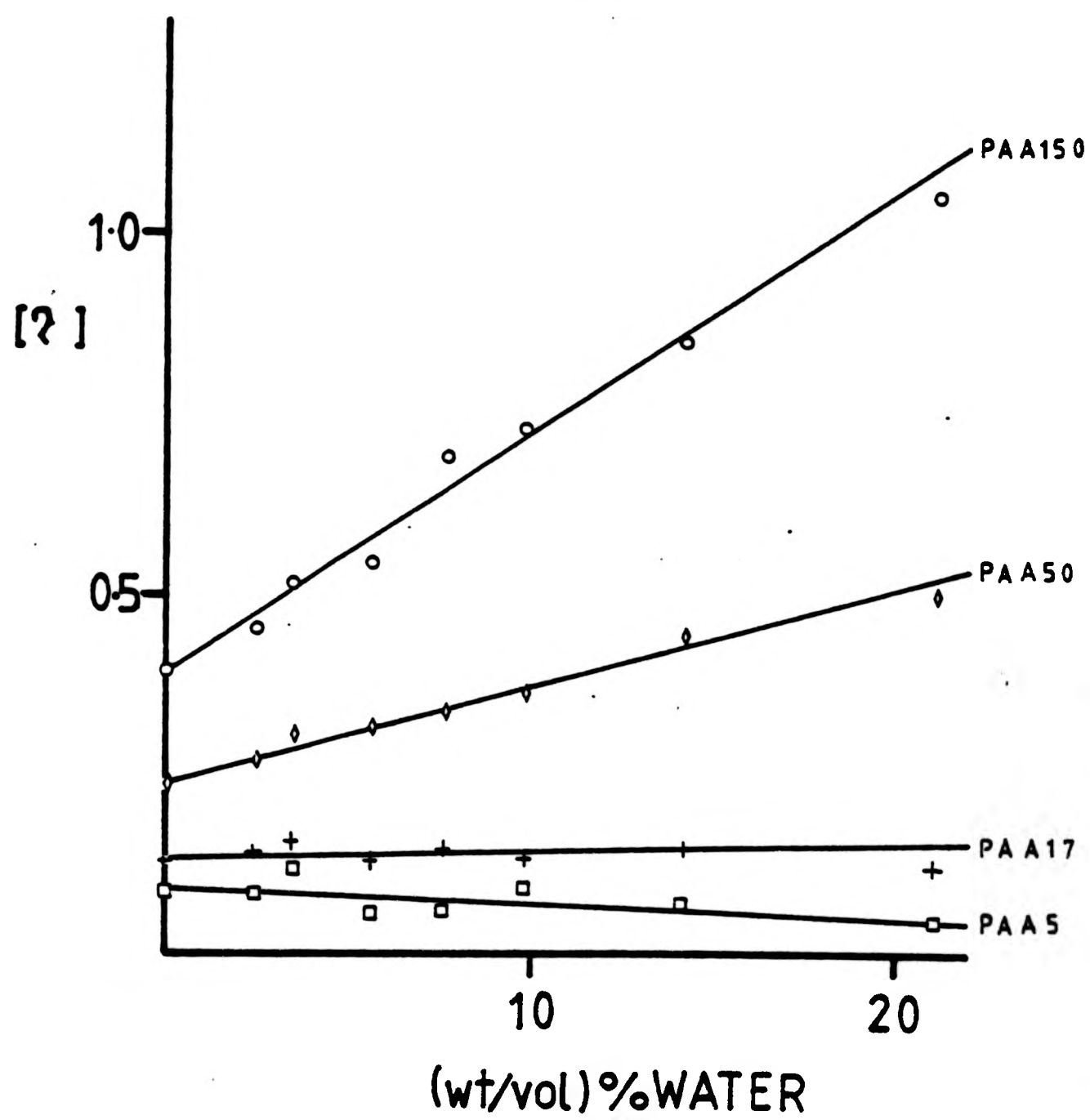
FIG 4.8 : Variation of intrinsic viscosity, $[\eta]$, for poly(acrylic acid) in dioxane/water as a function of water content at 303 K. (samples as indicated).
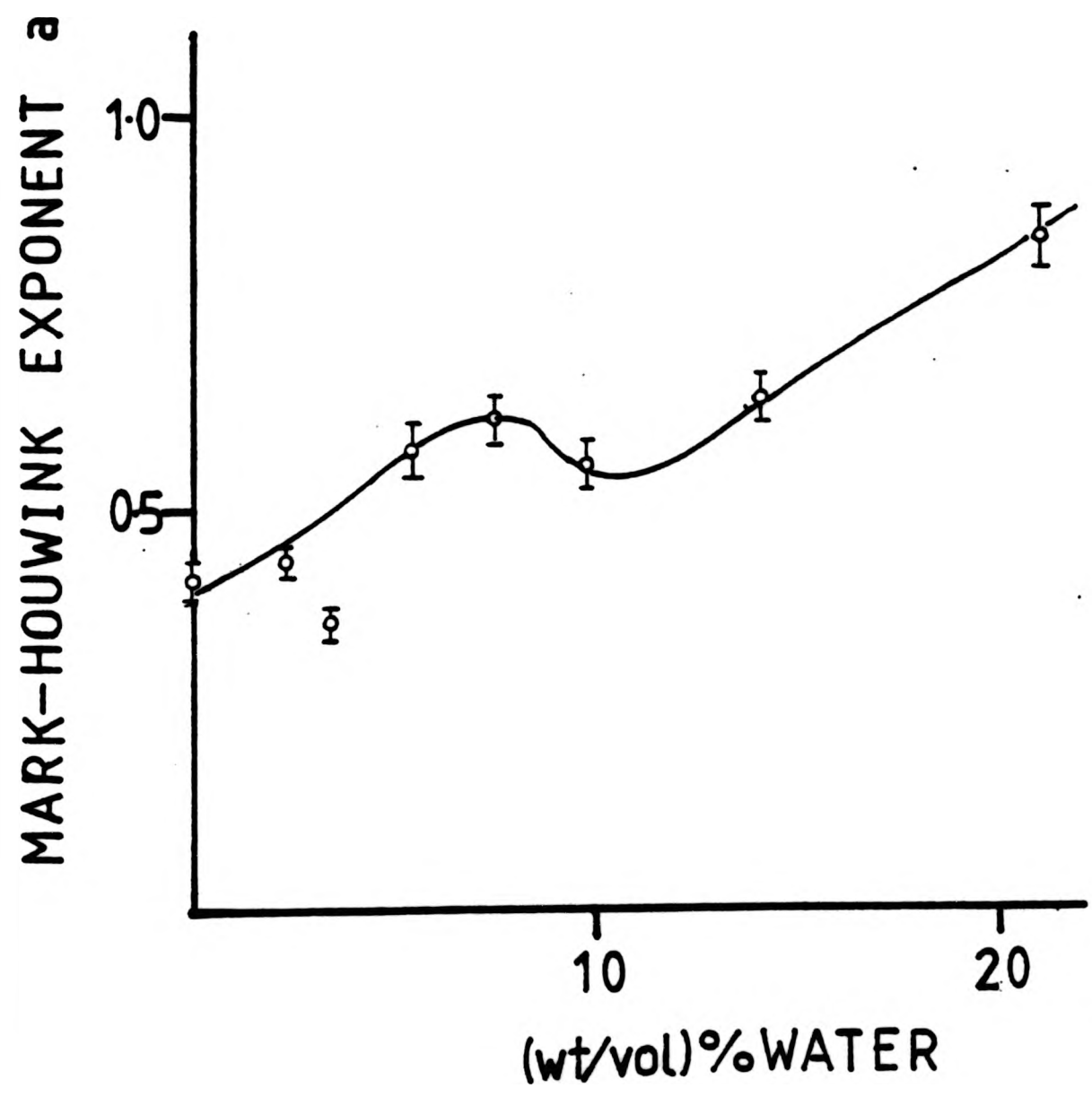
FIG 4.9 : Variation of Mark-Houwink exponent for poly(acrylic acid) in dioxane/water as a function of water content at 303°K.
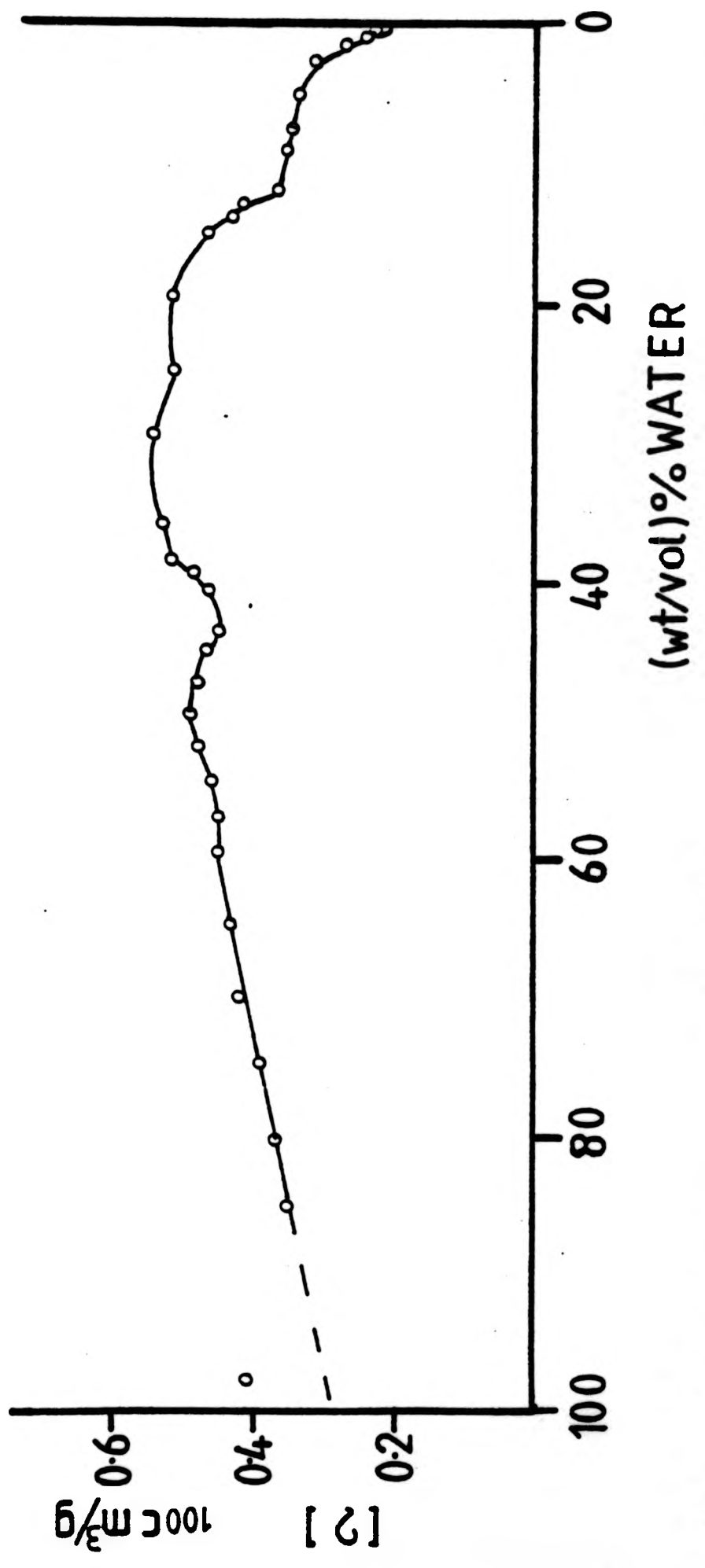
FIG 4.10 : Variation of intrinsic viscosity, [η], for poly(acrylic acid)
PA150 in dioxane/water as a function of water content
at 298 K.
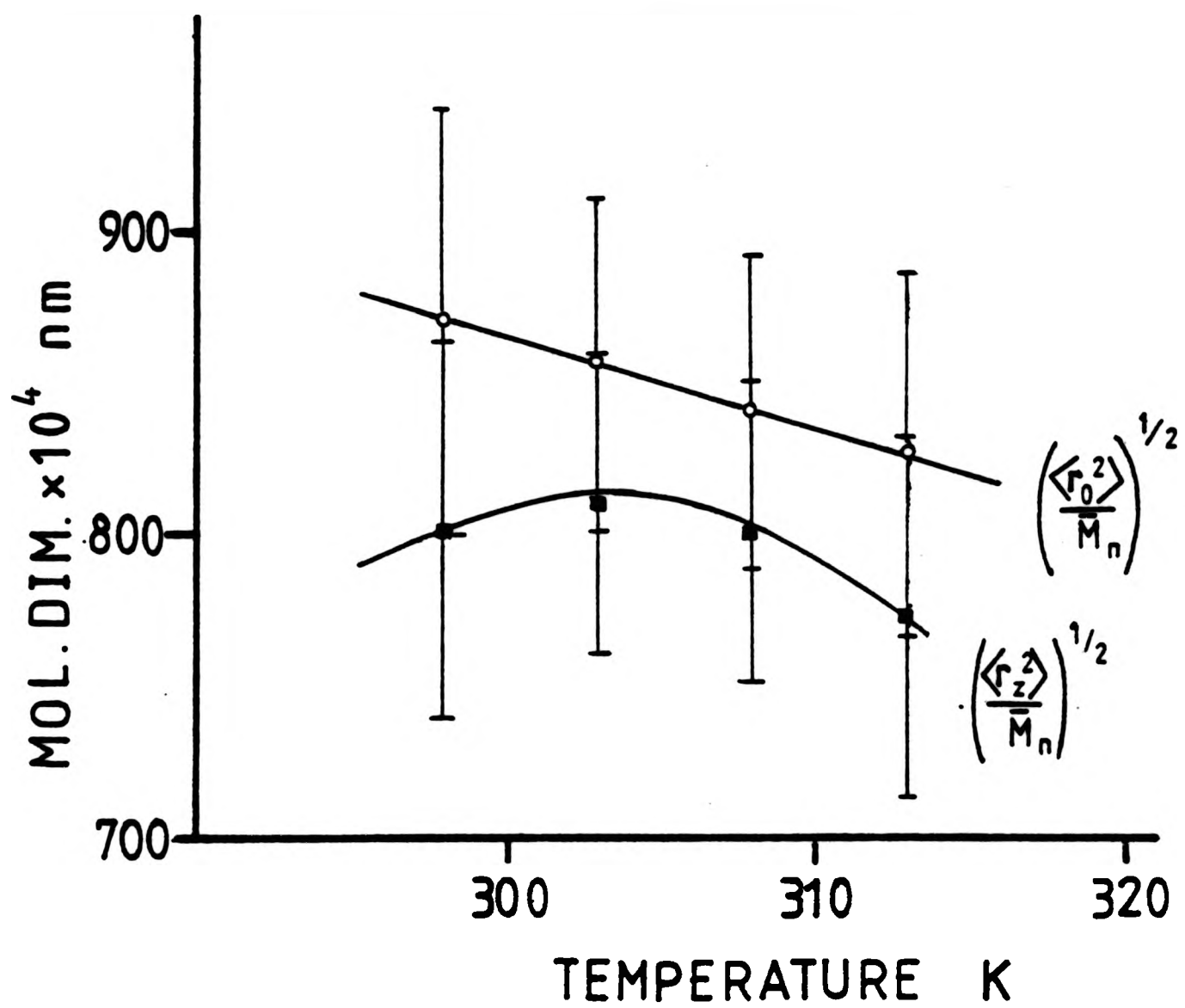
FIG 4.11 : variation of molecular, $(\langle r_z^2 \rangle / \overline{M}_n)^{\frac{1}{2}}$, and unperturbed, $(\langle r_0^2 \rangle / \overline{M}_n)^{\frac{1}{2}}$, dimensions for poly(acrylic acid) in dioxane as a function of temperature.
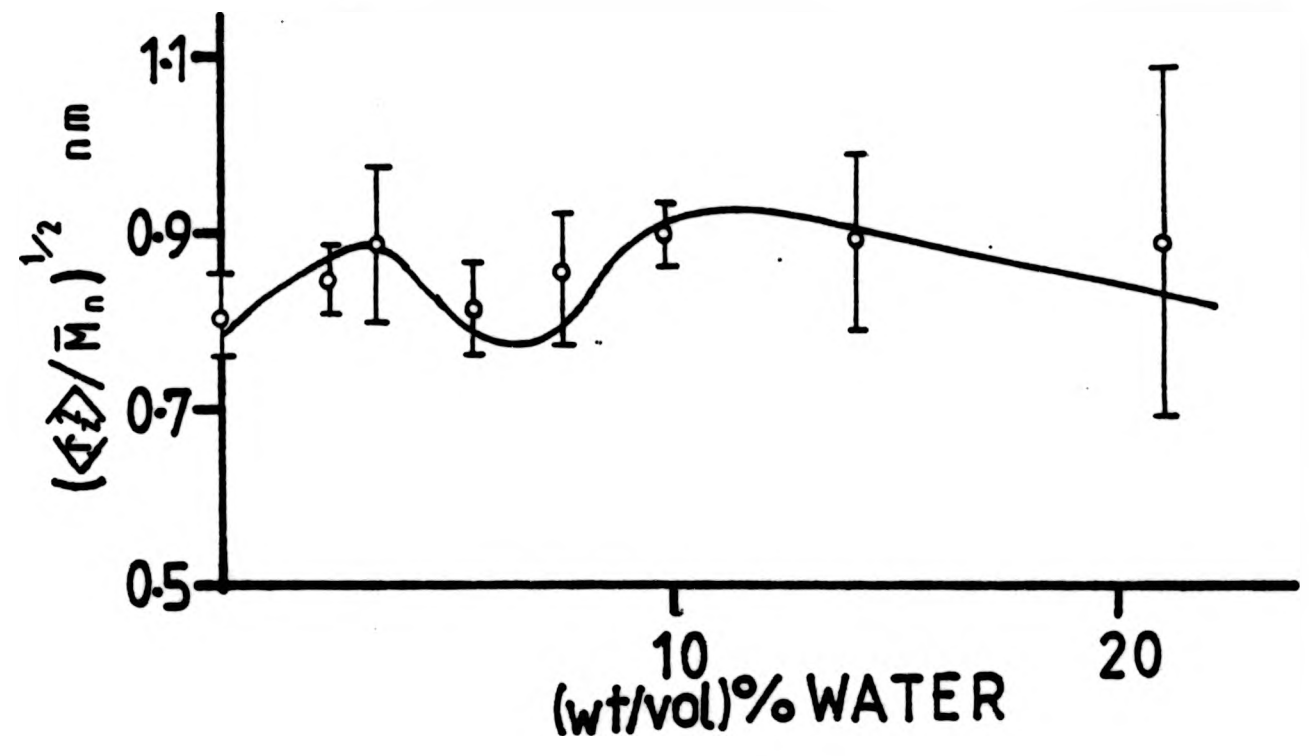
FIG 4.12 : Variation of molecular dimension, $(\langle r_z^2 \rangle / \bar{M}_n)^{\frac{1}{2}}$, for poly(acrylic acid) in dioxane/water as a function of water content at 303 K.
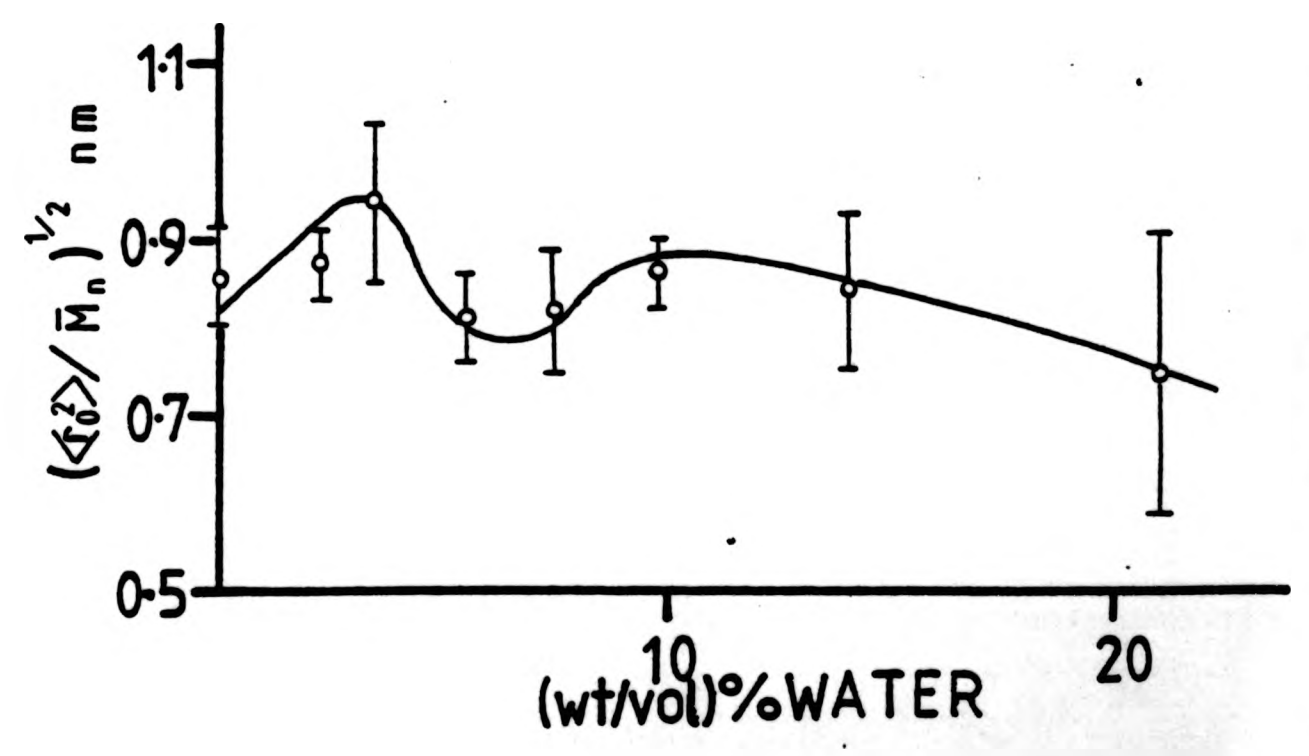
FIG 4.13 : Variation of unperturbed dimension, $(\langle r_0^2 \rangle / \bar{M}_n)^{\frac{1}{2}}$, for poly(acrylic acid) in dioxane/water as a function of water content at 303 K.
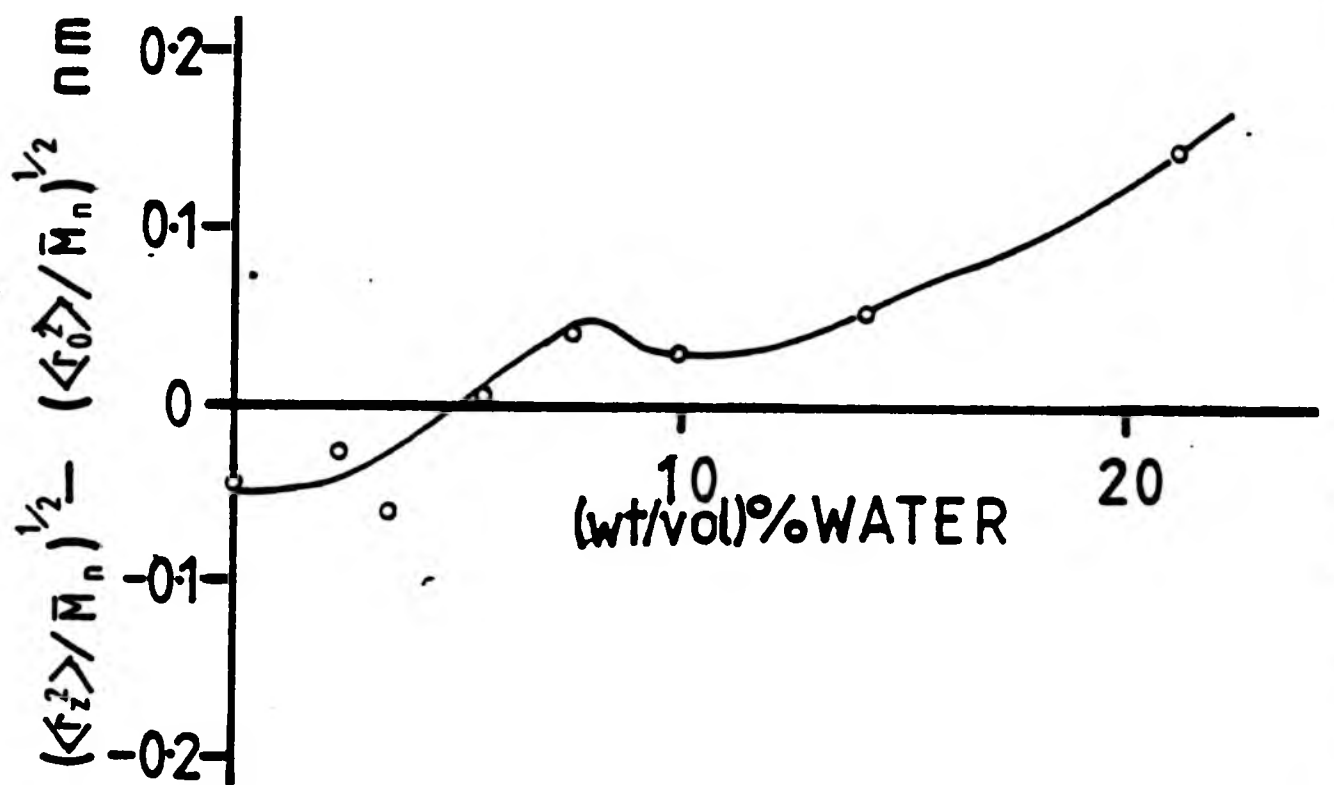
FIG 4.14 : Variation of $(\langle r_z^2 \rangle / \bar{M}_n)^{\frac{1}{2}} - (\langle r_0^2 \rangle / \bar{M}_n)^{\frac{1}{2}}$ for poly(acrylic acid) in dioxane/water as a function of water content at 303 K.

TABLE 4.1   Intrinsic viscosity, $[\eta]$ ($100cm^3/g$) for poly(acrylic acid) in dioxane as a function of temperature.

PAA	Temperature/K			
	298	303	308	313
PAA2	0.061 ± 0.003	0.058 ± 0.003	0.055 ± 0.003	0.054 ± 0.003
PAA5	0.091 ± 0.005	0.085 ± 0.004	0.083 ± 0.004	0.079 ± 0.004
PAA17	0.132 ± 0.007	0.134 ± 0.007	0.130 ± 0.007	0.127 ± 0.006
PAA20	0.172 ± 0.009	0.176 ± 0.009	0.158 ± 0.008	0.148 ± 0.007
PAA50	0.210 ± 0.011	0.234 ± 0.012	0.199 ± 0.010	0.180 ± 0.009
PAA90	0.295 ± 0.015	0.373 ± 0.019	0.360 ± 0.018	0.311 ± 0.016
PAA150	0.343 ± 0.020	0.398 ± 0.020	0.380 ± 0.020	0.359 ± 0.018
PAA300	0.634 ± 0.030	-	-	-

TABLE 4.2   Mark-Houwink relationship for poly(acrylic acid) in dioxane as a function of temperature.

Temp/K	$K \times 10^3$	a
298	3.39 ± 0.17	0.40 ± 0.02
303	2.88 ± 0.14	0.42 ± 0.02
308	2.75 ± 0.14	0.42 ± 0.02
313	3.02 ± 0.15	0.40 ± 0.02

TABLE 4.3   Stockmayer-Fixman relationship for poly(acrylic acid) in dioxane as a function of temperature.

Temp/K	$K_\theta \times 10^3/100cm^3mol^{\frac{1}{2}}/g^{3/2}$	$K' \times 10^6/100cm^3mol/g^2$
298	1.64 ± 0.12	-2.11 ± 0.16
303	1.57 ± 0.12	-1.34 ± 0.10
308	1.47 ± 0.11	-1.24 ± 0.09
313	1.41 ± 0.11	-1.39 ± 0.10

TABLE 4.4   Change in intrinsic viscosity, $[\eta]$, with time for poly(acrylic acid), PAA50, in dioxane at 298K.

Day	2	3	6	17	27	36
$[\eta]$	0.204 ± 0.01	0.210 ± 0.011	0.202 ± 0.01	0.212 ± 0.009	0.207 ± 0.01	0.194 ± 0.01

TABLE 4.5   Intrinsic viscosity for poly(acrylic acid) in dioxane/water
mixtures at 303K.

(wt/vol)% water	$[\eta]$ $\mathrm{d}l/_g$			
	PAA5	PAA17	PAA50	PAA150
0.00	0.085 ± 0.004	0.134 ± 0.007	0.234 ± 0.012	0.398 ± 0.020
2.36	0.082 ± 0.004	0.139 ± 0.007	0.274 ± 0.014	0.450 ± 0.023
3.43	0.122 ± 0.006	0.152 ± 0.007	0.304 ± 0.015	0.517 ± 0.026
5.49	0.055 ± 0.003	0.127 ± 0.006	0.314 ± 0.016	0.547 ± 0.027
7.51	0.058 ± 0.003	0.144 ± 0.007	0.331 ± 0.017	0.679 ± 0.034
9.82	0.089 ± 0.004	0.129 ± 0.006	0.360 ± 0.018	0.731 ± 0.037
14.11	0.068 ± 0.003	0.145 ± 0.007	0.437 ± 0.022	0.850 ± 0.043
21.12	0.038 ± 0.002	0.117 ± 0.006	0.495 ± 0.025	1.053 ± 0.053
100.00	0.124 ± 0.006	0.166 ± 0.008	0.256 ± 0.013	0.293 ± 0.015

TABLE 4.6   Mark-Houwink relationship for poly(acrylic acid) in dioxane/water mixtures at 303K.

(wt/vol)% water	$K \times 10^3 / 100cm^3/_g$	a
0.00	2.88 $\pm$ 0.14	0.42 $\pm$ 0.02
2.36	2.68 $\pm$ 0.13	0.44 $\pm$ 0.02
3.43	6.85 $\pm$ 0.34	0.36 $\pm$ 0.02
5.49	0.61 $\pm$ 0.03	0.58 $\pm$ 0.03
7.51	0.48 $\pm$ 0.03	0.62 $\pm$ 0.03
9.82	1.00 $\pm$ 0.05	0.56 $\pm$ 0.03
14.11	0.41 $\pm$ 0.02	0.65 $\pm$ 0.03
21.12	0.05 $\pm$ 0.01	0.85 $\pm$ 0.04
100.00	22.90 $\pm$ 1.15	0.21 $\pm$ 0.01

TABLE 4.7   Stockmayer-Fixman relationship for poly(acrylic acid) in dioxane/water mixtures at 303K.

(wt/vol)% water	$K_\theta \times 10^3$ / $100cm^3 mol^{\frac{1}{2}}/g^{3/2}$	$K' \times 10^6$ / $100cm^3 mol/g^2$
0.00	1.64 ± 0.12	-2.11 ± 0.16
2.36	1.65 ± 0.08	-1.14 ± 0.06
3.43	2.12 ± 0.11	-2.11 ± 0.11
5.49	1.31 ± 0.07	0.58 ± 0.03
7.51	1.35 ± 0.07	1.31 ± 0.07
9.82	1.62 ± 0.08	0.81 ± 0.04
14.11	1.52 ± 0.08	2.15 ± 0.11
21.12	1.03 ± 0.05	4.96 ± 0.25
100.00	2.30 ± 0.12	-4.03 ± 0.20

TABLE 4.8   Molecular dimensions for poly(acrylic acid) in dioxane as a
             function of temperature.

Temp K	$(\langle r_z^2 \rangle /\bar{M}_n)^{1/2}$ x 10^4/nm	$(\langle r_o^2 \rangle /\bar{M}_n)^{1/2}$ x 10^4/nm	σ	C_∞
298	801 ± 63	869 ± 69	1.65 ± 0.13	5.44 ± 0.44
303	810 ± 51	856 ± 54	1.63 ± 0.10	5.31 ± 0.33
308	797 ± 50	838 ± 53	1.59 ± 0.10	5.06 ± 0.32
313	772 ± 60	826 ± 64	1.57 ± 0.12	4.93 ± 0.38

TABLE 4.9 Molecular dimensions for poly(acrylic acid) in dioxane/water mixtures at 303K.

% water	$(\langle x_z^2\rangle/\bar{M}_n)^{1/2}$ $\times 10^4$/nm	$(\langle r_o^2\rangle/\bar{M}_n)^{1/2}$ $\times 10^4$/nm	σ	C_∞
0.00	810 ± 51	856 ± 54	1.63 ± 0.10	5.31 ± 0.33
2.36	842 ± 36	870 ± 37	1.65 ± 0.07	5.47 ± 0.23
3.46	887 ± 87	947 ± 93	1.80 ± 0.18	6.47 ± 0.64
5.49	813 ± 47	806 ± 47	1.53 ± 0.09	4.69 ± 0.27
7.51	856 ± 75	814 ± 71	1.55 ± 0.14	4.79 ± 0.42
9.82	898 ± 38	865 ± 37	1.64 ± 0.07	5.41 ± 0.23
14.11	897 ± 99	847 ± 93	1.61 ± 0.18	5.18 ± 0.57
21.12	887 ± 200	744 ± 167	1.41 ± 0.32	4.00 ± 0.90
100	818 ± 160	973 ± 190	1.85 ± 0.36	6.83 ± 1.33

TABLE 4.10 Comparison of molecular dimensions between present data and Newman data.[3].

	Newman Data	Present data
$(\langle r_z^2 \rangle / \bar{M}_w)^{1/2} \times 10^4$ nm	700 ± 100	680 ± 29
$(\langle r_o^2 \rangle / \bar{M}_w)^{1/2} \times 10^4$ nm	707 ± 14	693 ± 35
σ	1.95 ± 0.04	1.91 ± 0.10
C_∞	7.61 ± 0.15	7.29 ± 0.37

CHAPTER FIVE

PREFERENTIAL SOLVATION

5.1 PREFERENTIAL SOLVATION

A variety of expressions have been proposed for a 'preferential adsorption (solvation) parameter'.[1] They express the measure of the relative interactions between the components in a mixed solvent (components 1 and 2) and a polymer (component 3). The measurement of such a parameter, λ_i^*, can be made using a combination of light scattering and differential refractometry techniques utilising an expression of the form[2]

$$\lambda_i^* = \left[\left(\frac{M_{APP}}{M}\right)^{\frac{1}{2}} - 1\right] \left[\frac{(dn/dc_3)}{(dn/d\phi_1)}\right] \qquad 5.1$$

The molecular weight, M, of the polymer in a single solvent (component 1) is determined by light scattering and the 'apparent molecular weight', M_{APP} of the same polymer in a mixed solvent is then measured. Here ϕ_1 is the vol. fraction of component 1 in the mixed solvent and ϕ_2 is that of component 2. The refractive index increment (dn/dc_3) of the polymer in the mixed solvent is measured along with the refractive index increment of the solvent mixture with respect to one of the components $dn/d\phi_1$.

The weight average molecular weight, $\bar{M}_w$, of PAA50, PAA150 and PAA300 in dioxane were determined along with that for sample PAA300 in dioxane/water mixtures for water contents up to 32 (wt/vol)% in the solvent. From these measurements the parameters λ_i^* were determined for each solvent mixture and this along with other parameters, such as the second virial coefficient A_2 and the molecular dimension $<r_z^2>$, derived from light scattering and differential refractometry measurements

are shown in Tables 5.1 and 5.2 (see also Figs 5.1-5.7).

Above a water content of approximately 16(wt/vol)% the values of $dn/d\phi_1$ could not be determined in this experiment. The values, for $dn/d\phi_1$, for these experiments were derived from refractive index data given by Hovorka.[3] As can be seen in Fig 5.2 (open circles, o , my data; closed circles, ● , Hovorka data) both sets of refractive index increments appear to be in agreement in trends which give a maximum for the curve at approximately 24 (wt/vol)% water. A plot of the partial specific volume of dioxane in dioxane/water mixtures also gives a maximum at this water content.[4]

The plot of $(dn/dc_3)/(dn/d\phi_1)$ was a smooth curve which appears, in the range studied, to be asymptotic to both axes, Fig 5.3.

In the plot for M_{APP}/M a minimum is found at approximately 8(wt/vol)% water and a second maximum is seen at 24 (wt/vol)% water, Fig 5.4.

The A_2* measured by light scattering in the mixed solvents is an 'apparent second virial coefficient' which can be corrected to the true value, A_2, by taking into account the effects due to any preferential solvation, using equation 5.2.[5]

$$A_2 = A_2^* \left(\frac{M_{APP}}{M} \right) \qquad\qquad 5.2$$

A plot of these corrected values of A_2, as a function of water content shows that $A_2 = 0$ at 8, 18, 24 and 30 (wt/vol)% water, Fig 5.5. These points should reflect unperturbed states in a plot of the molecular dimension $<r_z^2>$. This value is derived from $<s_z^2>$, the radius of gyration, which is the quantity measured by light scattering,[6] and can be related to each other by equation 5.3.

$$\langle r_z^2 \rangle_o = 6 \langle s_z^2 \rangle_o \hspace{6cm} 5.3$$

Strictly this relationship only holds for unperturbed systems (denoted by the subscript zero) but it is used here to give a comparison with the appropriate molecular dimension derived from solution viscosity. Maxima are shown at 8, 16 and 29 (wt/vol)% water, in the $\langle r_z^2 \rangle$ plot, but a minimum occurs at 24 (wt/vol)% water, Fig 5.6.

Corresponding behaviour is also observed in the appropriate plot of dn/dc_3 with minima, this time, occurring at 8, 18 and 30 (wt/vol)% water and a maximum at 23 (wt.vol)% water, Fig 5.1.

The turning points in the λ_1^* plot are also in the same sense (ie maxima) for 8, 18 and 30 (wt/vol)% water with minima at 14 and 24 (wt/vol)% water. λ_1^* is defined here such that positive values indicate preferential solvation of dioxane and negative values indicate preferential solvation of water. The main solvent composition scale in all the figures are (wt/vol)% water content. The ancilliary scale, on all figures except Fig 5.2, indicates the corresponding mole ratios (water:dioxane) for these (wt/vol)% water contents.

5.2 DISCUSSION

The zero values for A_2, Fig 5.5, would indicate that at these water contents the polymer should be in its unperturbed state. Of the four solvent compositions that give $A_2 = 0$ those at 8, 18 and 30 (wt/vol)% water give values of $\langle r_z^2 \rangle$ of 19.5, 17.0 and 16.4nm respectively. They all occur as maxima in the curve. The values of $\langle r_z^2 \rangle$ at 24 (wt/vol)% water is 6nm which is a minimum in the curve. This water content (24 (wt/vol)%) corresponds to a maximum in

M_{APP}/M in Fig 5.4 indicating that this is also where the greatest solvation is occurring. The minima in the λ_1^* plot, at this point, indicates that the polymer is being solvated preferentially by water.

Strong interactions between dioxane and water are well established[4,7,8] with stoichiometries of mole ratios (water:dioxane) of $1:2$[12,11,10,12] $(2:1)$,$2:1$[4,9],$3:1$[13] and $5:1$[14] corresponding to weight/volume percentages of water of $8,18,30$, 39 and 51% respectively. The only one which has been quantified is the 5:1 complex where it has been shown that only 5% of the mixture is formally in the complex.[13] Morcellet and Loucheux[4] conceives that in poly(acrylic acid)/dioxane/water systems the polymer is solvated by a 3:1 complex in the range 0-61% dioxane and by a 1:1 complex of the mixed solvent at 80% dioxane (20% water).

The maxima in $\langle r_x^2 \rangle$ could be accounted for by the solvation of the polymer not by dioxane or water individually but by these complexes which break-up when the solvent composition changes from the stoichiometric values. The $A_2 = 0$ points are therefore associated not with 'unperturbed states' of the polymer in dioxane and water mixtures but with the polymer in a dioxane/water complexed mixture. The 'unperturbed states' occurring at 18 and 30 (wt/vol)% water can be associated with the 1:1 and 2:1 complexes with, as indicated by Fig 5.7, a preferential adsorption of water over dioxane in the immediate vicinity of the polymer.

The 'unperturbed state' at 8 (wt/vol)% water could be associated with a 1:2 complex. This would appear to be a reasonable assumption since the data in Fig 5.7 indicate that there is a preferential solvation of dioxane rather than water in this mixture. The value of $\langle r_x^2 \rangle_{max}$ at this water content is also larger than the other maxima. The results in Fig 5.4 would also appear to indicate that this

is a 'loose' association since M_{APP}/M is a minimum. The maxima for $\langle r_z^2 \rangle$ in the other cases are essentially the same, 17.0nm at 18 (wt/vol)% and 16.4nm at 30 (wt/vol)% water. This would appear to indicate that although the preferential solvation involves complexation of the mixed solvent it is the water that is almost exclusively in the immediate vicinity of the polymer, and this is substantiated by the similarity in the value of λ_1^* for these maxima as shown in Fig 5.7.

Where $\lambda_1^* = 0$ (see Fig 5.7) two 'non-preferentially solvated' states can be defined, at 5 and 10 (wt/vol)% water, which have similar $\langle r_z^2 \rangle$ values (16nm and 18nm respectively) and give $(M_{APP}/M)=1$. The slightly different values of $\langle r_z^2 \rangle$ could be due to the different processes occurring at these solvent compositions. At 5 (wt/vol)% a complex is forming whilst at 10 (wt/vol)% a complex is breaking-up.

It appears doubtful, although a solvent composition of 24 (wt/vol)% water corresponds to a mole ratio of 3:2, that this type of complex exists in this situation since the trends developed here are generally in the opposite sense to those corresponding to the complexes with stoichiometries of 1:2, 1:1 and 2:1.

The value of $\langle r_z^2 \rangle$ for the states where $\lambda_1^*=0$ is approximately three times that of the 'unperturbed' value at 24 (wt/vol)% water, possibly indicating that in the absence of any other interactions there is some self-association of the polymer (intermolecular). From Fig 5.7 it can be seen that at 24 (wt/vol)% water there are interactions between the polymer and solvent.

In general, preferential solvation by dioxane appears relatively to have expanded the coil, at 8 (wt/vol)% water, whereas there is a very small contraction of the coil when it is preferentially solvated by water, at 18 and 30 (wt/vol)% water, over the 'randomly' solvated

dimension given at 5 and 10 (wt/vol)% water, where there is no predominance of one solvent component over the other. In this sense, an alternative to the suggestion, above, of self-association, could be one of solvation of the polymer by water alone which results in a contracted species.

REFERENCES

1. J M G Cowie, Pure Appl.Chem. $\underline{23}$, 355, (1970)

2. B E Read, Trans. Faraday Soc. $\underline{56}$, 382, (1960).

3. F Hovorka, R A Schaefer, D Dreisbach, J.Am.Chem.Soc. $\underline{58}$, 2264, (1936).

4. M Morcellet, C Loucheux, Makromol.Chem. $\underline{179}$, 2439, (1978).

5. C Strazielle in 'Light Scattering from Polymer Solutions', ed M B Huglin, Academic Press, London, (1972).

6. T M Birshtein, O B Pitsyn, 'Conformations of Macromolecules', Wiley Interscience, New York, (1966).

7. G Kortum, V Valent, Ber.Bunsenges Phys.Chem. $\underline{81}$, 752, (1977).

8. M Baron, P Diaz de Vivar, C Henderson, An.Asoc.Quim.Argent. $\underline{64}$, 383, (1976).

9. G G Hammes, W Knoche, J.Chem.Phys. $\underline{45}$, 4041, (1966).

10. A Fratiello, D C Douglass, J.Mol.Spectrosc. $\underline{11}$, 465, (1963).

11. N A Trifonov, M Z Tsypin, Zhur.Fiz.Khim. $\underline{33}$, 1378, (1959).

12. N Muller, P Simon, J.Phys.Chem. $\underline{71}$, 568, (1967).

13. D Jannakoudakis, G Papanastasiou, P G Maurides, J.Chim.Phys. - Chim.Biol. $\underline{73}$, 156, (1976).

14. J A GEDDES, J. Am.Chem.Soc $\underline{55}$, 4832, (1933)
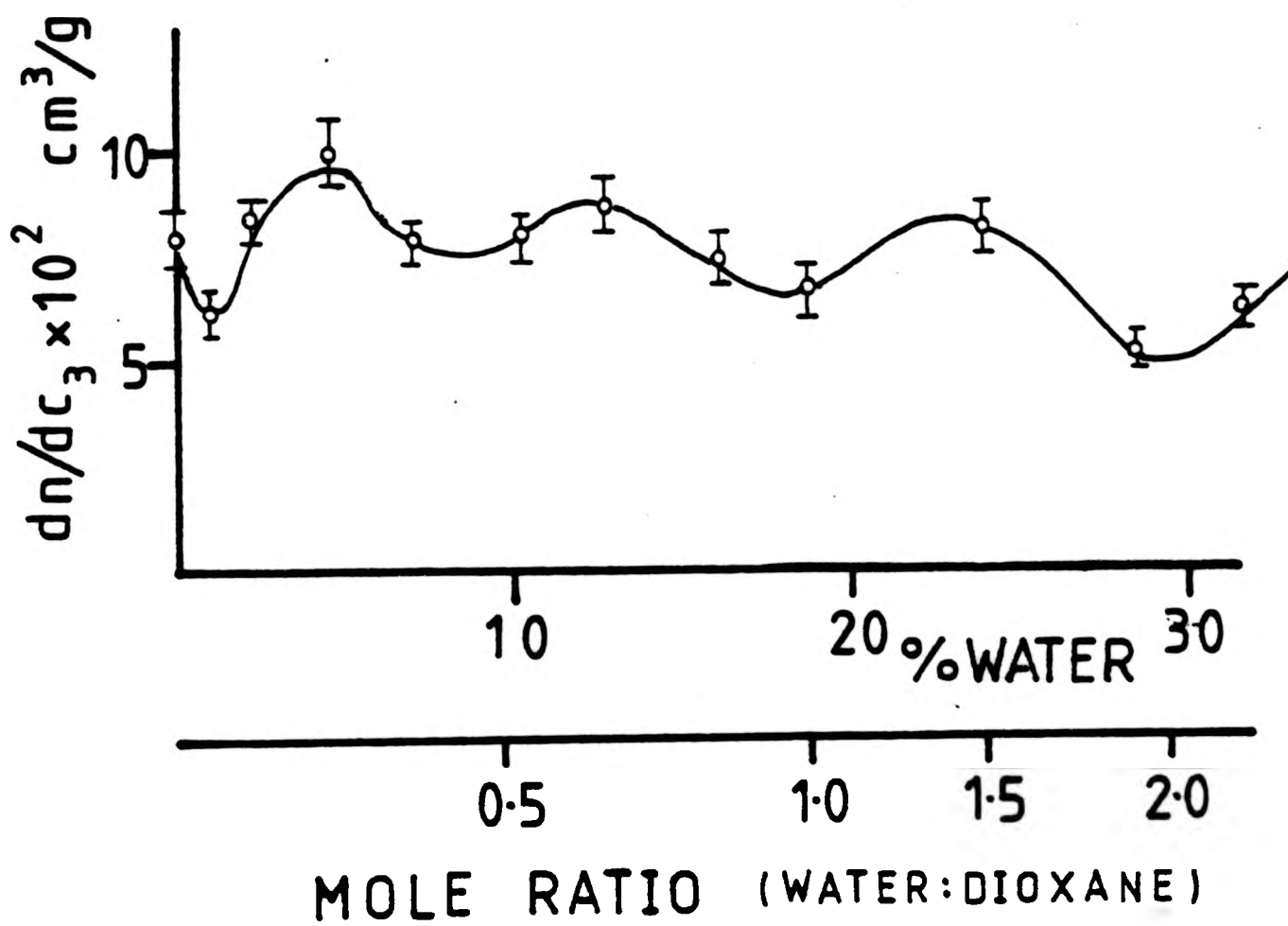
FIG 5.1 : dn/dc_3 for poly(acrylic acid) PAA300 in dioxane/water
at 298 K.
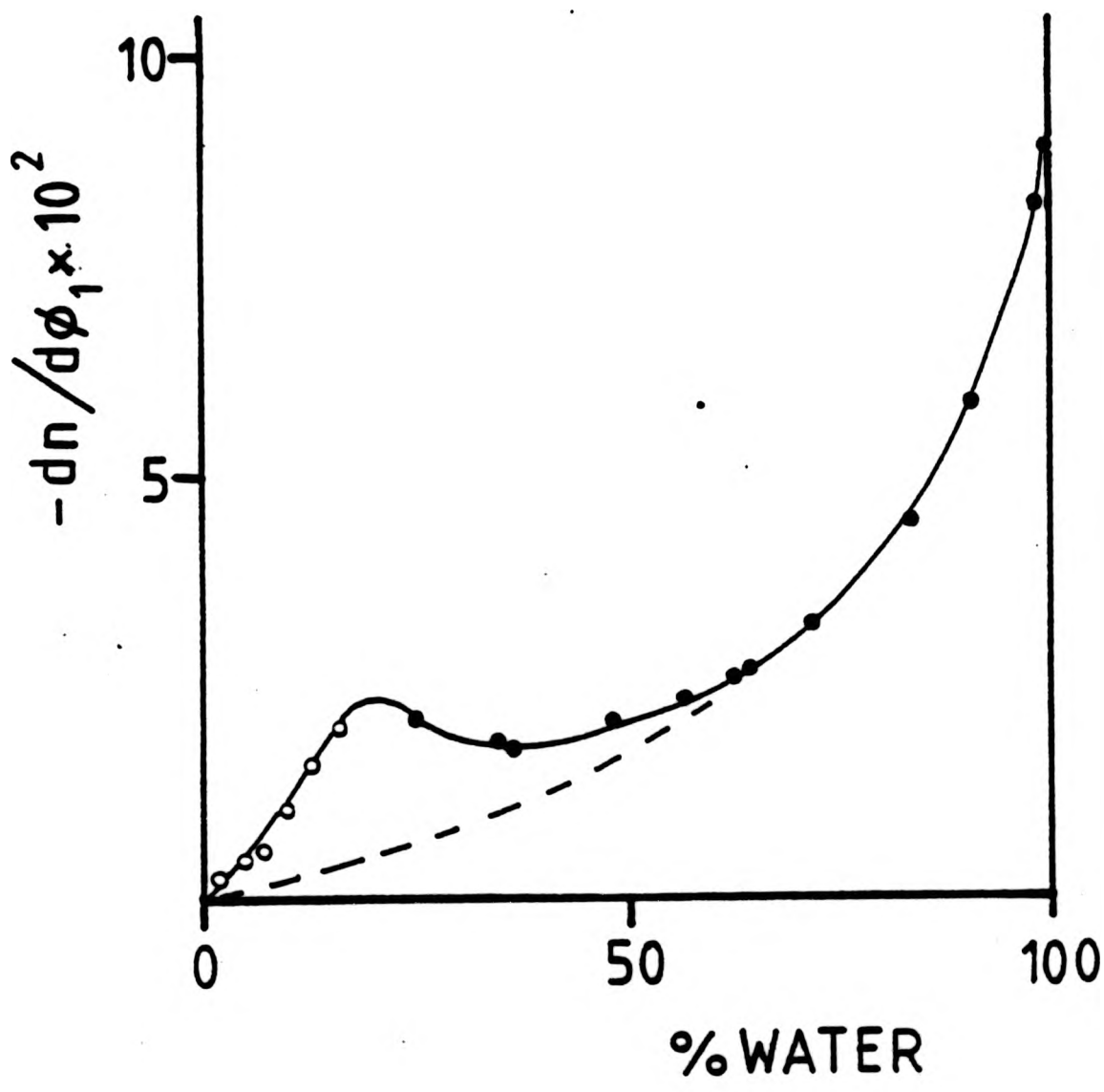
FIG 5.2 : $-dn/d\phi_1$ for poly(acrylic acid) PAA300 in dioxane/water at 298 K.
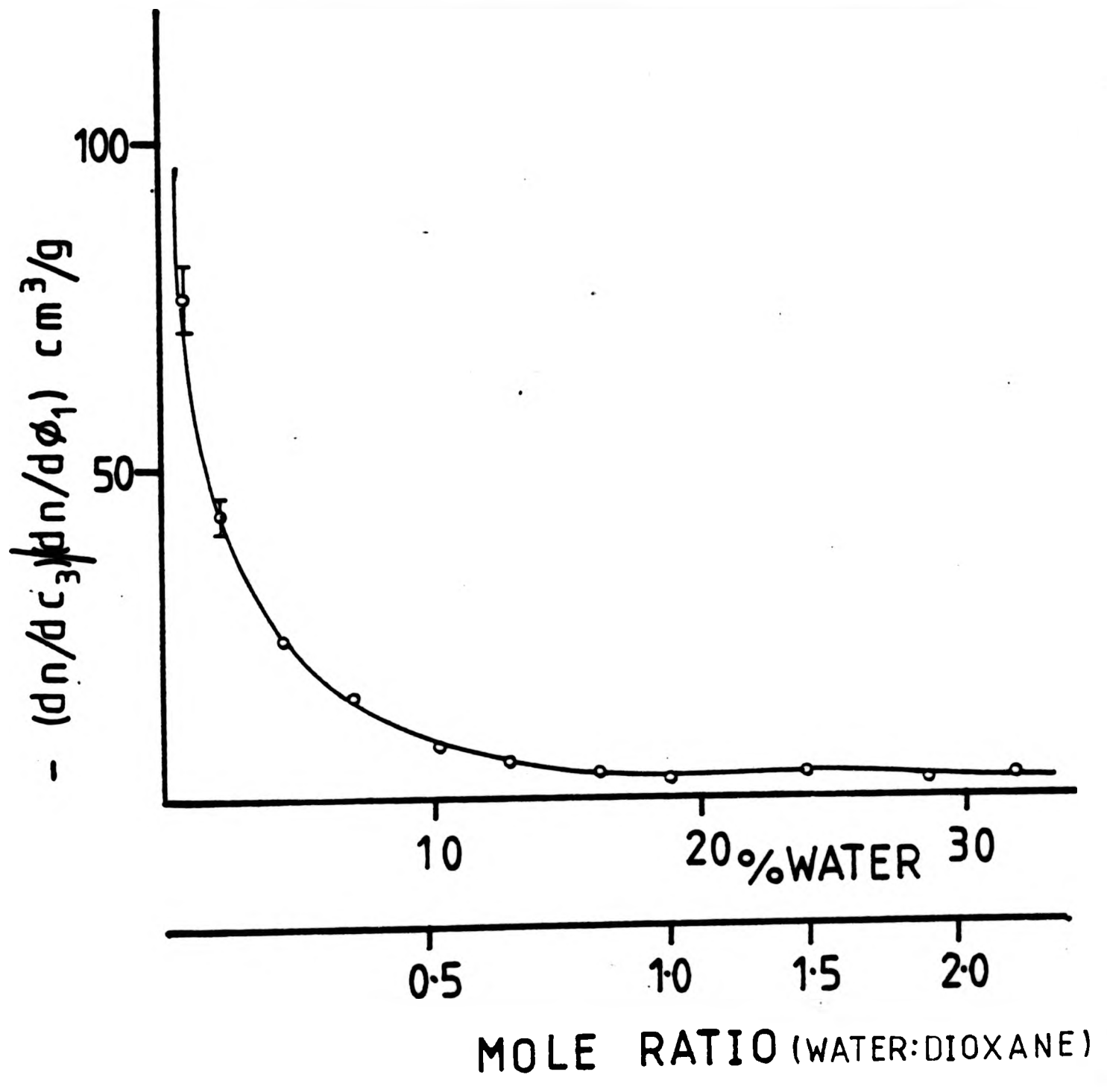
FIG 5.3 : $-(dn/dc_3)/(dn/d\phi_1)$ for poly(acrylic acid) PAA300 in dioxane/water at 298 K.
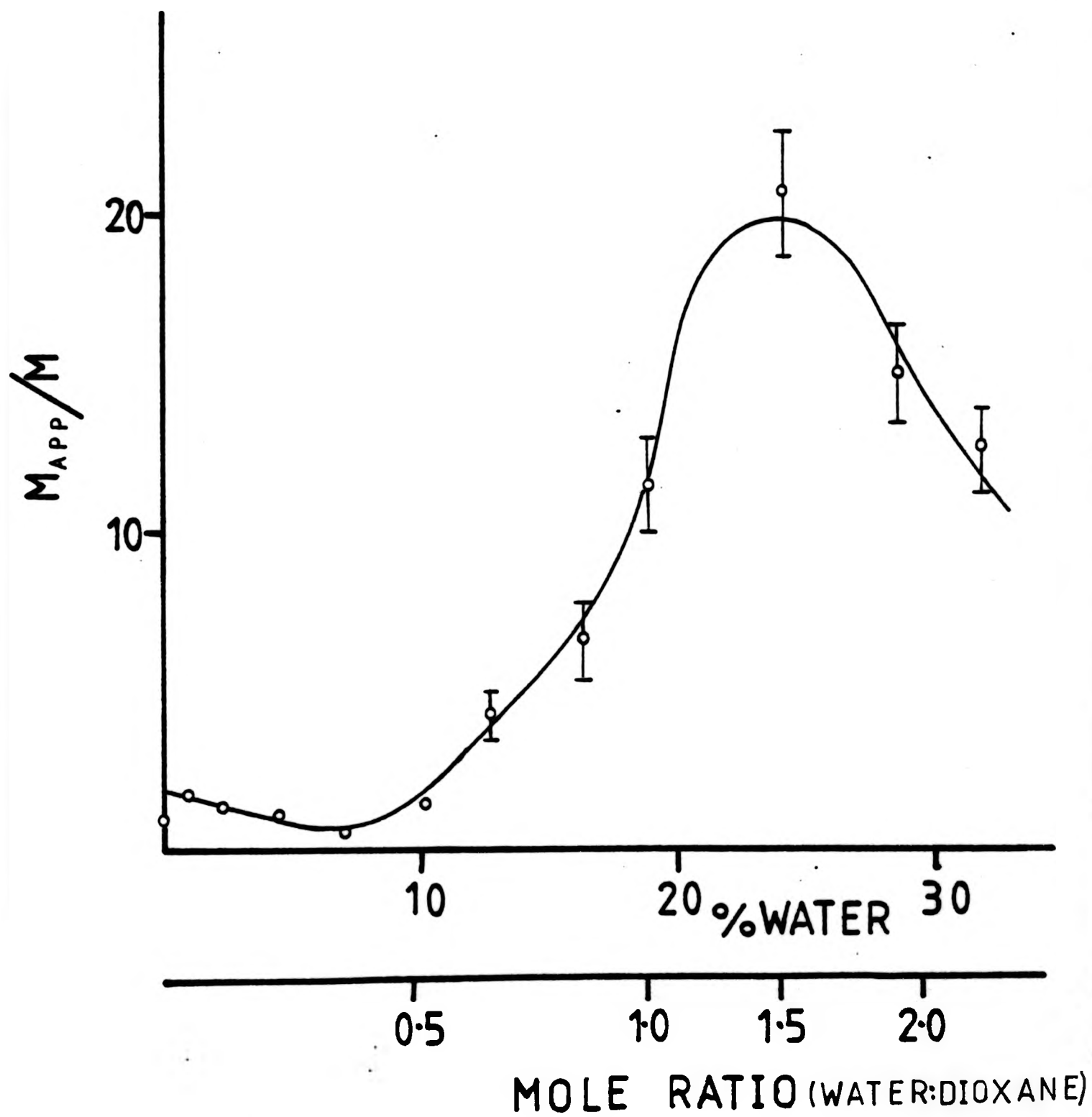
FIG 5.4 : M_{app}/M for poly(acrylic acid) PAA300 in dioxane/water at 298 K.
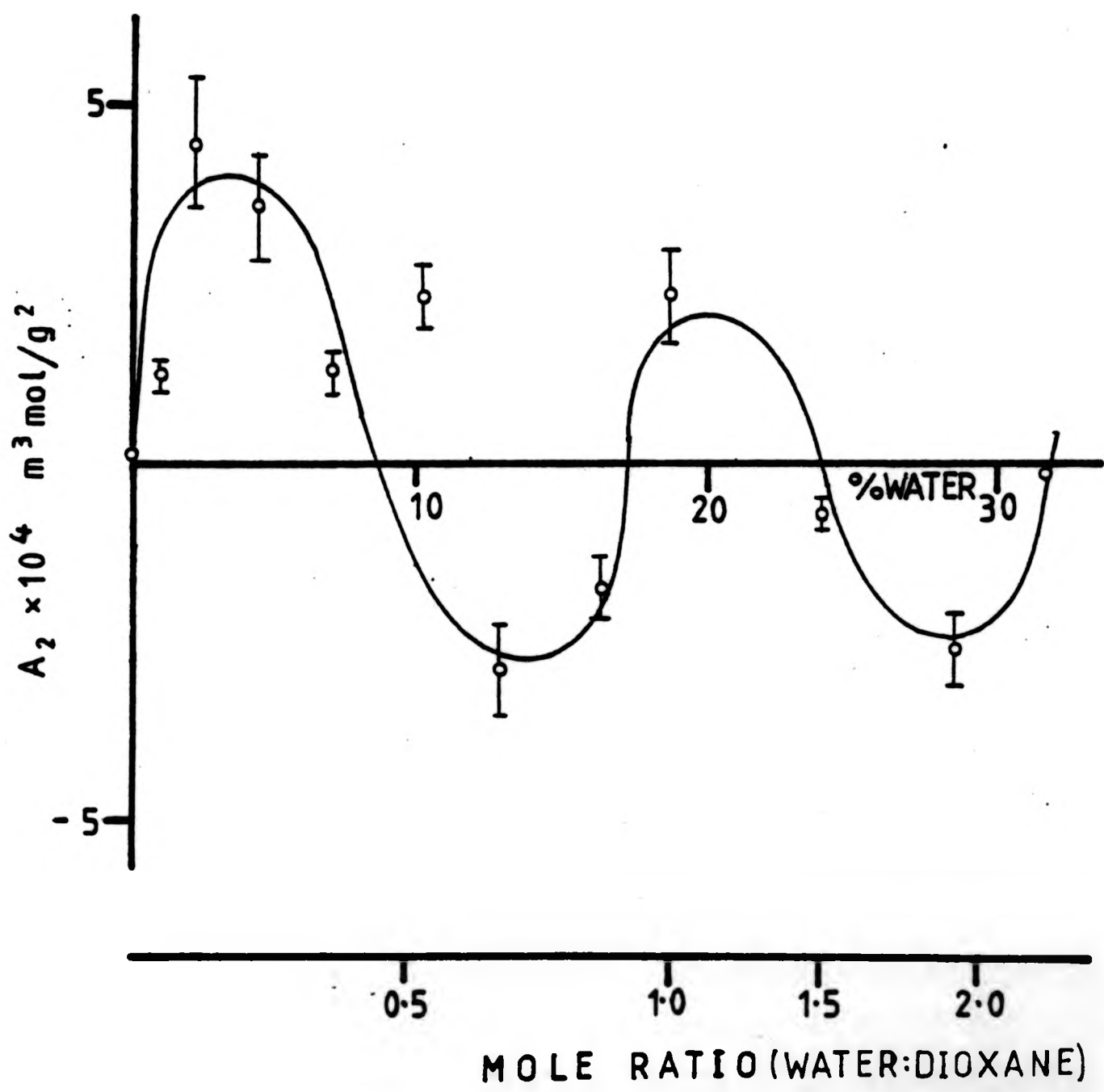
FIG 5.5 : Second virial coefficient, A_2, for poly(acrylic acid) PAA300 in dioxane/water at 298 K.
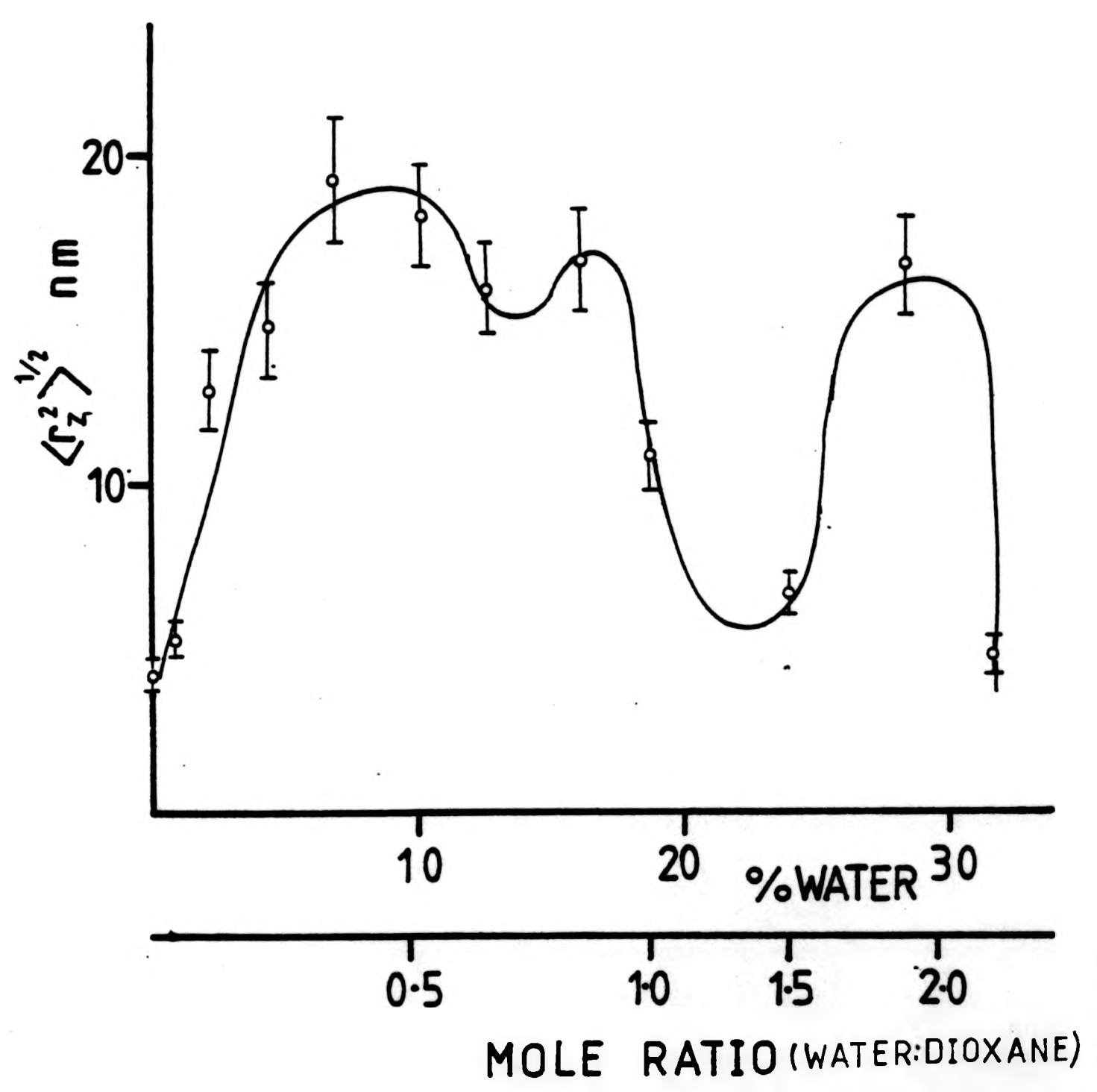
FIG 5.6 : Molecular dimension, $\langle r_z^2 \rangle^{\frac{1}{2}}$, for poly(acrylic acid) PAA300 in dioxane/water at 298 K.
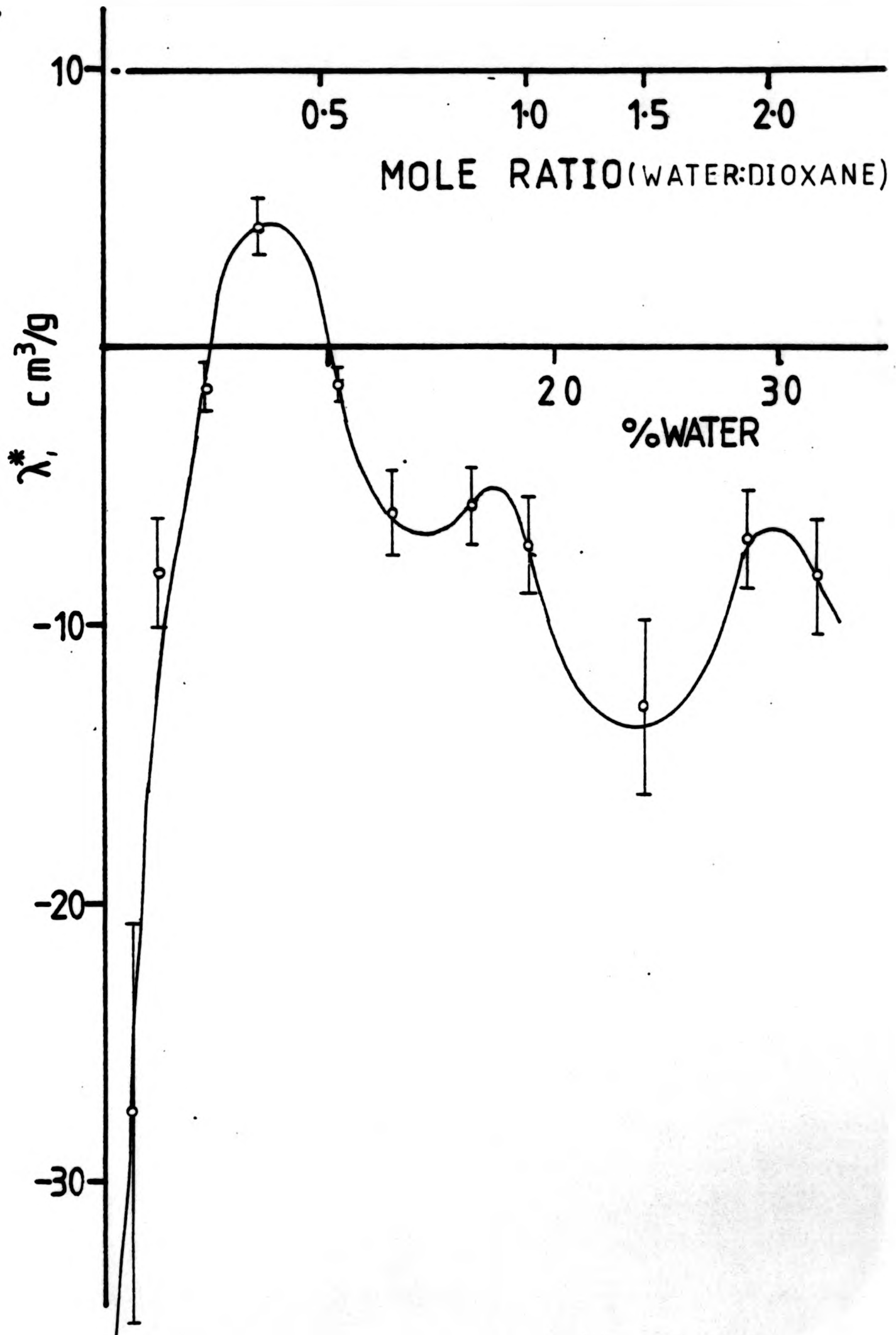
FIG 5.7 : Preferential solvation parameter, λ^*, for poly(acrylic acid) PAA300 in dioxane/water at 298 K.

TABLE 5.1 Light scattering data for poly(acrylic acid) in dioxane/water mixtures.

PAA	(wt/vol)% water	$\bar{M}_w \times 10^{-6}$ /g/mol	M_{APP}/M	$A_2^{\ddagger} \times 10^4$/ cm³mol/g²	$A_2 \times 10^4$/ cm³mol/g²	$<r_g^2>^{1/2}$/nm
PAA50	0.00	0.065 ± 0.007	-	+0.54 ± 0.05	+0.54 ± 0.05	8.56 ± 0.9
PAA150	0.00	0.307 ± 0.03	-	-0.11 ± 0.01	-0.11 ± 0.01	7.20 ± 0.7
PAA300	0.00	0.914 ± 0.09	1.00	0.13 ± 0.01	0.13 ± 0.01	4.2 ± 0.40
	1.13	1.69 ± 0.17	1.85 ± 0.06	0.62 ± 0.06	1.15 ± 0.23	5.18 ± 0.50
	2.25	1.29 ± 0.13	1.41 ± 0.28	3.10 ± 0.30	4.37 ± 0.90	12.82 ± 1.30
	4.51	1.03 ± 0.10	1.13 ± 0.23	3.11 ± 0.31	3.51 ± 0.70	14.74 ± 1.50
	7.00	0.47 ± 0.05	0.52 ± 0.05	2.32 ± 0.23	1.21 ± 0.24	19.22 ± 1.90
	10.33	1.27 ± 0.13	1.39 ± 0.28	1.57 ± 0.16	2.18 ± 0.44	18.05 ± 1.80
	12.76	3.86 ± 0.39	4.22 ± 0.84	-0.71 ± 0.07	-3.00 ± 0.60	15.80 ± 1.60
	16.00	6.08 ± 0.61	6.65 ± 1.33	-0.29 ± 0.03	-1.93 ± 0.39	16.74 ± 1.70
	18.67	10.52 ± 1.10	11.51 ± 1.50	+0.20 ± 0.02	+2.30 ± 0.46	10.84 ± 1.10
	23.88	19.03 ± 1.90	20.82 ± 2.08	-0.04 ± 0.004	-0.83 ± 0.17	6.53 ± 0.70
	28.58	13.80 ± 1.40	15.10 ± 1.50	-0.18 ± 0.02	-2.71 ± 0.54	16.47 ± 1.60
	31.73	11.56 ± 1.20	12.69 ± 1.30	-0.019 ± 0.002	-0.24 ± 0.05	4.71 ± 0.50

TABLE 5.2   Differential refractometry and preferential solvation data for poly(acrylic acid) in dioxane/water mixtures.

PAA No	(wt/vol)% water	$(dn/dc_3) \times 10^2 / cm^3/g$	$(dn/d\phi_1) \times 10^3$	$\dfrac{dn/dc_3}{dn/d\phi_1} / cm^3/g$	$\lambda_1^* / cm^3/g$
PAA50	0.00	7.9 ± 0.6	-	-	-
PAA150	0.00	6.0 ± 0.4	-	-	-
PAA300	0.00	7.9 ± 0.6	-	-	0.0
	1.13	6.2 ± 0.4	-0.81 ± 0.06	-76.84 ± 5.36	-27.57 ± 6.89
	2.25	8.4 ± 0.5	-1.94 ± 0.14	-43.37 ± 3.04	- 8.13 ± 2.03
	4.51	9.9 ± 0.7	-4.13 ± 0.29	-24.07 ± 1.68	- 1.52 ± 0.38
	7.00	7.9 ± 0.5	-5.17 ± 0.36	-15.28 ± 1.07	+ 4.26 ± 1.07
	10.33	8.0 ± 0.6	-10.54 ± 0.74	- 7.59 ± 0.53	- 1.36 ± 0.34
	12.76	8.7 ± 0.6	-15.21 ± 1.07	- 5.72 ± 0.40	- 6.03 ± 1.51
	16.00	7.4 ± 0.5	-20.00 ± 1.40	- 3.70 ± 0.26	- 5.84 ± 1.46
	18.67	6.8 ± 0.5	(E) -22.5	- 3.02 ± 0.21	- 7.23 ± 1.81
	23.88	8.2 ± 0.6	(E) -22.5	- 3.66 ± 0.30	-13.04 ± 3.26
	28.58	5.1 ± 0.3	(E) -21.0	- 2.42 ± 0.20	- 6.98 ± 1.75
	31.73	6.2 ± 0.4	(E) -19.5	- 3.18 ± 0.23	- 8.15 ± 2.04

(E) - estimated

CHAPTER SIX

pH MEASUREMENT

6. pH MEASUREMENT

The existence of strong interactions between water and dioxane has been shown by ir,[1-5] nmr,[6,7] and raman spectroscopy,[8] dielectric measurements,[9,10] ultrasonic absorption measurements[11] or density, refractive index, viscosity and partial specific volume measurements[12-15] although only the few cited in Chapter 5 report the existence of complexes of specific stoichiometry.

The pHs of dioxane/water and poly(acrylic acid)/dioxane/water systems were determined using an AgCl electrode. The measuring system was calibrated using mixtures of dioxane and hydrochloric acid adjusting the system to give a constant number of moles of H^+ ions in each mixture (0.96×10^{-3} moles). For the polymer solutions PAA50 was used with a concentration of 10^{-2} g/cm^3. At lower water contents, <10 (wt/vol)%, the readings are subject to uncertainty, Table 6.1, Fig 6.1.

The reduction of acidity of the mixtures (over that of water) in the region <50(wt/vol)% water confirms that there is complexation[16] in both the solvent and polymer systems. For mixtures with >50(wt/vol)% water the pH is essentially constant indicating no complex formation, or alternatively this can be interpreted as dioxane having a constant local environment.[17] It has been shown previously that there is complexation at these water contents but the constant pH may be due to an equilibrium between this complex formation and the 'structure-breaking effect' of the dioxane on the water.[16]

The results obtained confirm the studies that indicate that the addition of dioxane to water increases the basicity of the water.[18,19] Organic solvent/water mixtures can possess both acidic and basic properties but it is rare, with the exception of dioxane,[20] for one to be dominant as seen in this study.

The trend at low water contents is similar to that of poly(acrylic acid) in tetrahydrofuran/water mixtures.[21] A maximum has also been observed for a variety of aqueous salt solutions of poly(acrylic acid) which has been associated with hydrolysis. The apparent dissociation constant of weak polyacids decreases as the degree of dissociation increases and the apparent hydrolysis constant for alkali metal salts of the polyacid increases as the concentration increases leading to the observed maximum.[22] Thus the observed trends here are not unusual when the "solvent" interacts with this polyacid.

REFERENCES

1. W Gordy, J.Chem.Phys. 4, 769 (1936).

2. J Errera, R Gaspart, H Sack, J.Chem.Phys. 8, 63, (1940).

3. R Greinacher, W Luttke, R Mecke, Z Elektrochem. 59, 23, (1955).

4. A Fratiello, J P Luongo, J.Am.Chem.Soc. 85, 3072, (1963).

5. O D Bonner, Y S Choi, J.Phys.Chem. 78, 1723, (1974).

6. A Fratiello, D C Douglass, J.Mol.Spectrosc. 11, 465, (1963).

7. G Mavel, J.Phys.Radium 20, 1505, (1959).

8. C Fauconnier, M Harrand, Ann.Phys. (Paris) Ser 13, 1, 5, (1956).

9. S K Garg, C P Smyth, J.Chem.Phys. 43, 2959, (1965).

10. H A Rizk, Z.Phys.Chem. 66, 257, (1969).

11. G G Hammes, W Knoche, J.Chem.Phys. 45, 4041, (1966).

12. J A Geddes, J.Am.Chem.Soc. 55, 4832, (1933).

13. F Hovorka, R A Schaefer, D Dresibach, J.Am.Chem.Soc. 58, 2264, (1936).

14. G N Malcolm, J S Rowlinson, Trans.Faraday Soc. 53, 921, (1957).

15. D Jannakoudakis, G Papanastasiou, P G Maurides, J.Chim.Phys. - Chim.Biol. 73, 156, (1976).

16. K Ueberreiter, Colloid and Polymer Sci. 260, 37, (1982).

17. J R Goates, R J Sullivan, J.Phys.Chem. 62, 188, (1958).

18. D Feakins, D J Turner, J.Chem.Soc. 4987, (1965).

19. H P Bennetto, D Feakins, D J Turner, J.Chem.Soc.(A) 1211, (1966).

20. R G Bates in "Solute-Solvent Interactions", ed J F Coetzee, C D Ritchie, Marcel Dekker, New York, (1969).

21. S K Chatterjee, N Chatterjee, G Riess, Makromol.Chem. 183, 481, (1982).

22. H Daoust, M A Chabot, Macromolecules 13, 616, (1980).
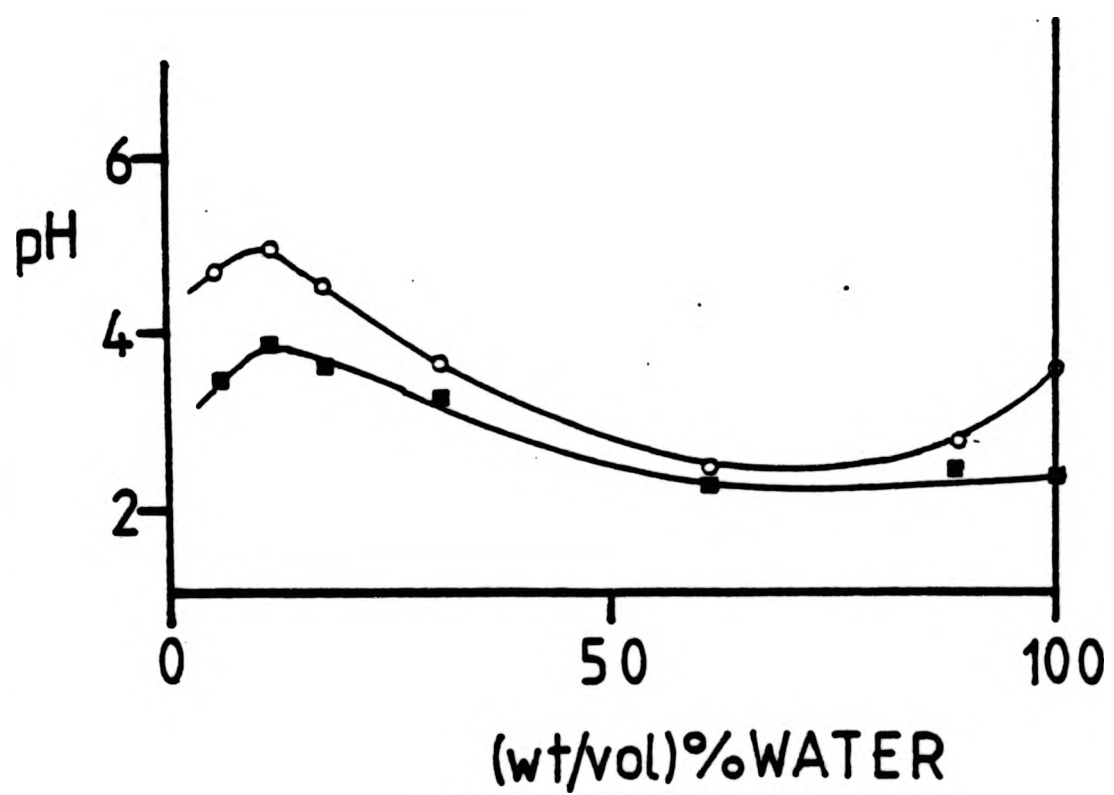
FIG 6.1 : Variation of pH for dioxane/water (o), and poly(acrylic acid) PAA50 in dioxane/water (■) as a function of water content. (polymer concentration = 10^{-2} g/cm^3).

TABLE 6.1   pH measurement for dioxane/water mixtures and 0.01 g/cm^3
            poly(acrylic acid), PAA50, solutions of these mixtures.

(wt/vol)% water	Solvent pH	Polymer/g/100cm^3	Polymer pH Soln
100	3.66	1.01	2.41
89.44	2.74	1.03	2.56
61.12	2.45	0.97	2.28
30.73	3.59	0.98	3.26
17.89	4.51	1.07	3.63
12.22	4.94	0.95	3.87
6.15	4.72	1.06	3.46

CHAPTER SEVEN

LASER RAMAN SPECTROSCOPY

7. LASER RAMAN SPECTROSCOPY

The Raman spectrum in the carbonyl stretching region ($1600-1800$ cm^{-1}) was determined for 10 g/100 cm^3 solutions of PAA50 in dioxane and dioxane/water mixtures containing 1.7 and 18.7 (wt/vol)% water, over various temperature ranges. A solution of 3.29 g/100 cm^3 PAA17 in dioxane was also studied (295-353K).

The main problem with these samples was the inability to get sufficient heat removal from the samples. This caused local heating and degradation which could be visually detected, after the experiments.

Sample PAA50 showed four peaks, in dioxane, at 1639, 1658, 1690 and 1730 cm^{-1}, Fig 7.1, whereas sample PAA17 showed only two peaks at 1648 and 1718 cm^{-1} with evidence of a shoulder at 1690 cm^{-1}, Fig 7.2. For PAA17, between 316K and 339K there is a distinct narrowing of the peak at 1718 cm^{-1} but with the shoulder at 1690 cm^{-1} retained. When water was added to the system the peaks at 1639, 1658 and 1690 cm^{-1} remained the same but the peak above 1700 cm^{-1} moved from 1730 to 1717 cm^{-1}, with 18.7 (wt/vol)% water, Fig 7.1. In the PAA50/dioxane system there is little change in the relative intensities of the peaks, Table 7.1. (NB These are weak signals when compared to the Raman spectrum of poly(acrylic acid) as a whole.) With PAA17, the relative intensity of the 1718 cm^{-1} peak increases over that at 1648 cm^{-1}, Table 7.2. When water is added there is a decrease in the relative intensities of all peaks over that at 1639 cm^{-1}, although analysis was made difficult by the sloping baselines, in all cases.

The peaks at 1658 and above 1700 cm^{-1} can be assigned in a similar way to those of propionic acid in dioxane and dioxane/water mixtures (see Chapter 8). That at 1658 cm^{-1} can be assigned to an intermolecular dimeric species whilst that at 1730 cm^{-1}, in dioxane, can be assigned

to a non-hydrogen bonded monomeric species which on additon of water moves to lower frequencies indicating the introduction of hydrogen-bonding. These peaks have been observed during polymerisation of acrylic acid[1] but the peak above 1700 cm^{-1} is absent in poly(methacrylic acid)[2]. The existence of a peak at 1690 cm^{-1} has been noted in aqueous solutions of poly(acrylic acid)[3,4] and identified with a hydrogen-bond interaction involving the solvent[4]

$$-C \overset{O}{\underset{OH}{\diagup\,}} \quad \longleftarrow \text{SOLVENT} \longrightarrow \quad \overset{HO}{\underset{O}{\diagdown\,}} C-$$
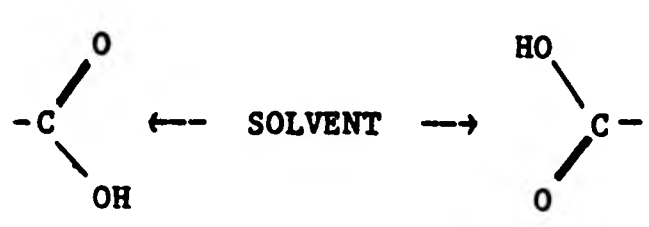
which disappears above a degree of neutralisation of 0.2[3] (sodium polyacrylate shows a conformational change at this degree of neutralisation[3]). This is the main peak for poly(methacrylic acid) and is associated with an intramolecular hydrogen-bond interaction.[2] The peak in water is broad, and there is some interference from the spectrum of water in this region,[2] but it is a sharp peak in this study, even with water present. This may possibly indicate that the interaction involves dioxane as well as, or instead of water[2] in a more specific interacting environment. The peaks at 1639 cm^{-1} can be associated with a dimeric species similar to that at 1658 cm^{-1} but intramolecular as opposed to an intermolecular one.[5] It is possible that these peaks have merged with sample PAA17.

The movement of the peaks at 1658 and 1730 cm^{-1}, for PAA50, to 1648 and 1718 cm^{-1}, for PAA17, in dioxane would appear to indicate that PAA17 is involved in hydrogen-bond interactions which are normally disfavoured in dioxane.[6] The distinct narrowing of the 1718 cm^{-1}

peak in PAA17 between 316K and 339K indicates a loss of some of the hydrogen-bonding character although this assertion should be treated with caution because the situation can be more complex.[7]

Since the solutions, for the two polymers, were prepared in a similar way, ie polymers and solvent were prepared in the same manner, by incorporation into sealed systems, the only differences are those of molecular weight and polymer concentration, and therefore proximity to the phase separation boundary. The existence of intramolecular interactions, in PAA50, to a greater extent than PAA17 which involves more intermolecular interactions, with polymer and solvent can only be attributed to their relative states in relation to their phase separation boundaries. It is interesting to note, in this context, the loss of some hydrogen-bond character between 316K and 339K, for PAA17, which is in the region of phase separation for the higher molecular weight poly(acrylic acids).

REFERENCES

1. A Simon, G Heintz, Wiss Z Tech.Hochschule Dresden 8, 217, (1958).

2. J L Koenig, A C Angood, J Semen, J B Lando, J.Am.Chem.Soc. 91, 7250, (1969).

3. L Bardel, G Cassanas-Fabre, M Alain, J.Mol.Struct. 24, 153, (1975).

4. A Simon, M Mucklich, D Kunath, G Heintz, J.Polym.Sci. 30, 201, (1958).

5. G C Pimental, A L McClellan, 'The Hydrogen Bond' Reinhold, New York, (1960).

6. G Allen, E F Caldin, Quart.Rev. 7, 255, (1953).

7. D Steele, 'The Interpretation of Vibrational Spectra', Chapman & Hall, London, (1971).
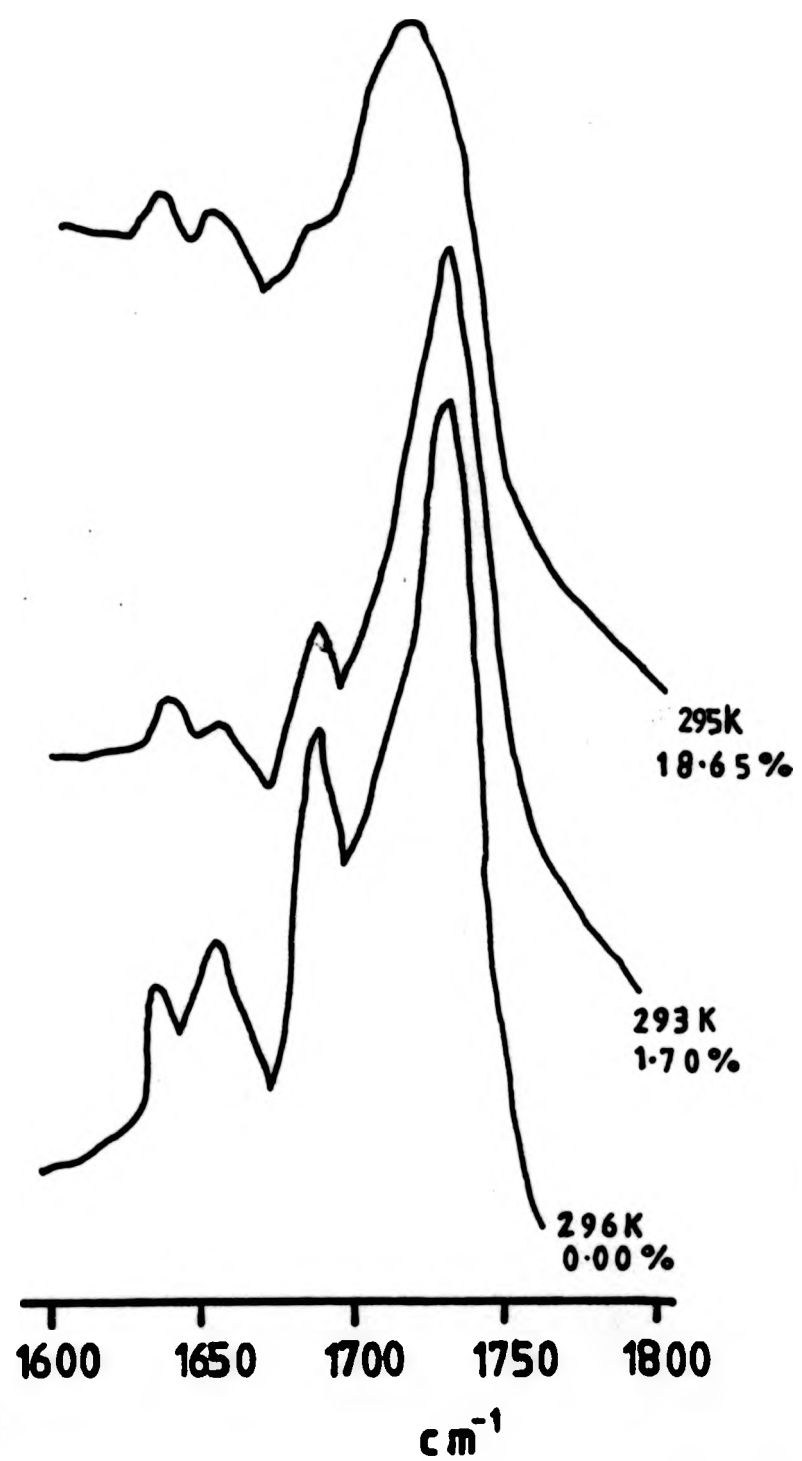
FIG 7.1 : Laser Raman spectra for poly(acrylic acid) PAA50
in dioxane and dioxane/water .
(polymer concentration 10 g/100cm^3 , water content as
indicated).
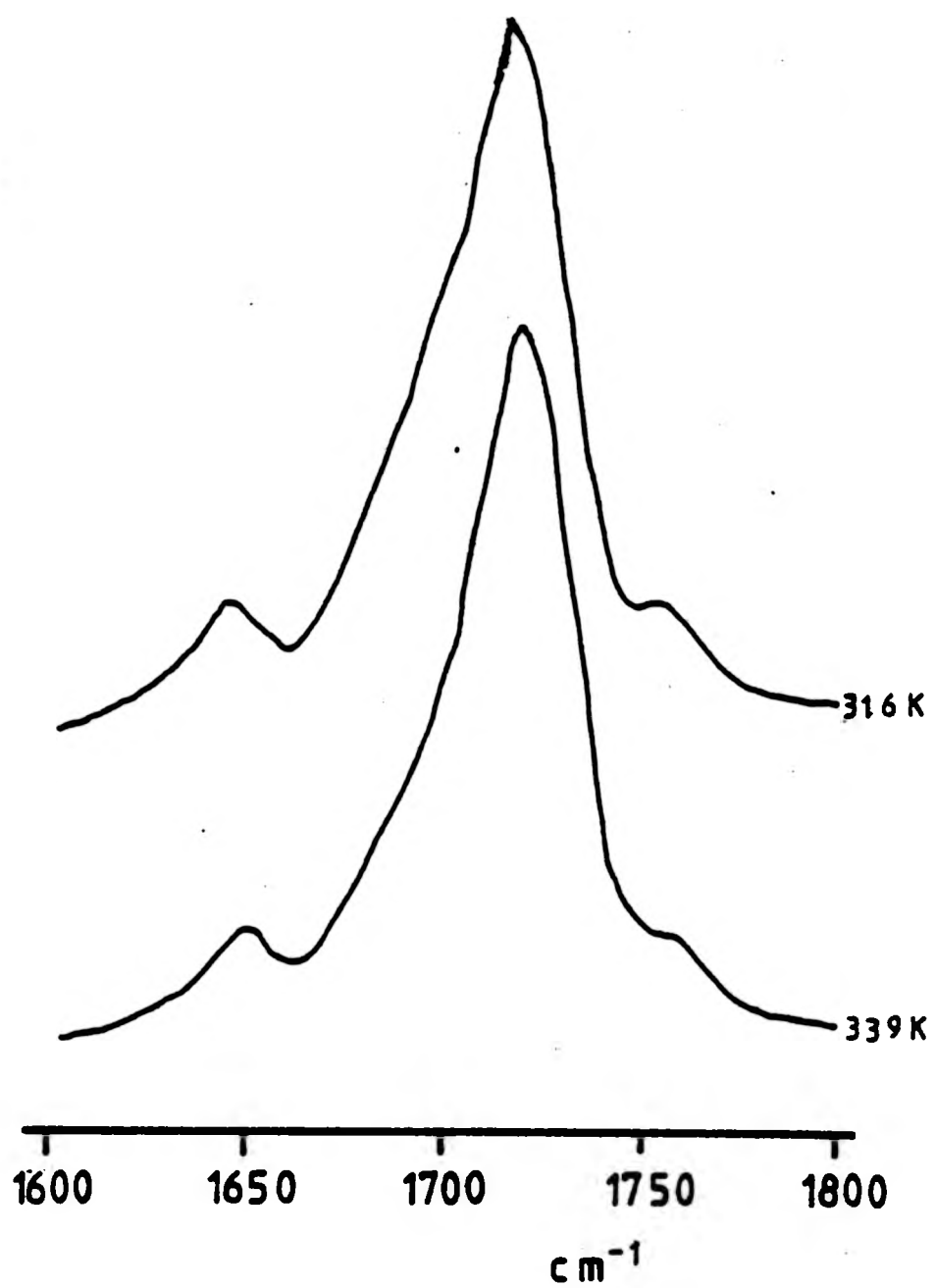
FIG 7.2 : Laser Raman spectra for poly(acrylic acid) PAA17
in dioxane.
(polymer concentration   3.29 g/100cm^3 , temperature as
indicated).

TABLE 7.1   Relative peak intensities of $\nu_{C=O}$ Raman peaks for poly(acrylic acid), PAA50, in dioxane and dioxane/water mixtures as a function of temperature.

(wt/vol)% water	Temp/K	Rel. peak intensity			
0.00		$1639cm^{-1}$	$1658cm^{-1}$	$1690cm^{-1}$	$1730cm^{-1}$
	296	1.0	1.3	2.6	4.5
	303	1.0	1.2	2.5	4.4
	308	1.0	1.4	2.8	4.7
1.70		$1638cm^{-1}$	$1658cm^{-1}$	$1690cm^{-1}$	$1728cm^{-1}$
	293	1.0	1.0	2.9	8.6
	304	1.0	1.4	3.0	8.5
	310	1.0	1.5	2.7	7.7
	322	1.0	1.0	2.2	6.3
	328	1.0	1.1	2.4	7.0
18.70		$1636cm^{-1}$	$1656cm^{-1}$	$1690cm^{-1}$	$1717cm^{-1}$
	295	1.0	1.6	4.0	10.4
	297	1.0	1.4	2.4	5.4

TABLE 7.2   Relative intensities of $\nu_{C=O}$ Raman peaks for poly(acrylic acid), PAA17, in dioxane as a function of temperature.

Temp/K	Relative peak intensity	
	$1648~cm^{-1}$	$1718~cm^{-1}$
295	1.0	6.2
298	1.0	4.7
304	1.0	4.7
309	1.0	5.2
316	1.0	5.9
327	1.0	5.7
339	1.0	6.4
353	1.0	7.0

CHAPTER EIGHT

PROPIONIC ACID/DIOXANE SOLUTIONS

8.   PROPIONIC ACID/DIOXANE SOLUTIONS

Because the determination of the heat of mixing of systems involving polymeric species is difficult, the use of a small molecule analogue system may provide information for comparative purposes.   In this case, propionic acid was used as a small molecule analogue for poly(acrylic acid).   Its heat of mixing and heat of dilution with dioxane and dioxane/water mixtures were determined.   The raman spectra for these systems were also recorded.

The heat of mixing, ΔH_m, of propionic acid with dioxane has been shown to be endothermic,[1] at 298K, with a maximum occurring at a dioxane mole fraction of 0.35 (136 J/mol).   Due to the different purification methods used the results obtained here differ by about 23% from the values in the literature.[1]   In this study ΔH_m is still endothermic but with a maximum of 104J/mol at a dioxane mole fraction of 0.49, Fig 8.1.   The dioxane used was prepared in a similar manner as that used in the phase separation studies whilst Inglese et al[1,2] use dioxane which has been fractionally distilled over sodium wire.   The propionic acid was purified by fractional distillation through a 0.35m Vigreux column followed by fractional distillation through a 0.4m column packed with glass rings whilst purging with nitrogen.   Inglese et al[1,3] use propionic acid which has been purified by fractional distillation through a 2m column packed with glass helices.

The determination of ΔH_m as a function of temperature (at 298, 304, 308 and 313K) shows the parameter to be decreasingly endothermic with increasing temperature, the maximum being at a mole fraction, of dioxane, of 0.49 in all cases, Table 8.1, Fig 8.1.

The heat of dilution, ΔH_d, of dioxane solutions of propionic acid by dioxane is also endothermic at 298K.   For solutions of propionic acid in dioxane/water solutions (5.72 (wt/vol)% water) ΔH_d became exothermic at this temperature, Table 8.2, Fig 8.2.   The initial solutions to be diluted contained a volume fraction of approximately 0.05 in propionic acid.   The

appropriate X_h function for these systems, Fig 8.3, gave linear relationships with $(\phi_1 + \phi_2)/2$, in the concentration range studied, with negative slopes and intercepts (the concentration independent parameter X_1) of +6.5 for the single solvent and -1.4 for the mixed solvent system.

The raman spectrum of the symmetrical carbonyl stretching frequency of propionic acid in liquid form shows a peak at 1659 cm^{-1} which has been interpreted as being due to a dimeric species,[4] Fig. 8.4. When the acid is dissolved in dioxane a new peak appears at 1740 cm^{-1} representing a non-hydrogen bonded species[5] and the peak at 1659 cm^{-1} is observed to weaken. When increasing amounts of water (2.93, 8.95 and 18.80 (wt/vol)%) are added to the solvent the peak at 1740 cm^{-1} broadens and moves to 1723 cm^{-1}, Fig 8.4. This is believed to denote the presence of a hydrogen bonded species which is not a dimer.[5] The peak at 1659 cm^{-1} diminishes progressively with increasing water content, Fig 8.4. The solutions used contained 20 g/100 cm^3 propionic acid.

A plot of the ratio of the intensities of the appropriate 'monomeric' species to that of the dimer as a function of temperature, on a log-log scale, (the temperature is expressed in terms of $^{\circ}C$ for convenience) shows a decrease in the relative amount of the dimeric species as the temperature increases, Fig 8.5.

When propionic acid is mixed with dioxane the predominant dimeric species of the acid are broken-up producing a non-hydrogen bonded species leading to an endothermic heat of mixing and heat of dilution. When the temperature is increased there is a decrease in the relative amount of this dimeric species in the pure acid. The reduction in ΔH_m with increasing temperature can then be attributed to the decrease in the relative amount of this species initially present, which leads to less bond-breaking.

When water is added to the system the dimer break-up is offset by the formation of hydrogen-bonded species between the acid and water

leading to an exothermic heat of dilution. These trends are reflected in the exothermic heat of solution, ΔH_s, (the heat of mixing at infinite dilution) of the acid in water. It has been variously determined at 298K as -1.544 ± 0.004,[6] -1.50 ± 0.16,[7] -1.7 ± 0.2[8] and -1.63 ± 0.005[9] kJ/mol. Studies, as a function of temperature also indicate a decrease in the heat of solution with increasing temperature (-2.062 ± 0.008 at 293K to -1.050 ± 0.008 kJ/mol at 303K[6]) reflecting the decrease in stability in the hydrogen-bonded species between the acid and water with increasing temperature.

REFERENCES

1. E Wilhelm, A Inglese, J-P Grolier, H V Kehiaian, J.Chem. Thermodynamics 14, 517, (1982).

2. A Inglese, E Wilhelm, J-P Grolier, H V Kehiaian, J.Chem. Thermodynamics 12, 217, (1980).

3. A Inglese, E Wilhelm, J-P Grolier, H V Kehiaian, J.Chem. Thermodynamics 14, 33, (1982).

4. R J Jakobsen, Y Mikawa, J R Allkins, G L Carlson, J.Mol.Struct. 10, 300, (1971).

5. N B Colthup, L H Daly, S E Wiberley, "Introduction to Infrared and Raman Spectroscopy", Academic Press, London, (1964).

6. J Konkek, I Wadsö, Acta.Chem.Scand. 25, 1541, (1971).

7. E M Arnett, J V Carter, quoted in ref 6.

8. R Aveyard, R W Mitchell, Trans.Faraday Soc. 64, 1757, (1968).

9. L Avedikan, J Juillard, J-P Morel, M Ducross, Thermochimica Acta 6, 283, (1973).
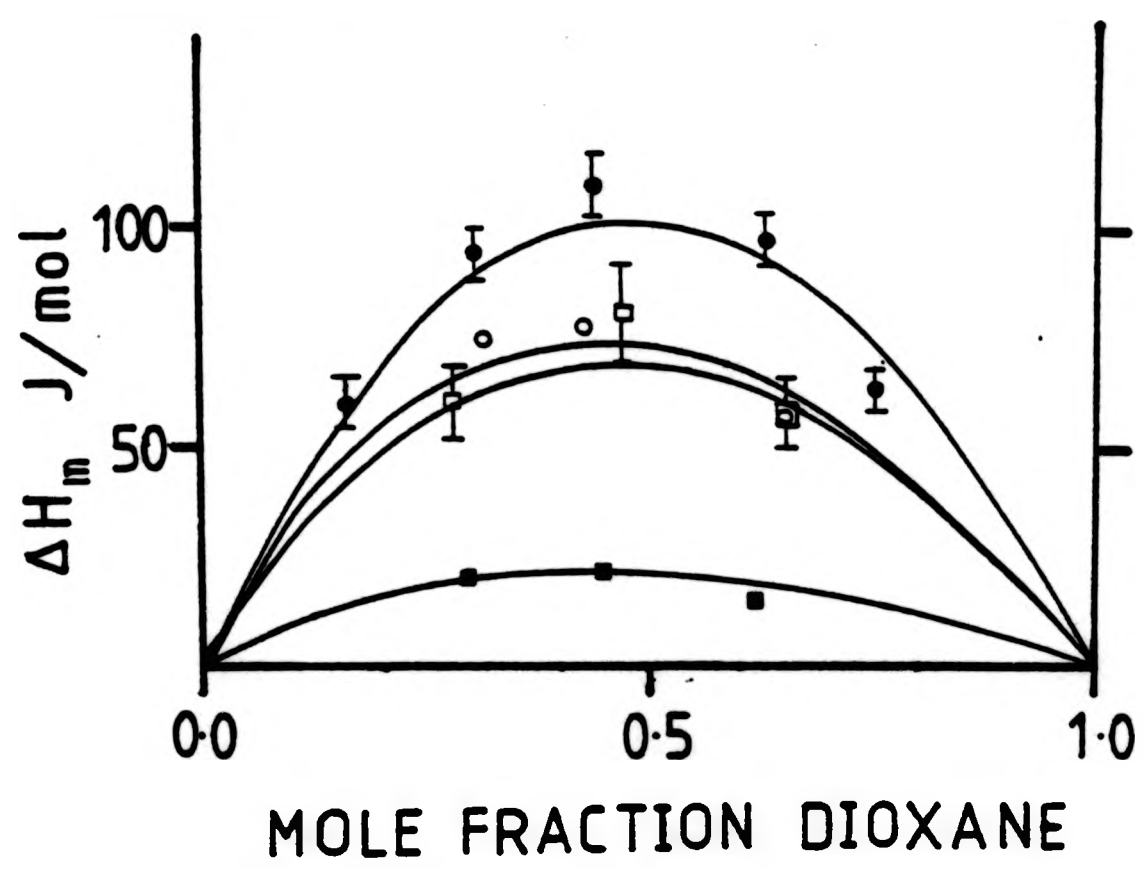
FIG 8.1 : Heat of mixing for propionic acid/dioxane as a
function of temperature.
(298 K(●), 304 K(○), 307 K(□), 312 K(■))
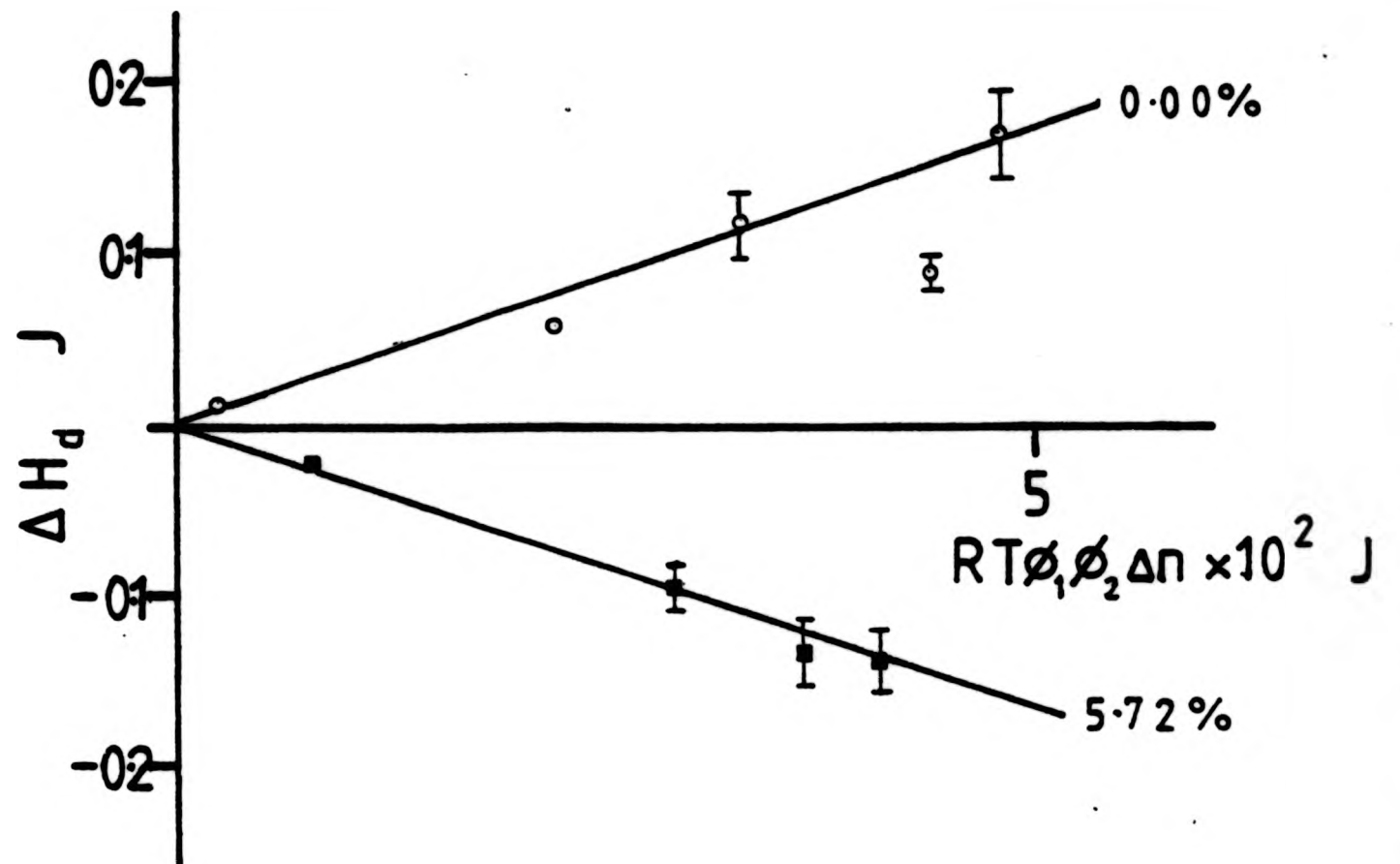
FIG 8.2 : Heat of dilution, ΔH_d, of propionic acid in
dioxane/water as a function of water content at 298 K.
(water content : 0.00(wt/vol)%(○), 5.72(wt/vol)%(■)).
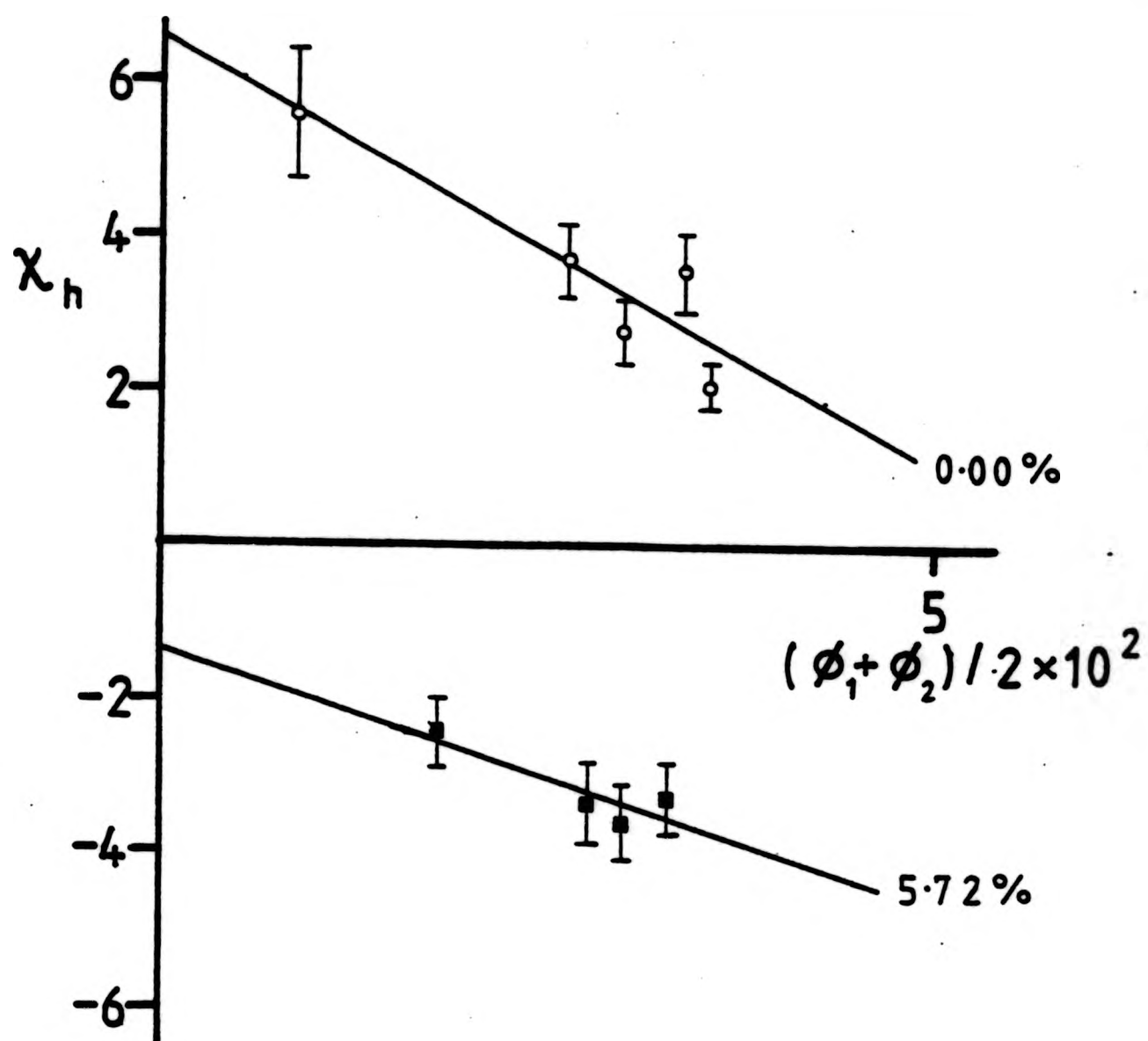
FIG 8.3 : Interaction parameter, χ_h, for propionic acid in
dioxane/water as a function of water content at 298 K.
(water content : 0·00(wt/vol)%(o), 5·72(wt/vol)%(■)).
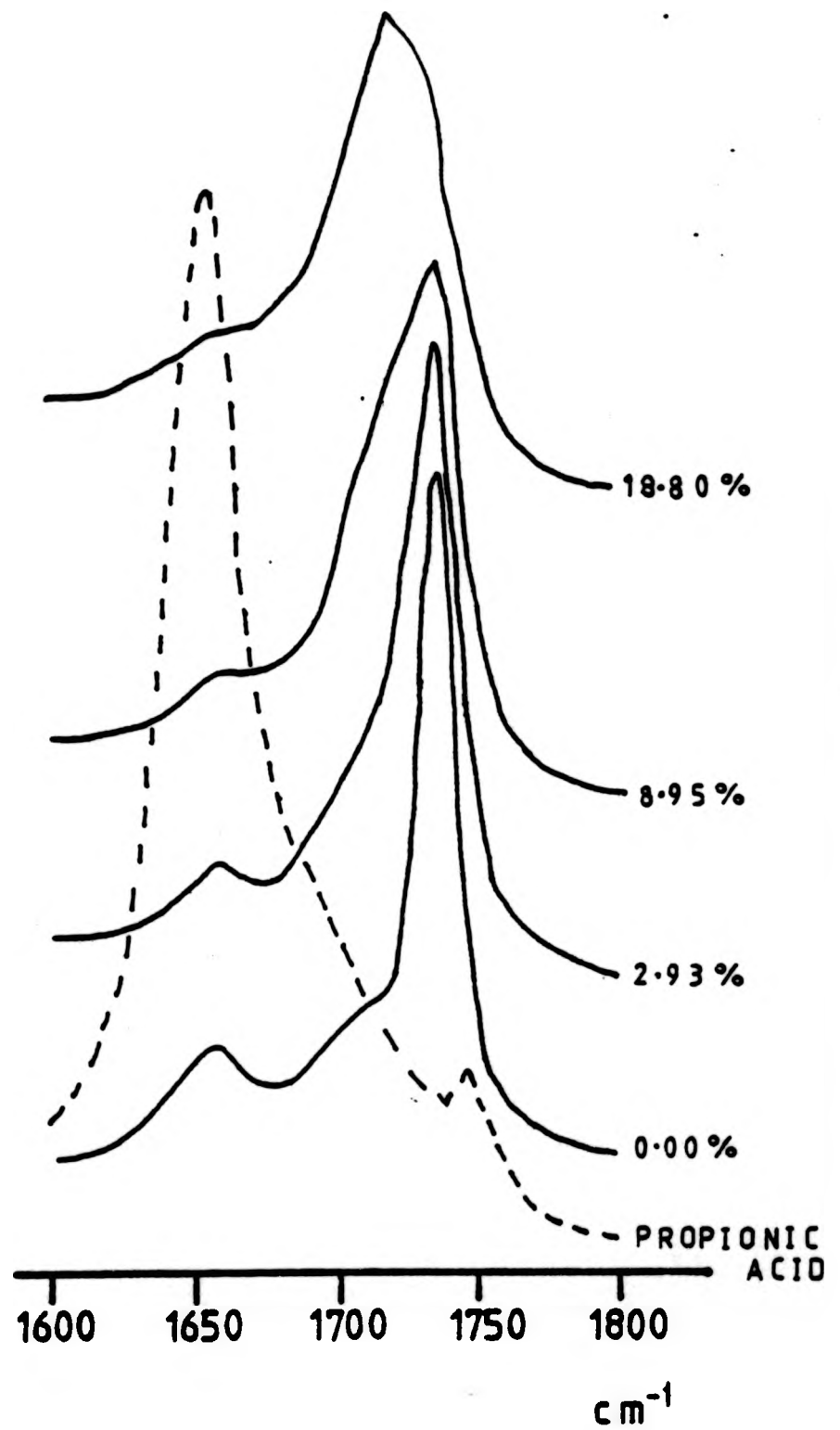
FIG 8.4 : Laser Raman spectra for propionic acid in dioxane,
dioxane/water and pure acid.
(acid concentration 20 g/100cm^3, water content as
indicated).
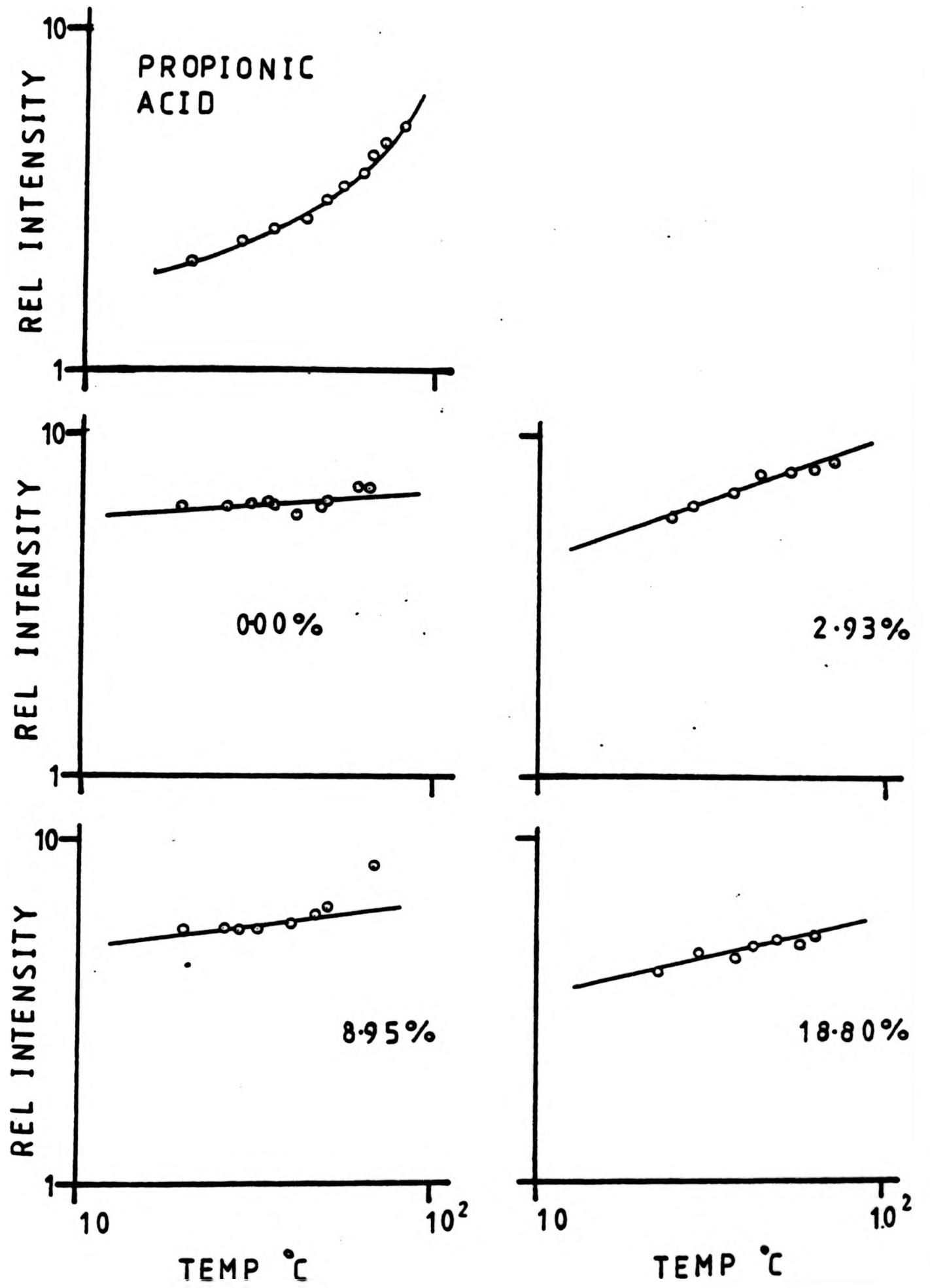
FIG 8.5 : Relative intensity (monomeric/dimeric) of Raman peaks for propionic acid in dioxane/water as a function of temperature. (water content as indicated).

TABLE 8.1   Heat of mixing of propionic acid with dioxane.

Temp/K	Mole Fraction Dioxane	$\Delta Hm/J/mol$
298	0.16	60.0 ± 4.20
	0.30	94.2 ± 6.6
	0.44	109.1 ± 7.7
	0.63	97.5 ± 6.8
	0.75	63.0 ± 4.4
304	0 31	74.2 ± 1.5
	0.43	77.4 ± 1.6
	0.65	58.0 ± 1.2
307	0.28	59.3 ± 8.3
	0.47	79.9 ± 11.2
	0.65	56.1 ± 7.9
312	0.30	20.0 ± 0.6
	0.45	21.5 ± 0.6
	0.62	14.2 ± 0.4

TABLE 8.1 Heat of mixing of propionic acid with dioxane.

Temp/K	Mole Fraction Dioxane	$\Delta Hm/J/mol$
298	0.16	60.0 ± 4.20
	0.30	94.2 ± 6.6
	0.44	109.1 ± 7.7
	0.63	97.5 ± 6.8
	0.75	63.0 ± 4.4
304	0 31	74.2 ± 1.5
	0.43	77.4 ± 1.6
	0.65	58.0 ± 1.2
307	0.28	59.3 ± 8.3
	0.47	79.9 ± 11.2
	0.65	56.1 ± 7.9
312	0.30	20.0 ± 0.6
	0.45	21.5 ± 0.6
	0.62	14.2 ± 0.4

TABLE 8.2   Heat of dilution of propionic acid with dioxane and dioxane/water mixtures at 298K.

(wt/vol)% water	$RT\emptyset_1\emptyset_2\Delta n$ $\times 10^2$/J	$\Delta H_d \times 10^2$/J	$(\emptyset_1+\emptyset_2)/2$ $\times 10^2$	x_h
0.00	0.27	1.50 ± 0.20	0.90	5.6 ± 0.8
	2.20	6.00 ± 0.90	3.01	2.7 ± 0.4
	3.30	12.20 ± 1.80	3.65	3.7 ± 0.6
	4.40	9.00 ± 1.30	3.55	2.1 ± 0.3
	4.80	17.10 ± 2.60	3.39	3.6 ± 0.5
5.72	0.82	-2.00 ± 0.30	1.80	-2.40 ± 0.4
	2.87	-9.60 ± 1.40	3.30	-3.3 ± 0.5
	3.64	-13.40 ± 2.00	3.00	-3.7 ± 0.6
	4.08	-13.70 ± 2.00	2.80	-3.4 ± 0.5

CHAPTER NINE

MICROCALORIMETRY

9.1 MICROCALORIMETRY

The heat of dilution, ΔH_d, was determined for solutions of PAA150 at 298K (Fig 9.1, 9.2) and PAA50 at 298K (Fig 9.3, 9.4), 303.5K (Fig 9.5, 9.6), 307K (Fig 9.7, 9.8), 312K (Fig 9.9, 9.10) and 316K (Fig 9.11, 9.12) in dioxane and for PAA50 in a dioxane/water mixture containing 5.06 (wt/vol)% water at 298K (Fig 9.3, 9.4) and 312K (Fig 9.9, 9.10). For all the systems a maximum initial polymer volume fraction of 0.02 was used. The values of the enthalpic interaction parameter, χ_h, for these systems were derived from computations of $\Delta H_d/RT\emptyset_1\emptyset_2\Delta n$, as previously defined. The values of the concentration independent parameter, χ_1, determined by an extrapolation procedure, are shown in Table 9.1.

PAA50 solutions in dioxane gave endothermic heats of dilution at all the temperatures studied. PAA150 solutions also gave an endothermic heat of dilution at 298K and both gave similar curves for both types of plot. The concentration independent parameter, χ_1, can be regarded as coincident for both molecular weights, at this temperature and this agrees with the observed similarities in the temperatures of phase separation. A plot of χ_1 as a function of temperature, for PAA50 solutions, indicates a decreasingly positive value of this parameter with increasing temperature, Fig 9.13. Extrapolation of the curve, to higher temperatures, also indicates that this parameter, and the heat of dilution, are positive at temperatures approaching the phase separation boundary, for this system, and hence it can also be deduced that the heat of mixing, ΔH_m, at these temperatures is also positive.

When water was added to the system the heat of dilution, and χ_h, became negative. A similar analysis to that applied above shows that there is little change in the shapes of the plots between the two

temperatures studied, Fig 9.3, 9.9 . The values of χ_1 can again be regarded as coincident and much smaller than the value obtained for this parameter, from the equivalent single solvent system, Fig 9.4, 9.10, Table 9.1 .

9.2 DISCUSSION

Calorimetric investigations of poly(acrylic acid) have generally been confined to studies in water[1-4] or in salt solutions at various degrees of neutralisation.[1-8] Both the heat of solution,[4] ΔH_s, (the heat of mixing at infinite dilution) and the heat of dilution[1,3,4] in water have been found to be endothermic and small, approximating to zero at 298K. The heat of dilution for acrylic acid in water has also been found to be endothermic[9] but that for propionic acid is exothermic.[4] This small caloric effect has been observed for poly(acrylic acid) in ethylene glycol[4] but in this case it is exothermic, whereas a much larger exothermic effect has been found with formamide.[4] This effect is due to dissociation of the $-CO_2H$ groups which is more pronounced in formamide than water because of its greater ionising capability.[4]

The heat of dilution for sodium salts of poly(acrylic acid) has been found to be exothermic.[1-3,5-7] It has also been determined that at very dilute concentrations it is endothermic, but small[4,8] (all determined at 298K). The heat of dilution was found to increase exothermically with increasing degree of neutralisation[3] and with increasing temperature.[7]

The heat of dilution of the tetraalkylammonium salts of poly(acrylic acid) with water, have been found to be increasingly endothermic in the order[6]

$$Me_4N < Et_4N < Pr_4N < Bu_4N$$
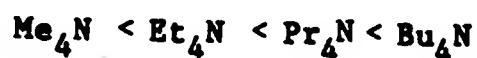
This can be accounted for by the structure-forming tendencies of the R_4N species.[6]

Previous workers have quoted the heat of dilution in dioxane as being endothermic, but from unpublished data.[10] A value of -1.46 kJ is quoted for the 'amount of heat absorbed by the system when one mole of poly(acrylic acid) is dissolved in an infinite amount of dioxane', at $302.2K$[10].

An alternative analysis of the data can lead to a measure of the parameter, κ, directly (χ_1 can be equated with κ_1)[11] using the equation

$$\Delta H_d = RT \kappa \Delta n_2 (\phi_1 - \phi_2) \qquad 9.1$$

where Δn_2 is the number of base moles of polymer in the solution and the other parameters have their previous meaning. A plot of κ as a mean function of the volume fraction (ie $(\phi_1 + \phi_2)/2$) gives curves similar to those for the corresponding plot for χ_h. The concentration independent parameters, κ_1, determined in this way are tabulated in Table 9.1. The values of χ_1 and κ_1 are in reasonable general agreement and qualitatively do show the same decreasingly positive trend with increasing temperature. A comparable analysis of the system in water, at 298K, leads to χ_1 and κ_1 values of 0.20 and 0.45 respectively and the extrapolation on this data is approximately a factor of ten larger than the experimental data quoted here.

The system in 0.2M hydrochloric acid also gives an endothermic heat of dilution and a χ_1 value (0.15) comparable to that of the water system.

REFERENCES

1. J-P Cartier, H Daoust, Can.J.Chem. $\underline{49}$, 3935, (1971).

2. V Crescenzi, F Delben, F Quadrifoglio, D Dolar, J.Phys.Chem. $\underline{77}$, 539, (1973).

3. V Crescenzi, F Quadrifoglio, F Delben, J.Polym.Sci. A2, $\underline{10}$, 357, (1972).

4. J Klein, W Scholz, Makromol.Chem. $\underline{180}$, 1477, (1979).

5. S Morimoto, Kobunshi Konbunshu $\underline{34}$, 851, (1977).

6. N Ise, K Mita, T Okubo, J.Chem.Soc. Faraday Trans. I $\underline{69}$, 106, (1973).

7. K Mita, T Okubo, J.Chem.Soc. Faraday Trans. I. $\underline{70}$, 1546, (1974).

8. J Škerjanc, Biophys.Chem. $\underline{1}$, 376, (1974).

9. J Pannell, J.Phys. E $\underline{6}$, 475, (1973).

10. A R Schultz, P J Flory, J.Am.Chem.Soc. $\underline{75}$, 3888, (1953).

11. M A Kabayama, A Y Daoust, J.Phys.Chem. $\underline{62}$, 1127, (1958).
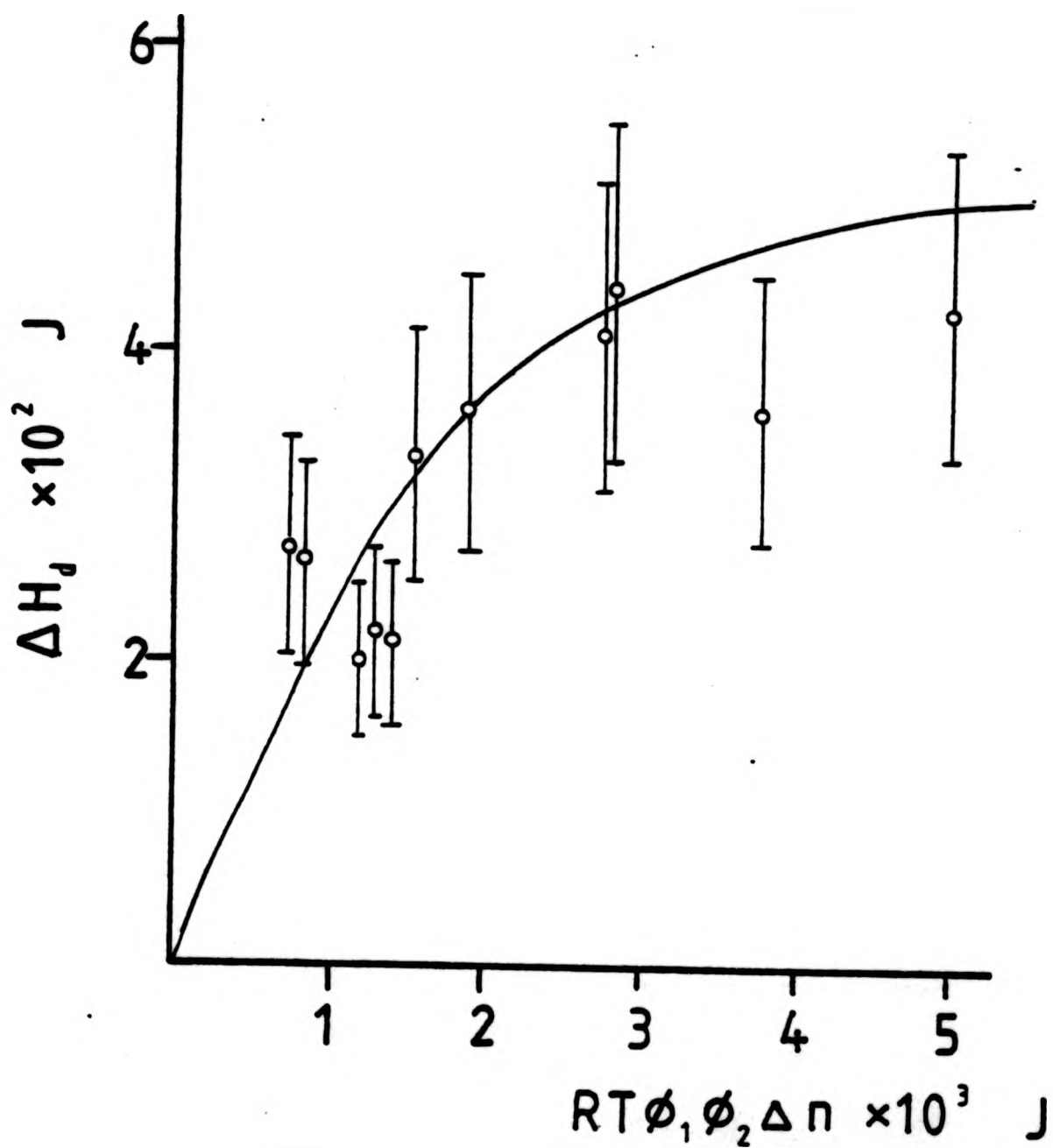
FIG 9.1 : Heat of dilution, ΔH_d, of poly(acrylic acid) PAA150 in dioxane at 298 K.
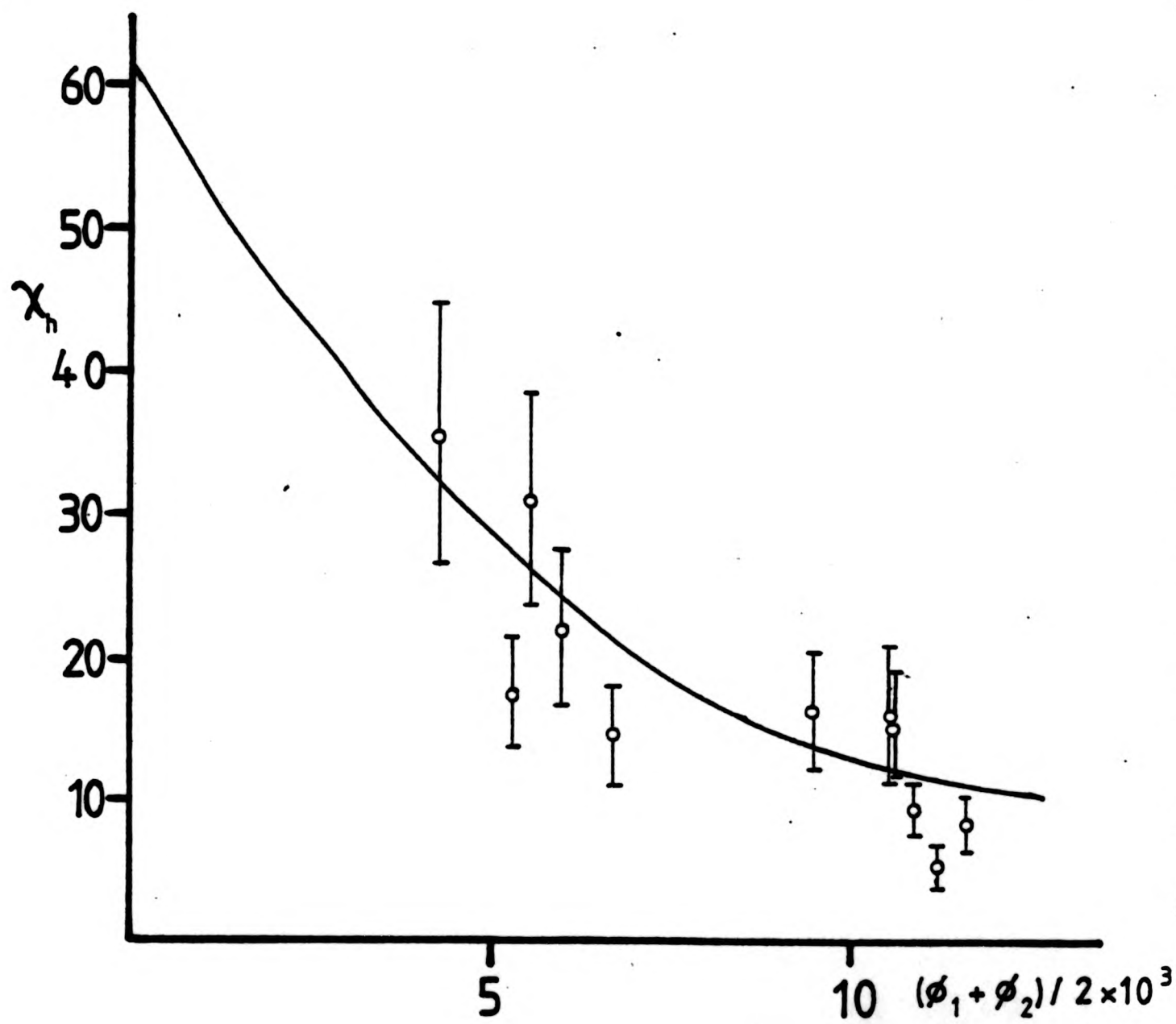
FIG 9.2 : Interaction parameter, χ_h, for poly(acrylic acid) PAA150 in dioxane at 298 K.
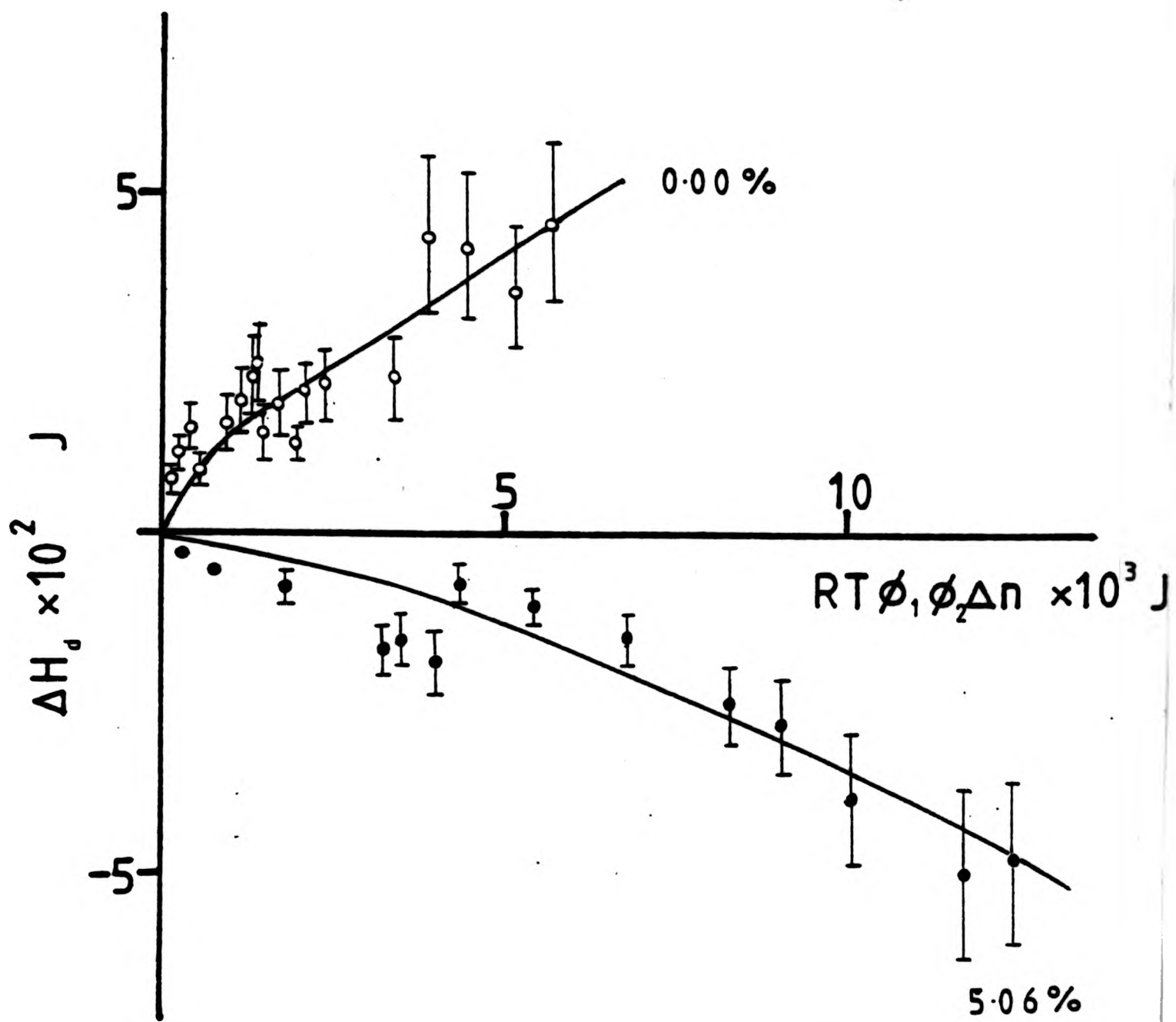
FIG 9.3 : Heat of dilution, ΔH_d, of poly(acrylic acid) PAA50 in dioxane (o) and dioxane/5·06(wt/vol)%water (●) at 298 K.
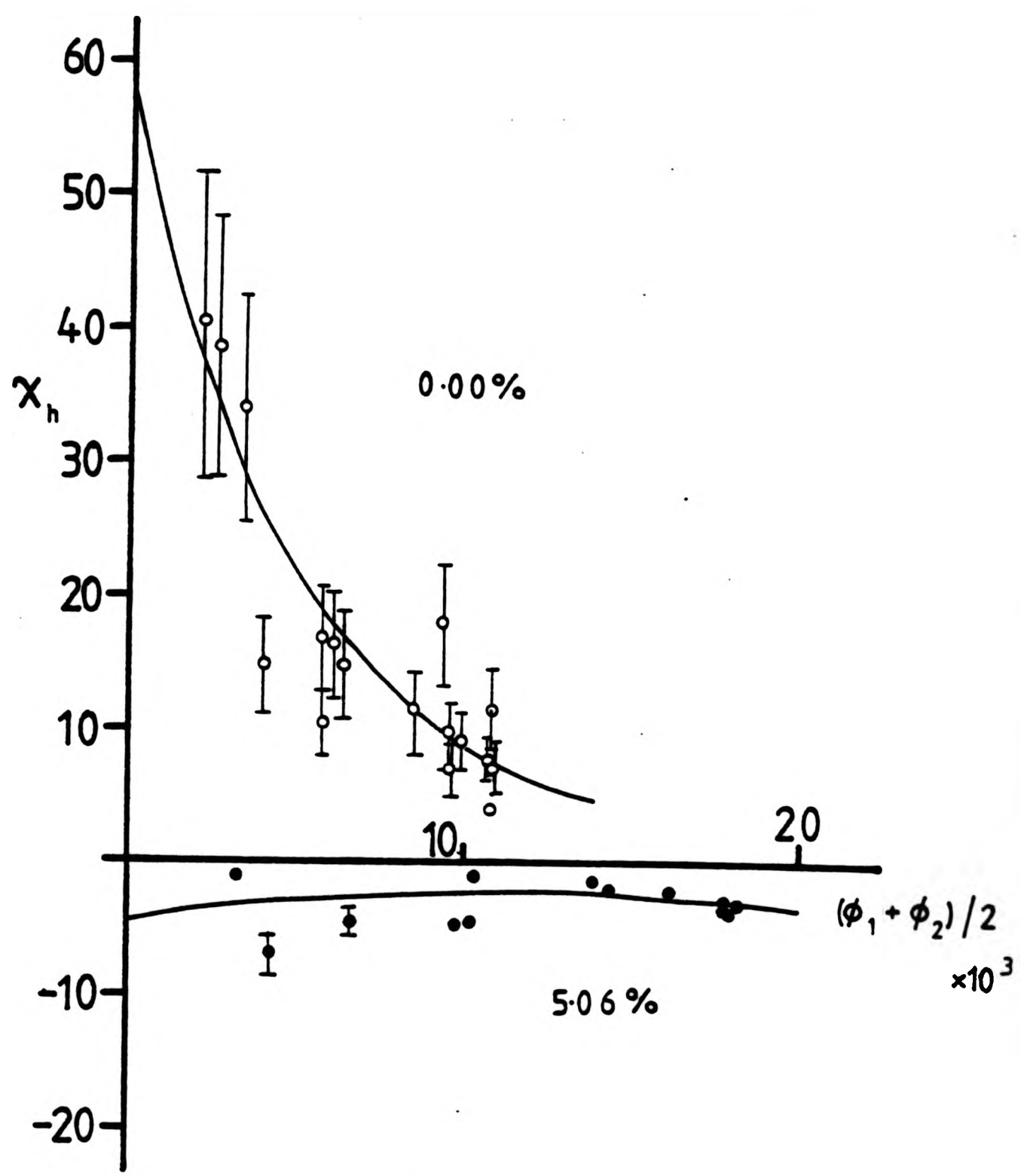
FIG 9.4 : Interaction parameter, χ_h, for poly(acrylic acid) PAA50
in dioxane (o) and dioxane/5·06(wt/vol)% water (●) at 298 K.
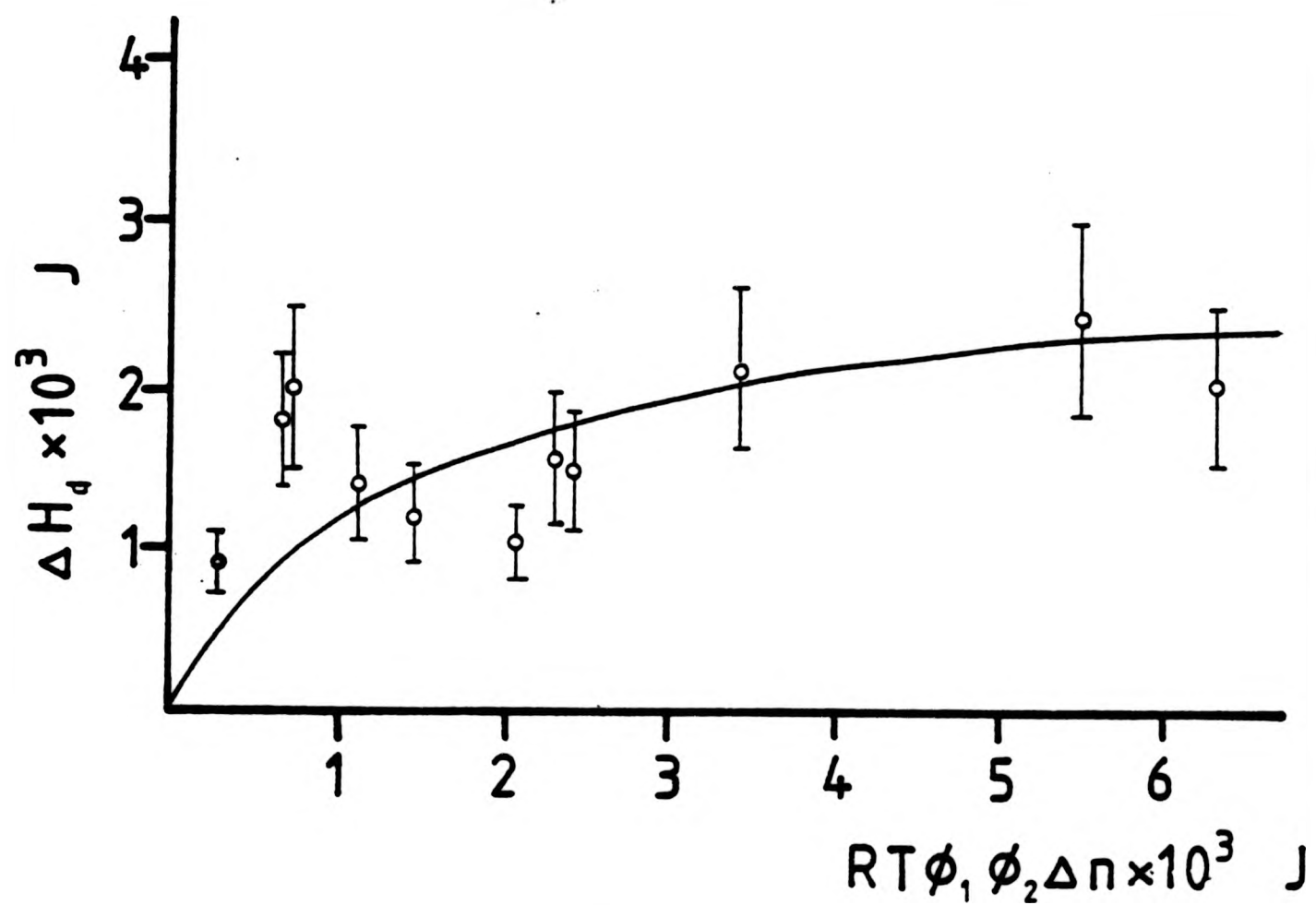
FIG 9.5 : Heat of dilution, ΔH_d, of poly(acrylic acid) PAA50
in dioxane at 303 K.
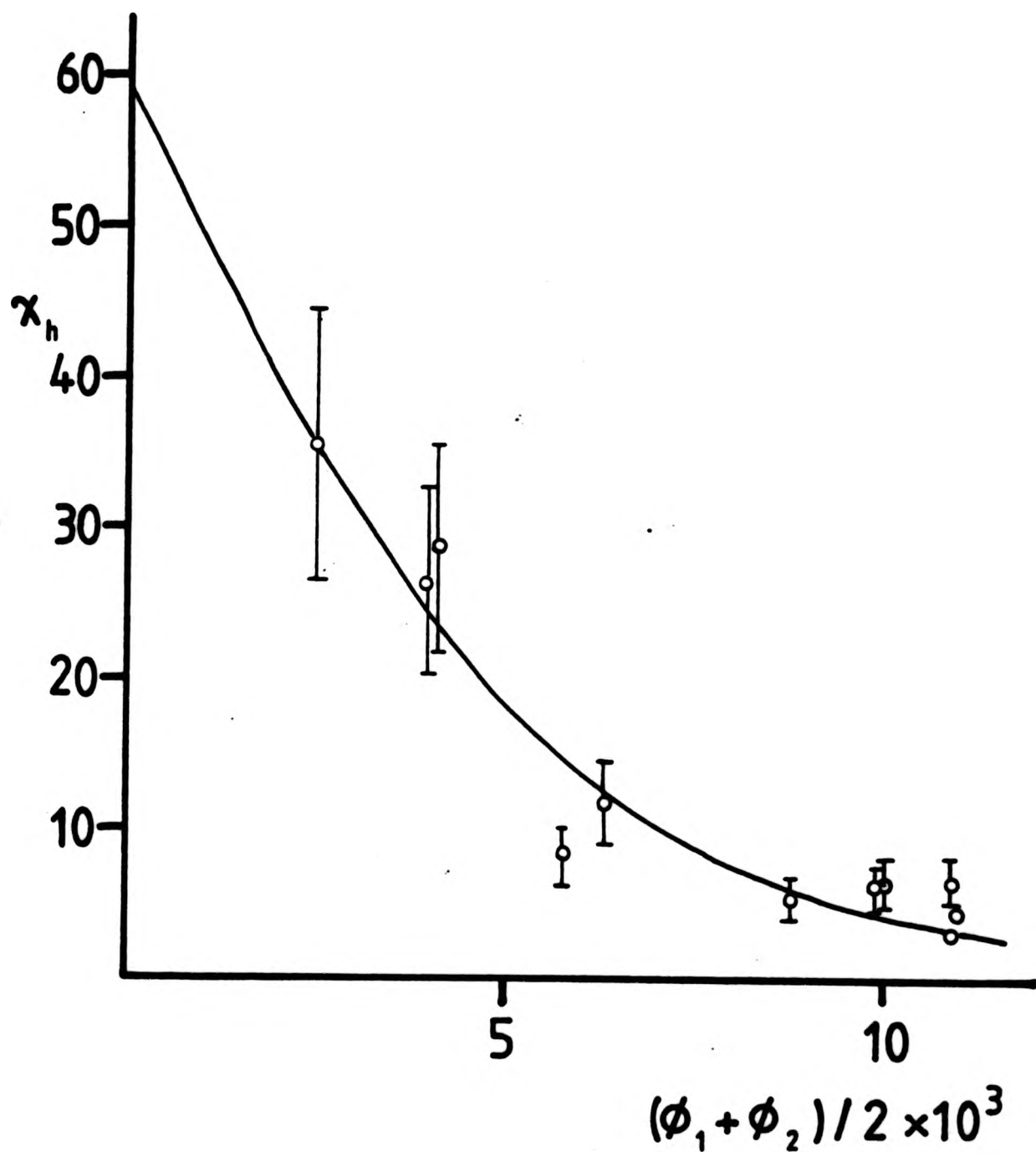
FIG 9.6 : Interaction parameter, χ_h, for poly(acryilic acid) PAA50 in dioxane at 303 K.
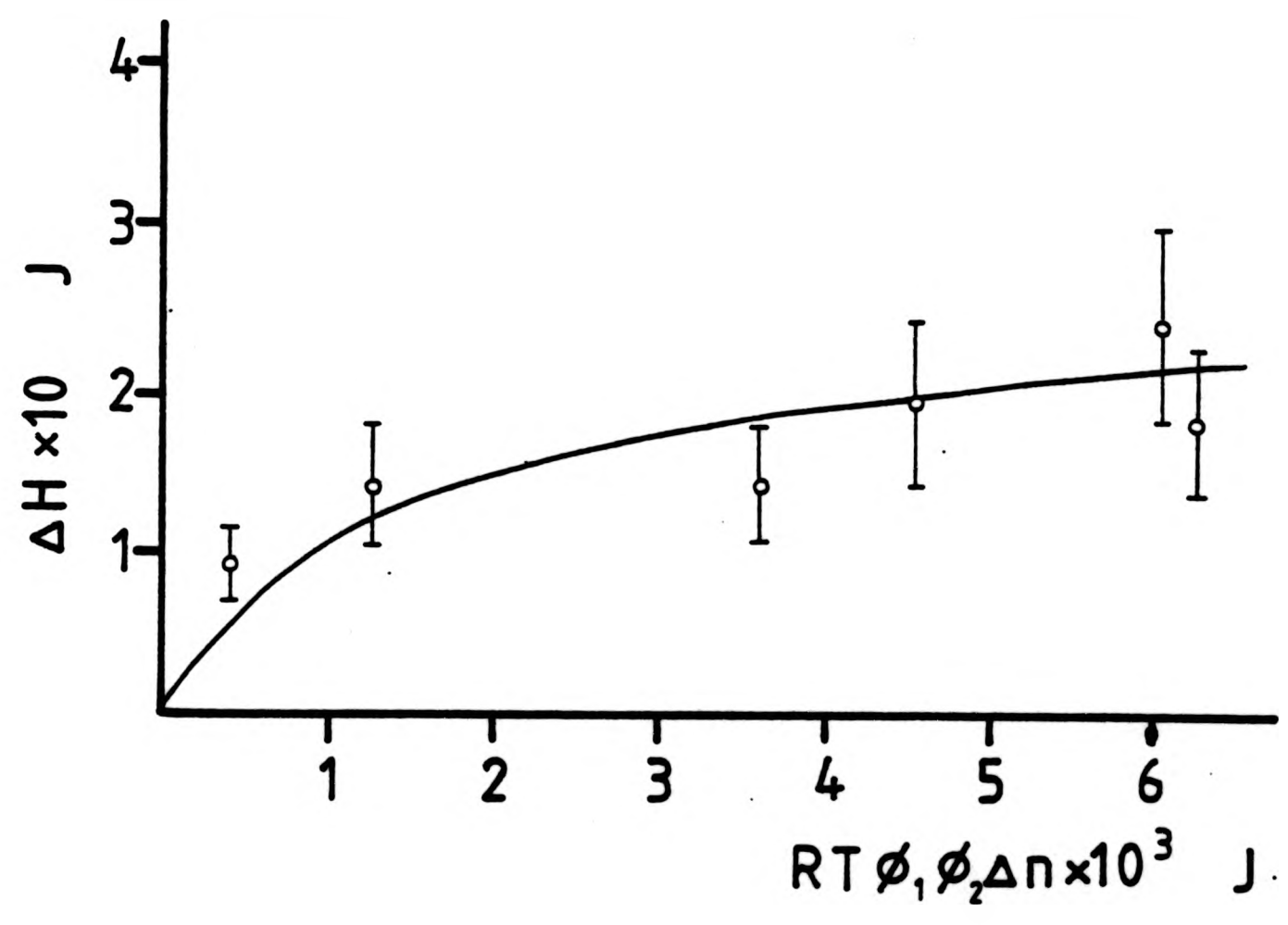
FIG 9.7 : Heat of dilution, ΔH_d, of poly(acrylic acid) PAA50
in dioxane at 307 K.
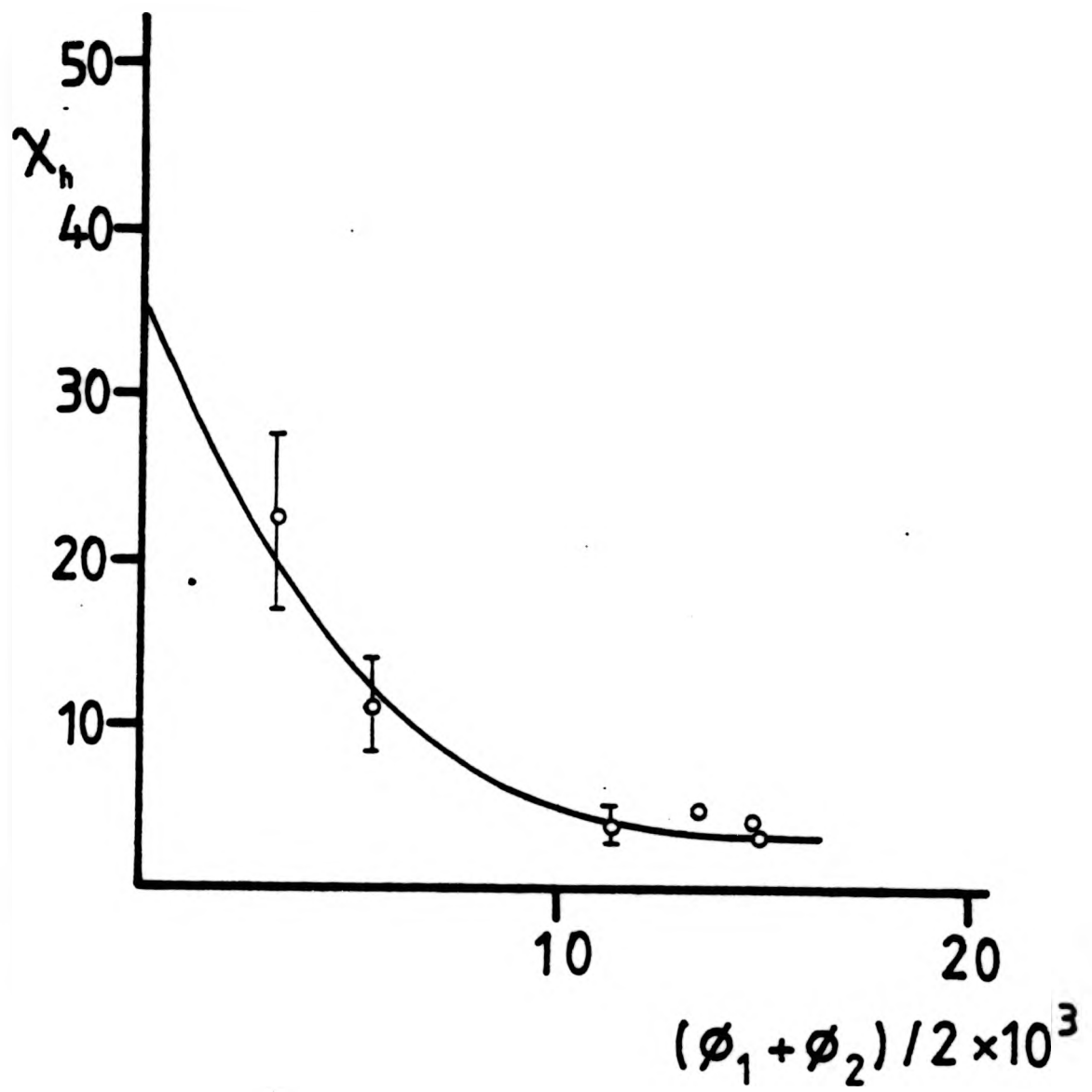
FIG 9.8 : Interaction parameter, χ_h, for poly(acrylic acid) PAA50 in dioxane at 307 K.
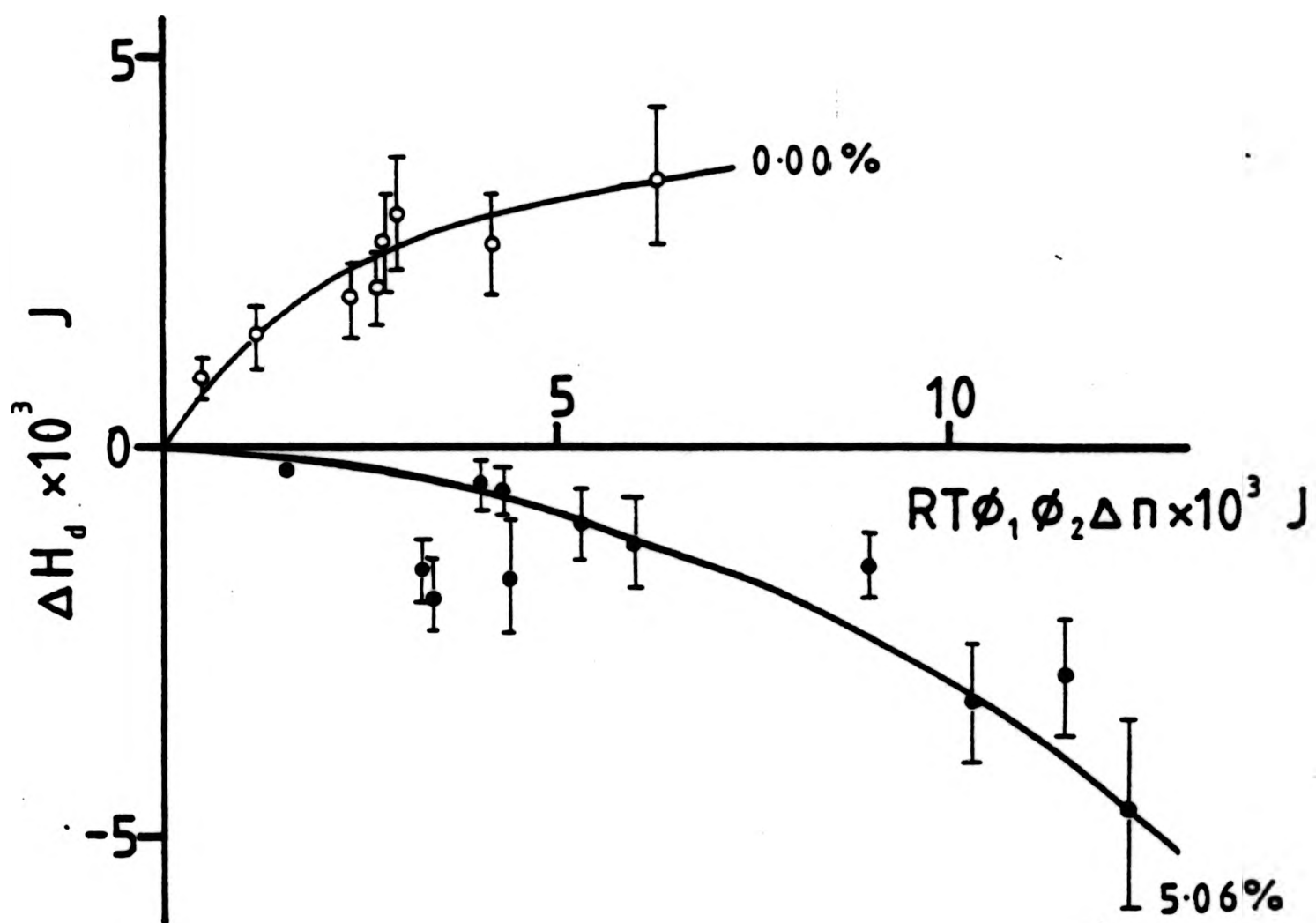
FIG 9.9 : Heat of dilution, ΔH_d, of poly(acrylic acid) PAA50
in dioxane (o) and dioxane/5·06(wt/vol)%water (●) at 312 K.
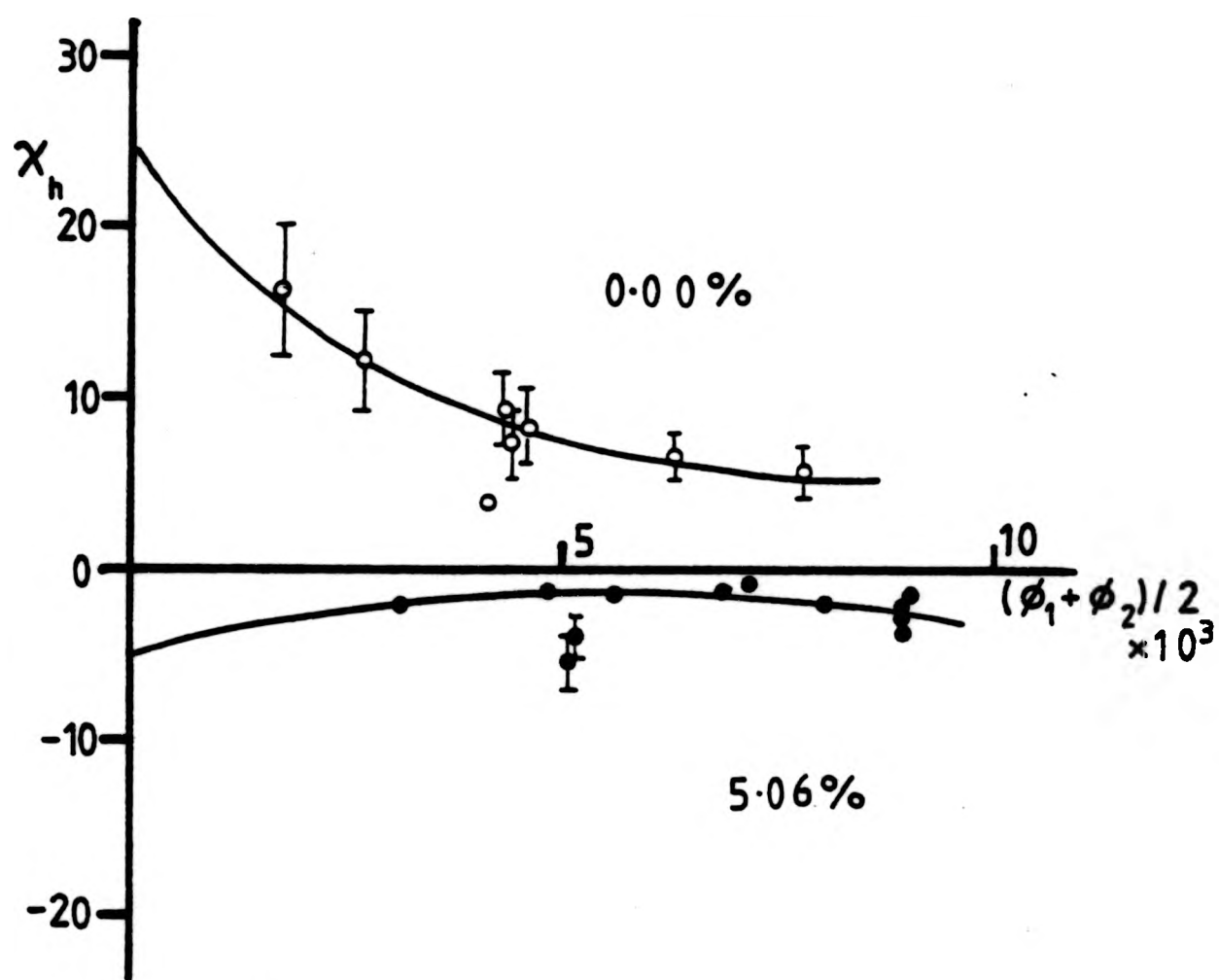
FIG 9.10 : Interaction parameter, χ_h, for poly(acrylic acid) PAA50
in dioxane (o) and dioxane/5·06(wt/vol)% water (●) at 312 K.
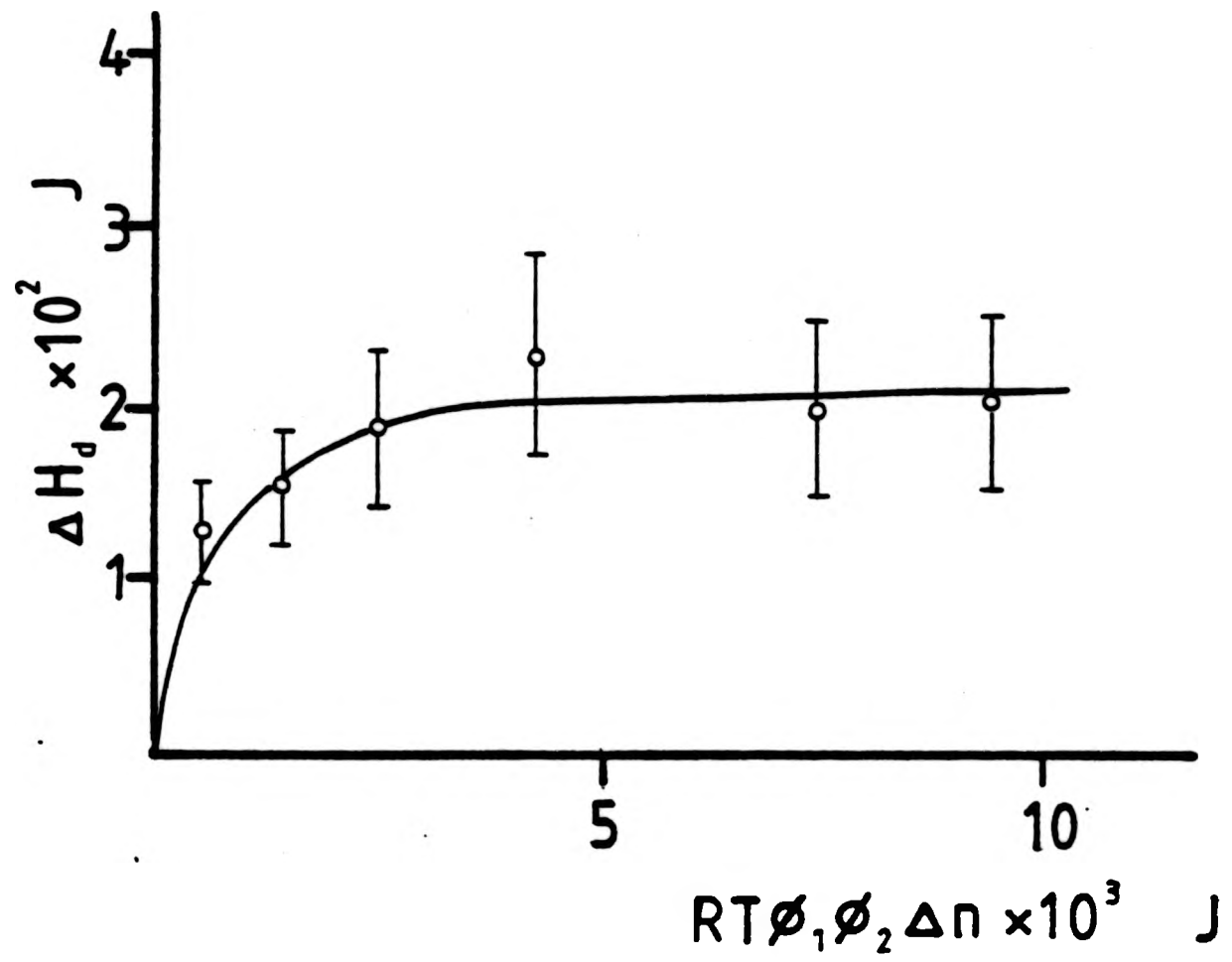
FIG 9.11 : Heat of dilution, ΔH_d, of poly(acrylic acid) PAA50 in dioxane at 316 K.
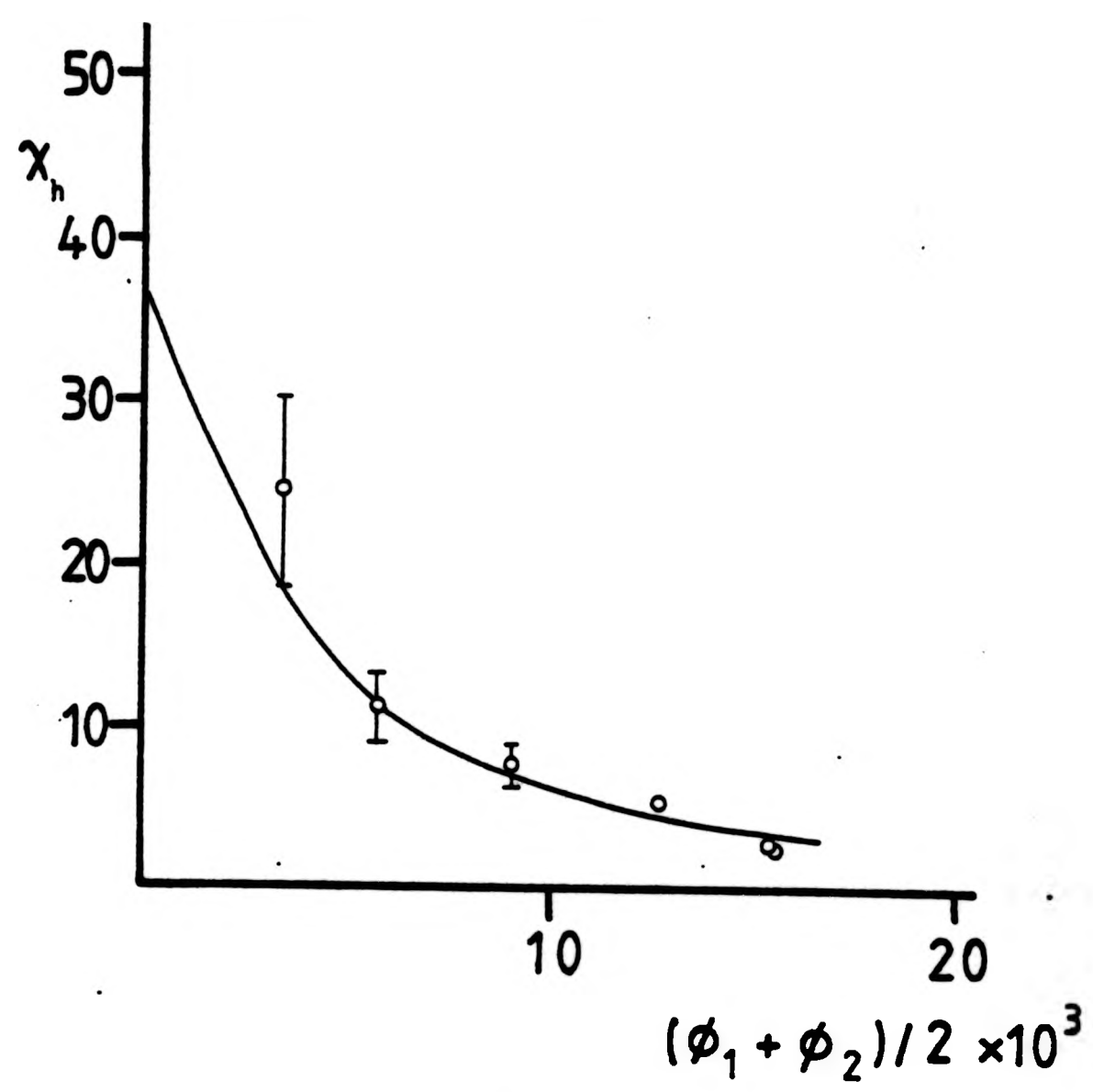
FIG 9.12 : Interaction parameter, χ_h, for poly(acrylic acid) PAA50 in dioxane at 316 K.
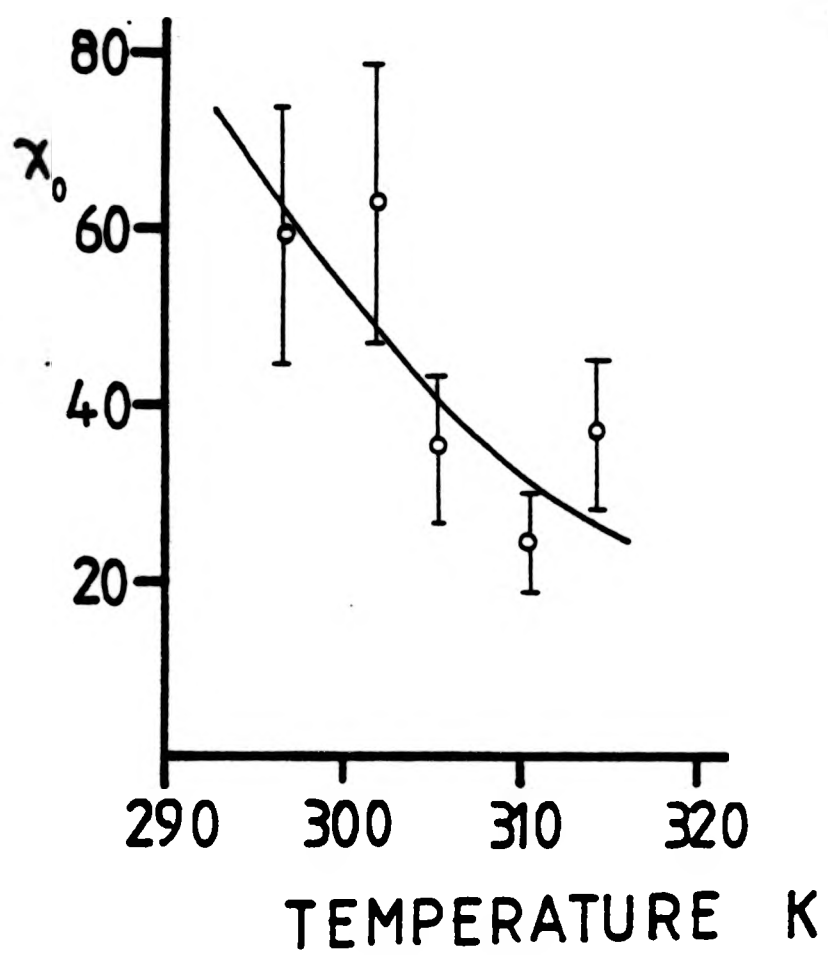
FIG 9.13 : (concentration independent) Interaction parameter, χ_0, for poly(acrylic acid) PAA50 in dioxane as a function of temperature.

TABLE 9.1 χ_1, κ_1, as a function of temperature for poly(acrylic acid) in dioxane and dioxane/water mixtures.

PAA No	(wt/vol)%water	Temp/K	χ_1	κ_1
PAA150	0.00	298	61 ± 15	55 ± 14
PAA50	0.00	298	60 ± 15	49 ± 12
		303.5	63 ± 16	20 ± 5
		307	35 ± 9	30 ± 7
		312	25 ± 6	18 ± 5
		316	37 ± 9	28 ± 7
PAA50	5.06	298	-4.5 ± 1	-11 ± 3
		313	-4.5 ± 1	-1.3 ± 0.3

CHAPTER TEN

NON-AQUEOUS TERNARY SYSTEMS

10.1 NON-AQUEOUS TERNARY SOLUTIONS - CLOUD POINT CURVES

Systems of poly(acrylic acid) in dioxane and a third 'non-aqueous solvent' component were studied.   The third component considered here is a 12-crown-4-ether (12-C-4).   Short chain poly(ethylene glycol)s and poly(propylene glycol)s as the third component are also considered.

The cloud point curves for PAA50 in dioxane/12-C-4 mixtures were determined in mixed solvents containing 2.02, 4.91, 10.07 and 19.18 (wt/vol)% of the 12-C-4, Fig 10.1-10.3,for polymer concentrations up to $15g/100cm^3$.   The binary system with 12-C-4 as a single solvent for PAA50 was also studied, Fig 10.2.   The 12-C-4 was used as supplied (Aldrich) without further purification.

At the lowest crown ether content, 2.02 (wt/vol)%, Fig 10.1 , behaviour which was similar to that of PAA300 in dioxane was observed, in which there was an hourglass type shaped phase separation boundary.   The gap between the two higher temperature phase separation boundaries was seen to close at a polymer concentration of approximately $1.5g/100cm^3$ and at temperatures which were lower than that of the corresponding aqueous systems, Fig 3.19.   The p-LCST phase separation boundary also occurred at lower temperatures than the aqueous system.   At higher crown ether contents a single LCST boundary was exhibited and the temperature of this boundary was found to increase with increasing crown ether content as shown in Fig 10.2.

A plot of the temperature minima of these phase separation boundaries against crown ether content showed that there was a linear increase with crown ether content at these low percentages, Fig 10.3, Table 10.1.   The polymer concentration of these minimum temperatures decreases with increasing 12-C-4 content.   The minimum in the cloud-point curve for the 2.02 (wt/vol)% 12-C-4 solutions occurred at

approximately the same polymer concentration as the limit of the
hourglass so that the corresponding values are not indicated in Fig 10.3.

The system with 12-C-4 as a single solvent also exhibited simple
LCST behaviour but at higher temperatures, at approximately 440K.
Degradation of the solutions was seen, however, at temperatures around
470K.

10.2.1   TERNARY POLYGLYCOL SYSTEMS OF POLY(ACRYLIC ACID)

The ternary system of poly(acrylic acid) in dioxane together with
short-chain poly(ethylene glycol)s or a short-chain poly(propylene
glycol) was studied.   The number average molecular weights of the
polyglycols were determined in both dioxane (328K) and in toluene (316K)
by vapour pressure osmometry.   Comparison between the two solvents
indicate that there is little self-aggregation of the polyglycol in
dioxane, Table 10.2.

The polyglycols were used as supplied (BDH - poly(propylene glycol)
425, poly(ethylene glycol)s 200, 400, 1000, 1500, 4000 and 6000
corresponding to PPG425 and PEG2, PEG4, PEG10, PEG15, PEG40 and PEG60
respectively).

The solutions were prepared by dissolving a known weight of
polyglycol, liquid or solid, in a volume of dried dioxane (wt/vol %).   A
known weight of poly(acrylic acid) was then added to a volume of this
mixture.

10.2.2   POLY(ETHYLENE GLYCOL) - CONSTANT $\bar{M}_n$

The cloud-point curves of the system of PAA50 in dioxane together
with PEG2 or PEG40, as the third component, were determined for
poly(ethylene glycol) contents up to 20 (wt/vol)%.   The contents used

were 1.63, 5.14, 9.92 and 18.5 (wt/vol)% for PEG2, and 1.85, 4.69, 9.44 and 20.01(wt/vol)% for the PEG40 system.   PAA50 concentrations up to 15g/100 cm^3 were used.

Both PEG2, Fig 10.4, and PEG40, Fig 10.5, solutions exhibited singular LCST phase separation boundaries which increased in temperature with increasing poly(ethylene glycol) content.   After an initial common rate of increase in the temperature minima, of the boundaries, with increasing poly(ethylene glycol) content as seen in Fig 10.6, the PEG2 system increased in temperature at a faster rate than that for PEG40. The PAA50 concentration at which the temperature minima occurred appeared to increase with increasing PEG2 content, but decrease with increasing PEG40 content,   Table 10.3, Figs 10.4, 10.5.

10.2.3   POLY(ETHYLENE-GLYCOL) - VARYING $\overline{M}_n$

The cloud-point curves were determined when a constant poly(ethylene glycol) content of approximately 3(wt/vol)% poly(ethylene glycol) in dioxane (wt/vol%) was used but the molecular weight varied from 200 to 4000.   Sample PAA150, with concentrations up to 15g/100cm^3 was used as the poly(acrylic acid) component, Table 10.4, Fig 10.7-10.10 .

The systems using the lowest molecular weight poly(ethylene glycol)s PEG2, Fig 10.7, and PEG4, Fig 10.8, exhibited 'hourglass' type cloud-point curves between the two higher temperature boundaries (UCST and LCST).   The temperatures at which both phase separation boundaries occurred were found to decrease with increasing poly(ethylene glycol) molecular weight.   Compared to the analogous single solvent dioxane system both the phase separation boundaries are at lower temperatures. The closure of the gap between the two boundaries for the dioxane single solvent system occurs at approximately 8g/100 cm^3 but for PEG2 and PEG4

solutions it occurs at 3g/100 cm^3 and 5g/100 cm^3 respectively. This
trend appears to be in an opposite sense to that expected since
poly(ethylene glycol) of higher molecular weight exhibit only a single
LCST cloud-point curve, Fig 10.9. However, the trends indicated here
can only be general since the poly(ethylene glycol) content does vary to
a small extent. Fig 10.9 shows a single LCST boundary which decreases
in temperature with increasing poly(ethylene glycol) molecular weight.
The PAA150 concentration at which the temperature minima of the
boundaries occurred was relatively constant over the whole range of
poly(ethylene glycol) molecular weight, Table 10.4. Poly(ethylene
glycol) of higher molecular weight was found to be insoluble in dioxane
at room temperature.

The general trends in the system can be seen in Fig 10.10. The
p-LCST phase separation boundary increases in temperature with
poly(ethylene glycol) molecular weight until the higher temperature
boundaries merge. From then on increasing the poly(ethylene glycol)
molecular weight decreases the temperature of the p-LCST boundary.

10.2.4 POLY(ETHYLENE GLYCOL)/POLY(ACRYLIC ACID) - SIMILAR $\bar{M}_n$

The cloud-point curves for a system in dioxane with a
poly(acrylic acid) and a poly(ethylene glycol) of similar molecular
weights were determined. Samples PAA5 and PEG40 were used. Solutions
were made up with PAA5 concentrations up to 15g/100 cm^3. PEG40
contents of 1.85, 4.69 and 9.44 (wt/vol)% were used.

All the systems exhibited simple LCST curves and are shown in
Fig 10.11, together with the corresponding PAA5 in dioxane, as a single
solvent. The temperature of the phase separation boundary decreases
with increasing PEG40 content, as can be seen in Fig 10.12. The PAA5

concentrations at which the temperature minima occur also decrease with increasing PEG40 content, Table 10.5, Fig 10.11.

In section 10.2.6 blends of these two samples, cast from dioxane, are studied to establish their phase behaviour.

10.2.5   POLY(PROPYLENE GLYCOL) TERNARY SOLUTIONS

The cloud-point curves for the sample PAA50 in dioxane/PPG425 mixtures were determined.   Poly(propylene glycol) contents of 1.43, 5.10, 10.38 and 19.65 (wt/vol)%, and poly(acrylic acid) concentrations up to 15g/100 cm^3 were used, Fig 10.13-10.15, Table 10.6.

The system with 1.43 (wt/vol)% PPG425, Fig 10.13, exhibited an 'hourglass' shaped cloud-point curve.   The closure of the gap between the two higher temperature phase separation boundaries occurred at a temperature lower than in the corresponding dioxane single solvent system.   The p-LCST phase separation boundary occurred at temperatures of $\sim$323K, similar to that of the single solvent system.   The solutions with higher PPG425 contents showed single LCST boundaries which slowly increased in temperature with increasing PPG425 contents, Fig 10.14, 10.15.   The PAA50 concentration at which the temperature minima occurred was relatively constant at 1.5g/100 cm^3 PAA50.

Comparison with the corresponding poly(ethylene glycol) system (section 10.2.2) indicates that both polyglycols exhibit similar phase separation behaviour.   In the poly(propylene glycol) system the rate of increase in temperature of the p-LCST boundary is slower than the corresponding poly(ethylene glycol) which would appear to indicate that the poly(propylene glycol) system is the 'poorer' one.   The presence of the two higher temperature boundaries in this case, and not in the poly(ethylene glycol) system, would, however, appear to contradict this.

10.2.6   BLENDS - POLY(ETHYLENE GLYCOL)/POLY(ACRYLIC ACID)

Blends of poly(ethylene glycol), PEG40, and poly(acrylic acid), PAA5, were made up over the entire composition range, by weight, by casting films onto Teflon sheets from the minimum amount of dioxane needed to dissolve both components.   The dioxane was allowed to evaporate over a period of 24-48 hours before the samples were placed in a vacuum oven until used, to prevent any moisture uptake from the atmosphere and to remove any residual solvent.

Using a differential scanning calorimeter, dsc, the blends were scanned for both glass transition temperatures, T_g, and melting temperatures, T_m, between 180-400K, using 20mg samples, at a heating rate of 20K/min under a helium atmosphere.   The results obtained are shown in Fig 10.16 and tabulated in Table 10.7.   An example scan is given in Fig 2.14.

The published value for the T_g of poly(ethylene oxide) is molecular weight dependent.[1]   For the molecular weight used here the Tg has been given as approximately 223K [1] but the signal was too weak to be observed here.   Its T_m is given as 333K [2] but this sample gave a T_m at 347K.   The PAA5 sample gave no transitions within the temperature range studied.

For all the blends studied a T_g was observed.   A maximum in the curve occurred at 270K for a 50(wt)% mixture.   For greater PAA5 contents there was a gradual decrease in T_g but at PAA5 contents less than this, the T_g was relatively constant at 245K.   A T_m was only observed below a PAA5 content of 60(wt)%.   It gave a decreasing trend with increasing PAA5 content, from 347K to 335K.

At low PAA contents a single T_m was observed by dsc and confirmed

visually using a hot-stage microscope (Reichart). For high PAA5 contents, no melting was confirmed by this method. The sample containing 40(wt)% PAA5 gave two distinct melting peaks with the dsc. This behaviour was also confirmed visually.

Repeat scans were carried out for each sample and these scans gave the various transitions within $\pm 4K$ of the initial value. The first run values were used in analysing the system since the morphology of some of the blends may have been affected by the melting of the poly(ethylene glycol) component.

The T_g of poly(ethylene oxide) has been characterised at 207K [2] but is molecular weight dependent. A variety of values have been quoted for that of poly(acrylic acid), 361,[3] 376,[4] 379,[5] 382,[6] and 439K.[7] A study of the change of T_g for poly(acrylic acid) with anhydride composition has shown that there is an increase from 376-413K as anhydride content increases. The highest T_g quoted is then likely to be that for the anhydride species.[4] A further complication is that decarboxylation occurs simultaneously as anhydride formation, but at a slower rate.[4]

Copolymerising poly(acrylic acid) has a different effect on the T_g depending on the crosslinking ability of the other structural unit. Acrylic acid-allyl acrylate copolymers show an increase in T_g with increasing allyl acrylate content which is due to increased crosslinking. This can be compared with acrylic acid - n-propyl acrylate copolymers which show a decrease in the T_g with increasing n-propyl acrylate content and which doesn't crosslink.[6]

Smith et al[8] have observed two melting points in one of these blend of poly(ethylene oxide)/poly(acrylic acid). They give T_m of 288K and 333K for a blend containing 25(wt)% poly(acrylic acid). The

lowest T_m was attributed to an intimate and compatible mixture of the two polymers and the second T_m was attributed to the melting of an independent poly(ethylene oxide) crystalline phase.   No T_m above a poly(acrylic acid) content of 60(wt)% here indicates that there is a single amorphous phase and indeed visual inspection of the blends show that these samples are clear whereas those below a 50(wt)% poly(acrylic acid) content are opaque, suggesting the presence either of crystallinity or a phase separated mixture.

With the addition of poly(acrylic acid) to poly(ethylene oxide) or poly(ethylene glycol) the amount of formal complex, between the two species, increases until, effectively, the crystallinity of the poly(ethylene oxide) is destroyed leaving ostensibly a single amorphous phase.[8]   Stiffness measurements,[8] however, show that the complex at high poly(acrylic acid) contents has a high stiffness whereas that at lower poly(acrylic acid) contents has a low stiffness.   These characteristics indicate that the complexation present is different in the two situations.   In this study, although closer together in composition, evidence of analogous interactions can be seen.

10.3 DISCUSSION OF THE NON-AQUEOUS TERNARY SYSTEMS

Both poly(ethylene glycol) (poly(ethylene oxide)) and poly(propylene glycol) in aqueous solutions have been found to exhibit closed-loop type phase equilibria.[9,10]   LCST phase separation behaviour has also been found for poly(ethylene glycol) in a variety of aqueous salt solutions[9,11-13] and a Hofmeister type series established for the salting-out process,[14] for a series of anions.   On a molar concentration basis the series given is

$$PO_4^{2-} > SO_4^{2-} \approx CO_3^{2-} > S_2O_3^{2-} > F^- > CH_3COO^- > Cl^- > NO_3^-$$
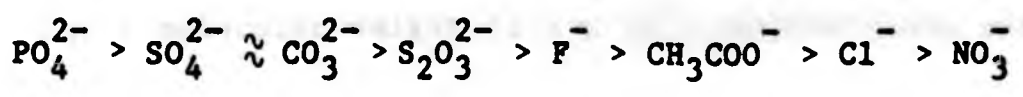
When aqueous solutions of poly(acrylic acid) and poly(ethylene glycol) with molecular weights greater than 4000 are mixed, precipitation has been observed.[8]   It has also been determined that poly(ethylene oxide) forms large aggregates in dilute solutions of benzene or chloroform but it is almost completely dispersed in methanol and dioxane.[15]

In aqueous solutions of poly(acrylic acid) and poly(ethylene glycol) a stoichiometric 1:1 interpolymeric complex is formed with the local exclusion of water.[16-18]   The complex is effectively a combination of two types of equilibrium complex, one on the macromolecular level where the equilibrium association increases rapidly with molecular weight, and one within the pairs of macromolecules which can be regarded as an equilibrium in a separate phase.[19,20]   A study of this system as a function of pH indicates that at low pH there is precipitation whereas at higher pH the system is soluble[16] which would appear to correlate with the Hoffmeister series previously cited.

Below a critical poly(ethylene glycol) chain length, ie the molecular weight being below 7500,[21] a complex is not formed since a definite number of binding sites are necessary for a stable interpolymer complex to be formed although the complex is stabilised by the presence of water.[22]   The molecular weight of the poly(acrylic acid) used was determined as 18.4×10^4 by viscometry.[21]   Cooperative interaction amongst the active sites plays an important role in the complex formation.[21]   A complex has been shown to be formed with poly(ethylene glycol) of molecular weight 2×10^4 but with a low degree of linkage.[23]

Higher molecular weight (3.5×10^4) poly(ethylene oxide) has been

shown to form a stoichiometric 1:1 complex with poly(acrylic acid) in tetrahydrofuran/water mixtures which is independent of solvent composition.[24] Molecular complexes have also been found, under appropriate pH conditions, to exist between poly(acrylic acid) with poly(ethylene imine)[25,26] and poly cations.[27-30]

It has been indicated that neither poly(acrylic acid) nor poly(ethylene glycol) participates in molecular interactions with dioxane but do form intermolecular complexes in water above a critical poly(ethylene glycol) molecular weight. A complex is also formed in the dioxane related system of tetrahydrofuran/water.

The quoted critical value of poly(ethylene glycol) molecular weight is 7500, in water, but it is interesting to note that in Fig 10.10 the change from three to one phase separation boundaries occurs at 1000 not 7500. (Fig 10.10 is the variation of temperature of phase separation as a function of poly(ethylene glycol) molecular weight.) At molecular weights higher than this the temperature of the p-LCST phase separation boundary decreases with increasing molecular weight. The behaviour could be indicative of an interpolymeric complex with the exclusion of dioxane. At molecular weights below this the system appears to be 'improving' ie the p-LCST phase separation boundary is increasing in temperature with increasing molecular weight (see Fig 10.10). Fig 10.6 shows the temperature of phase separation as a function of poly(ethylene glycol) content for two molecular weights. At low contents there is little change in phase separation temperature between the two molecular weights. At 3(wt/vol)% polyglycol content, the content referred to by Fig 10.10, the higher molecular weight, PEG40, does have a slightly higher phase separation temperature than the lower one PEG2. Taking into account the difference in molecular weight in poly(acrylic acid)

both these plots confirm an 'improving' system, in this region, but Fig
10.6 indicates that in general the 'solvent system' is getting 'poorer'
with increasing poly(ethylene glycol) molecular weight.   A complicating
factor in Fig 10.10 may be the presence of other phase separation
boundaries at higher temperatures.   Similar behaviour can also be seen
in the poly(acrylic acid) system with dioxane and poly(propylene glycol),
although it is less marked, Fig 10.15.   From the above it is clear that
for ternary dioxane systems where the poly(acrylic acid) has a much
greater molecular weight than poly(ethylene glycol) an interpolymeric
complex is formed above a poly(ethylene glycol) molecular weight of
approximately 1000.

From the study of the blends of these two polymers which have
similar, but low, molecular weight it is apparent that two different
complexes can be described depending on the relative amounts of the two
polymers present.   These complexes are a direct analogy of the complexes
formed in higher molecular weight polymeric blends.   These blends were
solvent cast from dioxane.   The temperature of phase separation for this
poly(acrylic acid) system as, effectively, the dioxane is replaced by
poly(ethylene glycol) is decreased with increasing polyglycol content, as
can be seen in the appropriate plot, Fig 10.12.   This decrease could be
due to complexation.   At the relatively low polymer concentrations, when
compared to dioxane, any complexation would be related to that seen for
the solutions with dissimilar polymer molecular weights.   But, since we
are 'dilute' in poly(ethylene glycol) we can make the assumption that
this complex is also related to that seen in blends which have a high
poly(acrylic acid) content relative to the poly(ethylene glycol).

If the short chain poly(ethylene glycol)s and poly(propylene
glycol)s are regarded as 'second solvents' in a similar way to water and

crown ether, 12-C-4, then a very general series of 'solvent qualities' can be proposed for high molecular weight poly(acrylic acid)s in dioxane, based on the appropriate phase separation behaviours as shown below.

$$H_2O >> PEG > 12-C-4 \sim PPG$$
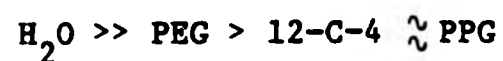
Water is a much better solvent for poly(acrylic acid) by itself, hence could be expected to improve on the 'solvent quality' of the dioxane. Although it has been shown that poly(ethylene glycol) can decrease the 'solvent quality' it is still better than poly(propylene glycol) and crown ether 12-C-4.

REFERENCES

1. J A Faucher, J V Koleske, E R Santee, J J Stratta, C W Wilson, J.Appl.Phys. 37, 3962, (1966).

2. 'Polymer Handbook' Ed J Brandrup, E H Immergut, Wiley-Interscience, New York, (1967).

3. E Jenckel, E Brucker, Z.Phys.Chem.(Leipzig) A185, 465, (1940).

4. A Eisenberg, J.Polym.Sci. A-1 7, 1717 (1969).

5. L J T Hughes, D B Fordyce, J.Polym.Sci. 22, 509, (1956).

6. A R Greenberg, R P Kusy, J.Appl.Polym.Sci. 25, 1785, (1980).

7. K H Illers, Z Elektrochem 70, 353, (1960).

8. K L Smith, A E Winslow, D E Petersen, Ind.Eng.Chem. 51, 1361, (1959).

9. S Saeki, N Kuwahara, M Nakata, M Kaneko, Polymer 17, 685, (1976).

10. G N Malcolm, J S Rowlinson, Trans.Faraday Soc. 53, 921, (1957).

11. E A Boucher, P M Hines, J.Polym.Sci.Polym.Phys.Ed. 14, 2241, (1976).

12. C F Cornet, H van Ballegooijen, Polymer 7, 293, (1966).

13. D N Napper, Polymer 10, 181, (1969).

14. M Atman, E A Boucher, J.Polym.Sci.Polym.Phys.Ed. 20, 1585, (1982).

15. D K Carpenter, G Santiago, A H Hunt, J.Polym.Sci.Polym.Symp. 44, 75, (1974).

16. F E Bailey Jr, R D Lundberg, R W Callard, J.Polym.Sci. A-2, 2, 845, (1964).

17. H-L Chen, H Morawetz, Macromolecules 15, 1445, (1982).

18. E Kokufuta, A Yokota, I Nakamura, Polymer 24, 1031, (1983).

19. Y Osada, A D Antipina, I M Papissov, V A Kabanov, V A Kargin, Vysokomol.Soedin.Ser A 14, 2462, (1972).

20. A D Antipina, V Yi Baranovsky, I M Papissov, V A Kabanov, Vysokomol.Soedin.Ser A 14, 941, (1972).

21. Y Osada, J.Polym.Sci.Polym.Chem.Ed. 17, 3485, (1979).

22. E Tsuchida, Y Osada, H Ohno, J.Macromol.Sci.Phys. B17, 683, (1980).

23. T Ikawa, K Abe, K Honda, E Tsuchida, J.Polym.Sci. A-1, 13, 1505, (1975).

24. S K Chatterjee, N Chatterjee, G Riess, Makromol.Chem. 183, 481, (1982).

25. A B Zezin, V V Lutsenko, V A Izumrudov, V A Kabanov, Vysokomol.Soedin.Ser. A 16, 600, (1974).

26. M Saito, K Abe, Y Osada, E Tsuchida, J.Chem.Soc.Jpn. 5, 977, (1974).

27. E Tsuchida, Y Osada, K Abe, Makromol.Chem. 175, 583, (1974).

28. E Tsuchida, Y Osada, Makromol.Chem. 175, 593, (1974).

29. E Tsuchida, K Abe, H Ohno, Macromolecules 9, 112, (1976).

30. R Subramanian, P Natarajan, J.Polym.Sci.Polym.Chem.Ed. 22, 437, (1984).
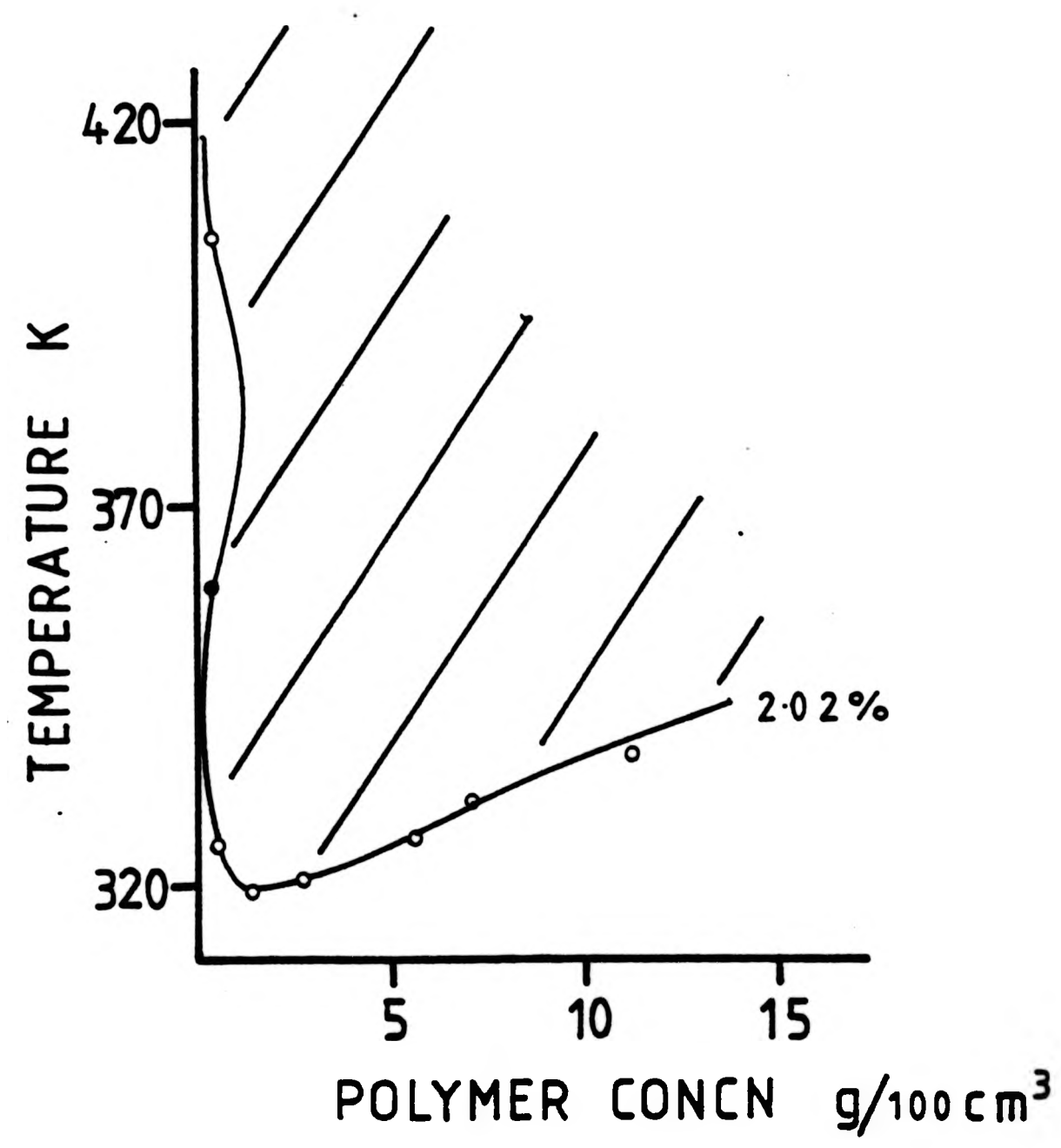
FIG 10.1 : Cloud point curve for poly(acrylic acid) PAA50 in
dioxane/2·02(wt/vol)% crown ether (12-C-4).
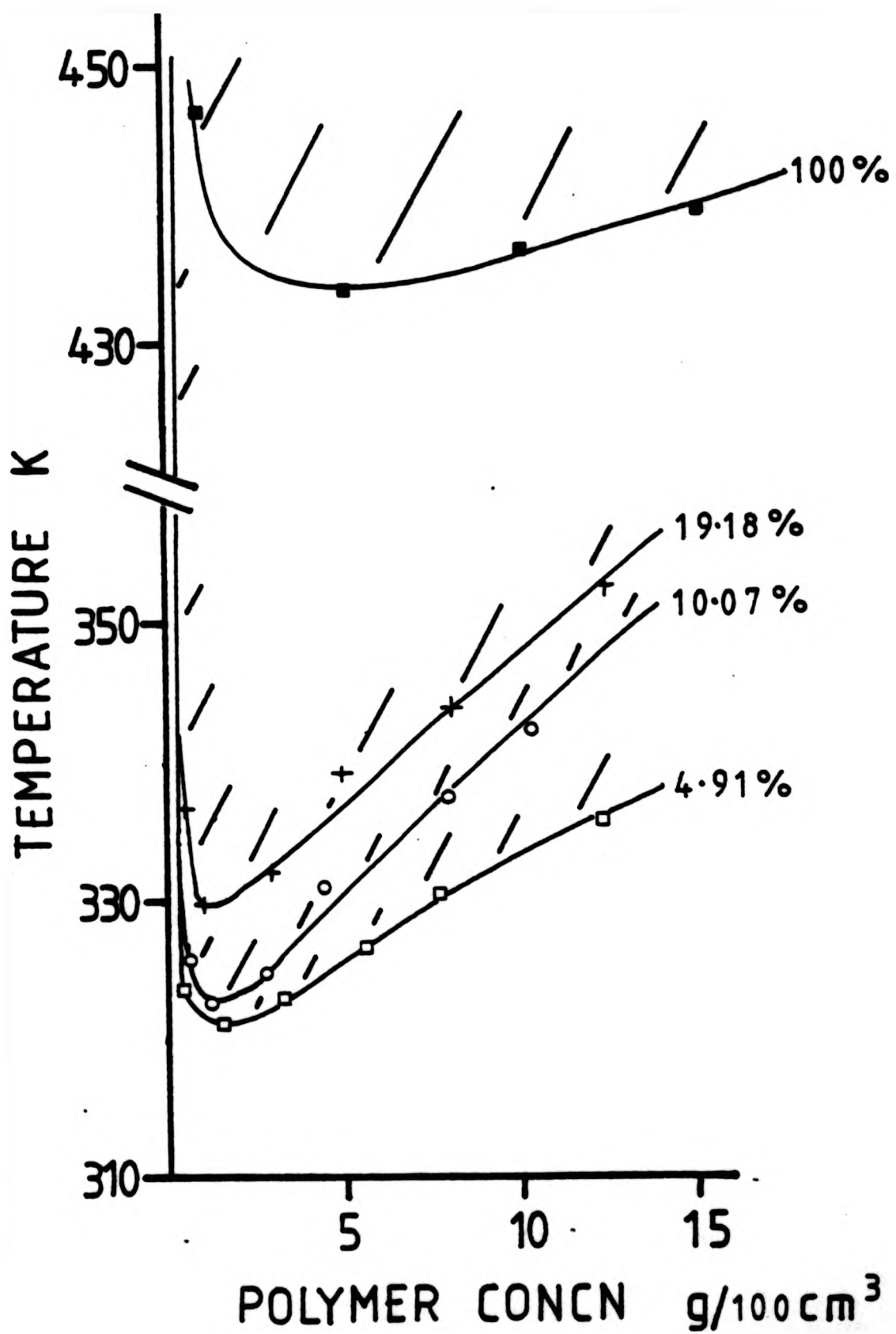
FIG 10.2 : Cloud point curve for poly(acrylic acid) PAA50 in
dioxane/crown ether(12-C-4),
(12-C-4 content : 4·91(□),10·07(o),19·18(wt/vol)%(+)),
and in crown ether (12-C-4)(■).
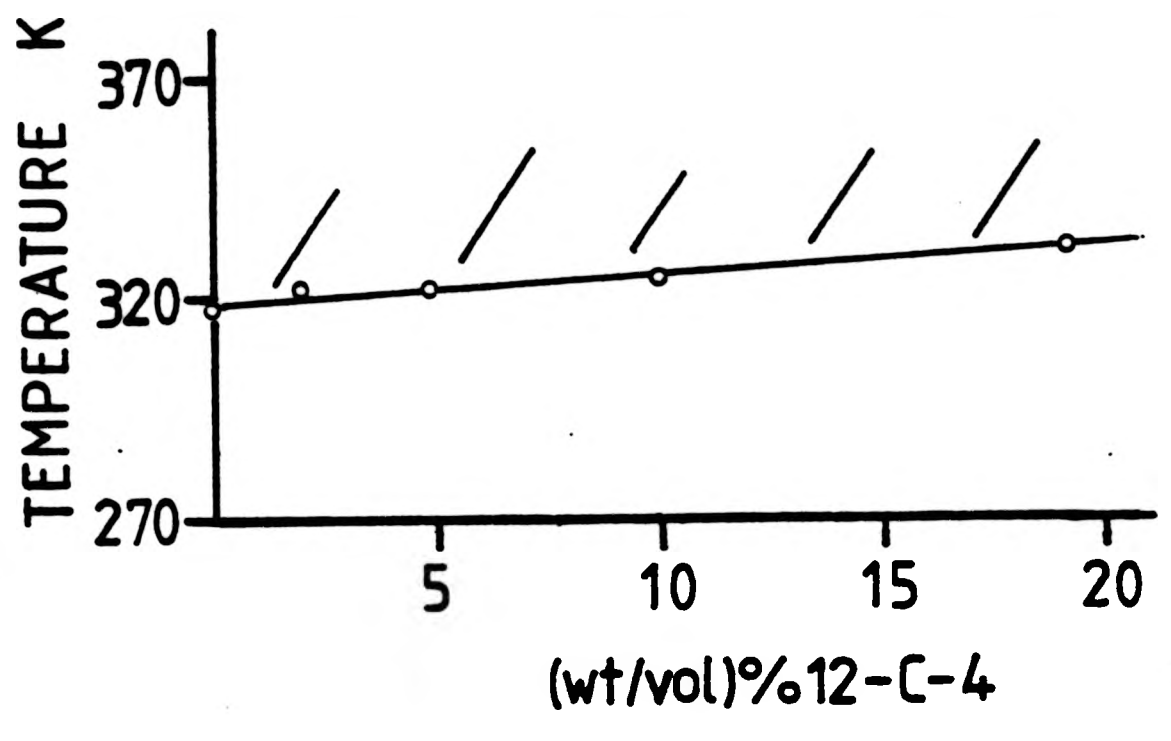
FIG 10.3 : Temperature of minimum in cloud point curve for
poly(acrylic acid) PAA50 in dioxane/crown ether (12-C-4)
as a function of crown ether content.
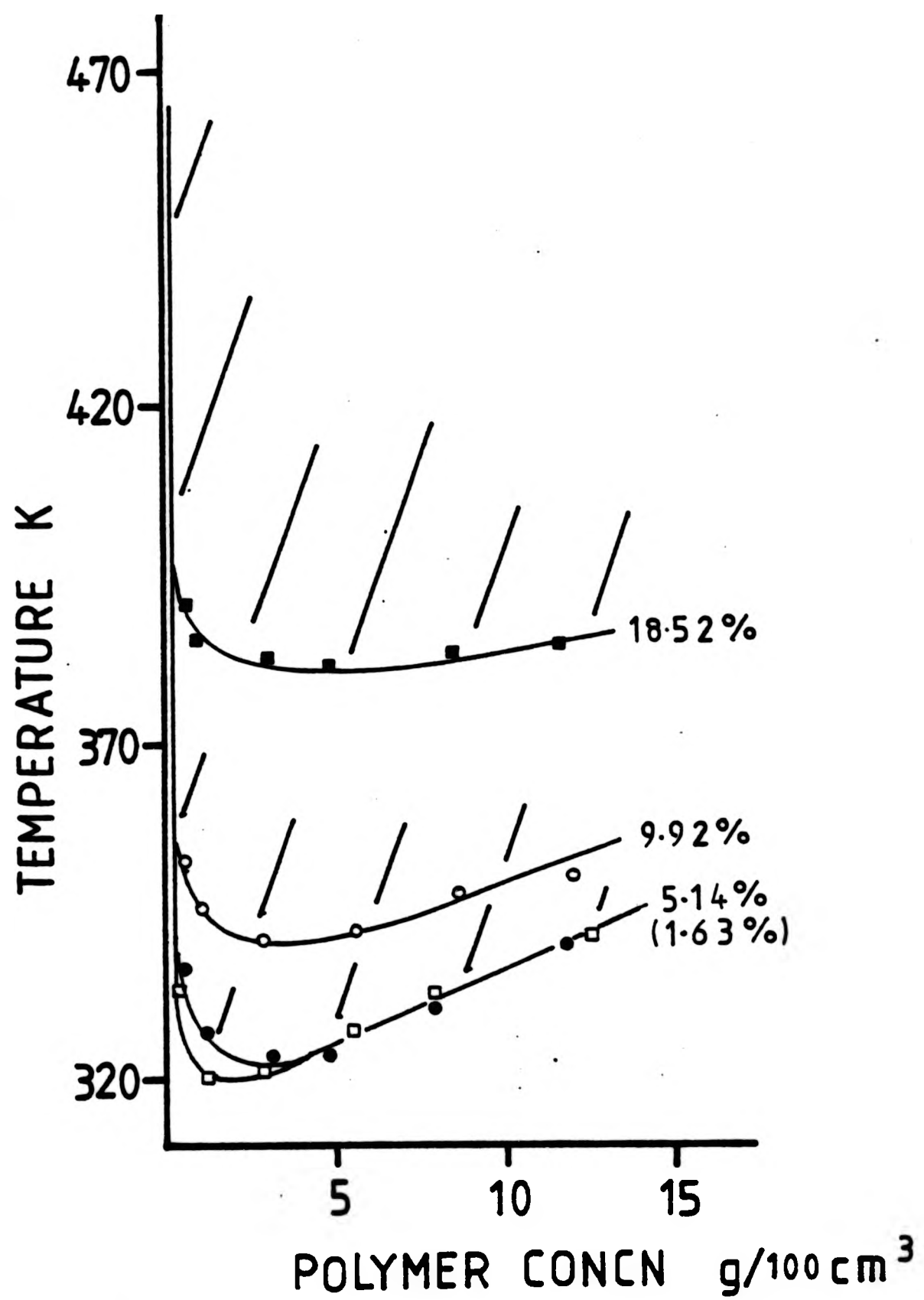
FIG 10.4 : Cloud point curve for poly(acrylic acid) PAA50 in
dioxane/poly(ethylene glycol) PEG2.
(PEG2 content : 1·63(□).5·14(●),9·92(○) and 18·52(wt/vol)%(■)).
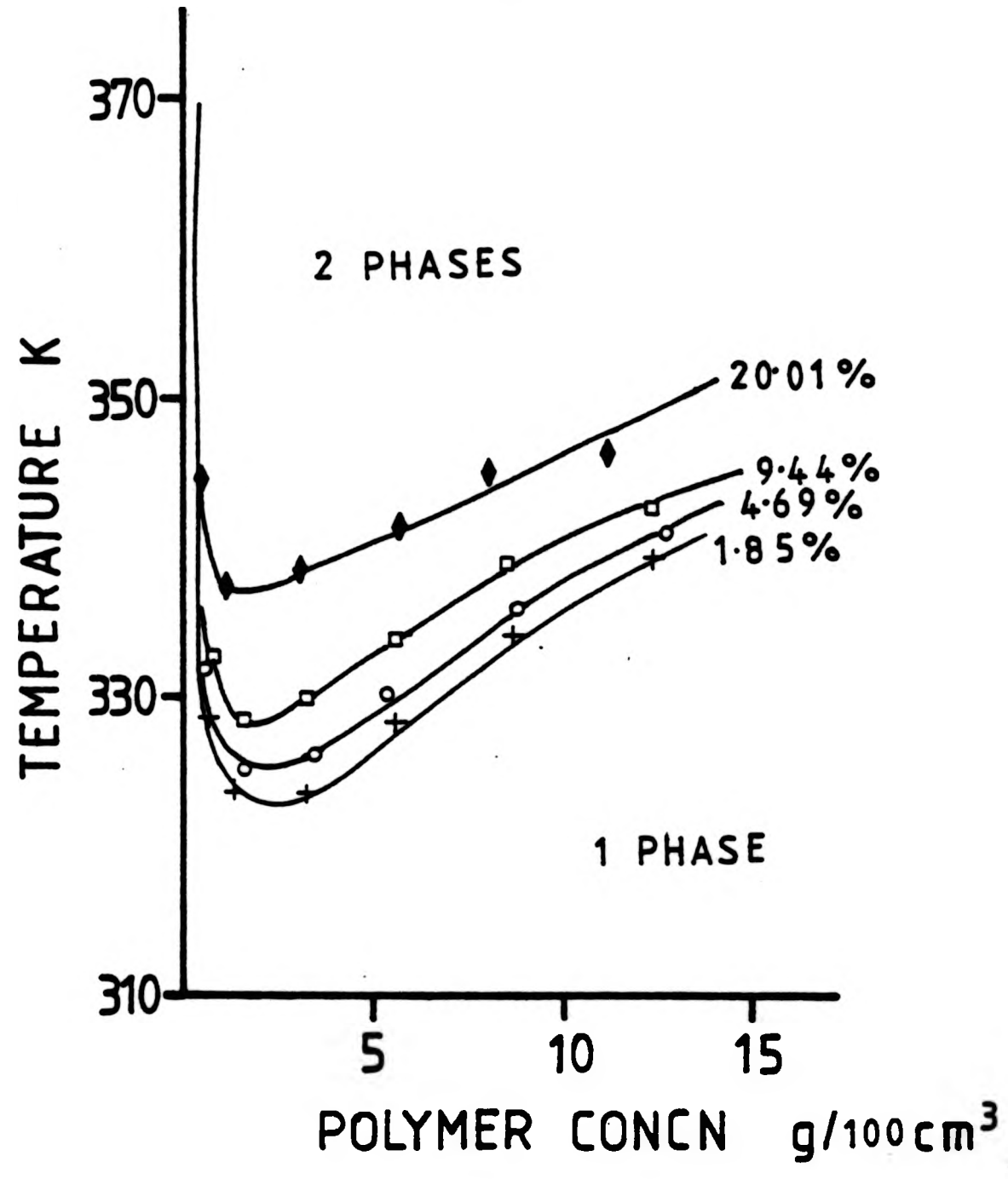
FIG 10.5 : Cloud point curve for poly(acrylic acid) PAA50 in
dioxane/poly(ethylene glycol) PEG40.
(PEG40 content : 1·85(+),4·69(o),9·44(□) and 20·01(wt/vol)%(♦)).
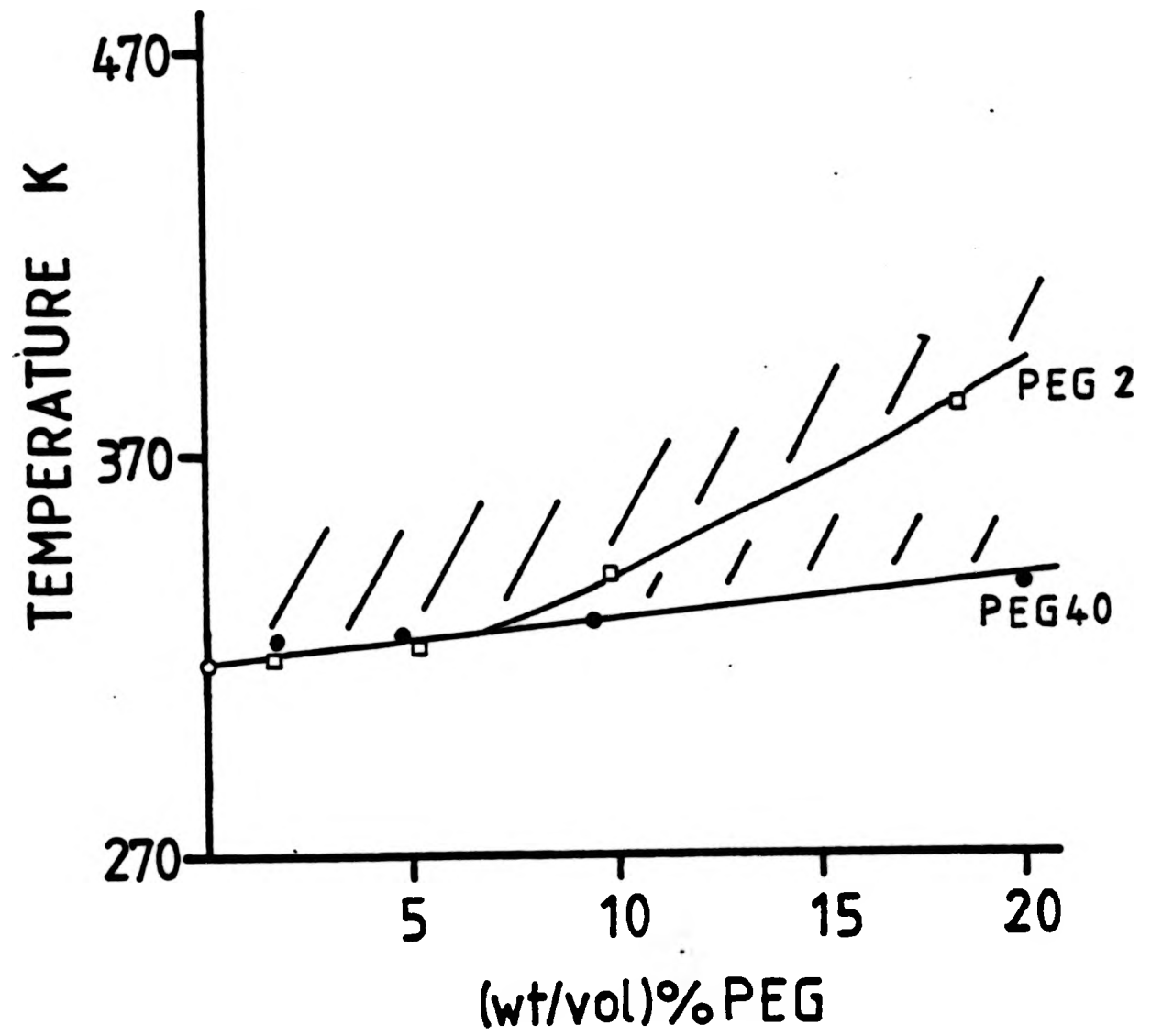
FIG 10.6 : Temperature of minimum in cloud point curve for
poly(acrylic acid) PAA50 in dioxane with
poly(ethylene glycol)'s PEG2 or PEG40 as a function of
poly(ethylene glycol) content.
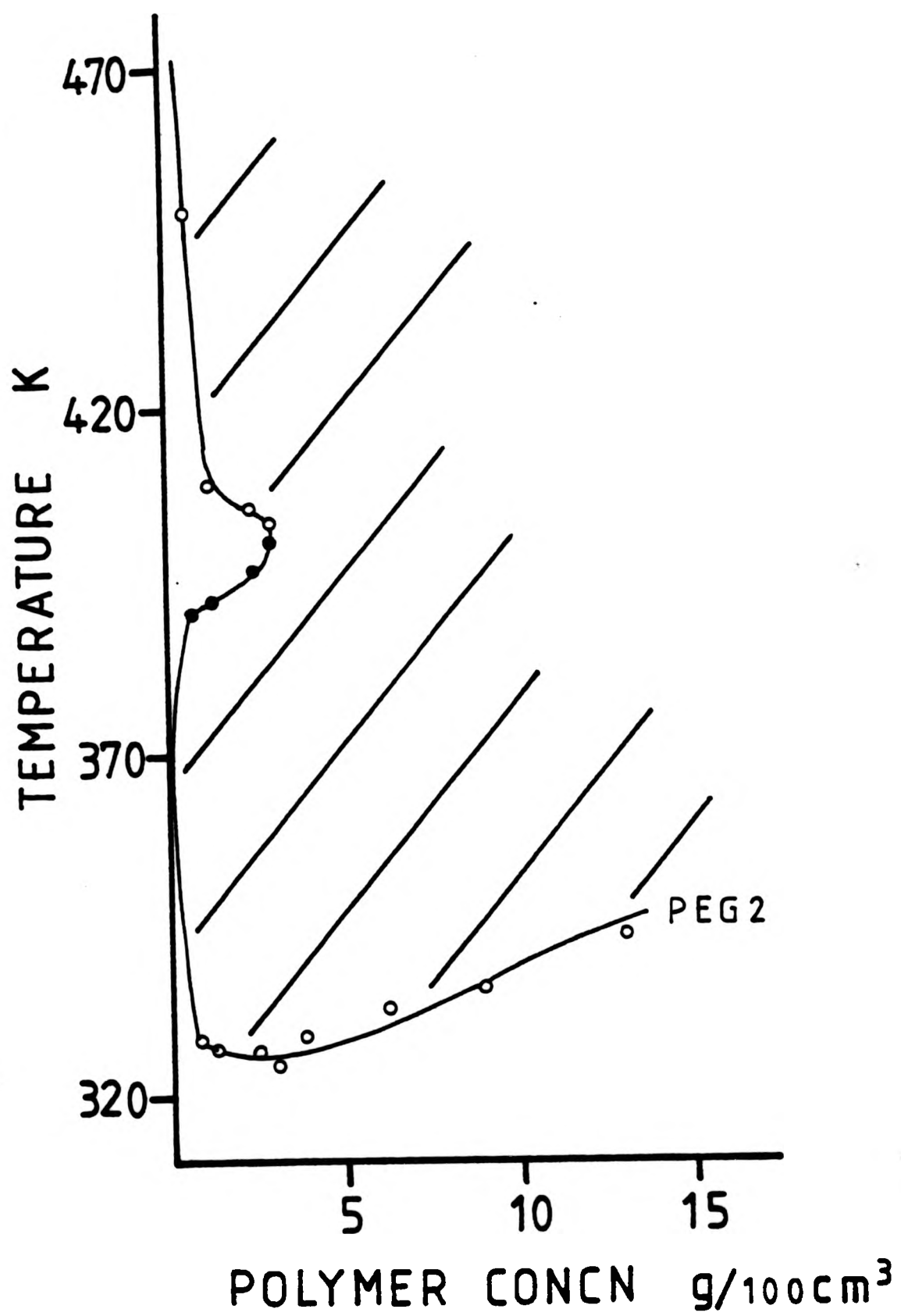
FIG 10.7 : Cloud point curve for poly(acrylic acid) PAA150 in
dioxane/3·10(wt/vol)% poly(ethylene glycol) PEG2.
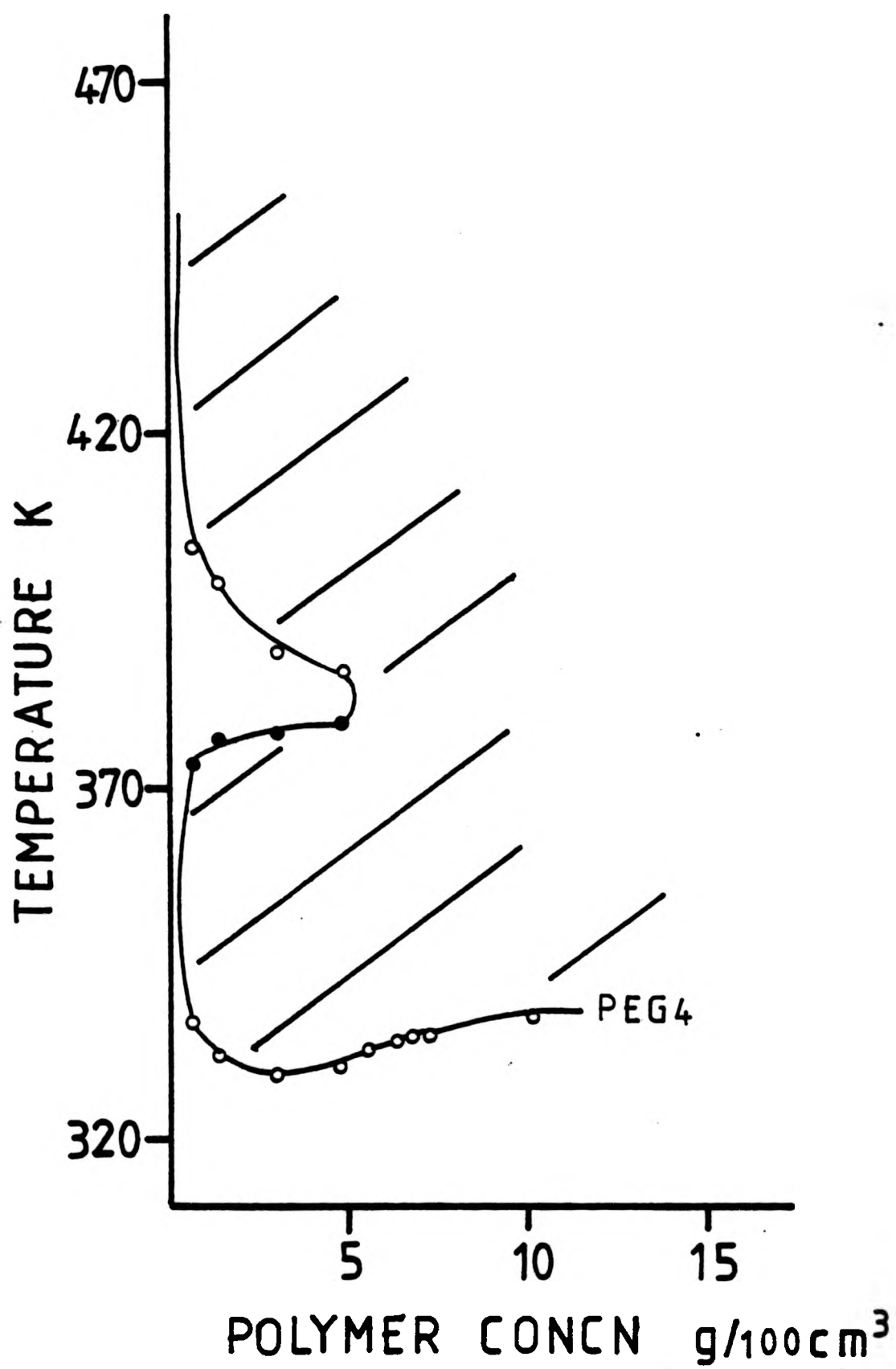
FIG 10.8 : Cloud point curve for poly(acrylic acid) PAA150 in
dioxane/2.97(wt/vol)%poly(ethylene glycol) PEG4.
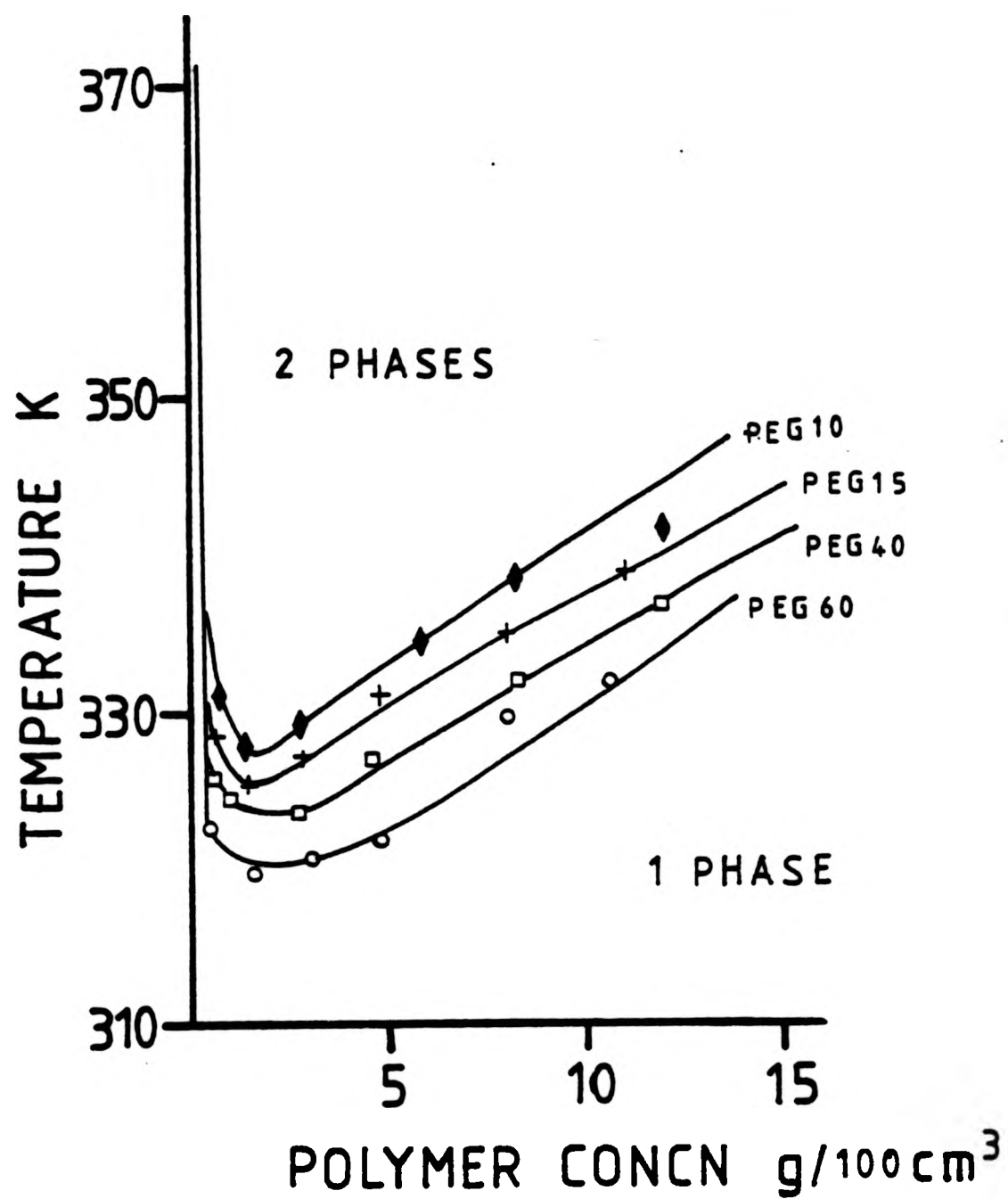
FIG 10.9 : Cloud point curve for poly(acrylic acid) PAA150 in
dioxane/poly(ethylene glycol) (varying molecular weight).
(PEG content : 3·02 PEG10(♦),3·02 PEG15(+),2·99 PEG40(□)
and 2·96(wt/vol)% PEG60(o)).
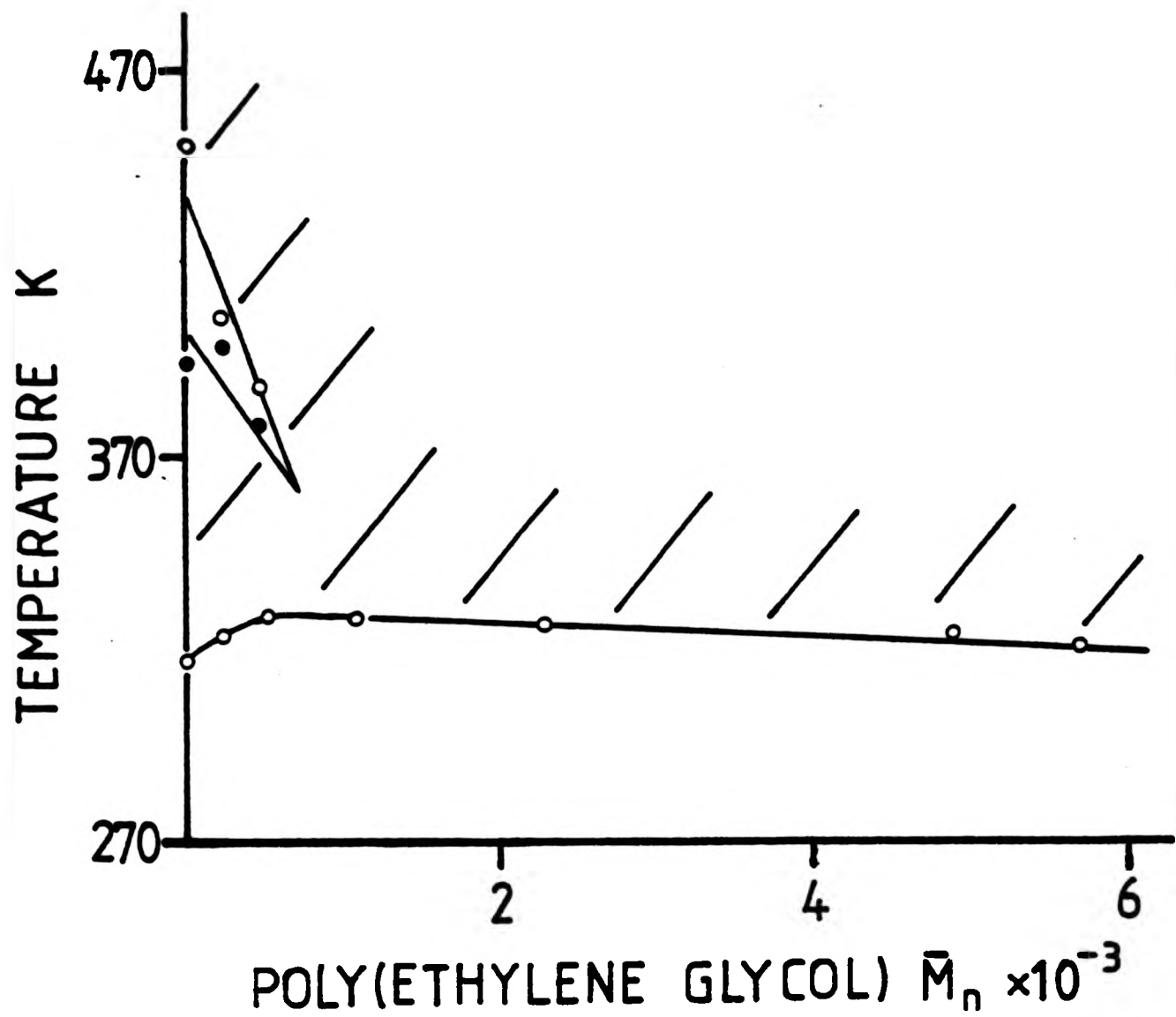
FIG 10.10 : Temperature of minimum in cloud point curve for
poly(acrylic acid) PAA150 in dioxane/poly(ethylene glycol)
as a function of poly(ethylene glycol) molecular weight.
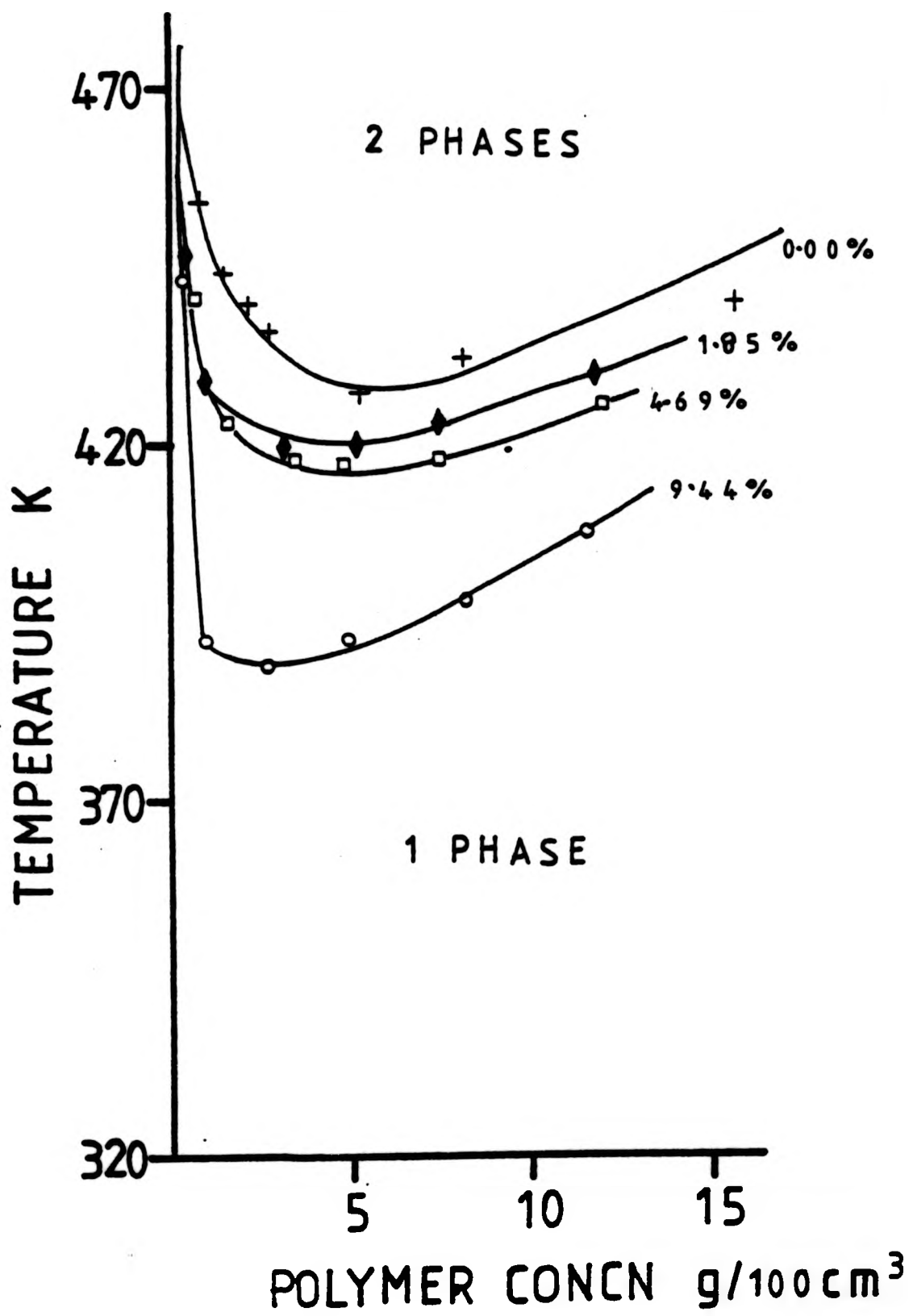
FIG 10.11 : Cloud point curve for poly(acrylic acid) PAA5 in
dioxane/poly(ethylene glycol) PEG40.
(PEG40 content : 0·00(+),1·85(♦),4·69(□) and 9·44(wt/vol)%(o)).
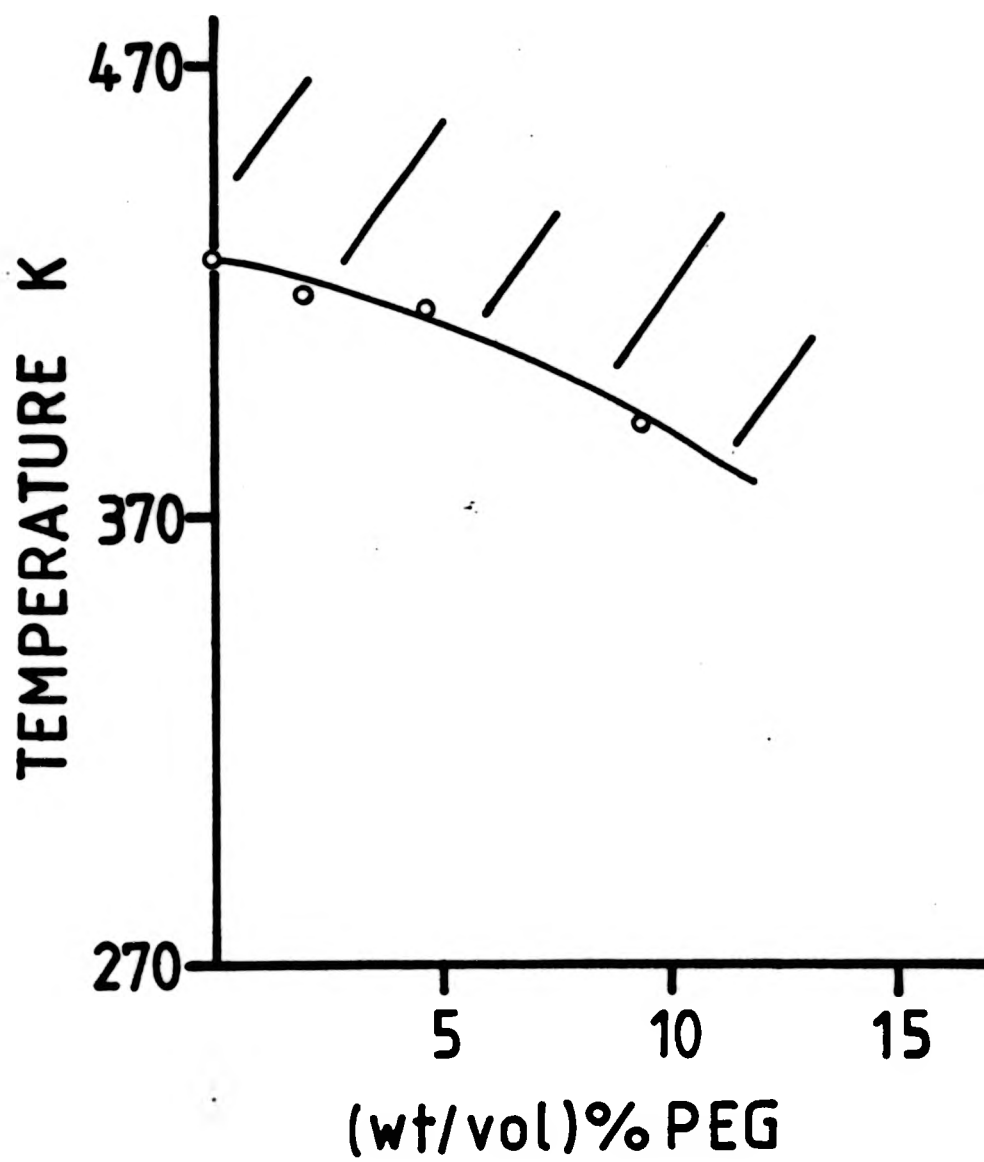
FIG 10.12 : Temperature of minimum in cloud point curve for
poly(acrylic acid) PAA5 in dioxane/poly(ethylene glycol)
PEG40 as a function of poly(ethylene glycol) content.
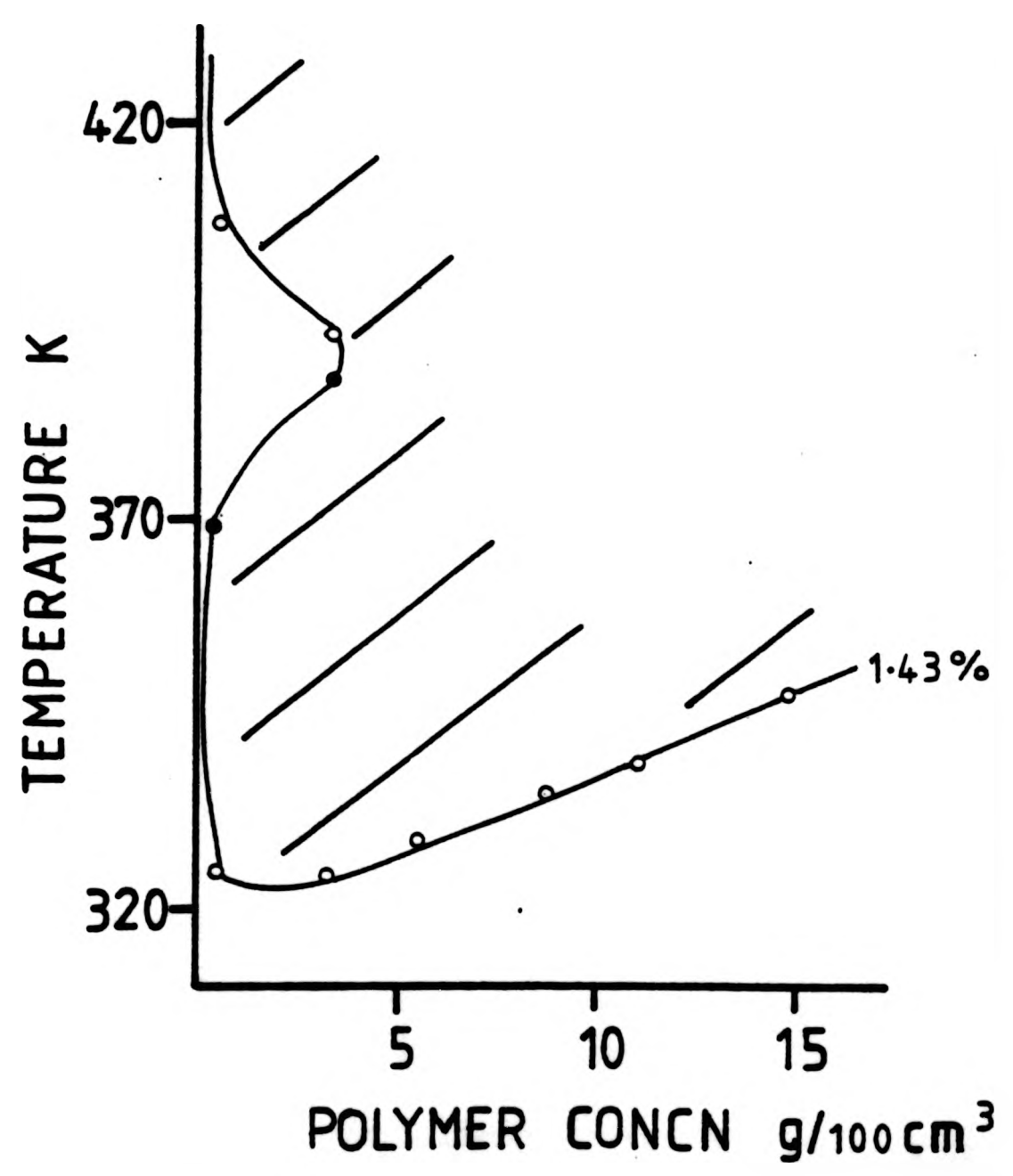
FIG 10.13 : Cloud point curve for poly(acrylic acid) PAA50 in dioxane/1·43(wt/vol)% poly(propylene glycol) PPG425.
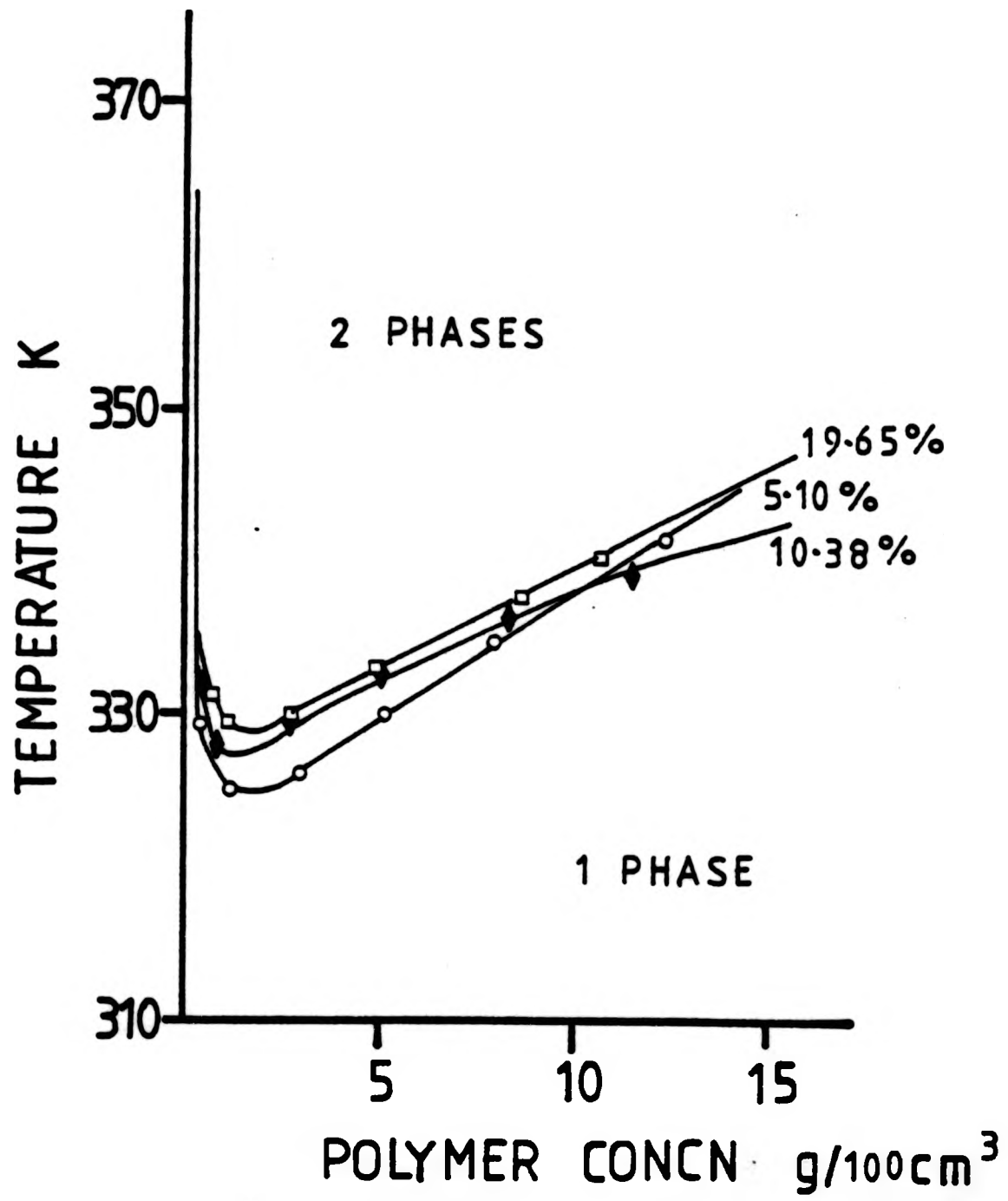
FIG 10.14 : Cloud point curve for poly(acrylic acid) PAA50 in
dioxane/poly(propylene glycol) PPG425.
(PPG425 content : 5·10(o),10·38(♦) and 19·65(wt/vol)%(□)).
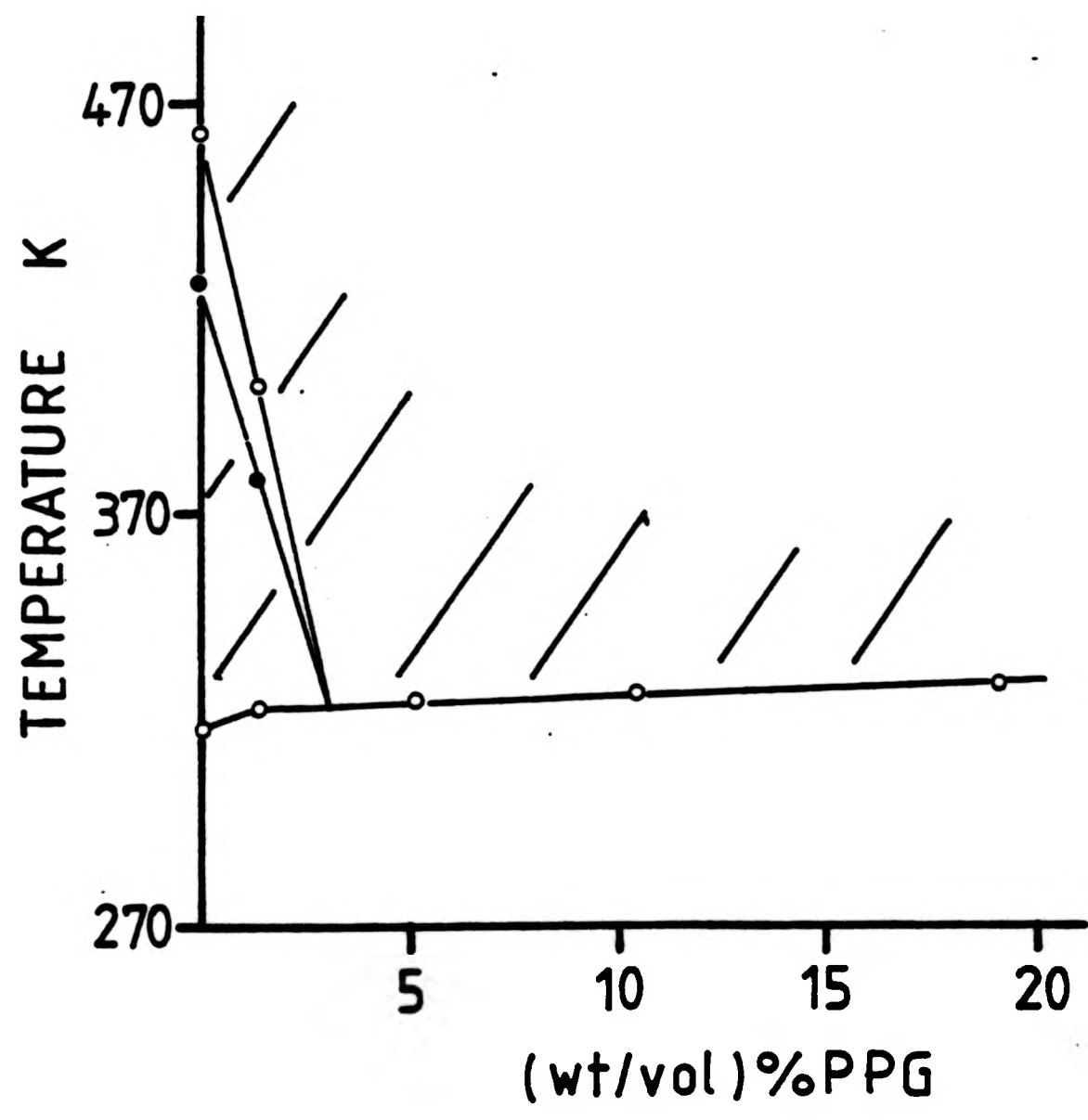
FIG 10.15 : Temperature of minimum in cloud point curve for
poly(acrylic acid) PAA50 in dioxane with
poly(propylene glycol) PPG425 as a function of
poly(propylene glycol) content.
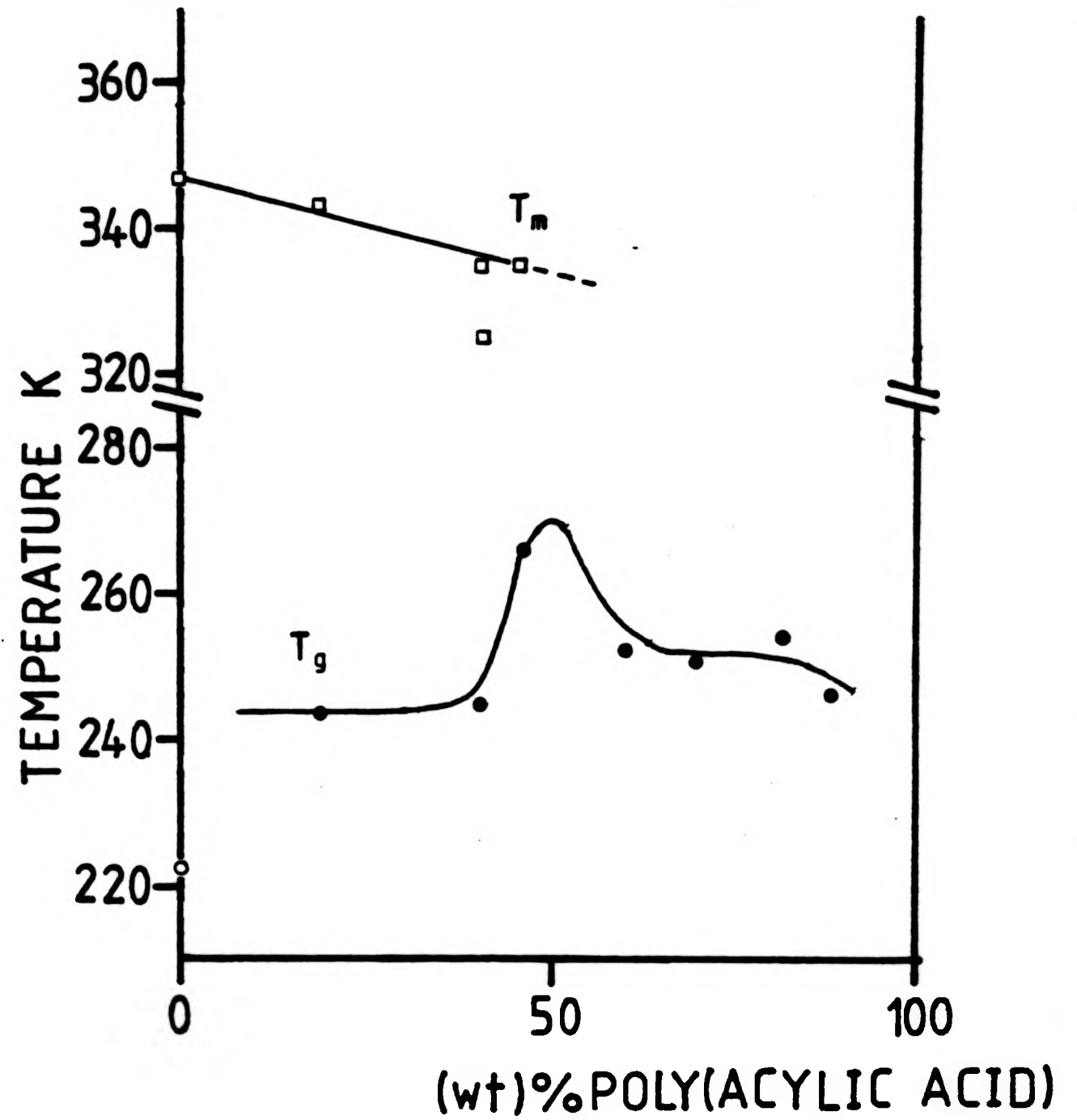
FIG 10.16 : Glass transition T_g and melting T_m temperatures for
poly(acrylic acid)/poly(ethylene oxide) (PAA5/PEG40)
blends as a function of (wt)% poly(acrylic acid).

TABLE 10.1 Temperature of phase separation of poly(acrylic acid) (PAA50) in dioxane/12-crown-4 ether (12-C-4)

%12-c-4	Min PAA/ g/100cm^3	Temp/K
0.00	2	318.5
2.02	1.5	322
4.91	1.5	322.5
10.07	1.25	324
19.18	1.25	331
100.00	5	435

TABLE 10.2 $\bar{M}_n$ for poly(ethylene glycol) (PEG) and poly(propylene glycol) (PPG)

Polyglycol	$\bar{M}_n$/g/mol Toluene 316K	$\bar{M}_n$/g/mol Dioxane 328K	$\bar{M}_n$(dioxane)/ $\bar{M}_n$(toluene)
PEG2	239 ± 10	238 ± 10	1.00
PEG4	400 ± 16	476 ± 19	1.19
PEG10	1008 ± 40	1074 ± 43	1.07
PEG15	1917 ± 76	2290 ± 91	1.19
PEG40	4173 ± 167	4908 ± 196	1.18
PEG60	4833 ± 193	5710 ± 228	1.18
PPG425	399 ± 16	490 ± 19	1.23

TABLE 10.3   Temperature of phase separation of poly(acrylic acid) (PAA50) in dioxane with poly(ethylene glycol)s

PEG	%PEG	Min PAA/g/100cm^3	Temp/K
—	—	2.00	318.5
PEG2	1.63	2.00	320
	5.14	3.00	322
	9.92	3.50	350.5
	18.52	5.00	381
PEG40	1.85	2.00	323
	4.69	2.00	325
	9.44	1.50	328
	20.01	1.20	337

TABLE 10.4   Temperatures of phase separations for poly(acrylic acid) (PAA150) in dioxane with 3(wt/vol)% poly(ethylene glycol)s

PEG	% PEG	$\bar{M}_n$/g/mol	Min PAA/ g/100cm^3	Temperature/K		
				p-LCST	UCST	LCST
—	—	—	1.25	317.5	395	450
PEG2	3.10	238	2.5	324.5	398	404
PEG4	2.97	476	3.5	328.0	377	387
PEG10	3.02	1074	2.0	327.5	—	—
PEG15	3.02	2290	2.0	325.5	—	—
PEG40	2.99	4908	2.0	323.5	—	—
PEG60	2.96	5710	2.0	319.5	—	—

TABLE 10.5   Temperature of phase separation of poly(acrylic acid) (PAA5) in dioxane with poly(ethylene glycol) (PEG40).

%PEG40	Min PAA5 /g/100cm^3	Min Temp/K
0.00	5	427
1.85	5	419
4.69	4.5	417
9.44	3	389

TABLE 10.6   Temperature of phase separation of poly(acrylic acid) (PAA50) in dioxane with poly(propylene glycol) (PPG425)

%PPG	Min PAA/ g/100cm^3	TEMP/K		
		p-LCST	UCST	LCST
0.00	2.00	318.5	426	464
1.43	1.5	322	380	400
5.10	1.5	324.5	-	-
10.38	1.5	327	-	-
19.65	1.5	328.5	-	-

TABLE 10.7 Variation of T_g, T_m with poly(acrylic acid) content in poly(ethylene glycol), (PEG40)/poly(acrylic acid), (PAA5) blends

Blend	(wt)%PAA	T_g/K	T_m/K
0	0.0	223*	347
2	18.9	244	343
4	40.6	245	325/335
5	46.5	266	335
6	60.0	252	-
7	68.4	251	-
8	81.0	254	-
9	87.7	246	-
10	100.0	-	-

* See ref 1

CHAPTER ELEVEN

POLY(N-ISOPROPYLACRYLAMIDE) SYSTEMS

11.1 POLY(N-ISOPROPYL ACRYLAMIDE)/WATER

The poly(acrylic acid) systems studied display three separate phase separation boundaries. Preliminary studies were therefore undertaken on simpler systems involving (a) only a single LCST phase separation boundary or (b) two phase separation boundaries, one of which was an LCST and the other a UCST boundary. This chapter describes the phase separation behaviour of poly(N-isopropyl acrylamide) in water which exhibits a single LCST type boundary. The next chapter (Chapter 12) describes the corresponding behaviour for the system of poly(vinyl alcohol) in water which exhibits two phase separation boundaries, one LCST and one UCST type. Neither showed any evidence of a third phase boundary, but as water was the solvent, these may prove to be experimentally inaccessible.

Studies of aqueous solutions of poly(N-isopropyl acrylamide) have shown that the system exhibits inverted solubility behaviour[1-4] (LCST behaviour) and the cloud-point curve over a wide range of polymer concentrations has been determined by Heskins and Guillet[4] for a single molecular weight. Inverted solubility has also been noted with polyacrylamide-poly(N-isopropyl acrylamide) copolymers in water[3] but not in the related systems of poly(N-methyl acrylamide)[5] or poly(N,N-dimethyl acrylamide)[6] in water.

11.2 SYNTHESIS OF N-ISOPROPYL ACRYLAMIDE

The most convenient route to N-substituted acrylamides is the reaction of a nitrile with an olefin or an alcohol which is a nucleophilic substitution reaction in the presence of a strong acid.

The reaction between the carbonium ion and the alcohol tautomerises to form the N-substituted amide,[7] Fig 11.1.

Acrylonitrile, propan-2-ol and 98% sulphuric acid in molar ratios 1:1:2 were added together in a flask cooled in an ice bath, initially to below 303K. During the addition of the alcohol and sulphuric acid the temperature was not allowed to rise above 303K, and 330-340K for the rest of the reaction period.

After 30 minutes the mixture was poured onto ice and the pH adjusted with ammonia solution until a precipitate was formed (pH 2). The mixture was filtered and extracted with ether. The monomer, recovered from the ether extract by evaporation, was recrystallised from a hexane/benzene mixture.[8] The resulting ir and nmr spectra are shown in Fig 11.2.

11.3 SYNTHESIS OF POLY(N-ISOPROPYL ACRYLAMIDE)

Acrylamides can generally be polymerised rapidly in the presence of free radicals in solution. Common initiators used include peroxides,[9] azo-compounds[10] or radiation-induced polymerisation.[11,12] In this case a redox pair ammonium persulphate/sodium metabisulphite was used[12] because of the relatively short reaction time when compared to the other initiators (30 min compared to >1 hr).

A flask was charged with monomer and water in molar ratio of 1:100. The monomer was allowed to dissolve whilst purging the flask with nitrogen to remove dissolved oxygen. The flask was purged for a further 30 min after dissolution.

To the flask was added, initially, ammonium persulphate $((NH_4)_2S_2O_8)$ followed by sodium metabisulphite $(Na_2S_2O_5)$ in 2 cm^3 of water, in amounts 0.2-2% by weight of monomer (see Table 11.1). The reaction was allowed to continue for 30 minutes, while continuing the nitrogen purge. An increase in temperature of approximately 7K during the reaction corresponds to 100% conversion to polymer.[13]

The water was removed on a rotary evaporator. The polymer was then dissolved in chloroform, filtered and the chloroform removed by evaporation. The resulting ir and nmr are shown in Fig 11.3.

The number average molecular weights, $\bar{M}_n$, of the samples, were determined in dioxane, at 306K, and ethanol, at 302K, (see Table 11.1). Their phase separation behaviour was determined in a variety of solvents (water, chloroform, dioxane, dimethyl formamide, dimethyl sulphoxide, methanol and tetrahydrofuran) for polymer concentration up to 20g/100 cm^3.

11.4 DISCUSSION

LCST behaviour was found only for the aqueous system, Fig 11.4. The polymer was completely soluble in the other solvents, within the temperature range studied. The coincidence of the LCST boundaries for a range of molecular weights could be due to incomplete substitution of the isopropyl group or to branching.

The spectra, both ir and nmr, show coincident peaks for all the polymers (eg see Fig 11.2, 11.3) and do not give any indication of these effects.

The heat of phase separation is 12kJ/base mol of polymer and the heat of solution has been found to be decreasingly endothermic with increasing temperatures from 0.213 J/(g of solution) at 293K to 0.163 J/(g of solution) at 303K.[4] The thermodynamic functions, calculated from the heat of phase separation and heat of solution for the aqueous system, indicate that although the enthalpy becomes less favourable the major factor is the large positive entropy difference between the system involving two phases as opposed to one phase in the vicinity, and above, the phase separation temperature.[4]

Studies[1,2] have shown that when poly(N-isopropylacrylamide) is dissolved in water there is a hydrogen-bond interaction between the amide group and the water which promotes the uncoiling of the molecules and a loss of its flexible chain character. When the temperature is increased these hydrogen-bonds are 'loosened' leading to instability of the extended polymer structure and this along with the association of these polymer molecules into larger aggregates[4] leads to phase separation.

REFERENCES

1. O Chiantore, M Guiata, L Trossarelli, Makromol.Chem. **180**, 969, (1979).

2. J Scarpa, D D Mueller, I M Klotz, J.Am.Chem.Soc. **89**, 6024, (1967).

3. C K Chiklis, J M Grasskoff, J.Polym.Sci. A-2, **8**, 1617, (1970).

4. M Heskins, J E Guillet, J.Macromol.Sci.Chem. **2**, 1441, (1968).

5. O Chiantore, M Guita, L Trossarelli, Makromol.Chem. **180**, 2019, (1979).

6. L Trossarelli, M Meirone, J.Polym.Sci. **57**, 445, (1962).

7. R O C Norman, "Principles of Organic Synthesis", Methuen, London, (1968).

8. H Plaut, J J Ritter, J.Am.Chem.Soc. **73**, 4076, (1951).

9. W M Kulicke, J Klein, Angew Makromol.Chem. **69**, 169, (1978).

10. L M Novichkova, E I Pokrovski, A G Koval'skaya, E N Rostovskii, Vysokomol.Soedin.Ser B. **10**, 813, (1969).

11. J Zurakowska-Orszagh, A Kaim, Polymer **19**, 720, (1978).

12. G Delzenne, S Toppet, G Smets, J.Polymer.Sci. **48**, 347, (1960).

13. W C Wooten, R B Blanton, H W Coover Jr, J.Polym.Sci. **25**, 402, (1957).

$$R-C\equiv N + H^+ \rightleftharpoons [R-C\equiv \overset{+}{N}H \longleftrightarrow R-\overset{+}{C}=NH]$$

(ACRYLONITRILE)

$$R-\overset{+}{C}=NH + R'OH \longrightarrow R-\underset{\underset{R'OH}{|}}{C}=NH$$

$$\downarrow -H^+$$

$$R-\underset{\underset{O}{\parallel}}{C}-NHR' \rightleftharpoons R-\underset{\underset{R'O}{|}}{C}=NH$$
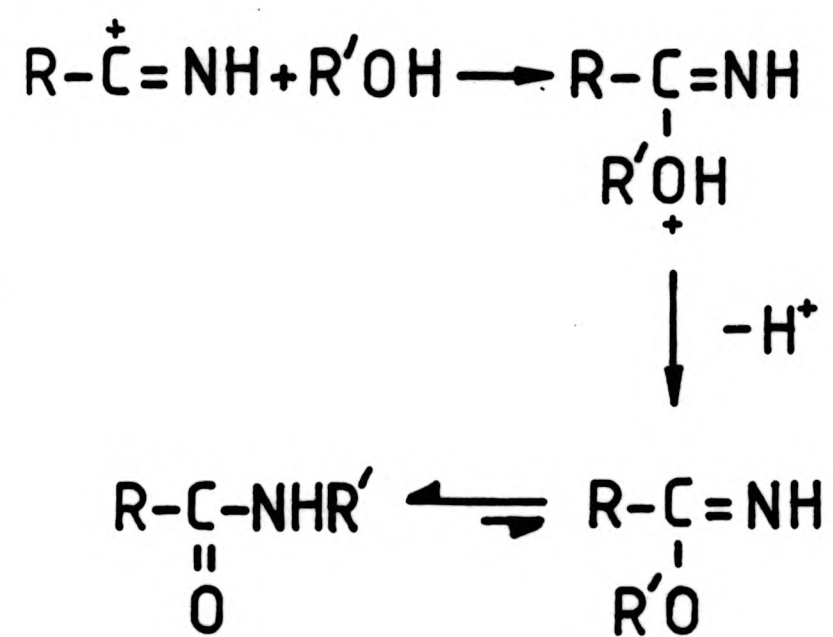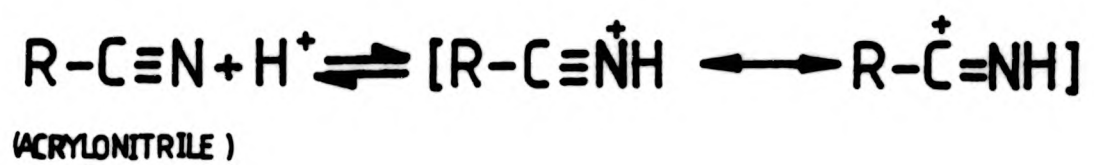
(N-ALKYL ACRYLAMIDE)

FIG 11.1 : Synthesis of N-isopropylacrylamide.

($R \equiv CH_2 = CH-$)
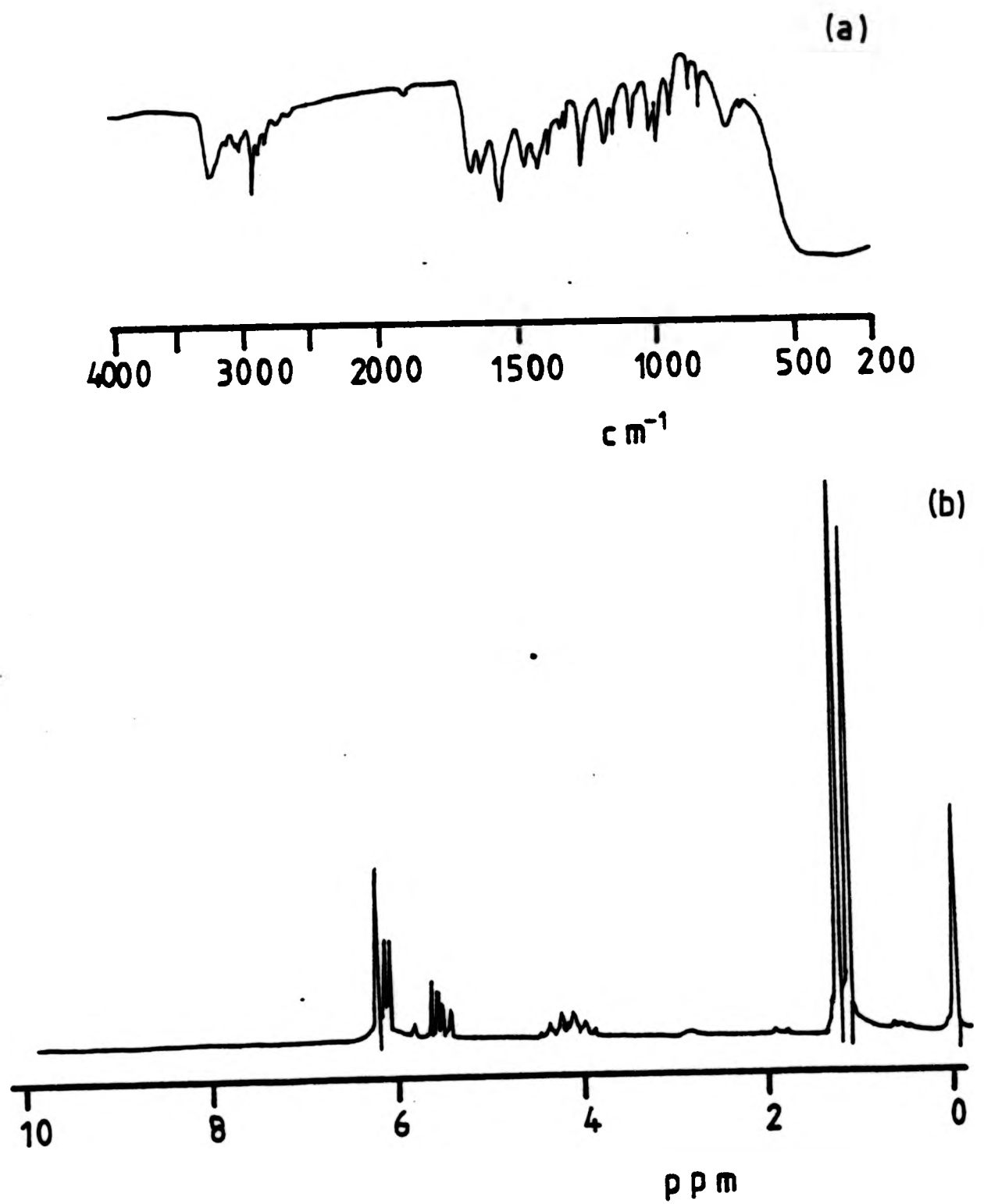
FIG 11.2 : N-isopropylacylamide :- (a) ir
                                   (b) nmr
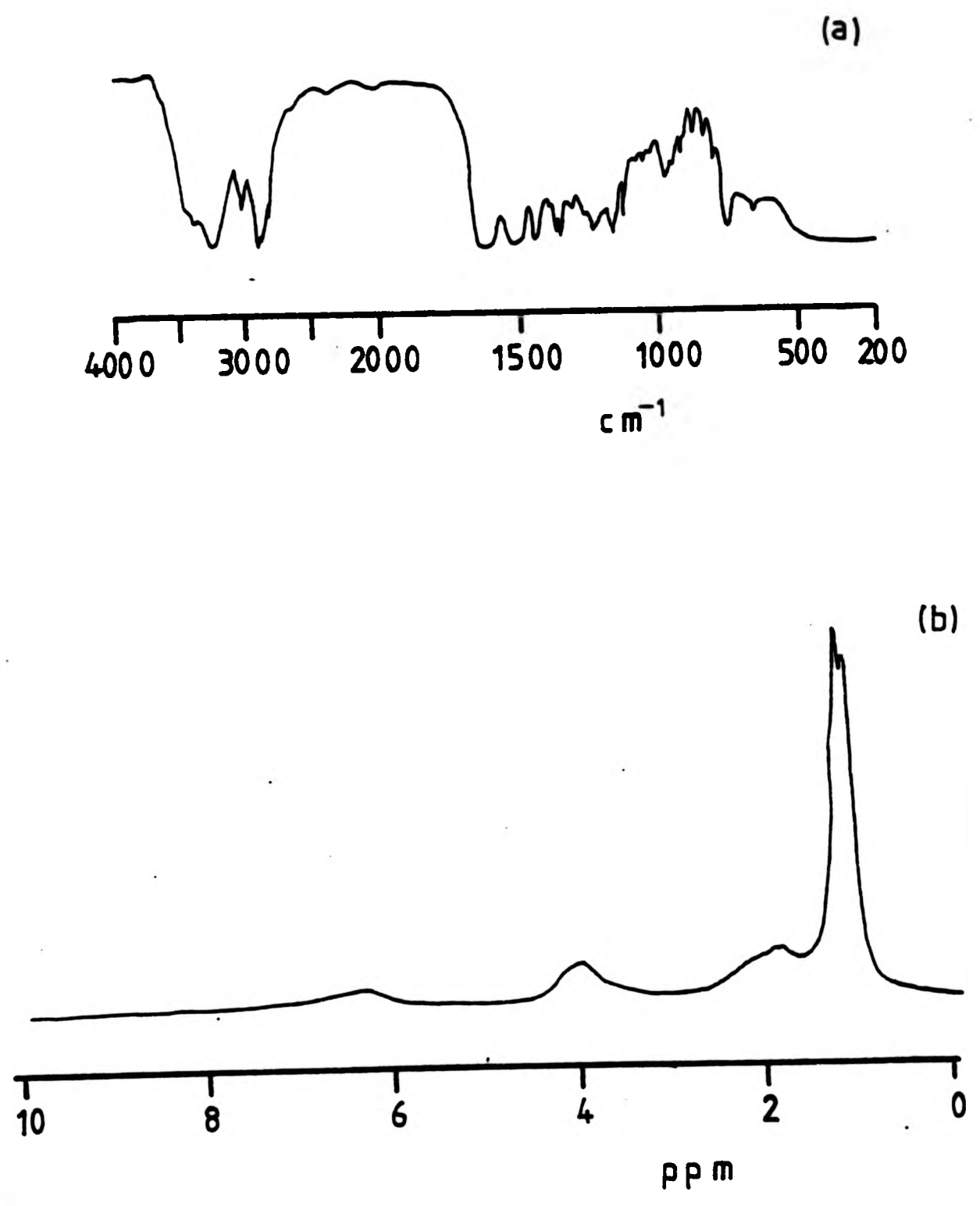
FIG 11.3 : Poly(N-isopropylacylamide) :- (a) ir
(b) nmr
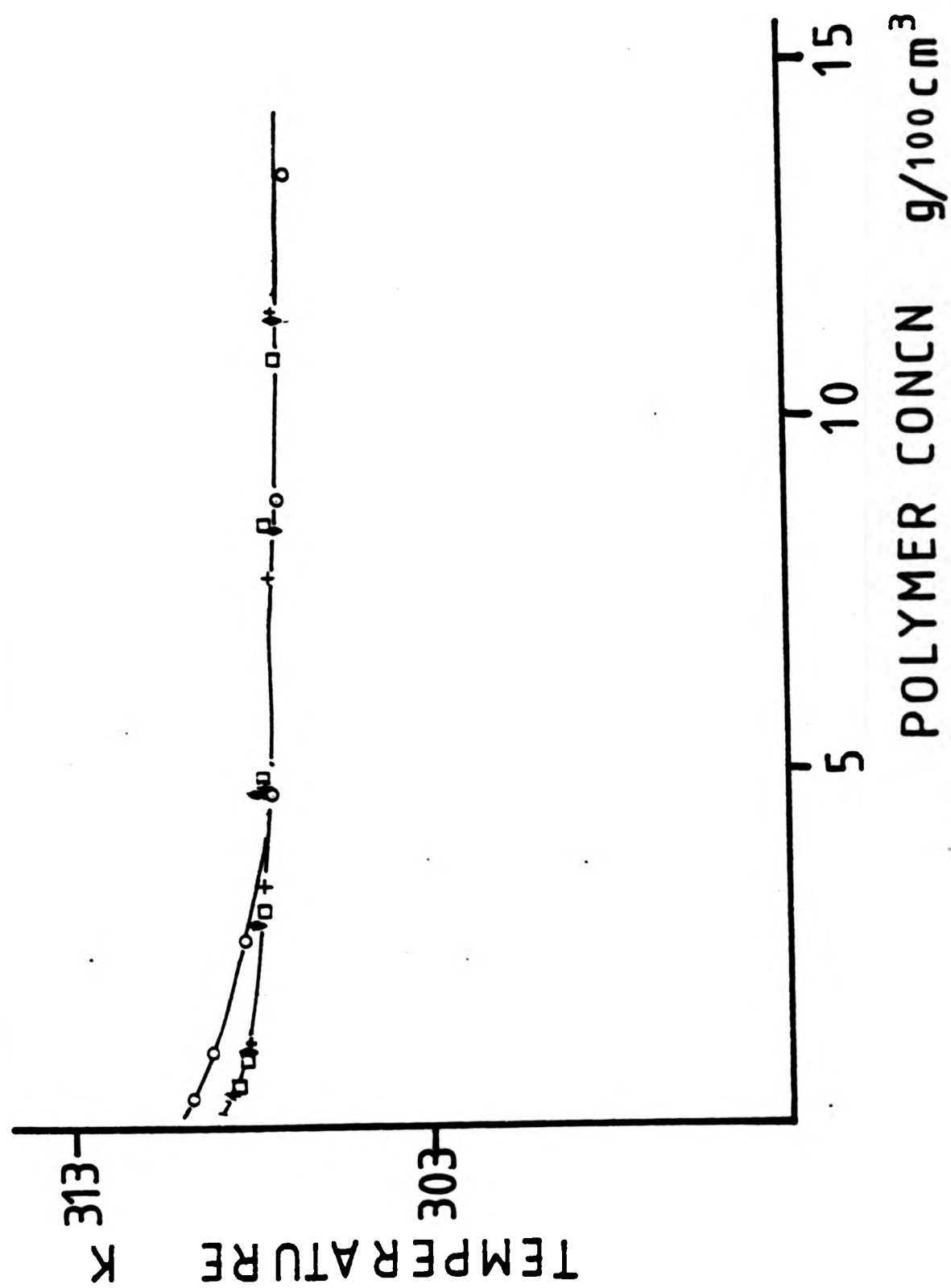
FIG 11.4 : Cloud point curve for poly(N-isopropylacrylamide) in water.
($\overline{M}_n$: $5 \cdot 7 \times 10^4$ (o), $20 \cdot 5 \times 10^4$ (+), $35 \cdot 2 \times 10^4$ (□), $62 \cdot 2 \times 10^4$ (♦)).

PREPARATION AND
TABLE 11.1 $\bar{M}_n$ for poly(N-isopropyl acrylamide) determined in dioxane (306K) and ethanol (302K) by membrane osmometry

Sample	%(NH$_4$)$_2$S$_2$O$_8$	%Na$_2$S$_2$O$_5$	wt% Yield	$\bar{M}_n$ x 10^{-4}/g/mol		
				Dioxane	Ethanol	Dioxane/Ethanol
8PN	0.23	0.25	52	62.2	12.7	4.90
5PN	0.47	0.48	60	35.2	15.6	2.26
6PN	0.91	0.93	75	20.5	9.30	2.20
7PN	1.93	1.91	40	5.77	5.92	0.97

CHAPTER TWELVE

POLY(VINYL ALCOHOL) SYSTEMS

12.1 POLY(VINYL ALCOHOL)/WATER

This chapter describes the preliminary investigation into the molecular weight variation of the phase separation behaviour of aqueous solutions of poly(vinyl alcohol) which exhibit two phase separation boundaries, an LCST boundary together with a UCST boundary. The behaviour can be compared with the more complicated three phase boundary system of poly(acrylic acid). It is worth noting, however, that the poly(vinyl alcohol) is actually a copolymer with vinyl acetate units present in the chain, and as such is a more complex structure.

A variety of authors have reported different types of solution behaviour for the system of poly(vinyl alcohol) in water.[1,2] Not only LCST behaviour[3-8] or UCST behaviour[9-11] but also combinations of both, classical[12] and closed-loop types,[8,13] have been reported. A study of the related Vinyl alcohol-Ethylene copolymer system in water[14] has indicated the existence of closed-loop type behaviour when the data were extrapolated to zero Ethylene content. A closed-loop system has also been examined for partially Butyralised Poly(vinyl alcohol)[15].

In this study four commercial Poly(vinyl alcohol)s (PVA49, PVA72, PVA100-Fluka, PVA125-BDH) were characterised and the phase equilibria in the system were established, Fig. 12.2. The $\bar{M}_n$ and A_2 for each sample were determined at 306K in 10^{-2}M aqueous NaCl solution, Table 12.1. The residual acetate contents were determined by nmr (Bruker WP80) in d_6-DMSO with NaTMS as internal reference at 343K, Table 12.1, Fig 12.1. The spectra shown in Fig 12.1 are for PVA72 and PVA100. In addition the corresponding spectrum for a poly(vinyl acetate) (BDH-$\bar{M}_n$ = 45000) is also shown. The spectra were analysed for acetate content by comparison of the methine proton signals which are adjacent to the hydroxyl or acetate groups (at 3.9 and 5.0 ppm respectively).[16,17] Only PVA125 and PVA100 showed regions of insolubility, PVA72 and PVA49 were completely soluble within the temperature and polymer concentration ranges studied.

12.2 DISCUSSION

Effectively this system can be regarded as an aqueous solution of vinyl alcohol-vinyl acetate copolymers leading to a variety of forms of cloud point curves. It has been found that where a low temperature LCST (the system, in this case, also exhibiting UCST behaviour at higher temperatures[18,19]) is seen, the temperature of phase separation decreases with increasing acetate content and for a given acetate content the temperature of phase separation decreases with increasing molecular weight.[18,19] The temperature of the UCST was found to be independent of acetate content at 398-408K.[8] The optimum water solubility occurs at 12 mol% acetate groups and has been attributed to the reduced hydrogen-bonding and lower crystallinity compared to poly(vinyl alcohol) homopolymers.[20] The results in Fig 12.2 are difficult to correlate with the above trends because both molecular weight and acetate content are varying.

The two samples (PVA125, PVA100) that gave closed-loop cloud point curves showed no higher temperature separations within the limits of polymer stability. The two other samples were completely soluble over the concentration and temperature range studied.

Insoluble material found after heating to higher temperatures (above 500K) has been explained by assuming that gelation has occurred due to the formation of a semicrystalline structure,[5] but at these higher temperatures there is also likely to be sample degradation and possible crosslinking taking place.

Direct comparisons between different studies of this system are difficult because not only is the system dependent on polymer molecular weight and acetate content but also on the general history of the polymer.[21] The temporal instabilities of the system[22-25] lead to the proposal that there are a variety of forms in which there is either partial crystallinity[1,2,25,26] or partial gelation,[12,27] but in general the phase separation behaviour has been described as the formation of a dilute liquid

phase and a concentrated swollen gel phase.[28]   Explanations of the system behaviour in terms of supermolecular structures formed by aggregates which are a result of the ageing process of the solution[18,22] suggest that eventually these stabilise the solution by the formation of internal crystalline regions, or microgel particles.

Investigation by light scattering attributes the association equilibrium to a diffusion process, the speed of equilibrium being dependent on both the molecular weight of the polymer, and the concentration of the solution.[24,27]   The supermolecular particles form semi-crystalline structures by internal hydrogen-bonding and turn the hydrophobic side of the gel inwards.   The LCST can then be attributed to the contraction of a hyper-coiled species similar to that in aqueous solutions of poly(methacrylic acid).[29,30]

This would account for the apparent negative A_2 during the ageing process[27] from an initial positive value[12,22,23,26] although difficulties in purification of the solution from contaminating and supermolecular particles is evident.[26]   The variation of A_2 with temperature shows a minimum at 363K indicating the decrease and then increase in solvent power with increasing temperature which also conforms with the lowering of intrinsic viscosity, the negative entropy parameter, ψ, and enthalpy parameter, κ, derived from viscometric data[3,4] and the interaction parameter X_h derived from heat of dilution measurements.[31,32]   This variation in A_2 would appear to be in agreement with the existence of closed-loop type behaviour.

REFERENCES

1. N A Peppas, Makromol.Chem. 176, 3433, (1975).

2. V J Klenin, O V Kleinina, N A Kolnibolotchuk, S Ya Frenkel, J.Polym.Sci.Polym.Symp. 42, 931, (1973).

3. A Dieu, J.Polym.Sci. 12, 417, (1954).

4. E D Pokhvalenski, T S Dimitrieva, 'Protessy Structurooerazov Rostvorakh Gelyakh Polim' (Univ. Saratov), 56, (1971).

5. V M Andreeva, A A Tager, A A Anikeyeva, T A Kuz'mina, Vysokomol.Soedin.Ser B 11, 555, (1969).

6. H Kunieda, Nippon Kagaku Kaishi 1134, (1974).

7. I Sakurada, V Sakaguchi, Y Ito, Kobunshi Kagaku 14, 289, (1951).

8. F F Nord, M Bier, S N Timasheff, J.Am.Chem.Soc. 73, 289, (1951).

9. O V Klenina, V I Klenin, S Ya Frenkel, Polym.Sci. USSR 12, 1448, (1970).

10. G N Kormanovskaya, E I Evko, V V Churakov, V M Lukyanovich, I N Vlodavets, Colloid J. USSR 30, 522, (1968).

11. I Sakurada, A Nakajima, K Shibatani, Makromol.Chem. 87, 103, (1965).

12. A A Tager, A A Anikeyeva, L N Adamova, V M Andreeva, T A Kuz'mina, M V Tsilipotkina, Vysokomol.Soedin.Ser A 13, 659, (1971).

13. G Rehage, Kunstoffe 53, 605, (1963).

14. K Shibatani, Y Ohyanagi, Kobunshi Kagaku 28, 361, (1971).

15. T Shiomi, K Imai, C Watawabe, M Miya, J.Polym.Sci.Polym.Phys.Ed. 22, 1305, (1984).

16. T Moritani, Y Fujiwara, Macromolecules 10, 532, (1977).

17. G Van der Velden, J Beulen, Macromolecules 15, 1071, (1982).

18. K Fujishinge, J.Colloid.Sci. 13, 193, (1958).

19. W R A D Moore, M O'Dowd, SCI.Monograph No 30, 77, (1968).

20. H Warson, SCI. Monograph No 30, 46, (1968).

21. A S Dunn, S R Naravane, Br.Polym.J. $\underline{12}$, 75. (1980).

22. T Matsuo, H Inagaki, Makromol.Chem. $\underline{53}$, 130, (1962).

23. T Matsuo, H Inagaki, Makromol.Chem. $\underline{53}$, 150, (1962).

24. M Matsumoto, Y Ohyanagi, J.Polym.Sci. $\underline{26}$, 389, (1957).

25. W I Priest, J.Polym.Sci. $\underline{6}$, 699, (1951).

26. V J Klenin, O V Klenina, B I Shvartsburd, S Ya Frenkel, J.Polym.Sci.Polym.Symp. $\underline{44}$, 131, (1974).

27. E Gruber, B Soehendra, J Schurz., J.Polym.Sci.Polym.Symp. $\underline{44}$, 105, (1974).

28. M M Zwick, J A Duiser, C Van Bochove, SCI.Monograph No 30, 188, (1968).

29. K Dialer, K Vogler, F Patat, Helv.Chim.Acta $\underline{35}$, 869, (1952).

30. T Kuroiwa, Chem. High Polymers (Japan) $\underline{9}$, 253, (1952).

31. K Amaya, R Fujishiro, Bull.Chem.Soc.Japan $\underline{29}$, 361, (1956).

32. K Amaya, R Fujishiro, Bull.Chem.Soc.Japan $\underline{29}$, 830, (1956).
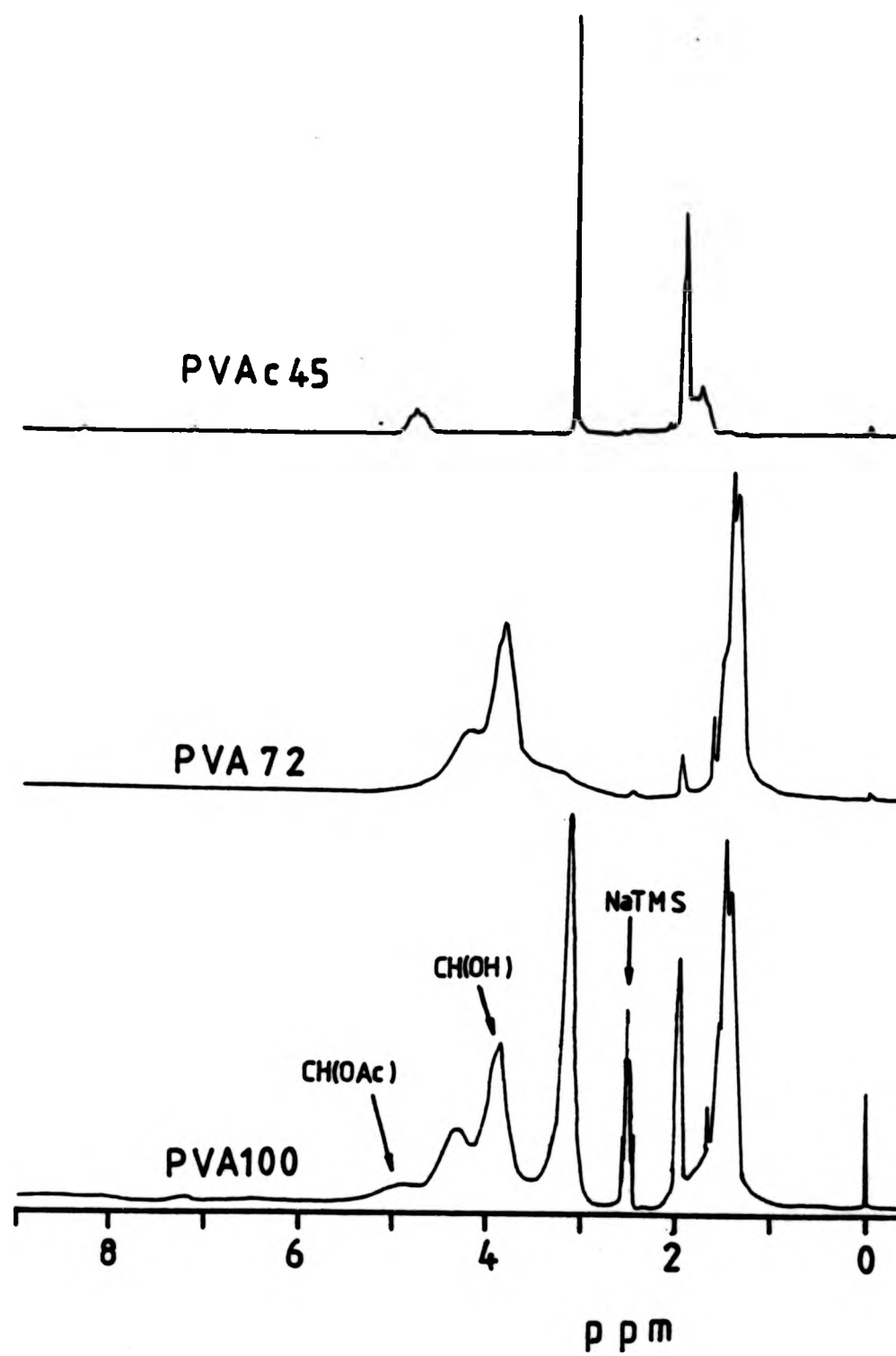
FIG 12.1 : nmr spectra of poly(vinyl acetate) PVAc45 and
poly(vinyl alcohol) PVA72,PVA100 in d_6-DMSO with
NaTMS as reference.
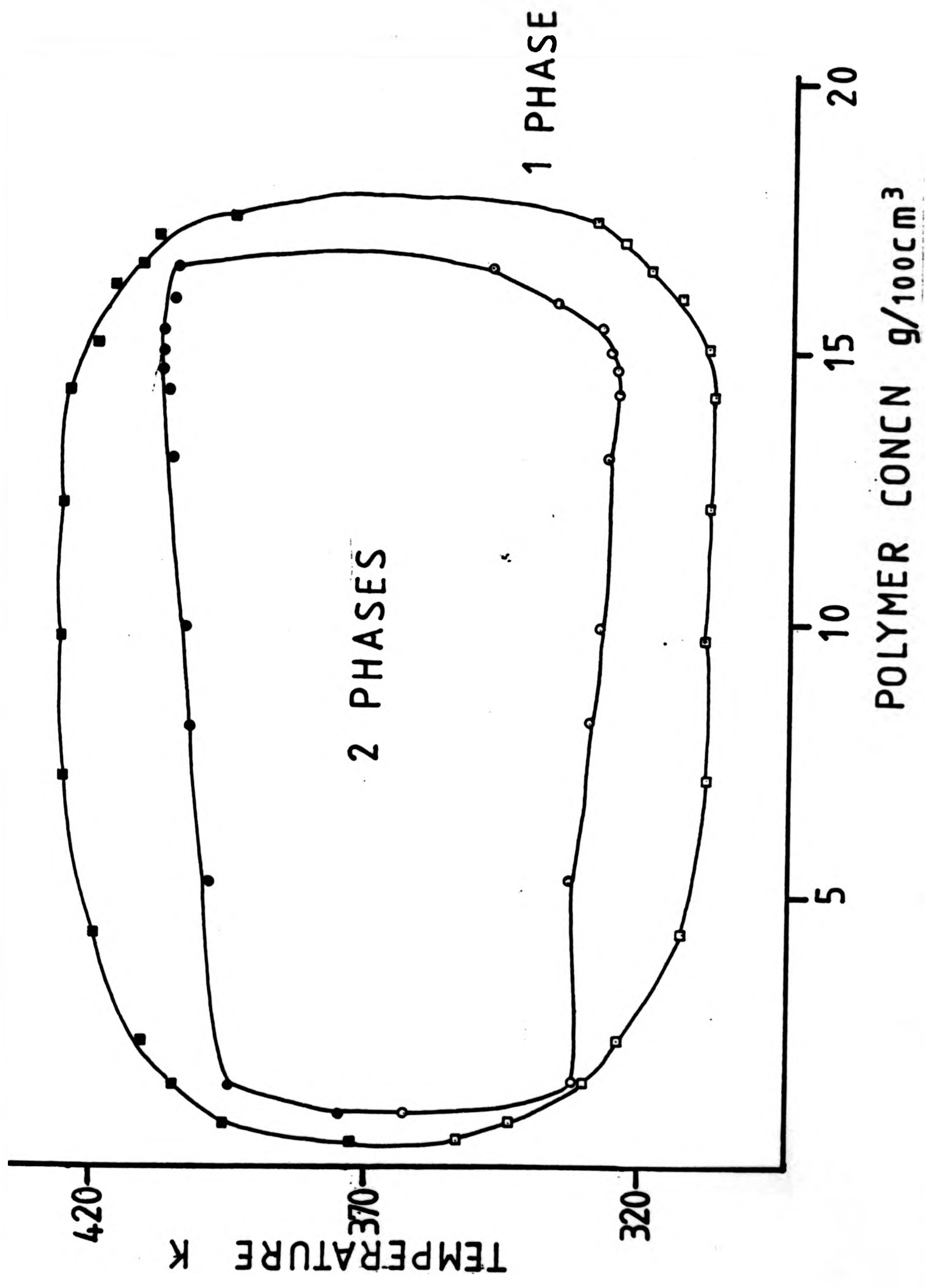
FIG 12.2 : Cloud point curve for poly(vinyl alcohol) in water.
($\bar{M}_n$: 10×10^4($\square$), 12.5×10^4($\circ$)).

TABLE 12.1 $\bar{M}_n$ and A_2 for poly(vinyl alcohol) determined by membrane osmometry in 10^{-2}M aq NaCl at 306K

PVA	$\bar{M}_n$ x 10^4/g/mol	A_2 x 10^4/cm^{3}mol/g^2	Acetyl mol%
PVA49	5.03 $\pm$ 0.25	8.85 $\pm$ 0.44	12
PVA72	8.09 $\pm$ 0.41	2.81 $\pm$ 0.14	-
PVA100	9.16 $\pm$ 0.46	4.93 $\pm$ 0.25	16
PVA125	12.60 $\pm$ 0.63	1.51 $\pm$ 0.08	7

CHAPTER THIRTEEN

GENERAL DISCUSSION

13.1 STRUCTURE IN DIOXANE SOLUTIONS OF POLY(ACRYLIC ACID)

It has been repeatedly stated that there are no molecular interactions in dioxane solutions of poly(acrylic acid).   It has been seen here, that in aqueous ternary systems of poly(acrylic acid), at least, there are interactions between the 'solvent' and the polymer which does involve dioxane.   Molecular complexes between dioxane and water are well-established but the preferential solvation study undertaken here shows that these complexes are also present in poly(acrylic acid) systems, depending on the water content in the solution.   That these complexes do exist has been demonstrated by a reduction in the acidity of the mixtures of dioxane and water, both with or without the polymer being present, over that of water alone (A)* (a pH cannot be defined for dioxane).   This reduction occurs over the entire range of solvent mixtures that are of interest in this study, ie less than 50% water.

It has been shown that these complexes occur at water contents of 8, 18 and 30(wt/vol)% in the solvent.   They can be quantified stoichiometrically as 1:2, 1:1 and 2:1 complexes, respectively, in terms of the mole ratio water:dioxane.   The complex at 8(wt/vol)% water has been shown to have a predominance of dioxane around the polymer.   The other complexes have a predominance of water around the coil.   The similarity of the value of the preferential solvation parameter, λ_1^* (B), and of the molecular dimension, $<r_z^2>$ (C), for the polymer at these different contents (18 and 30%) indicates that it is the water component

---

* A number of the figures referred to in the text are reproduced from previous chapters, at the end of this section.   See the letters in parenthesis.

which is almost exclusively in the vicinity of the coil. For sample PAA300 $<r_z^2>$ is 17nm and 16.4nm at 18 and 30(wt/vol)% water respectively (C). The value of $<r_z^2>$ at 8(wt/vol)% water is slightly larger at 19.5nm for sample PAA300.

The value of the second virial coefficient, A_2, derived from light scattering at these water contents is zero which would indicate that the coil is unperturbed (D). There is also another water content, 24(wt/vol)%, where $A_2=0$ which gives a value of $<r_z^2>$ which is approximately a third of the other values (6nm for PAA300). This water content gives the 'greatest' preferential solvation by water, in the region studied. It also corresponds to a complex of mole ratio of 3:2 but it would be unrealistic to consider this complex as a possibility since the other parameters used during the analysis of the preferential solvation data indicate that the $A_2=0$ at this water content has different characteristics from the other three. The molecular dimensions at 24(wt/vol)% water may be more akin to the unperturbed state associated with the polymer in water. The other three water contents must be considered as 'unperturbed states' not of water and dioxane mixtures but of water/dioxane complexed mixtures.

A more general unperturbed state for the system could be described where there is no preferential solvation, ie $\lambda_1^*=0$. This occurs at both 5 and 10(wt/vol)% water and the values of $<r_z^2>$ are similar for both water contents (16nm at 5% and 18nm at 10% water). The $<r_z^2>$ values are similar since both are linked to the same complex, the one at 8(wt/vol)% water. The value at 5(wt/vol)% associated with the complex formation whilst that at 10(wt/vol)% is associated with the break-up of the complex as the water content is increased.

Dondos and Benoit[1] have proposed the existence of two θ-points for

polymeric systems in a given binary mixture where one θ-point occurs when $A_2=0$ and the other when the coil obeys Gaussian statistics and A_2 is not necessarily zero. Only when there is no preferential solvation do the two θ-points coincide. It is not unreasonable, therefore, to define the points where $\lambda_1^*=0$ as unperturbed states as well as the mixtures where $A_2=0$. In this case when $\lambda_1^*=0$ at 5(wt/vol)% water, A_2 is positive, and at 10(wt/vol)% it is negative, which again could be due to the different 'complex environment' around the coil.

A comparison of the two different measurements of $<r_z^2>$ is shown in Fig 13.1. In general it can be considered that the trends are similar considering that one set of data is based on weight average molecular weights, $(<r_z^2>/\bar{M}_w)^{\frac{1}{2}}$, from light scattering and the other set is based on number average molecular weights, $(<r_z^2>/\bar{M}_n)^{\frac{1}{2}}$, derived from osmometry and solution viscosity. The quantitative agreement is disappointing however.

The study of the variation of intrinsic viscosity, $[\eta]$, with increasing water content was undertaken on a different sample, PAA50 (E), to that used in the preferential solvation study, PAA300. It is interesting, here, not to consider the position of the changes in trends of $[\eta]$ but to consider the mid-points between these changes. These mid-points occur at approximately 7, 18 and 31(wt/vol)% water in the solvent, which is in agreement with the stochiometric molar values of the complexes proposed for the system from the preferential solvation study. The changes in trends can then be correlated with changes in ordering in the solution, from predominantly one complex to another.

The Mark-Houwink exponent, which also gives a measure of the unperturbed state of the coil, as a function of water content was also studied, (F). This gave a value of 0.5 at approximately 3(wt/vol)%

water but the values at 5 and 10(wt/vol)% water are both close to 0.55.
The plot also gives a maximum at 8(wt/vol)% water which would be in
agreement with a maximum in the molecular dimensions as derived from
light scattering data as well as solution viscosity.

In the plot of [η] against water content, one of the changes in
trends occurs at 12(wt/vol)% water.   For the same poly(acrylic acid)
sample, PAA50, the transition from three phase separation boundaries to a
single phase separation boundary also occurs here, (G), but it is
interesting to note that although the predominant complexation in the
solution changes the phase separation is still associated with a p-LCST
phase separation boundary.

Although not strictly a 'solvent', poly(ethylene glycol) when used
as the third component in dioxane solutions of poly(acrylic acid) was
also found to form a 1:1 molar complex with the poly(acrylic acid).   It
is not altogether satisfactory to regard this interaction as a
polymer-solvent one since it is more associated with poly(ethylene
glycol) molecular weights which, although relatively small when compared
to the poly(acrylic acid) are large when compared to dioxane.   The
nature of the 'major solvent' is also not critical, in this case, since
an interpolymeric complex of similar character is also found in aqueous
solutions.

However, these are other examples of solution systems based on
poly(acrylic acid)/dioxane which do involve specific interactions between
the components which affect the phase separation behaviour in the
solutions.

The study so far has been into the characteristics of the solutions
which are effectively not approaching a phase separation boundary.   They
are single phase solutions well below the temperature at which the p-LCST

phase separation boundary occurs.

In the single solvent system of poly(acrylic acid) in dioxane the quoted θ-temperature is 303K (this point has been discussed elsewhere). The variation of intrinsic viscosity, $[\eta]$ with temperature, (H), does give a maximum, for higher molecular weight poly(acrylic acid)s, at this temperature and leads to a maximum in the appropriate molecular dimension plot, but the Mark-Houwink exponent which would be expected to be 0.5 is in fact 0.42, implying that the polymer coil is smaller than the expected unperturbed value. This is shown also by the fact that $\langle r_z^2 \rangle / \bar{M}_n$ is smaller than $\langle r_o^2 \rangle / \bar{M}_n$ for all the temperatures studied, (J). When the Mark-Houwink exponent is $0.5, \langle r_o^2 \rangle = \langle r_z^2 \rangle$. From Fig 4.11(J) it is difficult to conceive of a temperature where this occurs. In general, as might be expected, the value of $[\eta]$ decreases with increasing temperature, as phase separation is approached.

Interactions in the aqueous ternary solutions are also indicated by raman spectroscopy, (K), (Chapter 7) where there is evidence not only of hydrogen-bond interactions between different polymer molecules themselves, but also between the polymer and the solvent. The interactions between the polymer and the solvent increases with increasing water content but these interactions decrease with increasing temperature. In addition intrapolymeric hydrogen-bonding interactions involving the solvent also decreases with increasing temperature whereas both inter- and intra-polymeric dimeric interactions increase. Hence, the approach to phase separation could be described as the effect due to the decrease in hydrogen-bond interactions between the polymer and the solvent and an increase in dimeric interactions, both inter- and intra-polymeric, between polymer molecules. This effect has also been described as the increasing formation of intramolecular closed-loop

units, with increasing temperature, which exclude the solvent, or entrap it, which would lead to phase separation in polymeric species which is not possible in the analogous monomeric species.[2]

A measure of the χ-parameter can be obtained from the parameter B in the Stockmayer-Fixman relationship by

$$B = \frac{\bar{u}^2(1-2\chi)}{V_1 N_A} \qquad \qquad 4.13$$

where V_1 is the molar volume of the solvent, in the case of dioxane 85.21 cm^3/mol.[3]. $\bar{u}$, the partial specific volume of poly(acrylic acid) in dioxane has been measured in this study as 0.78 cm^3/g. Different values of B can be obtained depending on the form of the Stockmayer-Fixman relationship used. The values for χ are shown in Table 13.1. These values are relatively constant and are close to the critical value, χ_c, as defined by

$$\chi_c = 1/2 + 1/x^{\frac{1}{2}} \qquad \qquad 1.12$$

indicating that the system is close to a phase separation boundary. The negative values of K' are one of the consequences of having positive χ values. The excluded volume parameter, z, can also be determined from K' through the relationship

$$\frac{z}{M^{1/2}} = \left(\frac{3}{2\pi}\right)^{3/2} B \left(\frac{<r_o^2>}{M}\right)^{3/2} M^{-1/2} \qquad 13.1$$

The values obtained, as shown in Table 13.2, are negative.

The quantities $A_2M^2/<s^2>^{3/2}$ and $A_2M/[\eta]$, which are related to the excluded volume[4,5] have been used as measures of the interpenetration of coils in solution for both non-polar[4] and polyelectrolyte[5] systems. In good solvents the upper limit of these quantities, which represent coils behaving like unpenetrable spheres, are 5×10^{24} and 150 for $A_2M^2/<s^2>^{3/2}$ and $A_2M/[\eta]$ respectively[5]

when A_2 is in $cm^3 mol \ g^{-2}$ and $[?]$ is in $100cm^3/g$. The values obtained here are approximately 10^{14} and 40 respectively. It should be noted that these are approximate since the quantities depend on the molecular size of the coils. It can be seen from the values obtained that dioxane is indeed a poor solvent for poly(acrylic acid).

13.2 THE p-LCST PHASE SEPARATION BOUNDARY

In polar polymer solutions, such as poly(N-isopropylacrylamide) in water, when the components are mixed, interactions, for example hydrogen bonds, are formed between the polymer and the solvent resulting in a negative heat and entropy of mixing. As the temperature is increased, the system tends to move towards the phase separation boundary as these interactions are destroyed and the heat of mixing becomes less exothermic. The predominant factor here is the entropy of mixing. This parameter can become more negative if interactions are formed between like species during this process but there must be some entropy gain caused by the disruption in the polymer-solvent structure. An LCST boundary can then be associated with an entropically controlled process.

In non-polar systems the LCST boundary normally occurs at temperatures above the boiling temperature of the solvent. Here the occurrence of the boundary is due to the greater expansion of the solvent compared to the polymer with increasing temperature. The solvent needs to undergo a 'condensation' process onto the polymer for a homogeneous solution to be retained. This can also be associated with an entropically controlled process. As the temperature is increased across a UCST phase separation boundary from a two phase to a single phase system in non-polar solutions any polymer-polymer interactions, for example dipole interactions, are broken up by thermal motions. This

will be associated with a positive entropy of mixing which is also
dependent on temperature.   This process is also associated with a
positive heat of mixing.   A UCST boundary can then be regarded as a
process controlled by the enthalpic parameter.

In the case where two phase separation boundaries occur in a
solution resulting in closed-loop type behaviour, as shown by aqueous
poly(vinyl alcohol) solutions, hydrogen bond interactions between polymer
and solvent are formed at low temperatures.   On increasing the
temperature these interactions are again destroyed leading to the same
situation as with the single LCST boundary system.   This system also has
a second, higher temperature boundary, a UCST boundary.   It has been
seen that as the temperature increases the 'solvent quality' goes through
a minimum.   The subsequent improvement in the solvent leads to a UCST
boundary where the heat and entropy of mixing are both positive.

There is little effect on UCST behaviour on changing the pressure of
the system, but because the LCST behaviour (non-polar) is a consequence
of differences in free volume, changes in pressure will have a greater
effect on this phase boundary by reducing the free volume and
consequently increasing the polymer solubility with increasing
pressure.   It is interesting to note that the effect depends only on the
reduced volume of the solvent.[6]

As discussed in Chapter 1, the trends in the parameter χ, at phase
separation boundaries can be described by dividing it into combinatorial,
χ_{comb}, and free volume, χ_{fv}, parts.   As shown in Fig 1.5 and Fig
13.2, χ_{comb} is the important parameter at a UCST phase separation
boundary whilst χ_{fv} dominates at an LCST phase separation boundary.
How can the p-LCST phase separation boundary be described?   For a system
in which three boundaries p-LCST, UCST and LCST can be located as the

temperature of the system is increased, $\chi = \chi_c$ at three temperatures and the form of the χ function must be a cubic curve similar to that shown in Fig 13.2. If it is assumed that the higher temperature boundaries, UCST and LCST, are 'classical' in the sense described above, then the trends in χ_{comb} and χ_{fv} can be described as in Fig 13.2. The parameter χ can also be divided up into non-polar and polar contributions as suggested by Yamakawa[7]

$$\chi = \chi_{np} + \chi_p \qquad 1.25$$

where χ_{np} can be given by

$$\chi_{np} = \chi_{comb} + \chi_{fv} \qquad 13.2$$

Phase separation behaviour at and below the p-LCST can be described if we consider that now χ_p is a factor of some importance, and the behaviour can be accounted for if χ_p is considered to be a decreasingly negative function of the temperature which vanishes at temperatures around the p-LCST boundary, as shown schematically in Fig 13.2. χ_{np} will then become the dominant factor at higher temperatures where χ_p is vanishingly small and the components χ_{comb} and χ_{fv} become important in the 'classical' sense. The χ_p factor can best be represented as a negative inverse function of the temperature, $\chi_p \propto -1/T$.

The relationship between the heat of mixing, ΔH_m, and χ can be given generally as

$$\Delta H_m = -RT^2 \left(\frac{\partial \chi}{\partial T}\right) \phi_1 \phi_2 \qquad 1.20$$

This shows that ΔH_m also has a decreasingly negative value with increasing temperature, when χ_p is considered. Evidence suggests that

the level of hydrogen bonding in the system studied, poly(acrylic acid) in dioxane, is not excessive and it would be expected to have a positive heat of mixing. However, there are sufficient hydrogen bond interactions present, which are thermally labile, and their disruption would lead to an increasingly positive, and therefore a decreasingly negative, trend in the heat of mixing as a function of increasing temperature. This is in the same sense as that described above. It can be seen, then, that χ_p is predominantly enthalpic in character although there must be an entropic component associated with it which arises from the changes caused by disruption of specific interactions. As these would largely lead to a favourable entropic contribution the phase separation is likely to be enthalpically controlled. The overall χ-parameter can be described as a function of temperature by an equation of the form

$$\chi = b/T + a + cT^2 - d/T \qquad\qquad 13.3$$

The first two terms on the right hand side of the equation can be associated with χ_{comb}, the third term with χ_{fv} and the fourth term with χ_p which will be predominantly enthalpic in character being associated with specific interactions in the solution. It is a negative inverse function of temperature which vanishes at temperatures around the p-LCST phase separation boundary. Hence a p-LCST boundary can be associated with an enthalpically controlled process unlike a 'classical' LCST boundary which is normally associated with an entropically controlled process. Thus the two phase boundaries may be distinguished both in terms of the mechanism of phase separation and their thermodynamic description.

13.3 CONCLUSION

In this study a system, poly(acrylic acid) in 1,4-dioxane, has been found to exhibit three phase separation boundaries with increasing temperature.   An LCST boundary at low temperatures designated as pseudo-LCST (p-LCST) followed by a UCST boundary at higher temperatures. Another LCST boundary occurs at even higher temperatures.   It has been established that both p-LCST and LCST boundaries exhibit the general characteristics normally associated with an LCST type boundary.   They both decrease in temperature with increasing molecular weight and the temperature minimum moves to lower polymer concentrations the higher the molecular weight.   The UCST boundary, unexpectedly, also decreases in temperature with increasing molecular weight.   This three phase separation boundary system is also reflected in ternary solutions containing dioxane and poly(acrylic acid) together with water, crown ether (12-C-4) and with short chain poly(ethylene glycol)s and poly(propylene glycol)s.

Classical thermodynamic behaviour, at UCST and LCST phase separation boundaries, are followed by the two higher temperature boundaries. However, this is not the case with the lower temperature p-LCST boundary.   To explain this boundary the effect of specific interactions, X_p must be introduced into the 'classical' expressions for the X-parameter, which is a negative inverse function of temperature.   It is also predominantly an enthalpic parameter.   Therefore a p-LCST phase separation boundary can be associated with an enthalpically controlled process as opposed to the 'classical' LCST phase separation boundary which is normally associated with an entropically controlled process.

This behaviour and its relationship to specific interactions in solution are an important area for future study not only for polymer

solutions but also for their application to specific interactions in polymer blends and mixtures.

A recent development, not included in this thesis, is the pulse-induced critical scattering (PICS) study undertaken on the poly(acrylic acid)/dioxane system by L A Kleintjens at Dutch State Mines. This study has established the spinodal curve associated with the p-LCST phase separation boundary.[8]

REFERENCES

1. A Dondos, H Benoit, Polym.Lett. 7, 335, (1969).

2. G Allen, E F Caldin, Quart.Rev. 7, 255, (1953).

3. 'Polymer Handbook', Ed J Brandrup, E H Immergut ,
    Wiley-Interscience, New York, (1967).

4. T A Orofino, P J Flory, J.Chem.Phys. 26, 1067, (1957).

5. T A Orofino, P J Flory, J.Phys.Chem. 63, 283, (1959).

6. D Patterson, G Delmas, Trans. Faraday Soc. 65, 708, (1969).

7. H Yamakawa, S A Rice, R Corneliussen, L Kojin, J.Chem.Phys. 38,
    1759, (1963).

8. Private communication, from Dr. L.A. KLEINTSENS
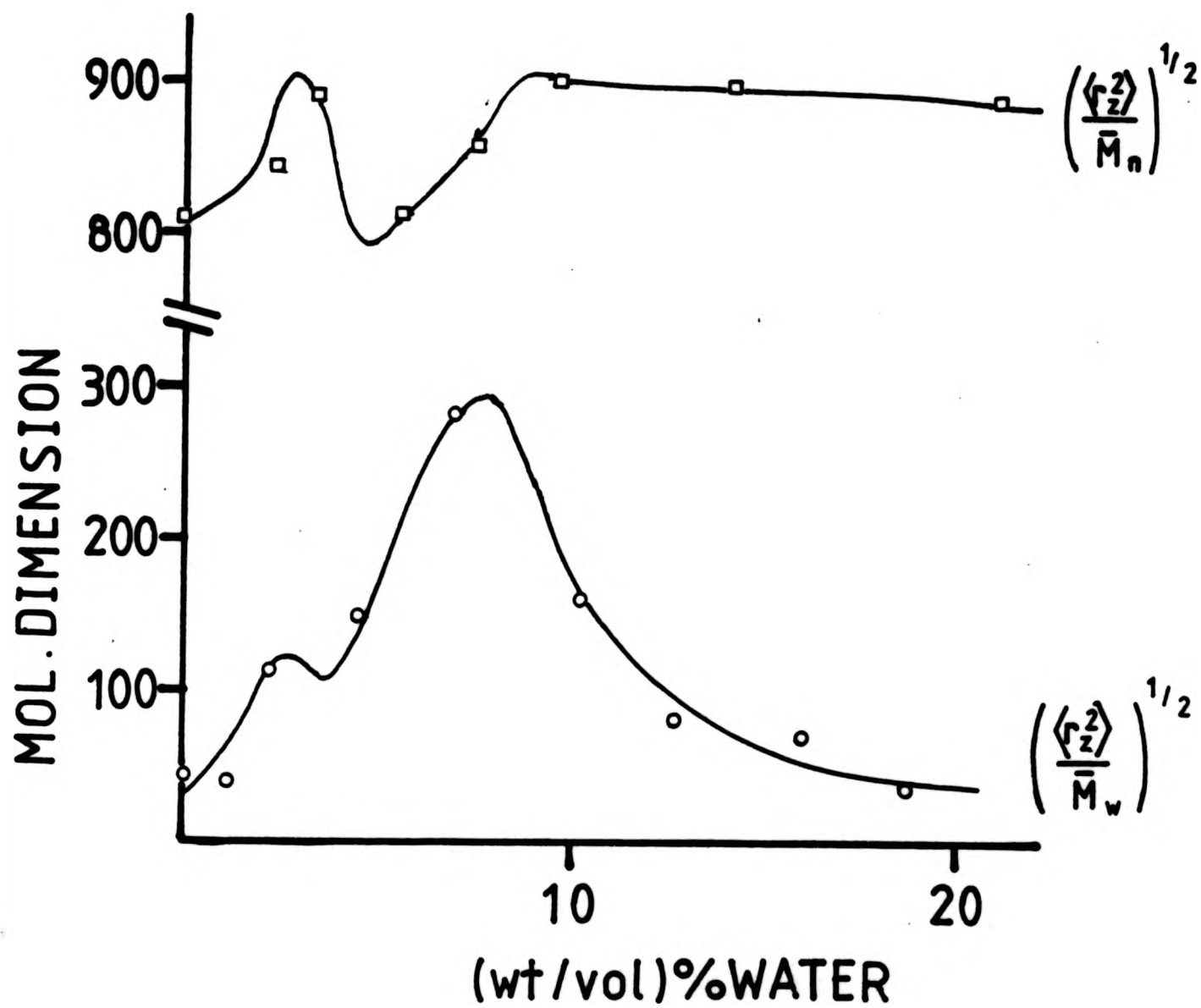
FIG 13.1 : Molecular dimension for poly(acrylic acid) in
dioxane/water as a function of water content
as derived from light scattering ($(\langle r_z^2 \rangle / M_w)^{\frac{1}{2}}$, o)
and solution viscosity ($(\langle r_z^2 \rangle / M_n)^{\frac{1}{2}}$, □).
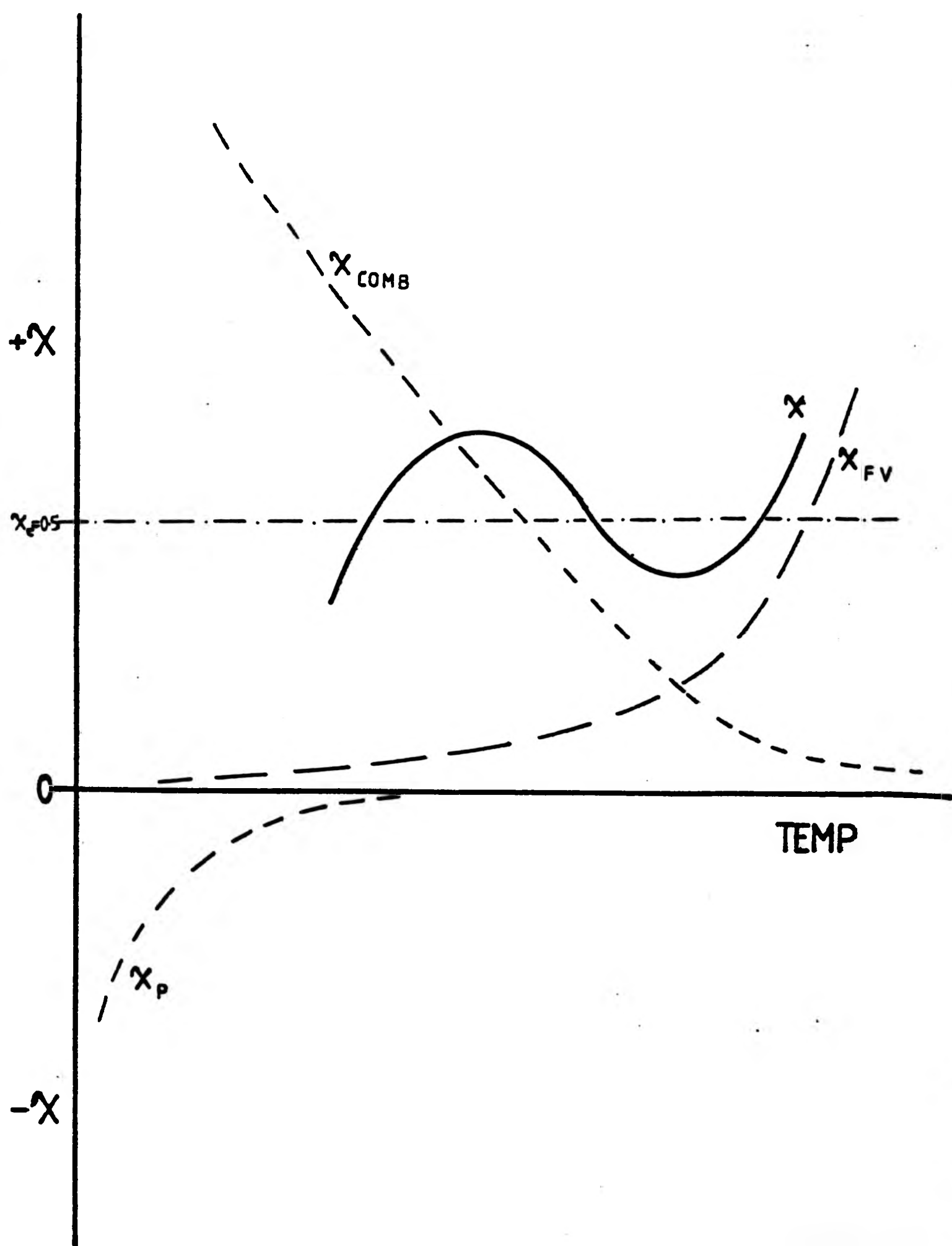
FIG 13.2 : Variation of χ and its components χ_p, χ_{comb}, χ_{FV} as a function of temperature.

TABLE 13.1   Values of X as a function of temperature for the different
forms of K'

Temp	K'		
	0.51ΦB	0.346ΦB	0.287ΦB
298	0.57	0.60	0.62
303	0.54	0.57	0.58
308	0.54	0.56	0.57
313	0.55	0.57	0.58

TABLE 13.2   Values of $(z/M^{\frac{1}{2}}) \times 10^{10}$ as a function of temperature for the
different forms of K'

Temp	K'		
	0.51ΦB	0.346ΦB	0.287ΦB
298	−8.32	−12.27	−14.79
303	−5.53	− 8.15	− 9.83
308	−5.45	− 8.04	− 9.69
313	−6.38	− 9.41	−11.34

(F)

(G)

(H)

(J)

(K)
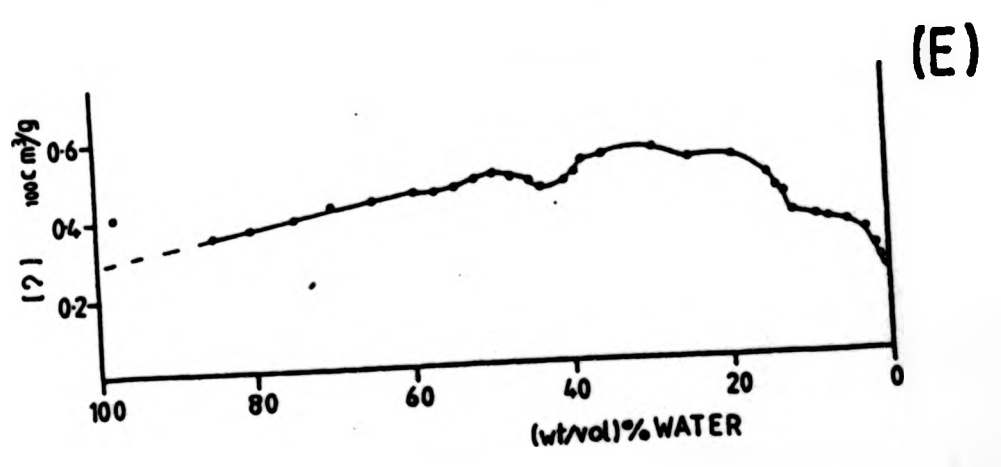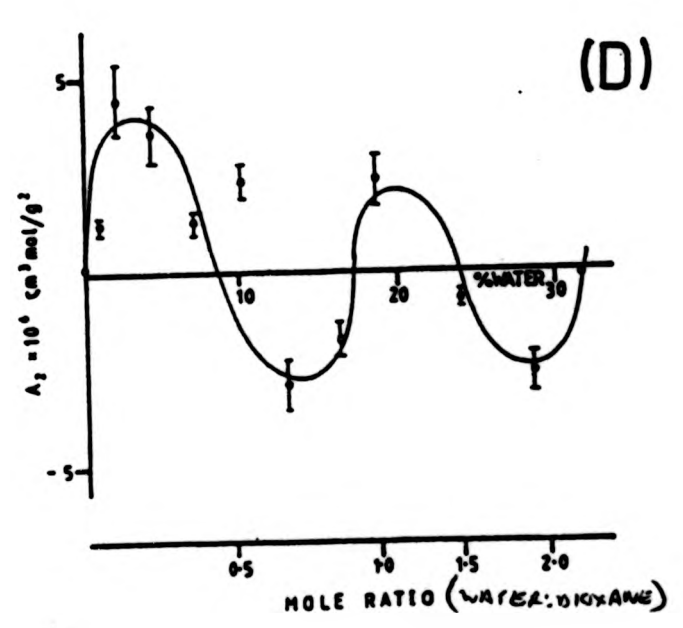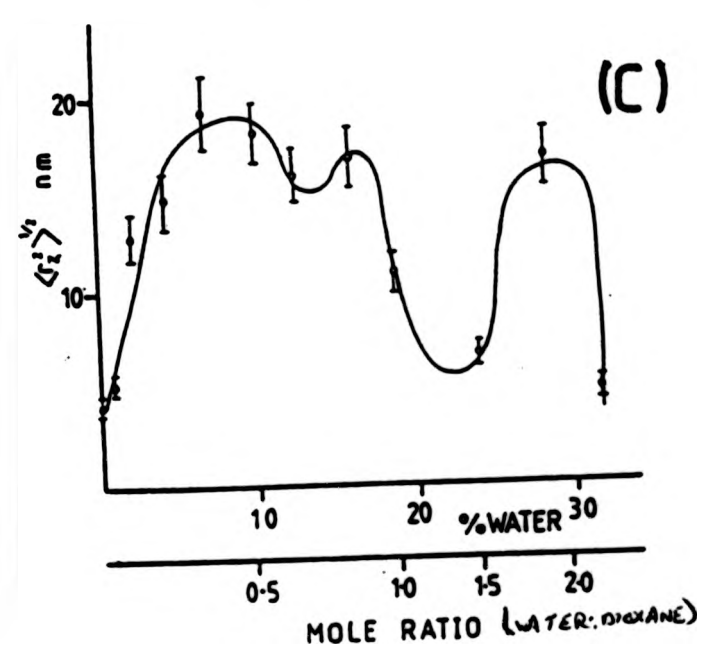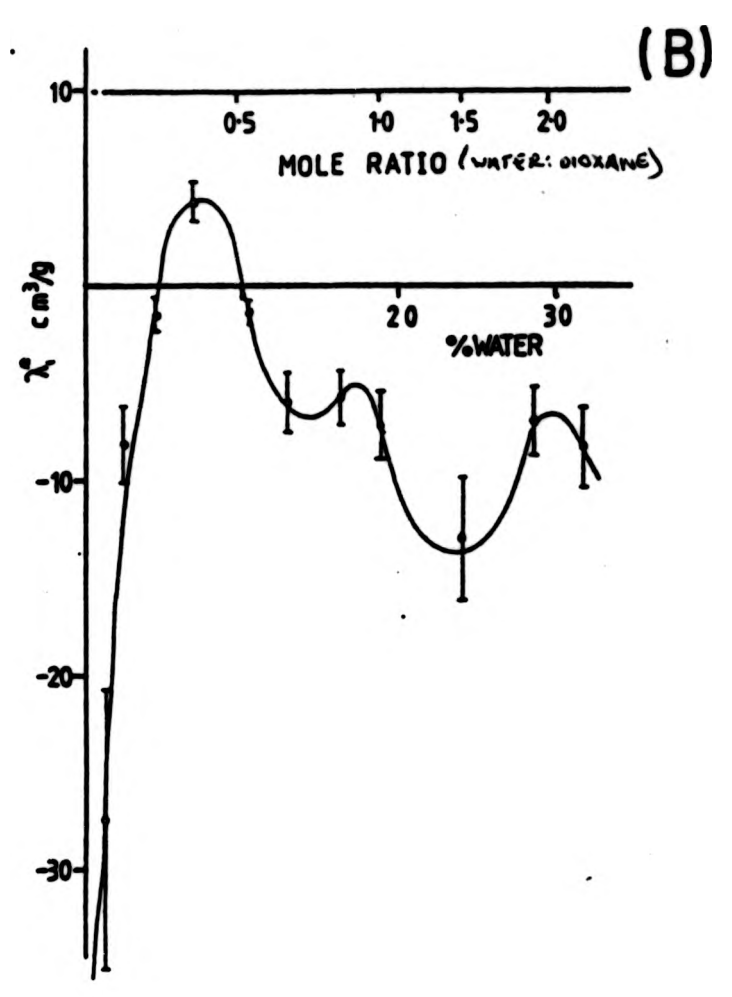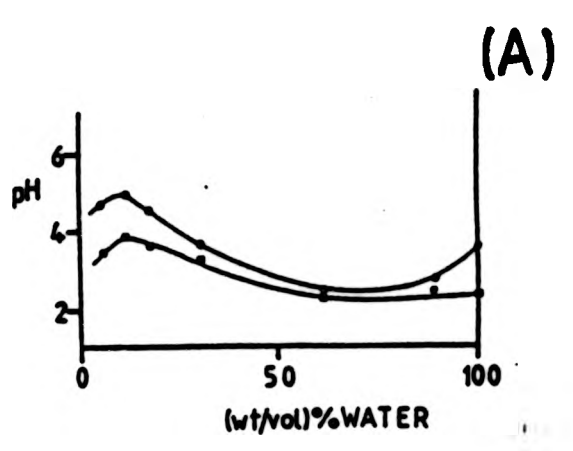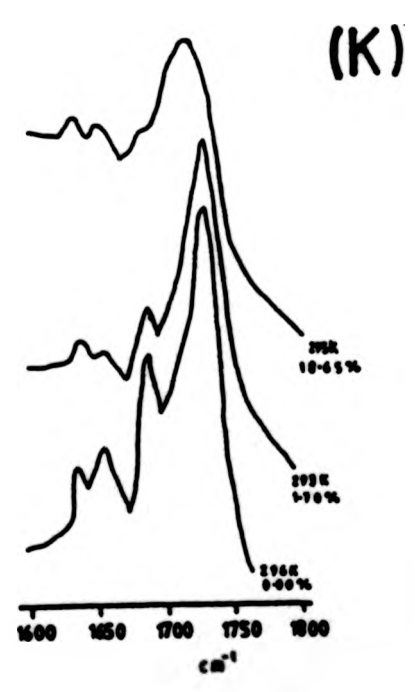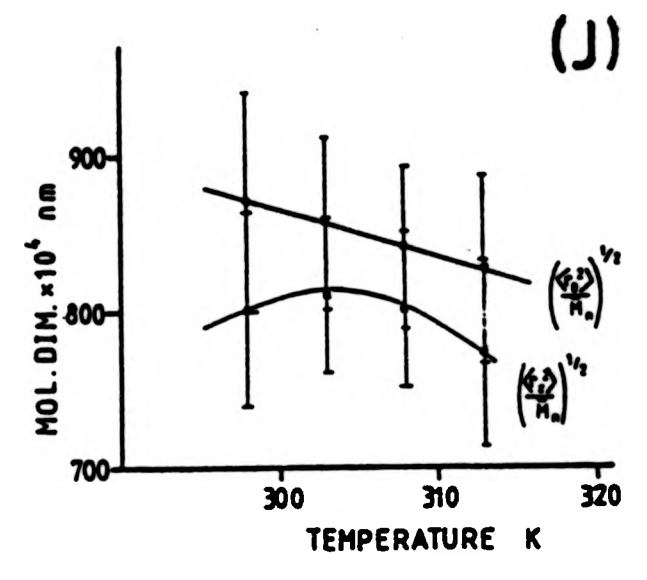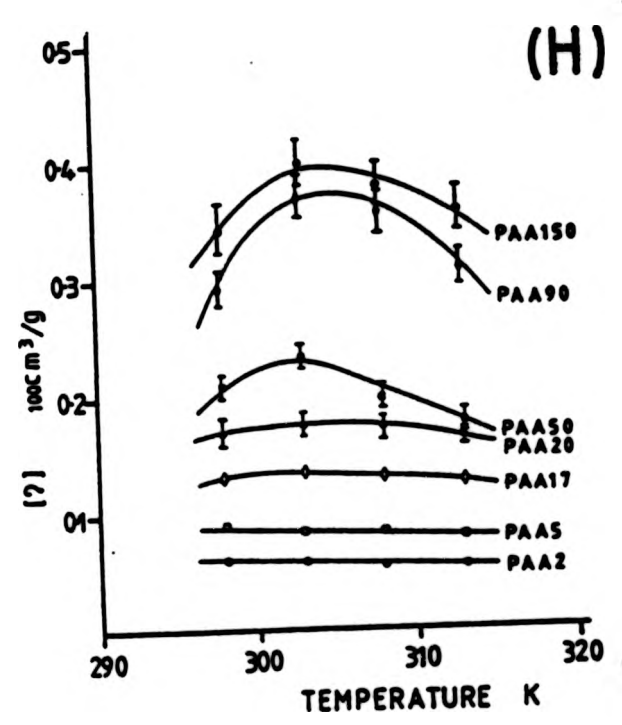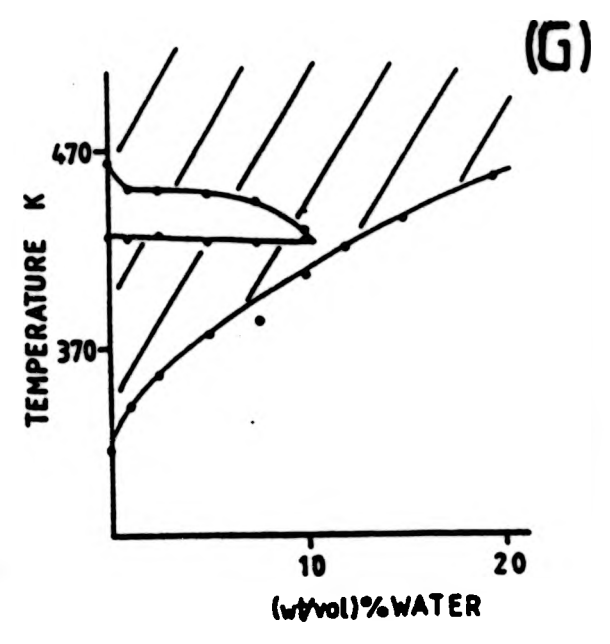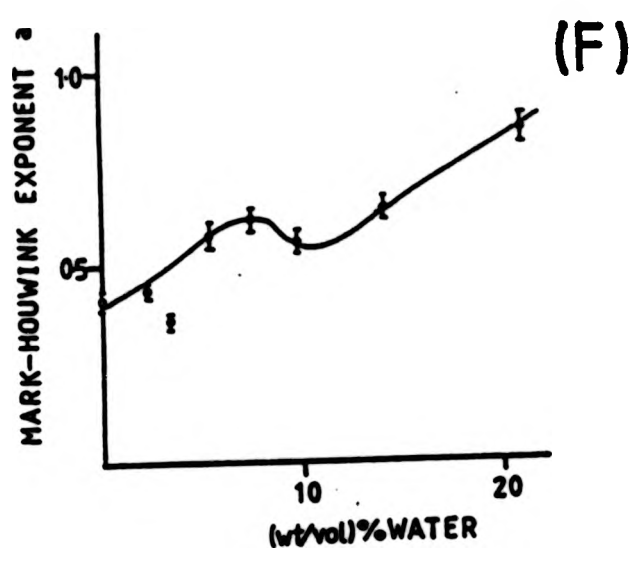
APPENDIX A

Data are given for the cloud-point curves for the various systems
studied.   The corresponding figures are given with each table.
Poly(acrylic acid) concentrations are given in $g/100cm^3$.   The
'solvents' are given as (wt/vol)% of the minor component.
Poly(N-isopropylacrylamide) and poly(vinyl alcohol) concentrations are
also given in $g/100cm^3$.

POLY(ACRYLIC ACID)/DIOXANE

(Fig 3.1)

PAA5 g/100cm^3	p-LCST K	PAA5 g/100cm^3	p-LCST K
0.81	454	7.22	432
1.44	444	8.16	433
2.08	439.5	8.91	434
2.84	436	15.74	440
4.38	427	19.41	449
5.30	427	25.10	459
5.59	429	30.06	468.5
5.82	430.5	39.83	477

(Fig 3.2)

PAA17 g/100cm^3	p-LCST K	UCST K	LCST K	PAA17 g/100cm^3	p-LCST K	UCST K	LCST K
0.53	392	408	–	14.01	395	425	436
1.09	379.5	413	–	14.41	397	427	433
1.64	379	416	459	15.09	398	–	–
2.90	378	419	452	15.63	399	–	–
5.55	379	420	448	17.64	403.5	–	–
7.77	386	421.5	438	21.55	408	–	–
8.61	388	420.5	438.5	25.62	412.5	–	–
8.91	386.5	422.5	438	29.88	417	–	–
9.47	388	424	437.5	37.96	422	–	–
10.00	389.5	425	437	38.22	426	–	–
11.88	391.5	425	436.5				
14.01	395	425	436				

(Fig 3.3)

PAA20 g/100cm³	p-LCST K	UCST K	LCST K	PAA20 g/100cm³	p-LCST K	UCST K	LCST K
0.35	387	401	-	10.10	380.5	419.5	430
0.56	379.5	409	-	11.88	383.8	419.5	429
1.15	375.2	422	-	14.54	385	419.5	428.5
1.78	374	423	-	16.07	389	420	427
3.70	375	421.5	456	18.25	393	421	426
4.98	375.5	421	448	19.55	395	422	425
5.90	376	420	437	24.69	400	-	-
6.96	377	416	436	29.71	403.	-	-
7.73	381	413	435	34.12	406.5	-	-
8.30	384	412	434.5	37.92	408	-	-
8.75	384	412	434	40.98	412.5	-	-
9.04	383	414	433				

(Fig 3.4)

PAA50 g/100cm³	p-LCST K	UCST K	LCST K	PAA50 g/100cm³	p-LCST K	UCST K	LCST K
0.25	361.6	375.5	-	3.26	320.9	427	451
0.51	323.4	403.5	-	4.15	323.1	427	451
0.69	320.6	408	-	5.64	326.4	427	450.5
1.06	319.8	414.9	495.5	7.19	329.7	427	449.5
1.32	319.3	422.7	483.6	15.64	331.5	423	448
1.80	318.6	425.9	466.1	20.61	333.5	423	446
2.21	319.6	427	462	24.93	335	422	445
2.22	318.7	426.5	461.5	29.27	336.5	421.5	441
2.50	318.8	426.5	457.8	39.79	339	421	440
2.60	319.2	426.5	457.8				

(Fig 3.5)

PAA90 g/100cm³	p-LCST K	UCST K	LCST K	PAA90 g/100cm³	p-LCST K	UCST K	LCST K
0.29	323	375	–	7.40	329.4	427	446
0.43	321.2	403.5	–	10.07	330.5	427	445.5
0.78	319.8	413.7	493	15.08	334.6	427	445.5
1.25	319.3	421.5	458	20.46	338.2	425	444
2.18	322.7	427	450.5	26.00	341	422	440
3.22	323.6	427	448	29.35	343	421	439
3.93	324.4	427	446.5	39.26	346.6	419.5	434
5.00	326.6	427	446				

(Fig 3.6)

PAA150 g/100cm³	p-LCST K	UCST K	LCST K	PAA150 g/100cm³	p-LCST K	UCST K	LCST K
0.24	322.7	312.5	–	7.52	328.5	402.5	410
0.49	318.9	386.5	–	8.55	329.1	–	–
0.90	318	392.1	468.8	9.18	330.2	–	–
1.37	317.8	395.6	441.8	11.98	331.5	–	–
2.25	319.9	401.5	421.6	19.64	335.9	–	–
3.19	321.9	401.5	413	25.33	339.5	–	–
3.77	321.9	401.5	411.9	29.61	343	–	–
5.15	319.4	402.5	410	40.56	347.4	–	–

(Fig 3.7)

PAA300 g/100cm^3	p–LCST K	UCST K	LCST K	PAA300 g/100cm^3	p–LCST K	UCST K	LCST K
0.27	336.9	355.7	–	5.27	306.6	–	–
0.38	306	359	475	7.40	307.3	–	–
0.72	300.9	365.1	425.6	10.80	317	–	–
1.04	299.8	366.7	417	19.27	318.5	–	–
2.02	299.7	377.8	395	24.12	320	–	–
3.24	305.1	383	393	28.94	321.4	–	–
4.62	307.5	383.8	392.7	40.59	326.5	–	–
5.12	307	391	392				

POLY(ACRYLIC ACID)/THF

(Fig 3.15)

PAA5 g/100cm^3	p-LCST K	UCST K	LCST K
0.40	–	–	–
1.05	391.5	–	–
4.92	365.5	–	–
7.40	367.5	–	–
11.21	376.5	–	–
14.13	380.5	–	–

(Fig 3.16)

PAA50 g/100cm^3	p-LCST K	UCST K	LCST K
0.46	308.6	367	–
1.15	293.8	396	432
3.08	292	405	419
4.95	289.2	408.5	416.5
7.29	289.8	408.5	415.5
7.82	290.4	408.5	415
8.66	290.6	408.5	409.5
9.00	290.5	–	–
11.14	291.5	–	–
14.83	292.3	–	–

POLY(ACRYLIC ACID) PAA50/DIOXANE/WATER

1.05% water (Fig 3.18)

PAA50 g/100cm^3	p-LCST K	UCST K	LCST K
0.00	–	–	–
0.44	344.5	418	452
1.00⁻	340.3	425	450
2.17	339.2	425	449
3.58	339	425	448.5
5.56	338.2	425	448.5
7.72	339.9	425	448.5
10.31	346.5	424	448
16.91	348.9	424	448

2.52% water (Fig 3.19)

PAA50 g/100cm^3	p-LCST K	UCST K	LCST K
0.00	–	–	–
0.58	361.5	415.8	–
1.13	356.4	426	449
2.19	355	426	449
3.41	355	426	449
5.54	354	426	449
8.17	354.6	426	449
10.31	355.9	426	448
14.58	355.5	426	448

4.99% water (Fig 3.20)

PAA50 g/100cm³	p-LCST K	UCST K	LCST K
0.00	–	–	–
0.55	388.5	420.5	–
1.10	379.4	422.5	448
2.10	378	423	448
3.22	372.5	423	448
3.55	374.5	423.5	448
5.18	373	424	448
8.17	370.6	424	448
9.61	372	424	448
12.54	373	424	448

7.49% water (Fig 3.21)

PAA50 g/100cm³	p-LCST K	UCST K	LCST K
0.00	–	–	–
0.53	401.5	415.5	–
0.94	398.4	419.5	452
2.17	391	422	442
3.79	389.2	422	441
6.02	388.8	422	440
7.43	386.4	–	–
9.74	388.5	–	–
14.77	389.5	–	–

9.99% water (Fig 3.22)

PAA50 g/100cm^3	p-LCST K	UCST K	LCST K
0.00	-	-	-
0.41	-	-	-
0.96	411.5	422	430
1.88	406.7	423	428.5
3.89	402.5	423.8	428.5
5.32	401	425	428.5
5.93	401	-	-
10.72	400	-	-

12.05% water (Fig 3.23)

PAA50 g/100cm^3	p-LCST K	UCST K	LCST K
0.00	-	-	-
0.59	431	-	-
0.99	422	-	-
1.83	421	-	-
2.61	419	-	-
5.36	415	-	-
7.51	414.5	-	-
10.15	416.5	-	-
14.96	417	-	-

14.87% water (Fig 3.23)

PAA50 g/100cm^3	p-LCST K	UCST K	LCST K
0.00	–	–	–
0.46	446	–	–
1.01	438	–	–
1.88	435	–	–
2.55	434	–	–
5.37	430.5	–	–
7.66	428.5	–	–
10.37	426	–	–
14.95	425	–	–

19.72% water (Fig 3.23)

PAA50 g/100cm^3	p-LCST K	UCST K	LCST K
0.00	–	–	–
1.02	461	–	–
5.03	453	–	–
7.49	451	–	–
9.88	451	–	–
14.37	453	–	–

POLY(ACRYLIC ACID) PAA17/DIOXANE/WATER

1.02% water (Fig 3.25)

PAA17 g/100cm^3	p-LCST K	UCST K	LCST K
0.00	-	-	-
0.42	-	-	-
0.82	401.5	409	450
1.89	395	417	443
3.77	394.5	419	435.5
6.18	397	421.5	425
8.08	399	-	-
8.51	396	-	-
8.99	396.5	-	-
12.13	398	-	-
14.64	404.5	-	-
19.99	411	-	-

2.55% water (Fig 3.26)

PAA17 g/100cm^3	p-LCST K	UCST K	LCST K
0.00	–	–	–
0.52	–	–	450
1.01	411	418.5	446
2.13	405	420	439
4.27	403	422.5	427
5.91	405	423	426
7.93	406.5	423	426
8.53	413	–	–
9.16	413.5	–	–
10.25	416	–	–
12.16	416.5	–	–
14.83	419	–	–
18.12	423.5	–	–

4.01% water (Fig 3.27)

PAA17 $g/100cm^3$	p-LCST K	UCST K	LCST K
0.00	–	–	–
0.39	–	–	–
1.23	418.5	420.5	437
1.95	416	421	432
3.90	414	422	427
6.40	415.5	423	425
7.86	417	–	–
8.53	422.5	–	–
9.04	423	–	–
10.25	424	–	–
10.88	424.5	–	–
15.32	429.5	–	–
20.24	432	–	–

POLY(ACRYLIC ACID) PAA50/THF/WATER

2.50% water (Fig 3.29)

PAA50 g/100cm^3	p-LCST K	UCST K	LCST K
0.00	–	–	–
0.49	318.5	362	–
1.14	317	365	397
2.01	317.3	375	392.5
2.69	315.5	–	–
5.18	314	–	–
7.25	314	–	–
10.78	315.2	–	–
14.96	321.5	–	–

POLY(ACRYLIC ACID) PAA50/DIOXANE/0.01M HCl

5.00% HCl (Fig 3.28)

PAA50 g/100cm³	p–LCST K	UCST K	LCST K
0.00	–	–	–
0.41	385.5	405.5	459
0.82	378.5	417	448.5
1.66	373.7	421	448.5
2.69	372.5	422.5	448.5
5.13	372	423.5	448.5
7.68	371.5	424	448.5
9.99	373	424.5	448
14.75	374	425	447

POLY(ACRYLIC ACID) PAA50/DIOXANE/CROWN ETHER 12-C-4

2.02% 12-C-4 (Fig 10.1)

PAA50 g/100cm^3	p-LCST K	UCST K	LCST K
0.00	–	–	–
0.46	328.4	362	408
1.41	322.4	–	–
2.74	323.7	–	–
5.61	329.9	–	–
7.96	334	–	–
11.28	340.2	–	–

4.91% 12-C-4 (Fig 10.2)

PAA50 g/100cm^3	p-LCST K
0.00	–
0.50	325
1.55	322.5
3.33	324.5
5.60	328.2
7.80	331.8
12.44	337

10.07% 12-C-4 (Fig 10.2)

PAA50 g/100cm^3	p-LCST K
0.00	–
0.66	327.4
1.17	323.9
2.74	326.1
4.40	332.6
7.99	338.8
10.45	343.6

19.18% 12-C-4 (Fig 10.2)

PAA50 g/100cm^3	p-LCST K
0.00	–
0.48	338
1.02	331
2.93	333.4
4.90	340.5
8.08	345
12.45	353.5

100% 12-C-4 (Fig 10.2)

PAA50 g/100cm^3	p-LCST K
1.14	448
5.26	435
10.23	438
15.24	441

POLY(ACRYLIC ACID) PAA50/POLY(ETHYLENE GLYCOL) PEG2/DIOXANE

1.63% PEG2 (Fig 10.4)

PAA50 g/100cm^3	p-LCST K
0.00	332.9
0.35	320.1
1.17	320.8
2.80	326.9
5.45	326.9
7.89	332.3
12.52	341.3

5.14% PEG2 (Fig 10.4)

PAA50 g/100cm^3	p-LCST K
0.00	–
0.52	335.9
1.17	326.5
3.18	322.1
4.73	323.1
7.72	331.2
11.84	339.9

9.92% PEG 2 (Fig 10.4)

PAA50 g/100cm^3	p-LCST K
0.00	–
0.52	352.2
1.09	344.9
2.89	340.5
5.55	342.4
8.64	347.1
12.05	349.3

18.52% PEG 2 (Fig 10.4)

PAA50 g/100cm^3	p-LCST K
0.00	–
0.68	390
1.01	385
3.14	382
4.85	381
8.50	383
11.74	384

POLY(ACRYLIC ACID) PAA50/POLY(ETHYLENE GLYCOL) PEG40/DIOXANE

1.85% PEG 40 (Fig 10.2)

PAA50 g/100cm^3	p-LCST K
0.00	–
0.61	328.8
1.09	323.8
3.05	323.5
5.41	328.2
8.55	334.4
12.21	339.6

4.69% PEG 40 (Fig 10.2)

PAA50 g/100cm^3	p-LCST K
0.00	–
0.42	332.1
1.43	325.2
3.31	326.3
5.21	330.1
8.55	335.6
12.47	340.2

9.44% PEG 40 (Fig 10.5)

PAA50 g/100cm^3	p-LCST K
0.00	–
0.59	332.5
1.41	328.3
3.08	329.9
5.45	333.6
8.38	338.8
12.23	342.6

20.01% PEG 40 (Fig 10.5)

PAA50 g/100cm^3	p-LCST K
0.00	–
0.40	344.5
1.06	337.2
2.98	338.3
5.49	341.3
8.03	344.9
11.13	346.0

POLY(ACRYLIC ACID) PAA150/POLY(ETHYLENE GLYCOL)/DIOXANE

3.10% PEG2 (Fig 10.7)

PAA150 g/100cm³	p-LCST K	UCST K	LCST K
0.00	-	-	-
0.68	327.3	390	448
1.30	326.5	392	408
2.47	325.7	396	405
2.87	324.4	400	403
3.84	328.0	-	-
6.19	332.3	-	-
8.96	335.0	-	-
12.86	342.3	-	-

2.97% PEG4 (Fig 10.8)

PAA150 g/100cm³	p-LCST K	UCST K	LCST K
0.00	-	-	-
0.65	335.5	372	403
1.38	331.3	375.8	398
3.07	328.5	376.5	388
4.81	329.4	378.0	385.5
5.60	331.9	-	-
6.36	332.8	-	-
6.82	333.4	-	-
7.33	333.2	-	-
10.21	336.4	-	-

POLY(ACRYLIC ACID) PAA150/POLY(ETHYLENE GLYCOL)/DIOXANE

3.10% PEG2 (Fig 10.7)

PAA150 g/100cm^3	p-LCST K	UCST K	LCST K
0.00	–	–	–
0.68	327.3	390	448
1.30	326.5	392	408
2.47	325.7	396	405
2.87	324.4	400	403
3.84	328.0	–	–
6.19	332.3	–	–
8.96	335.0	–	–
12.86	342.3	–	–

2.97% PEG4 (Fig 10.8)

PAA150 g/100cm^3	p-LCST K	UCST K	LCST K
0.00	–	–	–
0.65	335.5	372	403
1.38	331.3	375.8	398
3.07	328.5	376.5	388
4.81	329.4	378.0	385.5
5.60	331.9	–	–
6.36	332.8	–	–
6.82	333.4	–	–
7.33	333.2	–	–
10.21	336.4	–	–

3.02% PEG10 (Fig 10.9)

PAA150 g/100cm^3	p-LCST K
0.00	–
0.69	331
1.29	327.7
2.84	329
5.78	334.4
8.26	338.5
12.00	341.3

3.02% PEG15 (Fig 10.9)

PAA150 g/100cm^3	p-LCST K
0.00	–
0.65	328.3
1.37	325.4
2.79	327.0
4.69	331.0
7.93	335.2
11.02	338.8

2.99% PEG40 (Fig 10.9)

PAA150 g/100cm^3	p-LCST K
0.00	–
0.51	325.5
0.94	324.5
2.74	323.6
4.62	327.0
8.38	331.9
11.99	336.8

2.96% PEG60 (Fig 10.9)

PAA150 g/100cm^3	p-LCST K
0.00	–
0.54	322.5
1.51	319.4
3.07	320.6
4.78	321.5
8.06	329.3
10.56	331.9

POLY(ACRYLIC ACID) PAA5/POLY(ETHYLENE GLYCOL)PEG40/DIOXANE

1.85% PEG40 (Fig 10.11)

PAA150 g/100cm^3	p–LCST K
0.00	–
0.37	446
0.90	428
3.14	419
5.16	419
7.50	422
11.77	429

4.69% PEG40 (Fig 10.11)

PAA150 g/100cm^3	p–LCST K
0.00	–
0.55	441
1.45	423
3.39	418
4.74	417
7.40	418
12.04	426

9.44% PEG40 (Fig 10.11)

PAA150 g/100cm^3	p–LCST K
0.00	–
0.43	443
1.09	393
2.65	389
4.79	393
8.02	398
11.55	408

POLY(ACRYLIC ACID) PAA50/POLY(PROPYLENE GLYCOL) PPG425/DIOXANE

1.43% PPG425 (Fig 10.13)

PAA150 g/100cm^3	p-LCST K	UCST K	LCST K
0.00	–	–	–
0.46	324.3	368	407
3.25	323.7	387	393
5.54	328.4	–	–
8.83	334.9	–	–
11.15	338.2	–	–
14.75	347.0	–	–

5.10% PPG425 (Fig 10.14)

PAA150 g/100cm^3	p-LCST K
0.00	–
0.49	329.4
1.24	325
3.05	326
5.30	329.9
7.98	334.8
12.31	341.7

10.38% PPG425 (Fig 10.14)

PAA150 g/100cm^3	p-LCST K
0.00	–
0.58	331.4
0.89	327.3
2.65	329.1
5.08	332.9
8.35	336
11.45	338.7

19.65% PPG425 (Fig 10.14)

PAA150 g/100cm^3	p-LCST K
0.00	–
0.72	330.9
1.11	329.2
2.79	329.5
4.96	332.4
8.64	337.2
10.72	339.9
14.64	357.0

PNIPAM/WATER (Fig 11.3)

5PN

5PN g/100cm^3	LCST K
0.64	308.5
0.95	308.3
3.12	307.8
4.92	307.6
8.53	307.4
10.76	307.1

6PN

6PN g/100cm^3	LCST K
0.43	308.5
1.22	308.5
3.39	307.5
4.79	307.6
7.72	307.3
11.48	307.1

7PN

7PN g/100cm^3	LCST K
0.43	309.9
1.06	309.3
2.59	308.3
4.70	307.6
8.77	307.2
13.42	306.8

8PN

8PN g/100cm^3	LCST K
0.47	308.6
0.97	308.4
2.92	307.9
4.72	307.7
8.44	307.3
11.49	307.2

POLY(VINYL ALCOHOL)/WATER (Fig 12.2)

PVA100

PVA100 g/100cm^3	LCST K	UCST K	PVA100 g/100cm^3	LCST K	UCST K
0.46	353.4	372.4	14.23	306.7	423.5
0.79	344.0	395.5	15.05	308	419
1.51	330.4	404.6	16.12	313.5	416
2.29	323.8	410.5	16.50	319	411
4.31	312.5	419	17.02	323.7	408
7.06	308	424.5	17.35	328.7	394.5
9.73	308	425.5	18.00	–	–
12.10	307.5	425			

PVA125

PVA125 g/100cm^3	LCST K	UCST K	PVA125 g/100cm^3	LCST K	UCST K
0.33	–	–	14.24	324	406
0.61	–	–	14.62	324.7	407
0.96	363	375	15.03	325.5	407
1.53	332.1	395	15.40	326.9	407
5.17	333	398	15.91	335.5	405.5
8.07	329.3	402	16.53	348	404.5
9.87	327.7	403.5	16.84	–	–
13.00	326.6	405	17.53	–	–